UNIVERSITAT POLITÈCNICA DE CATALUNYA

ASSESSMENT OF GROUNDWATER SYSTEM UNDER GLOBAL CHANGE SCENARIOS: THE CASE OF KWALE (KENYA)

by

Núria Ferrer Ramos

Advised by Dr. Albert Folch Sancho

This thesis is submitted in the fulfilment of the requirements for the PhD degree to the doctoral school of the Universitat Politècnica de Catalunya

in the

Department of Civil and Environmental Engineering

Hydrogeology Group (UPC-CSIC)

June 2019

Grup d'**H**idrologia **S**ubterrània
UNIVERSITAT POLITÈCNICA DE CATALUNYA

UNIVERSITAT POLITÈCNICA DE CATALUNYA

Abstract

Department of Civil and Environmental Engineering

by Núria Ferrer Ramos

Global change is a term widely used to describe changes in the characteristics of inter-related climate variables, and derived changes in terrestrial processes, including human activities that affect the environment. One of the main drivers of the current global change is the climate change characterized by increased number and increased length of drought periods. Another relevant driver that will imply greater pressure on natural processes is the expected population growth, increasing the demand and competition for water for domestic, industrial, agricultural, and municipal uses. Global change effects on water resources are profound and need to be explored deeply, especially, in the developing countries since, projections of impacts due to global change are associated with large uncertainties.

In Africa, it is estimated that 75 % of population use groundwater as their main source of drinking water, particularly in rural areas that rely on low-cost dug wells and boreholes. It is an important resource for economic growth, food production, drinking water security and ecosystem services. However, groundwater quality in Africa is being hampered negatively by anthropogenic pollution sources and activities limiting the available water resources. Despite its importance, data of groundwater systems are sparse and the current state of knowledge is low and this is a serious limitation for the sustainable development of the groundwater resources. Therefore, it is needed to find new tools and approaches to understand these systems with lack of data and poorly understood, especially in Africa's coastal areas where threatens are even more important. In this context, where Africa's groundwater systems are a critical and poorly understood socio-ecological systems, born the project Gro for Good: Groundwater Risk for Growth and Development" founded by the UPGro (http://upgro.org/). The main objective of this interdisciplinary project is to support science and governance of managing groundwater risks for growth and development in Africa for the poorest benefit. As part of this project, the main objective of this dissertation focus on develop a combination and integration of different types of hydrogeological tools, climatic episodes, and social variables, in order to better understand the effects of global change on Sub-Saharan Africa. To do it, the coastal aquifer system of Kwale (Kenya) is taken as a reference, where local communities share groundwater resources with new water-reliant activities as mining, agriculture and tourism. The final goal is to understand the risks

and impacts in this context to improve water resources management in benefit of the poorest. The study area of this thesis is located in a rural area on the coastal plain of Kwale County, south of Mombasa and adjacent to northern Tanzania. The area is characterized by a bimodal rainfall pattern (average 1200 mm/year), and experiences increased climate variability. Between April and June occurs generally the long rains and between October and December the short rains period. The major portion of the area is based on local agriculture, but since 2012, two new and major water-reliant economic activities have been established in Kwale County. One is carried out by the Kwale International Sugarcane Company Limited (KISCOL), which has been progressively habilitating 5500 ha of drip-irrigated sugarcane. The other important recent economic activity is the country's largest mining operation: the Kwale Mineral Sands Project operated by Base Titanium Ltd. Furthermore, the study area has a long-established coastal tourism industry.

The aquifer system has been characterized integrating kilometric geophysical transects carried out by the Kenyan team, hydrochemistry, environmental isotopes and groundwater level data. Furthermore, the main quality groundwater problems, contamination by faecal bacteria (*E. coli*), have been also characterized. To evaluate the main drivers of this kind of pollution, several qualitative and quantitative variables as geology, hydrology, geochemistry, sanitary risk factors, well types, and maintenance have been statistical analysed to study its correlation with *E. coli* concentration. The other main quality problem in the area is the saline intrusion, so geochemical models to understand the geochemical processes occurring in the area affected by seawater intrusion dynamics have been developed using PHREEQC software. The groundwater sustainability of the system has also been determined under the new abstraction regime of the water-reliant users. In most developing countries, this information is unknown, so information from water users and simple information sources (interviews, Google Earth, Trip Advisor, basic analytical methods, etc.), has been used to estimate groundwater abstraction of the main water-reliant industries. This sustainability has been evaluated thought La Niña drought 2016/17. All this previous knowledge has helped to build a numerical groundwater flow model, using Modflow code from 2010 to 2017, in order to integrate all the information available, define the relationship between surface and groundwater, and to use it as a tool to study how the climate change and the future increased abstraction rate may affect the groundwater system and its management. Future rainfall scenarios have been constructed based on long historical data series (from 1959 to 2017) and the Standardized Precipitation Index. Future abstraction has been based on current abstraction and future estimations made by to Water Resources Authority water allocations. In addition, a new index has been defined and tested

in the study area to define the risk for a given household to have no access to drinking water (in terms of either quantity or quality).

The aquifer is a multi-layered system formed by a shallow and deep aquifer, which crop out in the western part of the area in the Shimba Hills range on the west of the study area. The hydrochemical facies and the water isotopic composition indicate that there is hydraulic connectivity across the materials that comprise the shallow aquifer and between all the deep geological formations that conform the deep aquifer. These two aquifer units are separated by the presence of a middle/low permeability aquitard emplaced between the young and old materials Furthermore, the deep aquifer is disrupted across the area by two in-filled palaeochannels. Equipotential lines of the shallow aquifer show that the groundwater flow direction is from the Shimba Hills on the west to the Indian Ocean on the east. The statistical analyses performed to improve understanding on faecal bacteria pollution indicate that well constructive characteristics are the most important variables to avoid bacteria presence in groundwater. Furthermore, low Eh, short water column and areas with fast infiltration are factors related with the presence of faecal bacteria. Saline intrusion is the other quality problem in the aquifer area. The geochemical mix models point out that the increase in salinity, as observed in 2016 during La Niña, and the dynamics of the sea water intrusion will tend to increase calcite dissolution with could induce other potential risks as increase the creation of sinkholes. The main effect of La Niña has been a reduction of the recharge of 69 % compared to a year with average annual rainfall as 2013 and there has been a groundwater level decline in 86 % of the measured shallow wells. During La Niña groundwater salinity increases during the rainfall season instead of being reduced, as occurs in normal years in the wells located near the coast. Despite the groundwater levels recover after the drought period in the wake of the long rains wet season of 2017, the quality of the coastal wells did not recover.

The estimation of the current abstractions has been the baseline to define future groundwater abstraction that together with a future climatic series (precipitation and temperature) based on historical data, global scenarios have been run future using the numerical model as a tool. The total anticipated volume abstracted will increase by around 85 % compared with current abstraction. However, the percentage of this increment will not significantly affect the aquifer storage in each of the future global scenarios, reducing the aquifer storage around 1 %-2 % depending on the global climatic conditions. Nevertheless, three followed dry year can induce a reduction of the groundwater levels of the aquifer system. Despite groundwater level decline observed during prolonged dry periods and abstraction increment, a dry period followed by a humid period leads to the

relatively swift recovery of the groundwater system in less than 3 years. Another applicability to the numerical groundwater flow model has been to use the outputs of these numerical future scenarios together with household field data to test the new developed index that can be widely applied to evaluate the risk to run out without water due to lack of water and/or low water quality threshold. This index helps to understand better the effect of the global change on households under a "transient state" instead of a "steady state", as most of the current indexes do. In this tested case, this index shows that the areas with highest risk respond to quality issues, no quantity, as those located near the coast affected by saline intrusion.

The present dissertation contributes to the hydrogeological knowledge in a context that represents much of East Africa. Methodologically, different tools have been presented in order to study these systems by limited understanding and lack of data. It shows the importance of integrating the hydrogeological data of stakeholders, and the alternative sources of information used (Google Earth, Trip Advisor…) to advance the knowledge in areas with lack of data. Furthermore, this dissertation presents how to use different tools and kinds of data to study the sustainability of the aquifer system, focusing on the groundwater availability as well as its quality. Furthermore, integrating hydrogeological and social household data let a bigger understanding of how the groundwater system changes, naturally or induced, can affect the groundwater availability to the water-reliant users.

UNIVERSITAT POLITÈCNICA DE CATALUNYA

Resumen

Department of Civil and Environmental Engineering

per Núria Ferrer Ramos

El cambio global es un término ampliamente utilizado para describir los cambios en las características de las variables climáticas interrelacionadas y los cambios derivados en los procesos terrestres, incluyendo las actividades humanas que afectan el medio ambiente. Uno de los principales impulsores de este cambio global es el cambio climático, caracterizado por un aumento en el número y duración de los períodos de sequía. El esperado crecimiento poblacional es otro factor relevante que producirá una mayor presión sobre los procesos naturales. Este aumento de población, generará un incremento en la demanda y en la competencia por el agua, tanto en los usos domésticos, industriales, agrícolas como municipales. Los efectos del cambio global en los recursos hídricos son profundos y deben explorarse en detalle, especialmente en los países en vías de desarrollo, pues es donde las proyecciones de los impactos debidos al cambio global están asociadas a mayores incertidumbres.

En África, se estima que el 75 % de la población utiliza el agua subterránea como su principal fuente de agua potable, especialmente en las áreas rurales que dependen de pozos excavados de bajo coste. Es un recurso importante para el crecimiento económico, la producción de alimentos, la seguridad del agua potable y los ecosistemas. Sin embargo, la calidad de las aguas subterráneas en África se ve afectada negativamente por las fuentes de contaminación antrópica y las actividades que limitan los recursos hídricos disponibles. A pesar de la importancia de este recurso, los datos de los acuíferos son escasos y el estado actual del conocimiento es bajo, constituyendo una serie de limitaciones para el desarrollo sostenible de los recursos subterráneos. Por lo tanto, es necesario desarrollar nuevas herramientas y enfoques para comprender estos sistemas con falta de datos y poco conocidos, especialmente en las zonas costeras de África donde las amenazas son aún más importantes. En este contexto, donde los sistemas de agua subterránea de África son sistemas socio-ecológicos críticos y poco conocidos, nace el proyecto Gro for Good, cuyas siglas significan “agua subterránea para el crecimiento y el desarrollo”, fundado por UPGro (http://upgro.org/). El objetivo principal de este proyecto interdisciplinario es apoyar la ciencia y la gobernanza de la gestión de los riesgos de las aguas subterráneas para el crecimiento y el desarrollo en África para beneficiar la población más pobre. Como parte de este proyecto, el objetivo principal de esta tesis es desarrollar, combinar e integrar

diferentes tipos de herramientas hidrogeológicas, episodios climáticos y variables sociales, a fin de comprender mejor los efectos del cambio global en África subsahariana. Para hacerlo, el acuífero costero de Kwale (Kenia) se ha tomado como referencia, pues es un ejemplo donde las comunidades locales comparten los recursos de agua subterránea con nuevas actividades como la minería, la agricultura y el turismo, las cuales también dependen del agua subterránea. El objetivo final es comprender los riesgos e impactos en este contexto a fin de mejorar la gestión de los recursos hídricos en beneficio de los más pobres. El área de estudio de esta tesis está ubicada en un área rural en la llanura costera del condado de Kwale, al sur de Mombasa y adyacente al norte de Tanzania. El área se caracteriza por un patrón de precipitación bimodal (promedio de 1200 mm / año) y sometida a una gran variabilidad climática. Entre abril y junio ocurren generalmente las lluvias prolongadas, y entre octubre y diciembre, es el período de lluvias cortas. La mayor parte del área se basa en la agricultura de subsistencia, pero desde 2012, se han establecido en el condado de Kwale dos nuevas e importantes actividades económicas que dependen del agua. Una es la realizada por *Kwale International Sugarcane Company Limited* (KISCOL), una empresa que ha estado habilitando progresivamente 5500 ha de caña de azúcar mediante riego por goteo. La otra actividad económica es la empresa minera más grande del país: *Kwale Mineral Sands Project* operado por Base Titanium Ltd. Además, el área de estudio tiene una industria de turismo costero establecida hace años.

El acuífero se ha caracterizado mediante la integración de largos transectos geofísicos realizados por el equipo de Kenia, datos hidroquímicos e isotópicos, y datos sobre el nivel del agua subterránea. Además, se han caracterizado los principales problemas de calidad de las aguas subterráneas, uno de ellos, la contaminación por bacterias fecales (*E. coli*). Para evaluar los principales causantes de este tipo de contaminación, se han analizado estadísticamente varias variables cualitativas y cuantitativas como la geología, hidrología, geoquímica, factores de riesgo sanitario, tipos de pozo y mantenimiento para estudiar su correlación con la concentración de *E. coli*. El otro principal problema de calidad en el área, es la intrusión salina, por lo que se han desarrollado modelos geoquímicos para comprender los procesos geoquímicos que se producen en el área afectada por la dinámica de intrusión de agua de mar mediante el software PHREEQC. Además, se ha determinado la sostenibilidad de las aguas subterráneas bajo un nuevo patrón de extracción por parte de los usuarios de la zona. En la mayoría de los países en vías de desarrollo, esta información es desconocida, por lo que la información directa de los usuarios y de fuentes de información simples (entrevistas, Google Earth, Trip Advisor, métodos analíticos básicos, etc.) ha servido para estimar la extracción de agua subterránea de las principales industrias que dependen de este recurso. La sostenibilidad del acuífero se ha evaluado durante la

sequía producida por el evento de La Niña 2016/17. Además, todo este conocimiento previo sobre el sistema hidrogeológico ha permitido a construir un modelo numérico de flujo de agua subterránea, utilizando el código Modflow del 2010 al 2017, y así poder integrar toda la información disponible y definir la relación entre las aguas superficiales y subterráneas. Este modelo se ha usado como herramienta para estudiar cómo la variabilidad climática y el futuro aumento del bombeo de agua subterránea puede afectar al acuífero y poder definir así, una mejor gestión de los recursos. Los escenarios futuros de lluvia se han construido mediante el método SPI (índice de precipitación estandarizado) aplicado en una serie de datos de precipitación históricos (de 1959 a 2017). El volumen de bombeo futuro se ha basado en el volumen de explotación actual y la futura estimación realizada por las autoridades gestoras del agua de la zona. Además, se ha definido un nuevo índice y éste se ha probado en el área de estudio para intentar definir el riesgo de que un hogar determinado no tenga acceso al agua potable (en términos de cantidad o calidad).

El acuífero estudiado es un sistema de múltiples capas formado por un acuífero superficial y uno profundo, el cual este último aflora en la parte occidental del área de estudio en la zona montañosa de las Shimba Hills en el oeste de la zona de estudio. Las facies hidroquímicas y la composición isotópica del agua indican que existe una conectividad hidráulica a través de los materiales que comprenden el acuífero superficial y entre todas las formaciones geológicas profundas que conforman el acuífero profundo. Estas dos unidades acuíferas están separadas por la presencia de un acuitardo de media / baja permeabilidad emplazado entre los materiales recientes y antiguos. Además, el acuífero profundo está interrumpido en toda el área por dos paleocanales. Las líneas equipotenciales del acuífero superficial muestran que la dirección del flujo de agua subterránea es desde Shimba Hills en el oeste hasta el Océano Índico en el este. El análisis estadístico realizado para mejorar la comprensión de la contaminación por bacterias fecales indica que las características constructivas del pozo son las variables más importantes para evitar la presencia de bacterias en el agua subterránea. Además, bajos valores de Eh, una columna de agua reducida y áreas con infiltración rápida son los principales factores relacionados con la presencia de bacterias fecales. La intrusión salina es el otro problema de calidad en el acuífero. Los modelos de mezcla geoquímicos señalan que el aumento de la salinidad, como se observó en el 2016 durante La Niña, y la dinámica de la intrusión de agua de mar tenderán a aumentar la disolución de la calcita la cual podría inducir otros riesgos potenciales, tales como el aumento de la creación de hoyos. El efecto principal de La Niña ha sido una reducción de la recarga del 69 % en comparación con un año con un promedio anual de precipitaciones (2013), y una disminución del nivel subterráneo en el 86 % de los pozos superficiales medidos. Durante La Niña, la salinidad del agua subterránea aumenta

en los pozos ubicados cerca de la costa durante la temporada de lluvias en lugar de reducirse, como ocurre en años normales. A pesar de que los niveles de agua subterránea se recuperaron después del período de sequía gracias a la temporada de lluvias de 2017, la calidad de los pozos costeros no se recuperó.

La estimación de las explotaciones actuales ha servido de base para definir la futura extracción que junto con la serie climática futura (precipitación y temperatura) basada en datos históricos, han permitido estimar los efectos del cambio global mediante la utilización del modelo numérico como herramienta. Se ha estimado que la explotación futura aumentará alrededor de un 85 % en comparación con el volumen actual. A pesar de este incremento, el almacenamiento del acuífero no se ve significativamente afectado en los escenarios futuros analizados, ya que sólo se reduce el almacenamiento en torno al 1 % -2 %, dependiendo de las condiciones climáticas globales. Tres años secos seguidos pueden inducir una reducción de los niveles subterráneos. A pesar de esta disminución de los niveles observada durante los períodos secos prolongados y el incremento de la extracción, un período seco seguido de un período húmedo conduce a una recuperación relativamente rápida del sistema en menos de 3 años. Otra aplicabilidad del modelo numérico ha sido utilizar los resultados de estos escenarios futuros numéricos junto con datos de hogares para probar el nuevo índice. Este índice evalúa el riesgo que tiene un hogar de quedarse sin agua y/o una reducción de la calidad del agua. Este índice ayuda a comprender mejor el efecto del cambio global en los hogares bajo un "estado transitorio" en lugar de un "estado estacionario", como lo hacen la mayoría de los índices actuales. En el área de estudio, este índice muestra que las áreas con mayor riesgo responden a problemas de calidad, como es el caso de aquellos hogares ubicados cerca de la costa afectados por la intrusión salina.

La presente tesis contribuye al conocimiento hidrogeológico en un contexto que representa gran parte de África oriental. Metodológicamente, se han presentado diferentes herramientas para estudiar estos sistemas que presentan una comprensión limitada y falta de datos. Se muestra la importancia de integrar los datos hidrogeológicos de los usuarios de una zona y la utilización de fuentes alternativas de información (Google Earth, Trip Advisor ...) para poder avanzar el conocimiento en un área con falta de datos. Además, esta tesis presenta cómo utilizar diferentes herramientas y tipos de datos para estudiar la sostenibilidad de acuíferos, centrándose en la disponibilidad de aguas subterráneas, así como en su calidad. Además, la integración de datos hidrogeológicos y sociales permite comprender mejor cómo los cambios en un sistema de agua subterránea, naturales o inducidos, pueden afectar la disponibilidad de este recurso a los usuarios que dependen del agua.

UNIVERSITAT POLITÈCNICA DE CATALUNYA

Resum

Department of Civil and Environmental Engineering

por Núria Ferrer Ramos

El canvi global és un terme àmpliament utilitzat per descriure els canvis en les característiques de les variables climàtiques interrelacionades i els canvis derivats en els processos terrestres, incloent les activitats humanes que afecten el medi ambient. Un dels principals impulsors d'aquest canvi global és el canvi climàtic caracteritzat per un augment en el nombre i la durada dels períodes de sequera. L'esperat creixement poblacional és un altre factor rellevant que implicarà una major pressió sobre els processos naturals. Aquest augment de població, produirà un increment en la demanda i en la competència per l'aigua tant en els usos domèstics, industrials, agrícoles com municipals. Els efectes del canvi global en els recursos hídrics són profunds i s'han d'explorar en detall, especialment en els països en vies de desenvolupament, ja que és on les projeccions dels impactes deguts al canvi global estan associades a incerteses majors.

A l'Àfrica, s'estima que el 75 % de la població fa servir l'aigua subterrània com la principal font d'aigua potable, especialment en les àrees rurals que depenen de pous i pous excavats de baix cost. És un recurs important per al creixement econòmic, la producció d'aliments, la seguretat de l'aigua potable i els ecosistemes. Malgrat això, la qualitat de les aigües subterrànies a l'Àfrica es veu obstaculitzada negativament per les fonts de contaminació antròpica i les activitats que limiten els recursos hídrics disponibles. Tot i la importància d'aquest recurs, les dades dels aqüífers són escasses i l'estat actual del coneixement és baix, constituint una sèrie de limitacions per al desenvolupament sostenible dels recursos subterranis. Per tant, cal trobar noves eines i enfocaments per comprendre aquests sistemes amb manca de dades i poc coneguts, especialment a les zones costaneres d'Àfrica on les amenaces són encara més rellevants. En aquest context, on els sistemes d'aigua subterrània d'Àfrica són sistemes socio-ecològics crítics i poc coneguts, neix el projecte Gro for Good, les sigles signifiquen "aigua subterrània per al creixement i el desenvolupament", fundat per UPGro (http: / /upgro.org/). L'objectiu principal d'aquest projecte interdisciplinari és donar suport a la ciència i la governança de la gestió dels riscos de les aigües subterrànies per al creixement i el desenvolupament a l'Àfrica per tal de beneficiar la població més pobra. Com a part d'aquest projecte, l'objectiu principal d'aquesta tesi és desenvolupar, combinar i integrar diferents tipus d'eines hidrogeològiques, episodis climàtics i variables socials, per tal d'entendre més bé els efectes del canvi global a l'Àfrica

subsahariana. Per fer-ho, l'aqüífer costaner de Kwale (Kenya) s'ha pres com a referència, ja que és un exemple on les comunitats locals comparteixen els recursos d'aigua subterrània juntament amb noves activitats com la mineria, l'agricultura i el turisme, les quals també depenen d'aquest recurs. L'objectiu final és entendre els riscos i impactes en aquest context per tal de millorar la gestió dels recursos hídrics en benefici dels més pobres. L'àrea d'estudi d'aquesta tesi està ubicada en una àrea rural a la plana costanera del comtat de Kwale, al sud de Mombasa i adjacent al nord de Tanzània. L'àrea es caracteritza per un patró de precipitació bimodal (mitjana de 1200 mm / any) sotmesa a una gran variabilitat climàtica. Entre abril i juny tenen lloc generalment les pluges prolongades, i entre octubre i desembre, és el període de pluges curtes. La major part de l'àrea es basa en l'agricultura local, però des de 2012, s'han establert al comtat de Kwale dues noves i importants activitats econòmiques que depenen de l'aigua. Una és la realitzada per *Kwale International Sugarcane Company Limited* (KISCOL), una empresa que ha estat habilitant progressivament 5500 ha de canya de sucre mitjançant reg per degoteig. L'altra activitat econòmica és l'empresa minera més gran del país: *Kwale Mineral Sands Project* el operat per Base Titanium Ltd. A més, l'àrea d'estudi té una indústria de turisme costaner establert de fa anys.

L'aqüífer s'ha caracteritzat mitjançant la integració de llargs transsectes geofísics realitzats per l'equip de Kenya, dades hidroquímiques i isotòpiques, i dades sobre el nivell de l'aigua subterrània. A més, s'han caracteritzat els principals problemes de qualitat de les aigües subterrànies, un d'ells, la contaminació per bacteris fecals (*E. coli*). Per avaluar els principals impulsors d'aquest tipus de contaminació, s'han analitzat estadísticament diverses variables qualitatives i quantitatives com la geologia, hidrologia, geoquímica, factors de risc sanitari, tipus de pou i manteniment per a estudiar la seva correlació amb la concentració d'*E coli*. L'altre principal problema de qualitat de l'àrea, és la intrusió salina, per la qual cosa s'han desenvolupat models geoquímics per comprendre els processos geoquímics que es produeixen a l'àrea afectada per la dinàmica d'intrusió d'aigua de mar mitjançant el programari PHREEQC. A més, s'ha determinat la sostenibilitat de les aigües subterrànies sota un nou patró d'extracció per part dels usuaris de la zona. En la majoria dels països en vies de desenvolupament, aquesta informació és desconeguda, de manera que la informació directa dels usuaris i de fonts d'informació simples (entrevistes, Google Earth, Trip Advisor, mètodes analítics bàsics, etc.) ha servit per estimar l'extracció d'aigua subterrània de les principals indústries que depenen d'aquest recurs. La sostenibilitat de l'aqüífer s'ha avaluat durant la sequera produïda per l'esdeveniment de La Niña 2016/17. A més, tot aquest coneixement previ sobre el sistema hidrogeològic ha ajudat a construir un model numèric de flux d'aigua subterrània, fent servir el codi Modflow del 2010 al 2017, i així poder integrar tota la informació disponible i definir la relació entre les aigües superficials i

subterrànies. Aquest model s'ha fet servir com a eina per estudiar com la variabilitat climàtica i el futur augment del bombament d'aigua subterrània afecta l'aqüífer i així, millorar la gestió dels recursos. Els escenaris futurs de pluja s'han construït mitjançant el mètode SPI (índex de precipitació estandarditzat) aplicat a una sèrie de dades de precipitació històriques (de 1959 a 2017). El volum de bombament futur s'ha basat en el volum d'explotació actual i la futura estimació realitzada per les autoritats gestores de l'aigua de la zona. A més, s'ha definit un nou índex i aquest s'ha provat en l'àrea d'estudi per a intentar definir el risc de que una llar en concret no tingui accés a l'aigua potable (en termes de quantitat o qualitat).

L'aqüífer estudiat és un sistema de múltiples capes format per un aqüífer superficial i un profund, el qual aquest últim aflora a la part occidental de l'àrea d'estudi a les Shimba Hills a l'oest de la zona d'estudi. Les fàcies hidroquímiques i la composició isotòpica de l'aigua indiquen que hi ha una connectivitat hidràulica a través dels materials que comprenen l'aqüífer superficial i entre totes les formacions geològiques profundes que conformen l'aqüífer profund. Aquestes dues unitats aqüíferes estan separades per la presència d'un aqüitard de mitjana / baixa permeabilitat emplaçat entre els materials recents i antics. A més, l'aqüífer profund està interromput en tota l'àrea per dos paleocanals. Les línies equipotencials de l'aqüífer superficial mostren que la direcció del flux d'aigua subterrània és des de les Shimba Hills a l'oest fins a l'Oceà Índic a l'est. L'anàlisi estadístic realitzat per millorar la comprensió de la contaminació per bacteris fecals indica que les característiques constructives del pou són les variables més importants per evitar la presència de bacteris en l'aigua subterrània. A més, baixos valors d'Eh, una columna d'aigua reduïda i àrees amb infiltració ràpida, són els principals factors relacionats amb la presència de bacteris fecals. La intrusió salina és l'altre problema de qualitat a l'aqüífer. Els models de mescla geoquímica assenyalen que l'augment de la salinitat, com es va observar al 2016 durant La Niña, i la dinàmica de la intrusió d'aigua de mar tendiran a augmentar la dissolució de la calcita la qual podria induir altres riscos potencials, com ara l'augment de la creació de forats. L'efecte principal de La Niña ha sigut una reducció de la recàrrega del 69 % en comparació amb un any amb una mitjana anual de precipitació (2013), i una disminució del nivell de l'aigua subterrània en el 86 % dels pous superficials mesurats. Durant La Niña, la salinitat de l'aigua subterrània augmenta en els pous situats a prop de la costa durant la temporada de pluges en lloc de reduir-se, com passa en anys normals. Tot i que els nivells d'aigua subterrània es van recuperar després del període de sequera gràcies a la temporada de pluges de 2017, la qualitat dels pous costaners no es va recuperar.

L'estimació de les explotacions actuals ha servit de base per definir la futura extracció que juntament amb la sèrie climàtica futura (precipitació i temperatura) basada en dades

històriques, han permès estimar els efectes del canvi global mitjançant la utilització del model numèric com a eina. S'ha estimat que l'explotació futura augmentarà al voltant d'un 85 % en comparació amb el volum actual. Tot i aquest increment, l'emmagatzematge de l'aqüífer no es veu significativament afectat en els escenaris futurs analitzats, ja que només es redueix l'emmagatzematge entorn de l'1 % -2 %, depenent de les condicions climàtiques globals. Tres anys secs seguits poden induir una reducció dels nivells subterranis. Malgrat aquesta disminució dels nivells observada durant els períodes secs prolongats i l'increment de l'extracció, un període sec seguit d'un període humit condueix a una recuperació relativament ràpida del sistema en menys de 3 anys. Una altra aplicabilitat del model numèric ha estat utilitzar els resultats d'aquests escenaris futurs numèrics juntament amb dades de llars per provar el nou índex. Aquest índex avalua el risc que té una llar a quedar-se sense aigua i/o una reducció de la qualitat d'aquesta. Aquest índex ajuda a comprendre més bé l'efecte del canvi global en les llars sota un "estat transitori" en lloc d'un "estat estacionari", com ho fan la majoria dels índexs actuals. A l'àrea d'estudi, aquest índex mostra que les àrees amb més risc responen a problemes de qualitat, com és el cas d'aquelles llars situades a prop de la costa afectades per la intrusió salina.

La present tesi contribueix al coneixement hidrogeològic en un context que representa gran part d'Àfrica oriental. Metodològicament, s'han presentat diferents eines per estudiar aquests sistemes que presenten una comprensió limitada i manca de dades. Es mostra la importància d'integrar les dades hidrogeològiques dels usuaris d'una zona i la utilització de fonts alternatives d'informació (Google Earth, Trip Advisor ...) per poder avançar en el coneixement d'una àrea amb manca de dades. A més, aquesta tesi presenta com utilitzar diferents eines i tipus de dades per estudiar la sostenibilitat d'aqüífers, centrant-se en la disponibilitat d'aigües subterrànies, així com en la seva qualitat. A més, la integració de dades hidrogeològiques i socials permet comprendre millor com els canvis en un sistema d'aigua subterrània, naturals o induïts, poden afectar la disponibilitat d'aquest recurs als usuaris que depenen de l'aigua.

Contents

List of Figures

List of Tables

Chapter 1

General introduction and objectives

1.1. Global change

We live in a world where humans are having profound impacts on the global environment. Climate is warming, the populations of many species are in decline, pollution is affecting ecosystems and human health, and human societies now face new risks in terms of sea level changes, food security, and climate extremes. Global change is a term widely used to describe changes in the characteristics of inter-related climate variables in space and time, and derived changes in terrestrial processes, including human activities that affect the environment. In recent decades, a wide array of scientific research has been carried out to better understand how water resources might respond to global change (Green et al., 2011).

One of the main drivers of this global change is the climate change. Most scenarios predict that climate change increase mean global temperature, affect mean precipitation, increase extreme events and decrease the predictability of these abiotic factors (Allan and Soden, 2008; Easterling et al., 2000; Stocker et al., 2013). Other consequences are increased number and increased length of drought periods (Allan and Soden, 2008; Dai, 2011; Stocker et al., 2013), and decreased ice cover (Arnell, 1999; Barnett et al., 2005; Stocker et al., 2013). Climate change is projected to change global hydrologic behaviour (Hansen et al., 2016) altering water resource availability and distribution (Bin Hu et al., 2019). All these effects will be felt by humans mainly through its impacts on water resources globally, including groundwater resources and water-related disasters such as floods and droughts. Direct impacts of climate change on natural processes (recharge, groundwater discharge, storage and quality) may be exacerbated by the human response to these impacts, such as increased groundwater abstraction due to extended and more frequent droughts (UNESCO-IHP, 2015).

Another relevant driver of the global change that will imply greater pressure on natural processes and thus on water resources in the future is the expected population growth trends (UN, 2015). Population growth is a major contributor to water scarcity. Growth in populations means mounting demand and competition for water for domestic, industrial, agricultural, and municipal uses. Water is also needed for agriculture and industrial use, and for the evacuation of waste materials. The most water scarce or stressed areas are typically those with few water resources, high population densities, and high population growth rates (FAO, 2011). A growing population requires more food and so, more water is needed to produce that food. Agricultural productivity is a crucial component of global food security and, therefore, water scarcity and hunger are closely interrelated. Population growth, along with development, will double global food demand by 2050. The main concern is that people alter the properties of water as they use it, often degrading the

quality with each successive use. Waters that have been used for a variety of purposes may contain harmful constituents, including sewage, that pose threats to the environment and to the public health.

Global change effects on water resources are profound and need to be explored deeply, especially, in the developing countries (Okello et al., 2015a). Accurate knowledge of freshwater availability is indispensable for water resources management at regional or national level. In addition, in this context of global change, the coastal water resources are the most vulnerable, since coastal regions are zones occupied by dense human population; many living in rapidly growing cities and highly economically productive. However, overall projections of impacts due to global change on water resources in these countries are associated with large uncertainties (Kusangaya et al., 2014). This information has historically been very difficult to obtain because of difficulties in the aggregation of spatial information, and problems in the quantification of distributed hydrological processes (Schuol et al., 2008). Furthermore, institutional capacity to govern interactions between economic activities, water resource demands and poverty outcomes are currently constrained by insufficient knowledge and lack of effective management tools (Fulazzaky, 2014).

In this context of global change, African countries are the areas where more affection on the water resources are provided due to diverse causes. Africa is the continent which present the highest population growth rate. The current population in Africa is five times the size that had in 1950. In addition, the population expansion is set to continue, with its inhabitants doubling from 1.2 billion to 2.4 billion between 2015 and 2050, and eventually reaching 4.2 billion by 2100 (www.forbes.com). Moreover, the African coastal regions will be the areas that will experience the highest rates of population growth in the coming decades (Lichter et al., 2011). Furthermore, this population growth is companied by continent industrialization. Much of this new economic activity in African countries is based on tourism, mainly in coastal areas (World Tourism Organization, 2013) and extractive industries, such as oil, mining and intensive harvesting of maize, rice and sugar, among others. In many African countries, coastal areas provide the main tourism resource, with the greatest concentration of tourism investment and facilities. As a result of rapid population growth and increased industrial activity, water demand in Africa is projected to more than double by the end of the 21st century (Wada et al., 2010), which may compromise the future livelihoods and living standards of millions of people. Global climate change is expected to exacerbate this issue, as it will bring more extreme climate conditions, such as droughts (Carvalho Resende et al., 2018). African nations are the most vulnerable

to the effects of climate change due to the slow pace of economic development and inadequate institutional capacity (Ongoma and Onyango, 2014).

In Africa, groundwater is the major source of drinking water and its use for irrigation is forecasted to increase substantially to combat growing food insecurity (MacDonald et al., 2012). An estimated 75 % of Africans use groundwater as their main source of drinking water (UNEP, 2011), particularly in rural areas that rely on low-cost dug wells and boreholes. It is an important resource for economic growth, food production, drinking water security and ecosystem services. The total groundwater storage estimated in Africa is 0.66 million km^3 (0.36–1.75 million km^3). However, not all of this groundwater storage is available for abstraction (MacDonald et al., 2012). In this context of global change, groundwater plays an important role in society's adaptation to climate change and variability, in particular because it is more resilient to the effects of climate change than surface water (Green et al., 2011; Taylor et al., 2013; Treidel et al., 2011; Van der Gun, 2012). Groundwater's unique buffer capacity provides a major strength to reduce the risk of temporary water shortage and to create conditions for survival in areas where global change is expected to cause water stress (Falkenmark, 2013).

Groundwater quality in Africa is increasingly being hampered negatively by anthropogenic pollution sources and activities. Contaminating sources such as human settlement developments (demographic dynamics, ignorance, improper watershed and waste management, advanced agricultural production and industrial activities) are the major threat that compromise groundwater quality and quantity (Oke and Fourie, 2017). It must be present that poor quality of water affects the plant growth and human health causing diseases like diarrhoea, cholera among others. Official estimates suggest that in Africa, 50 % of the people lack access to water free from microbial contamination (Bain et al., 2014).

In order to maintain the quality and quantity of water supply and irrigation water in this continent, it is essential doing a well management of groundwater, which has become the major source of water supply for domestic, industrial and agricultural sectors of many African countries (UNEP, 2011) as cited before. However, data of groundwater systems are sparse and the current state of knowledge is low and this is a serious limitation for the sustainable development of the groundwater resources (Gaye and Tindimugaya, 2018). This lack of information has hampered groundwater development and protection (Oke and Fourie, 2017), i.e. 5 of the 8 large aquifer system considered as over-exploited are located in Africa (Richey et al., 2015a, 2015b). Therefore, spatially explicit information on groundwater in this continent, mainly related to Africa's coastal aquifers (Steyl and Dennis, 2010), is required to characterize this resource in ways that can usefully let to develop

strategies to adapt to growing water demand associated not only with population growth but also climate change. Improved management of coastal groundwater resource requires the acquisition of suitable groundwater inventory information and how to disseminate the information for the benefit of coastal communities (Oiro and Comte, 2019).

1.2. Motivation and objectives

In this context, where Africa's groundwater systems are a critical and poorly understood socio-ecological system born the project Gro for Good: Groundwater Risk for Growth and Development" founded by the UPGro (http://upgro.org/). This interdisciplinary project has the main idea that groundwater is essential for economic growth and can contribute to human development if resources are used sustainably to benefit the poor. However, competing groundwater use (commercial, community, ecosystem) requires new tools to understand risks from natural and human-induced changes. Therefore, the aim of this project is to support interdisciplinary science and governance of managing groundwater risks for growth and development in Africa: (I) a new Groundwater Risk Management Tool to support government regulation and management in Kenya; (II) an automated, daily monitoring network for shallow groundwater levels; (III) improved theory and evidence linking groundwater governance to poverty and health dynamics and outcomes (http://upgro.org/consortium/gro-for-good/). This thesis is carried out as part of Gro for Good project.

The main objective of the thesis focuses on developing a combination and integration of different types of hydrogeological tools, climatic episodes, and social variables, in order to better understand the effects of global change on sub-Saharan Africa taking as a reference the coastal aquifer system of Kwale (Kenya).The final goal is to understand the risks and impacts on this context to improve water resources management in benefit of the poorest.

To accomplish this broad objective, specific goals are identified:

- To define the hydrodynamics of the studied aquifer system, which has a geological structure that is representative of an important portion of the East Coast of Africa.
- To study the quality issues of the aquifer system with special effort onto faecal bacteria pollution drivers, the main pollution problem in many developing countries.
- To assess the sustainability of the system including the increment of groundwater demand caused by the diverse water-reliant users in the study area.

- To evaluate the effects of the climate change in the aquifer system, taking as a reference La Niña 2016/2017, as example of an extreme climatic event.
- To develop a numerical groundwater flow model, as a tool to study the vulnerability of the aquifer system to global change by:
    - Integrating all the data available in the study area including the relation between surface and groundwater.
    - Manage the future global change basing on the future climate variability and increase of abstraction rate.
- To create an index based on the groundwater numerical model outputs and household data to understand better the effects of the global change on the communities.

1.3. Study area

The 660 km^2 study site of this thesis is located in a rural area on the coastal plain of Kwale County, south of Mombasa and adjacent to northern Tanzania (Fig. 1.1). The physiography of the region is divided into three units: The Coast Plain at an elevation generally below 30 m a.s.l.; the Foot Plateau which has an elevation ranging from 60 to 135 m a.s.l., and the Coastal Range formed by the Shimba Hills with elevation ranging generally from 150 to 455 m a.s.l (Buckley, 1981) (Fig. 1.1). The area slopes toward the sea.

The area is characterized by a bimodal rainfall pattern and experiences considerable climate variability (Mumma et al., 2011). Between April and June occurs generally the long rains and between October and December the short rains period (CWSB, 2013). In the coastal area, the precipitation range is between 900 and 1500 mm/yr and the average temperature is about 26.5 °C. Inland, west of the Shimba Hills, the precipitation ranges from 500 to 600 mm/yr and the temperature is about 26.6 °C (County Government of Kwale, 2013).

The county, which has one of the highest poverty rates in Kenya, has a population around 720.000 (GoK, 2013), most of whom reside in rural areas (82 %) (CWSB, 2013a; Foster and Hope, 2016), concentrated manly along the coast. Only 65.8 % of Kwale's population has access to improved water in households in 2009 and 49 % to improved sanitation (Commission on Revenue Allocation, 2013).

The population in the study area live in small scattered communities and extensive stockbreeding. The coastal areas host the urban communities such as Ukunda, Msambweni and Diani. Population decreases inlandwards. The major portion of the area is based on local agriculture, but since 2012, two new and major water-reliant economic activities have

been established in Kwale County, increasing the pace of environmental, economic, social and political change in the area. One is carried out by the Kwale International Sugarcane Company Limited (KISCOL), which has been progressively habilitating 5500 ha of drip-irrigated sugarcane. The other important recent economic activity is the country's largest mining operation: the Kwale Mineral Sands Project operated by Base Titanium Ltd. Furthermore, the study area has a long-established coastal tourism industry in the Diani zone, with approximately 109 hotels (Fig. 1.1). This new water reliant industries, tourism sector and communities, schools and health centres are supplied by groundwater, exploiting the aquifer system of the study area by deep boreholes, shallow wells and handpumps.

The study area is divided into 4 zones (Fig.1.1) that represent the areas where each economic activity takes place. Zone 1 covers the area where the sugar fields irrigated with groundwater from in-situ boreholes are located; Zone 2 includes the mine and its well field; Zone 3 is the area where the sugar fields are irrigated with surface water from the Mtawa River but not from boreholes; and Zone 4 includes the area where most of the hotels are located.

Thus, Kwale County captures the complex reality of Africa's groundwater science and policy challenges at a unique historical moment prior to a generation of social, environmental and economic change (http://upgro.org/).

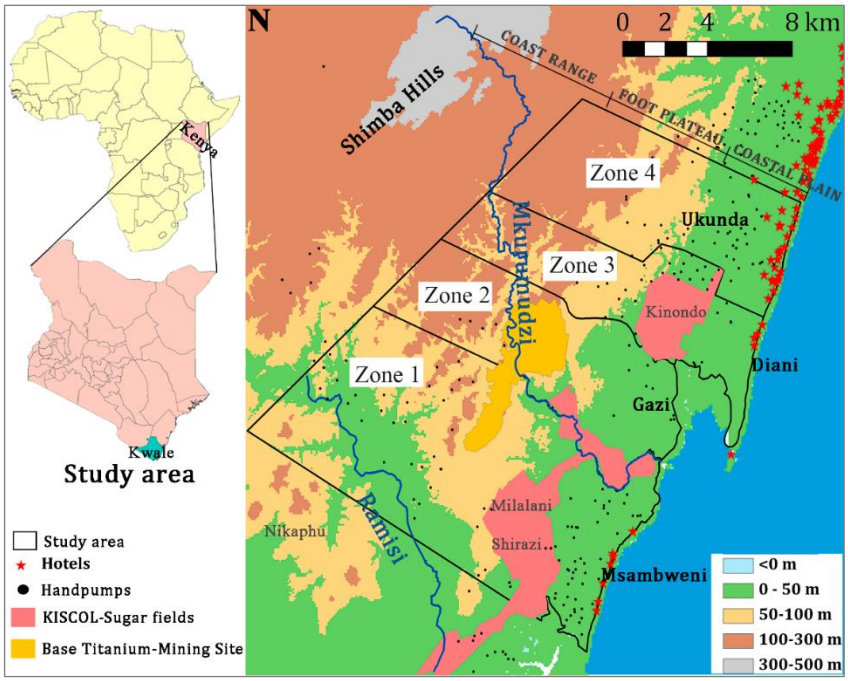

Figure 1.1. Location of the study area in Kwale county (Africa). The orange area is the Base Titanium mining site, the red one corresponds to the KISCOL sugar fields, the star are the hotels and the black dots refer to the community handpumps. The study area is divided into the four zones shown, which have been set to help the reader throughout this manuscript.

1.4. Thesis outline

The resulting document is structured in seven chapters. Even though each of these chapter is focused on answering specific question, all of them are intended to understand the groundwater system located in Kwale (Kenya) under global change scenarios.

The introduction to the problem is presented in Chapter 1. Chapter 2 characterizes the coastal aquifer system by the integration of kilometric geophysical profiles, hydrochemistry, hydrochemistry, environmental isotopes and groundwater levels. Once the conceptual model is defined, the last goal is to study the impacts on groundwater quality and quantity caused by the climatic event of La Niña 2016/17 that gave, as a result, an important drought in the study area.

Chapter 3, focus on fecal bacteria pollution, the main quality problem detected in the study area. The aim of this chapter is to discern what are the most significant sanitary, hydrogeological, geochemical and physical variables influencing the presence *Escherichia coli* (*E. coli*) in groundwater by means of statistical multivariate analyses. The statistical

analyses carried out have been Principal Component Analysis and generalized mixed models with Poisson error.

In Chapter 4, the conceptual model defined in Chapter 2 is used to study the sustainability of the aquifer system under the new abstraction rate by the water-reliant industries settled in the study area. The goal is to explore how irrigated agriculture, mining and tourism dependent on a multi-layered groundwater system could affect the groundwater system by analyzing the sustainability of the new abstraction regimes before, during and after La Niña event 2016/17. As part of the approach, induced changes in seawater intrusion are also studied. Geochemical models to understand the geochemical processes occurring in the area affected by seawater intrusion dynamics are developed using PHREEQC software.

Chapter 5 presents the regional numerical groundwater flow model built based on the conceptual model presented in Chapter 2 and the abstraction data presented in Chapter 3. The calibrated numerical flow model has been used as a tool to run different future scenarios. The final goal of this chapter is to analyze the effect of climate change and increased groundwater demand in the coastal studied aquifer in Kwale County. The groundwater flow model has been constructed using Modflow-2005 to simulate the period 2010 to 2017, and eight potential future model scenarios developed that cover six hypothetical years under different conditions (very dry, wet, etc.). Future rainfall scenarios have been constructed based on a long historical data series (from 1959 to 2017) and the Standardized Precipitation Index. Future abstraction has been based on current abstraction and future estimations made by to Water Resources Authority water allocations.

In Chapter 6 a new methodology is presented to assess the risk of a household to run out without water due to lack of water and/or low water quality threshold. This method combines household field data with groundwater numerical model outputs. This methodology is applied in the study area to evaluate the current situation as well as future conditions according to developed scenarios.

Finally, Chapter 7 presents a summary of the conclusions obtained during the performed research.

The Appendix includes all the extra information used to understand the different results obtained in the previous chapters.

Chapter 2

Conceptual model and La Niña effects

Ferrer, N., Folch, A., Lane, M., Olago, D., Odida, J., Custodio, E., 2019. Groundwater hydrodynamics of an Eastern Africa coastal aquifer, including La Niña 2016–17 drought. Sci. Total Environ. 661, 575–597.

2.1. Introduction

El Niño Southern Oscillation (ENSO) is a quasi-periodic invasion of warm sea surface waters into the central and eastern tropical Pacific Ocean, returning at least once in a ten-year period (Baudoin et al., 2017). Studies have shown correlations between ENSO conditions and monthly and seasonal rainfall patterns over East Africa (Mutemi, 2003). Oscillations in sea-surface temperatures in the Indian Ocean (known as the Indian Ocean Dipole) have also been shown to influence rainfall in the region (Behera et al., 2005; Ogwang et al., 2015). ENSO and IOD conditions triggered a severe drought in East Africa in 2016-17 (Uhe et al., 2018, 2017). The most affected areas include most of Somalia, south-eastern Ethiopia, north-eastern and coastal Kenya, and northern Uganda. Somalia and parts of Kenya faced severe famine. In South Sudan and Somalia, drought conditions made it harder to cultivate land and hampered humanitarian access, and in consequence, the drought led to the displacement of millions of people. In parts of Somalia and coastal Kenya, 70 % to 100 % crop failure was registered (Mpelasoka et al., 2017).

In Kenya, the first signals of an impending drought were experienced in October-December 2016 (Uhe et al., 2017). Kenya usually receives the majority of its rainfall during two periods: the 'long rains' during March, April and May (MAM) and the 'short rains' during October, November and December (OND) (Uhe et al., 2017). In 2016, the International Federation of Red Cross and the Red Crescent Societies (IFRC) noted that the south-eastern coast and north-western parts of Kenya received poor OND short rains, leading to an extension of the dry lean season that usually lasts from August to October. The south-east area had also suffered from poor MAM rains, intensifying the drought episode. The most affected Kenyan counties classified as "alarm stage" by the National Drought Management Authority were Turkana and Marsabit on the north-west and Kwale, Kilifi, Mombasa and Lamu on the south-east coast. The IFRC noted that the last drought reduced agricultural production and grazing lands for pastoralist communities and that the failed rains lead to decreased power and water supply to some of Kenya's communities (Uhe et al., 2017).

Due to the higher resilience of groundwater availability to droughts compared with surface water, groundwater resources are of particular importance during dry periods. However, aquifer water budgets and groundwater hydrodynamics are also affected by reduced rainfall. For this reason, it is important to characterize aquifer systems and understand their limitations in the face of future drought episodes (MacDonald et al., 2009). There are many African aquifer systems that have not yet been fully characterized, despite the importance of groundwater for growth and development (Comte et al., 2016). Poorly understood groundwater resources could be being used below their actual capacity, or be at risk of

over-exploitation. Further research is required to underpin sustainable use and development of Africa's groundwater resources.

From a global comparison of scenario-based projections of population growth in low-elevation coastal zones, African coastal regions appear set to experience the highest rates of population growth and urbanization in the coming decades (Neumann et al., 2015), underlining the importance of groundwater resource management to meet population needs. Groundwater availability along the African coast was briefly reported in Steyl and Dennis, (2010) but only some of the most populated areas have been studied in more detail. The South-east Tanzania Quaternary aquifer, which is the main water resource for the populated city of Dar es Salaam and its adjacent suburbs where around 80 % of Tanzanian industry is located (Mtoni et al., 2013; Sappa et al., 2015; Van Camp et al., 2013), and the recently discovered regional Neogene aquifer (SE of Dar es Salaam) (Bakari et al., 2012), were studied in recent years. Of the Sub-Saharan African countries, South Africa has also had a number of hydrogeological investigations to define the country's aquifers (Day, 1993; Demlie and Titus, 2015; Kelbe et al., 2016; Ndlovu and Demlie, 2016). In Sub-Saharan Africa's low-income countries or regions, there have been very few additional studies. In Kenya, for example, coastal aquifers have been described by defining the current state of seawater intrusion (Obura, 2001; Okello et al., 2015a) and Ezekiel et al., (2016) provide an assessment of the vulnerability of the Mombasa coastal aquifer. In many areas of Africa, the lack of groundwater monitoring and/or geological studies makes adequate aquifer characterization difficult.

ENSO and IOD-related droughts must be considered as one of several threats to groundwater availability in coastal Africa in coming decades. In order to improve water resources management and planning, this study provides evidence of the effect of the drought which began in 2016 on the groundwater systems of the East African coast. The groundwater system located in Kwale has a geological structure that is representative of an important portion of the East Coast of Africa (Rais-Assa, 1988) and was thus chosen as a paradigmatic example for study aimed at understanding the impact of severe drought on a coastal aquifer system in a rural area of relatively low population. This contrasts the recent studies carried out in Dar es Salaam and South Africa which focused on aquifers in highly populated urbanized zones. This chapter has two specific objectives: 1) Define the hydrodynamics of the Kwale hydrogeological system, and 2) Show the effects of La Niña 2016/17 drought on the groundwater system.

This chapter includes the results of a geophysical survey conducted to define the aquifer geometry forming the basis of the conceptual model. Local meteorological and soil data,

hydrochemical field surveys and groundwater level were used to describe aquifer recharge, groundwater flow direction, connectivity between aquifer levels and prevalence of pollution. The effects of La Niña on the hydrogeological system were assessed by comparing data from before and during the drought episode.

2.2. Study area

The study area is defined in Section 1.3 (Fig. 1.1).

As already said, the area is characterized by a bimodal rainfall pattern and experiences considerable climate variability (Mumma et al., 2011). From May 2016 to early 2017, the study area experienced unusually dry conditions. Local weather data suggest that this period represents the most extreme drought since 1974 in this area: The precipitation in the rain gauge at Kwale Agricultural Department Station (KMD 9439001) in Kwale town in the north-west of the study area was 636 mm/yr in 2016. Rainfall in the same station in 2013, 2014 and 2015 was 1286, 1604 and 1345 mm/yr respectively. In recent years, from 2012 to 2017, the average rainfall depth is around 1145 mm. 2013 (1286 mm) and 2017 (1265mm) were close to the average whilst 2012 and 2016 were both well below the average, and 2014 and 2015 were well above. During 2016, some community wells dried up completely.

2.3. Geology

The main rocks in the area range from the Carboniferous to Plio-Pleistocene in age and overlie the metamorphic rocks of the Mozambiquan system (Caswell, 1953; Rais-Assa, 1988). Much of the geology to the east is covered by the Magarini and Kilindini sands. The Rais-Assa (1988) nomenclature is adopted to describe the stratigraphy of the sedimentary rocks, which comprise six formations. The oldest of these formations is the Taru Fm. (Upper Carboniferous to Middle Permian) which is made up of tillite that suggests a periglacial environment, overlain by arkosic sandstones and arkose and conglomerates that point to a fluviatile environment. The Maji ya Chumvi Fm. (Mid-Permian to Mid-Triassic) overlies conformably on top of the Taru Formation and comprises sandstones and Carboniferous shales, sandy shales with fossil fish fauna, and argillaceous sandstones that reflect a lacustrine deposition palaeoenvironment (Rais-Assa, 1988) and a period of fluctuating climate (wet to dry) with possible evaporate deposits (Caswell, 1953). The Mariakani Fm. (Middle to Upper Triassic) covers conformably the Maji ya Chumvi Fm. (Rais-Assa, 1988); it has mottled and flaggy sandstones as well as silty shales and shale lenses that represent deltaic facies (Caswell, 1953; Rais-Assa, 1988). Caswell (1953) describes them as fine-

grained, flaggy sandstones and silty shales. Two sets of joints are often present, trending ENE-WSW and NW-SE, while a third set, which is less prominent, trends N-S (Caswell, 1953). The joints are regular, clean-cut and closely spaced. The Matolani Fm. (Upper Triassic to the start of Lower Jurassic) is dominated by feldspathic sandstones (Cannon et al., 1981; Caswell, 1953; Rais-Assa, 1988), corresponding to a deltaic facies, and ends with a major angular unconformity (Rais-Assa, 1988). None of these formations outcrop in the study area. Based on drilled boreholes they have low groundwater potential and thus they can be considered the substratum. The Taru Fm. and the others up to the Mazeras Fm. have a regional dip of 5-10° to the east-south-east (Caswell, 1953).

The formations that outcrop in the study area are the Mazeras Fm. (Lower Jurassic to the start of Middle Jurassic), the Kambe Fm. (Start of Middle Jurassic to middle Upper Jurassic), and the Mtomkuu Fm. (from the Middle of the Upper Jurassic to the Cretaceous) (Rais-Assa, 1988). These are overlain, following a long hiatus, by Cenozoic rocks and unconsolidated materials that include the Magarini sands (Upper Pliocene) dunes, coral reefs (Lower to Middle Pleistocene), the lagoonal Kilindini sands (Upper Pleistocene) and younger mostly sandy deposits (Caswell, 1953; Rais-Assa, 1988). The Mazeras Fm. is divided into two, the Lower and Upper Mazeras (Rais-Assa, 1988). The Lower Mazeras has coarse sandstones with silicified wood horizons, while the Upper Mazeras (roughly constrained above the 272 m contour line) comprises quartz-feldspathic sandstones and grits (Shimba grits) at the top (Caswell, 1953, 1956; Cannon et al., 1981; Rais-Assa, 1988). The Mazeras rocks have been estimated to attain a total thickness of at least 305 m (Caswell, 1953) and are ascribed to a deltaic to aeolian facies (Rais-Assa, 1988). The Kambe Fm., a marine facies, has conglomerates and limestones in the lower part and shales, sandstones and limestones in the upper parts (Rais-Assa, 1988), and sits above on a major angular erosional discordance that separates it from the Shimba grits. (Caswell, 1953; Rais-Assa, 1988). The Mtomkuu Fm. rests upon a major angular unconformity with the Upper Kambe Fm., and has silty clays in the lower part and shales, sandstones and limestones in the upper part, representing a transgressive marine facies (Rais-Assa, 1988). These three formations and the overlying Cenozoic sediments constitute the medium to high potential aquifers in the study area.

Related geological and geophysical work that was undertaken as part of this project has revealed that there are two palaeochannels in the study area, located in zone 1 and 4 (Fig. 2.1) (Olago D., Odida J. and Lane M., pers. comm.). They were formed by the erosion of Kambe Fm. and Mtomkuu Fm. during the last low sea stand and subsequent infilling by fluviatile sediments with very likely thin impermeable derived layers of e.g. fine consolidated fluvial sands, clays and indurated bioclastic sands. Clusters of high capacity boreholes lie within these palaeochannels at Milalani (zone 1) and Kinondo (zone 4).

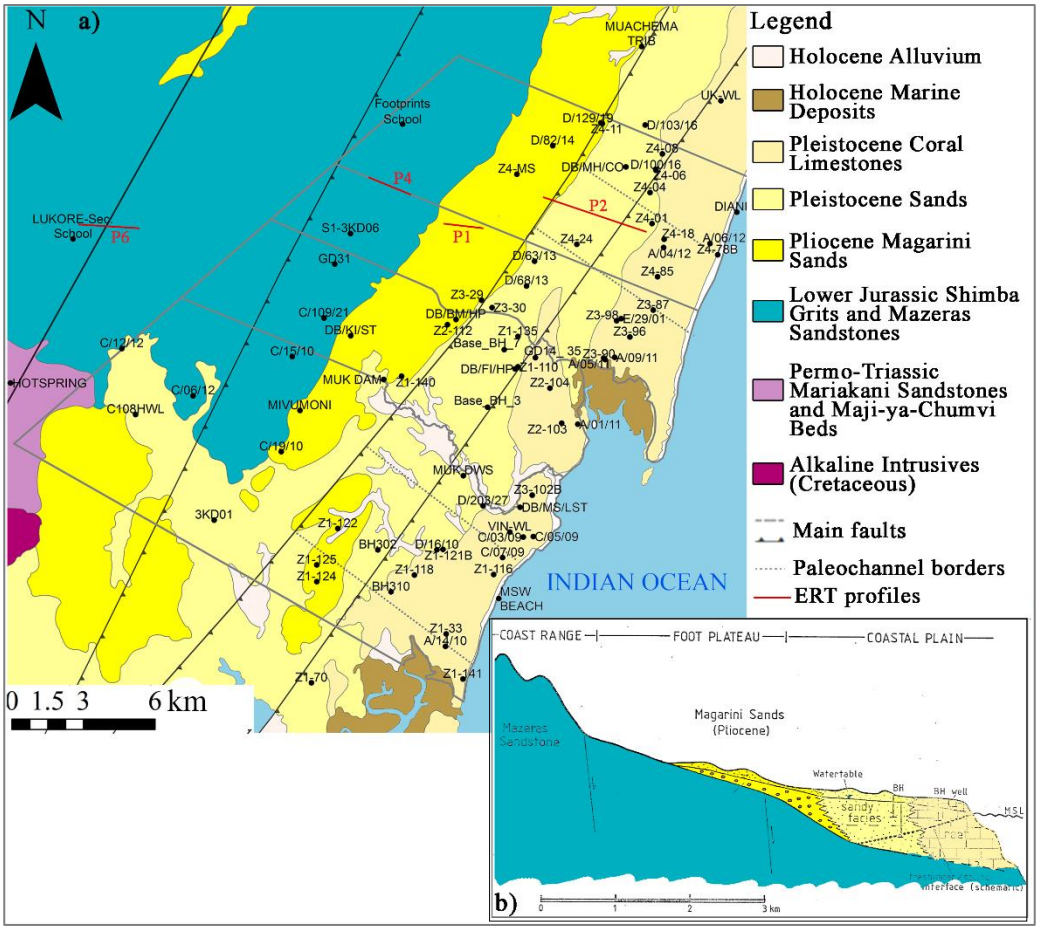

Figure 2.1 Geological map with the main faults, the main paleochannels (grey dotted lines). Geologically surveyed by D.O. Olago, J. Odida, and M. Lane (2018), ©University of Nairobi. The sampled points in June 2016 and the general cross-section of the study area (modified from Buckley, 1981). In red the ERT profiles.

2.4. Methodology

In order to construct the conceptual model and characterize the hydrogeological system during La Niña event in 2016, different surveys were carried out in the study area.

Water samples were taken from wells and boreholes at different depths and in different geological formations to characterize all aquifer systems in the study area. Because of the complexity of the available sampling points, the efforts were focused on identifying distinct hydrogeological interactions and on providing a complete description of groundwater dynamics.

2.4.1. Geophysical surveys

An ERT (electro-resistivity tomography) study was conducted between December 2015 and June 2016 to define the aquifer geometry in the study area. This was supported by geological field studies. A 2-D electrical imaging/tomography survey equipment was used. The field set of the tomography system used in this research included an ABEM SAS 1000 Terrameter, LUND ES464 switchbox (an electronic switching unit), 4 multi-core cables each with 21 current take out points at constant spacing of 10 metres interval, battery, communications cables, electrode jumpers, electrodes, laptop, and data transfer cable. The profile length was 800 m, comprising four multi-core cables. Roll-along technique was used during data acquisition. After completing the sequence of measurements, the cable was moved past one end of the line by two cables. The investigated depth was 149 m bgl (meters below ground level). This set-up provides a 2-dimensional inversion of the resistivity measurements along a profile line. The data was acquired in E-W orientation and NNE-SSW orientation, parallel to the coastline. ERT data was analysed using RES2DINV inversion software.

2.4.2. Recharge

In order to estimate the effect of La Niña drought on the seasonal and annual recharge patterns, groundwater recharge was estimated for the period 2012 to 2017. Groundwater recharge was calculated for the main land cover of the study area, with 65 % of it defined as open: broadleaved deciduous trees with closed to open shrubs, based on Africover database (DiGregorio, 2002).

Rainfall data was obtained from Kwale Agricultural Department rainfall station manned by Kenya Meteorological Department (KMD) located in Kwale Town. The other meteorological parameters such as temperature, wind speed, evaporation and humidity were obtained from the SWAT Global Weather (Soil and Water Assessment Tool), NASA, Kenya Meteorological Department and TAMHO (Gathenya, Thomas, pers.com). ETP was calculated by Hargreaves equation (Hargreaves and Samani, 1982). The recharge rate was estimated based on the soil mass balance by considering soil composition, root deep and threshold runoff. Soil composition was obtained from Kensoter ver.2 database (Kempen, 2007). This database consists of a soil inventory, which includes the geographical distribution of the soil units, the percentage of clay, silt and sand characteristic of each soil type, and their specific TAWC (Total Available Water Content) value. The root depth of the land cover was obtained from the Food and Agricultural Organization (FAO) (www.fao.org). Finally, the

threshold runoff was calculated for each land use by applying data from theoretical tables (Miller, 1994).

2.4.3. Background monitoring

An aquifer monitoring program was developed to measure groundwater level and physicochemical parameters (temperature, electrical conductivity (EC) and pH) from January 2014 until present. A total of 43 points in the Magarini sands, Kilindini sands and Pleistocene corals were monitored every two weeks (from 4 m bgl to 27 m bgl).

This data was complemented with information from Base Titanium's monitoring network composed of piezometers and community wells (from 5 m bgl to 107 m bgl) spread mainly around the mining site starting in March 2007 (field water quality) and August 2011 (water level data).

2.4.4. Hydrochemical and isotopic sampling surveys

Sampling campaigns were carried out in the study area in March (end of dry season) and June (end of wet season) to enable assessment of hydrochemical conditions in different seasons of a wet year (2014) and in La Niña-affected year (2016). During the field campaigns carried out in 2014, 32 and 34 wells/boreholes up to 30 m deep were sampled in the dry (March) and wet (June) season respectively. During the field survey of 2016, the number of sampling points was increased to 75 in March and 80 in June, since more samples were needed to better define the groundwater system. This included an additional sampling of wells/boreholes in the Shimba Hills and a number of deep boreholes across the study area. The 2016 surveys also included surface water samples: 2 in Ramisi River (C108HWL and 3KD01), 3 in Mkurumudzi River (S1-3KD06, MUK DAM and MUK DWS) and 1 in Mwachema River (MWACHEMA TRIB) (Fig.1). In 2016 water isotopes were also analysed in both field surveys.

Samples for hydrochemical and isotopic analysis were taken from wells used daily. For boreholes fitted with a handpump, it was ensured that at least three casing volumes of groundwater were removed before sampling. In the case of open wells, samples were taken using an electrical pump when the water column allowed. A bucket was used as a last option. The physicochemical parameters measured in situ during the 2016 sampling campaign were: temperature, pH, EC_{25} (electric conductivity at 25 ºC), DO (dissolved oxygen) and Eh measured with a YSI Professional Plus multiparameter probe with a flow cell to avoid contact with the air. pH and EC_{25} measurements are automatically temperature compensated. In 2014 the field parameters were measured with a Eutech COND 6+

conductivity meter (EC_{25} and temperature) and Eutech pH 6+ pH/ORP meter (pH and Eh). The pH was periodically calibrated against pH 7.00 and 4.04 references before and during the field surveys. EC_{25} was periodically calibrated against a 1413 µS/cm reference solution before and during the field surveys. All probes were washed in distilled water before and after each measurement and the probes were kept with distilled water all time. In addition, in 2016, ammonium concentration (mg/L NH_4-N and mg/L NH_4^+) was measured in situ by a field colorimeter test with a colour card comparator manufactured by Merck Millipore. Alkalinity concentration (carbonate, CO_3^{2-} and bicarbonate, HCO_3^-) was also measured in situ, after filtering the sample with 0.2 µm filters, by field titration using a digital titrator manufactured by Merck Millipore in the 2016 field surveys, and by field titrator manufactured by HACH in 2014 field surveys.

Samples for cation, anion and trace element analysis were filtered in the field with 0.2 µm GNWP (Millipore) nylon membrane in 15 mL polypropylene bottles, in 2016. In 2014, samples were filtered with 0.45µm filters (Sartorius) and collected in 130 mL polypropylene bottles. One membrane was used for each sampled point. After filtering, the bottles for cation and trace elements samples were acidified with 70 % pure HNO_3^- to ensure that pH < 2. Water isotopes were collected in 2 mL special crystal chromatography tubes with their respective septum cup without headspace. Total Organic Carbon (TOC) was sampled with crystal bottles (previously sterilized in a muffle furnace), filled without headspace and acidified in the field with HCl 2N. Water isotopes and TOC were analysed only in 2016 field surveys.

The samples were kept at 4 °C in a dark cool box during the field day and stored at 4 °C until they were analysed in the laboratory. The cations, trace metals and TOC collected in 2016 were analysed by the Institute of Environmental Assessment and Water Research (IDAEA) by ICP-AES, ICP-MS and by an infrared detector using the NPOC method (Shimatzu TOC-Vcsh) respectively. In the 2014 campaigns, cations were analysed by ICP-OES. Anions (campaigns in 2016) were processed by the Catalan Institute of Water Research (ICRA) using ionic chromatography. Bromide was analyzed at the Grup de Tècniques de Separació (GTS) of the Autonomous University of Barcelona by ICP-MS. In 2014 field campaigns, the laboratory used a Water Analyzer to measure anion concentrations. Water isotopes (δ^2H and $\delta^{18}O$) were measured in the Centro de Hidrogeología de la Universidad de Málaga (CEHIUMA) using Picarro equipment. The notation is expressed in terms of δ ‰ relative to the international standard V-SMOW (Vienna Standard Mean Oceanic Water) for δ^2H and $\delta^{18}O$. The precision of the samples calculated from international and internal standards systematically interspersed in the analytical batches was ±0.3 ‰ for δ^2H and ±0.05 ‰ for $\delta^{18}O$. The quality of the chemical analysis was checked by performing the ionic mass

balance. The hydrochemical composition of samples with error >10 % was not taken into account in the hydrochemical results.

2.5. Results

2.5.1. Aquifer structure based on geological and geophysical data

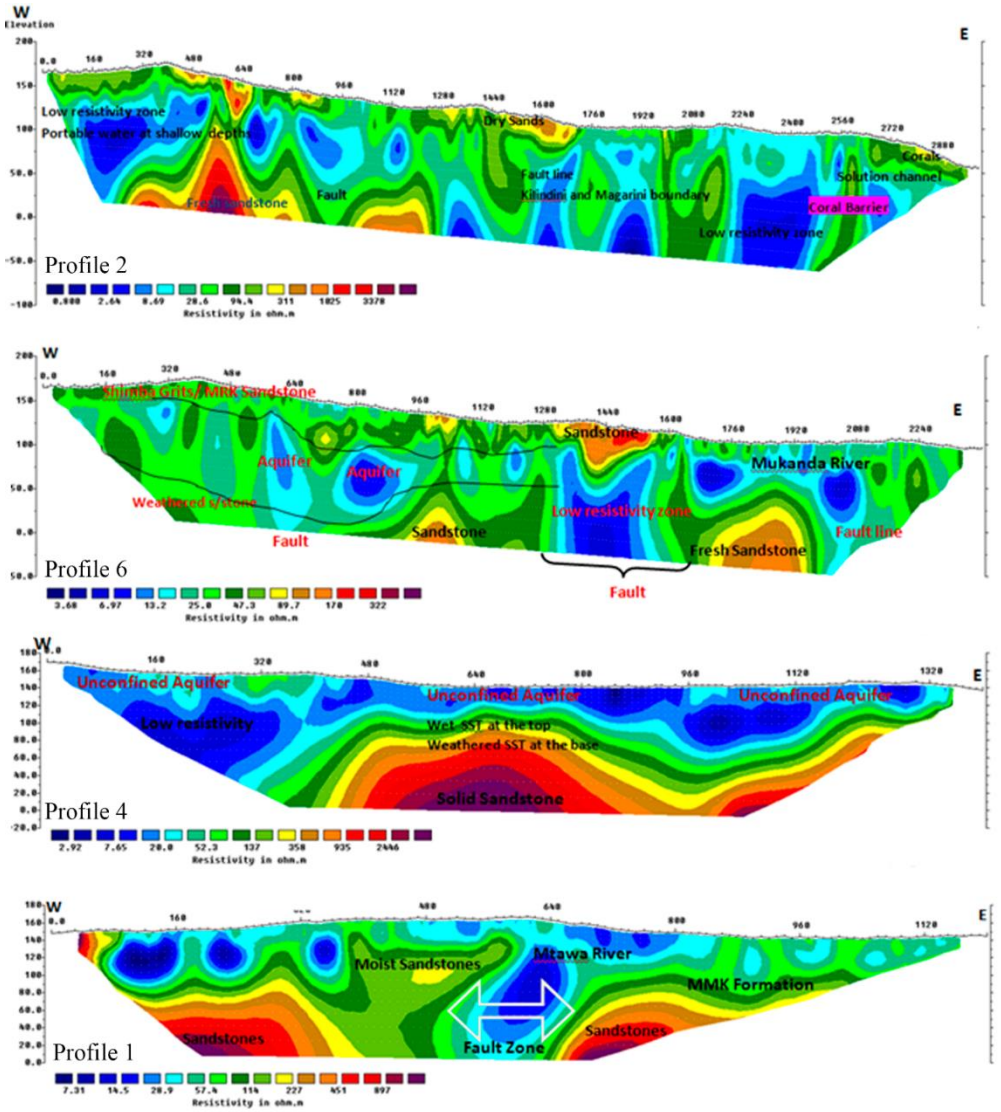

Figure 2.2. Geophysical profiles located on the study area in Figure 2.1.

The profiles, from west to east, are in sequence 6, 4, 1 and 2 (Fig. 2.2). In Profile 6 the surface geology is weathered Mazeras sandstones with some only slightly weathered patches. At depth, there are no clearly defined lithological structures and this probably reflects the spatially and vertically heterogeneous nature of these deltaic and aeolian-derived, folded and compacted sediments, with occasional aquifers. The highly weathered fracture zone(s) in the sandstones are potential aquifers, with good water quality reported at Lukore Dispensary, Lukore Secondary and Mukanda sites. Profile 4 clearly shows two aquifer layers; a shallow (up to 30 m) unconfined aquifer with generally low resistivities reflecting lenses of saline water, and a deeper aquifer with higher resistivity (50-200 Ω m). Profile 4 sub-surface topography indicates that the rocks of the Mazeras, Kambe and Mtomkuu Fm. are folded, consistent with Rais Assa's (1988) observations. While the Mazeras sandstone can easily be differentiated on the basis of its relatively high resistivity (>300 Ω m), the Kambe and Mtomkuu Fm. are geophysically indistinguishable, perhaps partly due to their relatively high water bearing capacity or their relatively small thickness. Profile 1 surficial geology consists of Magarini sands with relatively flat topography. The geophysical results indicate possible potential aquifers between 20 m and 80 m bgl. Multiple rivers were observed traversing the area. Fresh (low resistivity, 30-100 Ω·m) to saline (very low resistivity, <30 Ω·m) unconfined groundwater is indicated, depending on the locality, up to depths of ca. 30 m. A major fracture zone trending NNE-SSW with a down throw to the east is inferred (fault 3 on Figure 2.1), with a surface expression 380 m long. Profile 2 was 3000 m long. Its surface geology comprised Kilindini sands to the west and Pleistocene corals to the east. From the geophysical results, the tongue-shaped structure at the eastern end of the profile depicts a possible underground cavern from the dissolution of corals. There is a barrier that restricts movement of saline water further inland. In the subsurface and close to the present-day shoreline, corals can be inferred to a depth of about 100 m bgl.

Consequently, the outline of the hydrogeology of the area is fairly simple. The groundwater system comprises a shallow aquifer system recharged directly by rain infiltration, and a deeper aquifer that is recharged laterally from the Shimba Hills area acting as a mountain-front area.

2.5.2. Recharge

Groundwater recharge evolution according to the soil water balance is shown in Fig. 2.3. Despite the very short time series, only 5 years, there is significant variation over time. In 2014, the wettest year of the period, precipitation was 1591 mm while in 2016, during the drought event, precipitation was 636 mm, less than half of that and 13 % less than total precipitation in the second driest year.

Groundwater recharge occurs mainly during the wet season and for 97 % of the studied period (2012-2016) no recharge is observed. Fig. 2.3 shows that unless accumulated rainfall in a given rain period is greater than 104 mm, little or no recharge occurs. These observed thresholds reflect the requirement of prolonged rainfall events to generate recharge due to high rates of evapotranspiration and soil moisture deficit. Daily potential evapotranspiration is often higher than daily rainfall depth in the area. The relationship between rainfall and groundwater recharge is nonlinear. Seasonal rainfall depth is important, as is rainfall pattern across the seasons. This observation agrees with Taylor et al. (2012), which notes that intense seasonal rainfall associated with the El Niño Southern Oscillation and the Indian Ocean Dipole mode of climate variability contributes disproportionately to recharge. Indeed, infrequent recharge associated with heavy rainfall events is common in semiarid climates with retentive soils (Custodio et al., 1997).

During the wet year 2014, the main recharge periods are well differentiated: April to June (long rains) has the highest recharge with less recharge in October to December (short rains). During La Niña event, groundwater recharge was reduced during both wet seasons. During the long rains period, there was a recharge peak due to rainfall events of over 145 mm/d in April 2016. However, as stated in Uhe et al., (2018, 2017), the OND short rainfall period was particularly badly hit by La Niña event, and the results indicate no recharge during this period (Fig. 2.3).

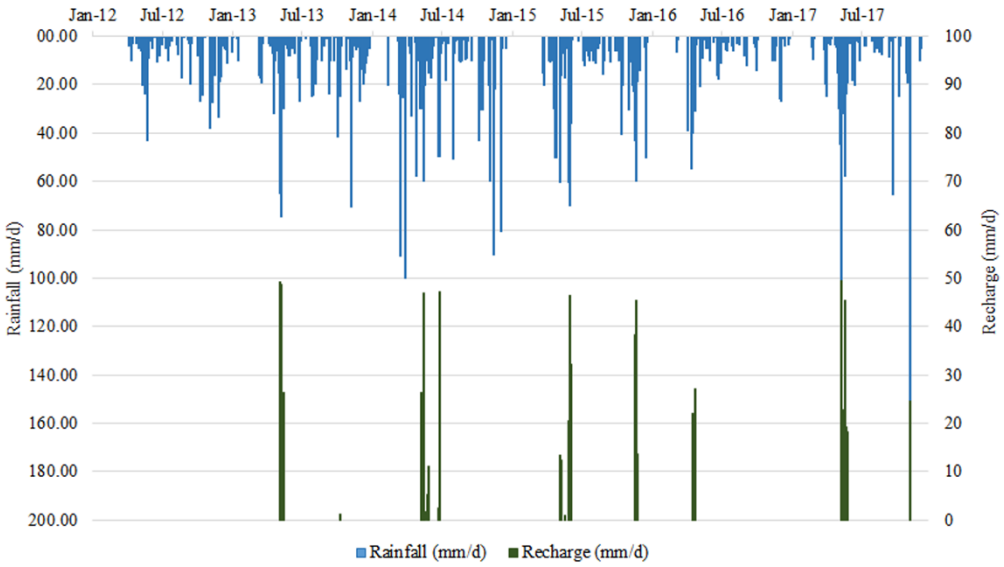

Figure 2.3. Recharge rate based on daily soil mass balance vs rainfall at Kwale Agricultural Department station (Kenya Meteorological Department) (mm/d); January 2012 to October 2017.

2.5.3. Groundwater distribution and trends

Groundwater flow in the shallow aquifer is from the upper part of the study zone to the lowest zones at the coast, discharging littoral and offshore into the sea (Fig. 2.4). The majority of discharge from both aquifers is assumed to be submarine to the Indian Ocean. There are a number of brackish groundwater emergences in the tidal zone observed along Diani coast and Msambweni Beach. In the middle part of the study area, the shallow aquifer feeds the gaining Mkurumudzi River while the surface-groundwater interaction in the Ramisi River cannot be defined with available water level data.

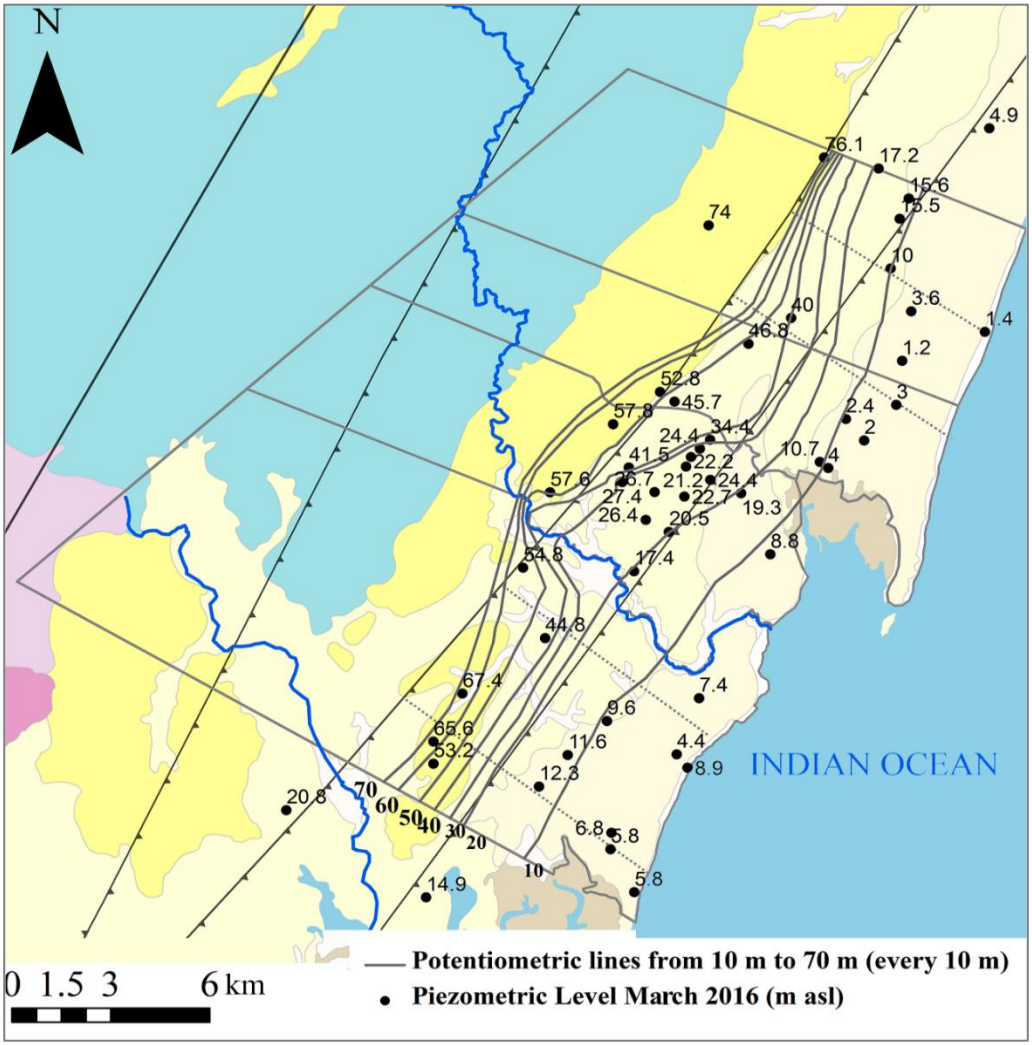

Figure 2.4. Groundwater contour map for the shallow aquifer in March 2016 after the field survey. Potentiometric lines are represented every 10 m.

The Kilindini sands constitute the main extension of the shallow aquifer in the study area. Most of the groundwater recharge in this geological formation occurs during intense rains or long rainy periods from April to June (Fig. 2.5a). The response of the water table to important rains is relatively fast, with peak water level occurring between 7 and 20 days after the main rainfall (Fig. 2.5a). Increasing groundwater level is accompanied by decreasing EC (Table 2.1).

The effect of La Niña 16/17 event on groundwater level variation in the Kilindini sands aquifer is shown in a well (GS9) located in this geological formation (Fig. 2.5a). During the low rainy periods, such as during La Niña, the descent of groundwater level continues until the next relevant rainfall event. The year 2012 was a very dry year with low OND rainfall, only slightly more than that in 2016. From January to December 2016, the groundwater level variation measured in wells located in this geological formation was between a maximum of 3.4 m and a minimum of 1.4 m (Table 2.1).

However, some wells located in the Kilindini formation in the north of the study area (points Z4-06, Z4-08, Z4-04 and Z4-01 in Fig. 2.1) show a different pattern in the response of groundwater level to rainfall (Table 2.1). These wells show lower increases in groundwater level after large rainfall events (Fig. 2.5b).

Rapid infiltration after rainfall events in the Pleistocene corals, attributed to high hydraulic diffusivity, causes recharge peaks in wells in this formation to dissipate rapidly, (Fig. 2.5a grey dots). The same process explains the sharper response of groundwater levels to rainfall compared to that seen in the unconfined Kilindini sands (Table 2.1). These observations are to be expected due to karstification of the geological formation. The reaction is not observed after all the main rainfall events due to the low frequency of measurements (every 15 days).

The deep aquifer is exploited by some community wells, KISCOL, and Base Titanium. Only Base Titanium has monitoring points not directly affected by dynamic groundwater levels due to abstraction. For this reason and because of the geological heterogeneity in the study area, the deep aquifer behaviour can be only described in the middle part of the study area. Groundwater level in deep boreholes also reacts to rainfall, as the shallow aquifer piezometers do, but there are somewhat longer lags between the start of recharge and the groundwater level maximum in the confined aquifer compared with the shallow aquifer; this time lag is 13-20 days (Table 1, Appendix A).

Water level measurements from the Base Titanium shallow piezometers show a limited effect of pumping from the deep aquifer on shallow groundwater level. This limited/nil

effect is attributed to a low permeability aquitard between the two aquifers, which was observed during the drilling of the Base Titanium boreholes. Groundwater level in the deep aquifer shows the influence of groundwater abstraction in this area, which started in 2014 (Fig. 2.6). The marked drawdown during the 2016 drought may have been enhanced by groundwater abstraction during the same period made by Base Titanium.

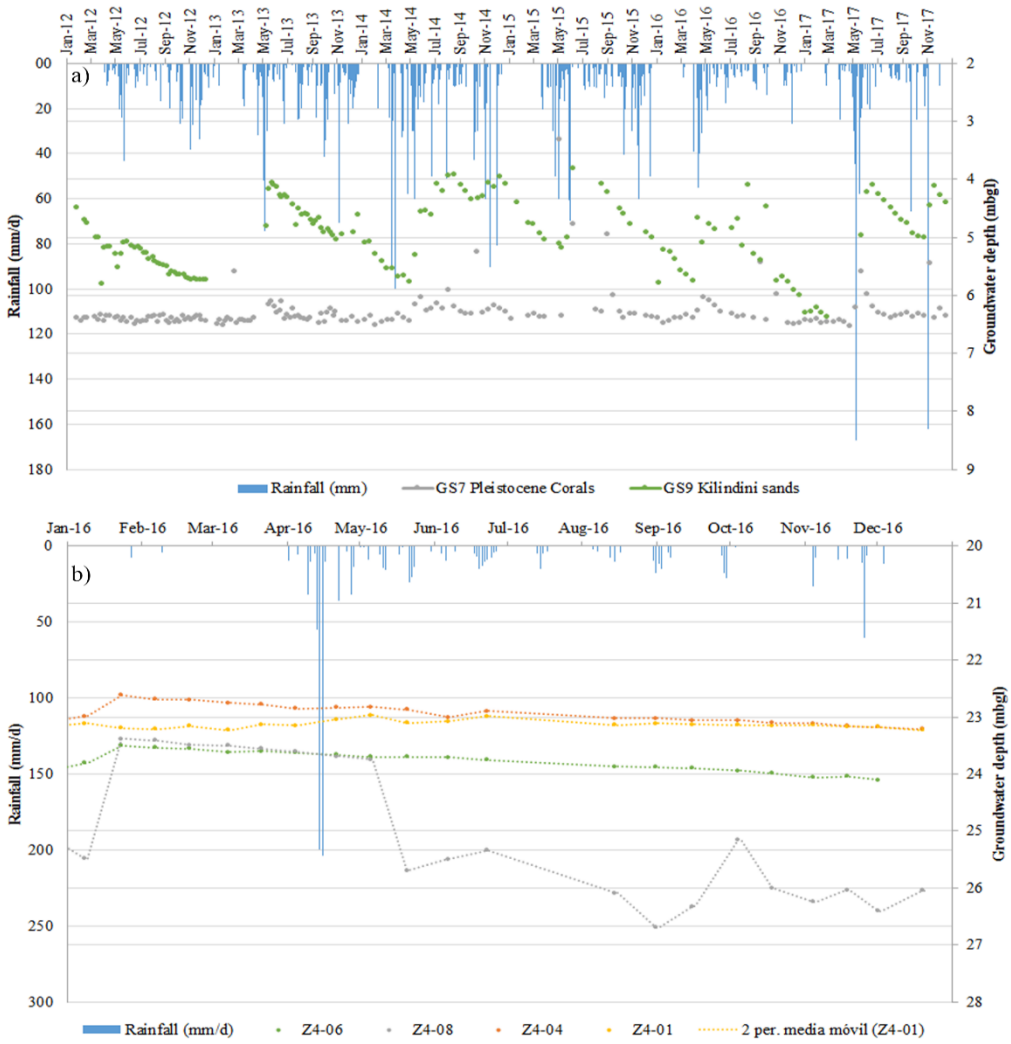

Figure 2.5. a) Groundwater level over time in well located in the Kilindini sands (GS9) and in well located in the Pleistocene corals (GS7). Peaks are insinuated in the corals during some recharge events indicating the fast response of the aquifer to rains. They did not show up in other recharge events due to the low frequency of measurements. b) Groundwater level in 2016 in community wells located to the North of the study area in the Kilindini sands see Figure 2.1). Plots also show rainfall at Kwale Agricultural Department station (Kenya Meteorological Department) (mm/d).

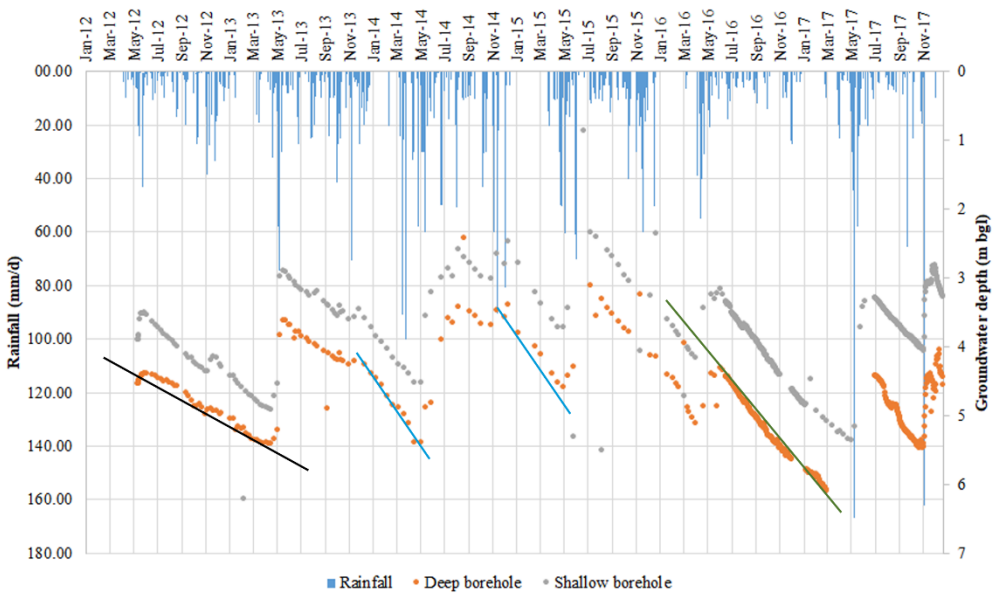

Figure 2.6. Base Titanium shallow and deeper control piezometers at an elevation of 24.6 m asl. The black line shows the groundwater recession that occurred in 2012 and early 2013 under natural conditions, since the wellfield was not intensively pumped until October 2013. The blue lines show the reduction in groundwater level occurring between recharge events once abstraction had commenced. The green line shows the slope increment of groundwater recession possibly caused by increased abstraction during La Niña event of 2016. The recession is taken as a line as the total drawdown is much smaller than the final stage controlled by the sea level.

Table 2.1. Groundwater level range and EC range of some monitored points from 2016 to April 2017.

Point	*Geology*	*Zone*	*Aquifer*	*Dates*	*EC range*	*EC tendency during 2016*	*GWL range*	*GWL tendency during 2016*	*Well depth/Screened section*	*D18 isotopic signal (june 2016)*
Z4-MS	Magarini s.	4	Shallow Aquifer	04/2016-02/2017	311-380	down	27.25-27.55	down	29	-3.12
Z4-85	P. corals	4	Shallow Aquifer	01/2016-04/2017	698-973	stable	9.62-9.9	down	10.4	-2.94
Z4-78	P. corals	4	Shallow Aquifer	01/2016-04/2017	2418-2652	stable	8.04-8.4	not clear	no data	-2.74
Z4-24	Kilindini s.	3	Shallow Aquifer	01/2016-03/2017	184-326	not clear	6.21-7.65	stable	7.5	-2.44
Z4-18	P. corals	4	Shallow Aquifer	01/2016-04/2017	705-960	stable	15.24-15.5	stable	15.9	-3.14
Z4-11	Magarini s.	4	Shallow Aquifer	01/2016-04/2017	102-621	up	12.63-16.1	down	17.87	-2.80
Z4-08	Kilindini s.	4	Shallow Aquifer	01/2016-06/2016	585-768	stable	23.38-27.69	down	28	-3.17
Z4-06	Kilindini s.	4	Shallow Aquifer	01/2016-12/2016	675-840	stable	23.5-24.1	down	24.6	-3.23
Z4-04	Kilindini s.	4	Shallow Aquifer	01/2016-04/2017	538-644	stable	22.62-23.5	down	23.6	-3.00
Z4-01	Kilindini s.	4	Shallow Aquifer	01/2016-04/2017	615-692	stable	22.97-23.48	down	no data	-3.24
Z3-98	P. corals	3	Shallow Aquifer	01/2016-04/2017	728-920	up	11.35-11.76	stable	12	-2.59
Z3-96	P. corals	3	Shallow Aquifer	01/2016-04/2016	2985-3090	not clear	7.08-8.19	not clear	8.3	-2.58

Z3-90	P. corals	3	Shallow Aquifer	01/2016-04/2017	1674-3655	up	6.22-8.49	down	no data	-2.62
Z3-87	P. corals	3	Shallow Aquifer	01/2016-04/2017	1659-2120	up	4.84-5.1	stable	no data	-2.59
Z3-30	Kilindini s.	2	Shallow Aquifer	01/2016-04/2017	535-1375	down	3.37-5.62	down	no data	-2.54
Z3-29	Kilindini s.	2	Shallow Aquifer	01/2016-04/2017	225-390	down	9.94-11.13	down	12.04	-2.68
Z3-102B	P. corals	2	Shallow Aquifer	04/2016-04/2017	507-640	up	11.24-11.8	down	12	-2.40
Z2-112	Magarini s.	2	Shallow Aquifer	01/2016-04/2017	55-128	down	6.75-8.11	down	no data	-2.40
Z2-104	P. corals	2	Shallow Aquifer	01/2016-04/2017	628-697	stable	no data	no data	no data	-2.64
Z2-103	P. corals	2	Shallow Aquifer	01/2016-04/2017	606-900	stable	11-11.51	stable	no data	-2.69
Z1-70	Kilindini s.	1	Shallow Aquifer	01/2016-04/2017	510-911	down	2.73-5.44	down	6.6	-2.29
Z1-33	Kilindini s.	1	Shallow Aquifer	01/2016-04/2017	531-759	up	9.86-10.47	down	10.65	-2.64
Z1-140	Magarini s.	2	Shallow Aquifer	01/2016-04/2017	529-669	up	11.06-12.94	stable	13.4	-3.12
Z1-135	Kilindini s.	2	Shallow Aquifer	01/2016-04/2017	190-360	down	3.18-5.05	down	no data	-1.97
Z1-125	Magarini s.	1	Shallow Aquifer	01/2016-04/2017	88-182	up	14.11-16.99	down	17.1	-2.70
Z1-124	Magarini s.	1	Shallow Aquifer	01/2016-01/2017	207-350	not clear	13.62-15.19	not clear	15.2	-2.61
Z1-122	Magarini s.	1	Shallow Aquifer	01/2016-04/2017	122-217	down	10.82-12.82	down	no data	-2.25

Z1-121	Kilindini s.	1	Shallow Aquifer	01/2016-04/2017	560-671	up	no data	no data	no data	-1.40
Z1-110	Kilindini s.	2	Shallow Aquifer	01/2016-04/2017	92-206	down	4.78-6.4	down	6.4	-2.18
DB/FI/HP	Kambe	2	Deep Aquifer	04/2016-04/2017	516-695	stable	no data	no data	no data	-3.07
DB/BM/HP	Kambe	2	Deep Aquifer	04/2016-04/2017	236-208	stable	no data	no data	no data	-3.14
C/15/10	Mazeras snd.	1	Deep Aquifer	04/2016-04/2017	379-677	up	no data	no data	no data	-3.15
C/109/21	Mazeras snd.	2	Deep Aquifer	04/2016-04/2017	483-790	up	no data	no data	no data	-3.16
C/06/12	Mazeras snd.	1	Deep Aquifer	04/2016-04/2017	248-760	up	no data	no data	no data	-3.10

2.5.4. Hydrochemical facies

The survey having more points sampled (June 2016) was chosen to represent the hydrochemical results of the study area. Although two field campaigns were carried out and each one represents a different season (dry and wet), the year 2016 was very dry and recharge in the rainy season were lower than usual because of La Niña 2016/2017 event, as stated in Section 2.5.2 (Fig. 2.3).

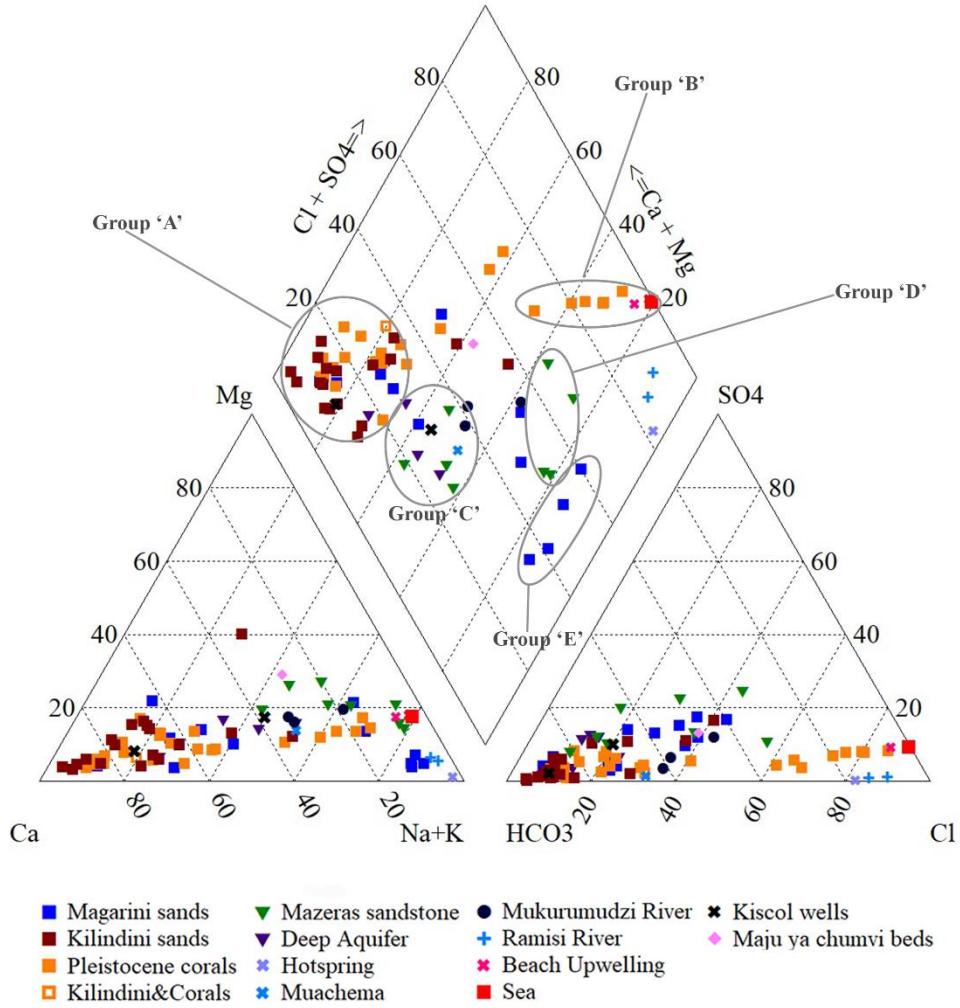

Figure 2.7. Piper diagram of all points sampled during June 2016 field survey.

Hydrochemical data shows the groundwater pattern in space and in depth. From it, the flow paths and the main hydrochemical processes that are taking place in the study area can be

deduced. Based on hydrochemical datasets, some groundwater hydrochemical facies are defined according to their major ion content. A total of 5 hydrochemical groups are described according to geology and the hydrochemical facies (Fig. 2.7 and Fig. 2.8):

Hydrochemical group 'A' comprises samples with a Ca-HCO_3^- facies that are hosted mainly in Pleistocene materials, Kilindini sands ('Pls') and Pleistocene corals ('Plc'), and a few samples from the deep aquifer in Mazeras sandstone (Fig. 8). This is the dominant group, comprising 63 % of the samples. pH is over 6.0 (6.1 to and 7.2). Some samples of this group are saturated with respect to calcite, most of them located in the limestone materials closest to the shoreline (Table 2, Appendix A).

Other facies present in Pleistocene materials are Na-Cl^- waters, located on the coastal line around Gazi bay and north coast (Fig. 2.8). The group 'B' consists in 7 samples representing the points affected by the saline intrusion, which is also supported by the average EC around 2850 µS/cm and a maximum value of 4061 µS/cm.

Group 'C' comprises 15 % of the samples and has a Na-Ca-HCO_3^- facies. Most samples in this group are located in the Mazeras sandstone outcropping at Shimba Hills and in their extension as the deep aquifer emplaced under the Magarini and Kilindini sands. These wells stand out by its lower Ca content, yet higher Na (Table 3, Appendix A) (Fig. 2.9a).

Group 'D' is represented by the 4 samples in Mazeras sandstone but having Na-Cl^--HCO_3^- facies. These samples are located up to Shimba Hills and they are enriched in Si (>20 mg/L Si or >40 mg/L SiO_2) (Table 3, Appendix A). The presence of quartz-feldspar minerals and silicified units in this formation with oversaturation relative to quartz (SI>1) indicates that the main process governing the Si content in this water is silicate weathering (Table 2, Appendix A). The sample labeled Maji ya Chumvi beds (pink symbol) corresponds to a point located at Lukore, up to the Shimba Hills, which present also this kind of facies but with a greater concentration of HCO_3^-, Na and Cl^- than the other samples of the group. This Cl^- and Na enrichment can be due to the greater water retention in the soil, thus increasing evapo-concentration or due to the presence of bluish-black gritty shales and muddy sandstones with possible salt remnants deposited during a period of fluctuating climate. Hydrochemically, this sample does not follow the sodium enrichment line and moves out the left side (Fig. 2.9c), suggesting a process that incorporates further HCO_3^- to groundwater from the soil gas (Armengol et al., 2017). A similar composition in sample C/12/12 points to connectivity between Triassic (Maji ya Chumvi Fm.) and Jurassic materials (Mazeras sandstone) (Fig. 2.9a).

Group 'E' represents the samples located in the Magarini sands (shallow aquifer) with Na-HCO_3-Cl^- facies. These samples also show high Si content and their Na concentration could come from silicate weathering process.

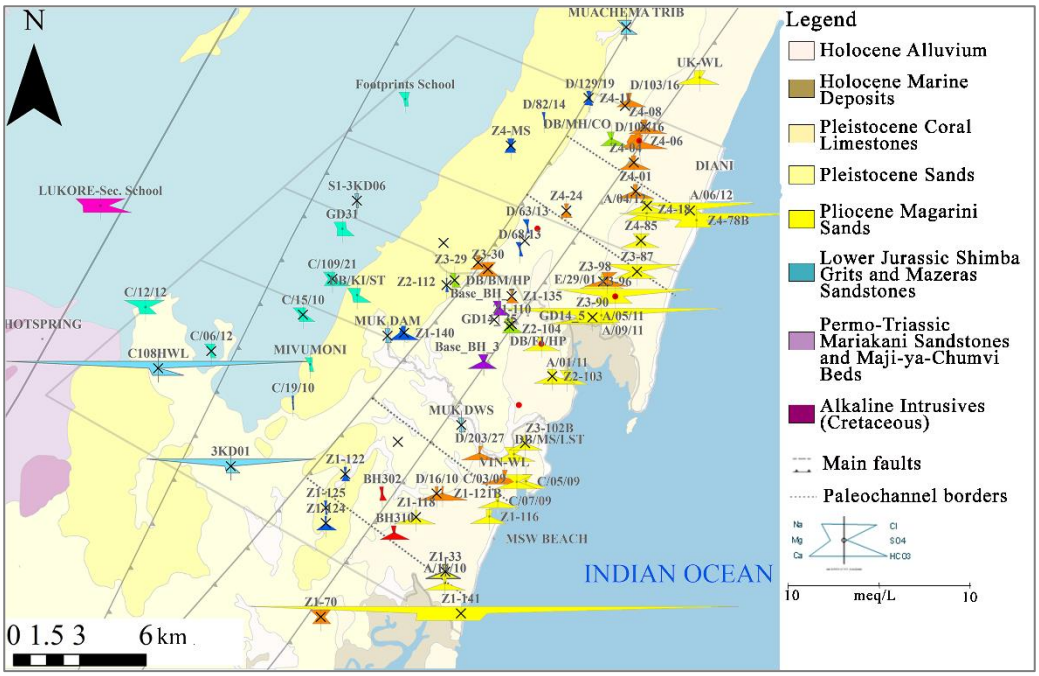

Figure 2.8. Modified Stiff diagram for points sampled in June 2016. Crosses indicate points monitored fortnightly and red dots the points at which fortnightly sampling was cut down due to various problems. The purple and green modified Stiff diagrams correspond to samples from the deep confined aquifer.

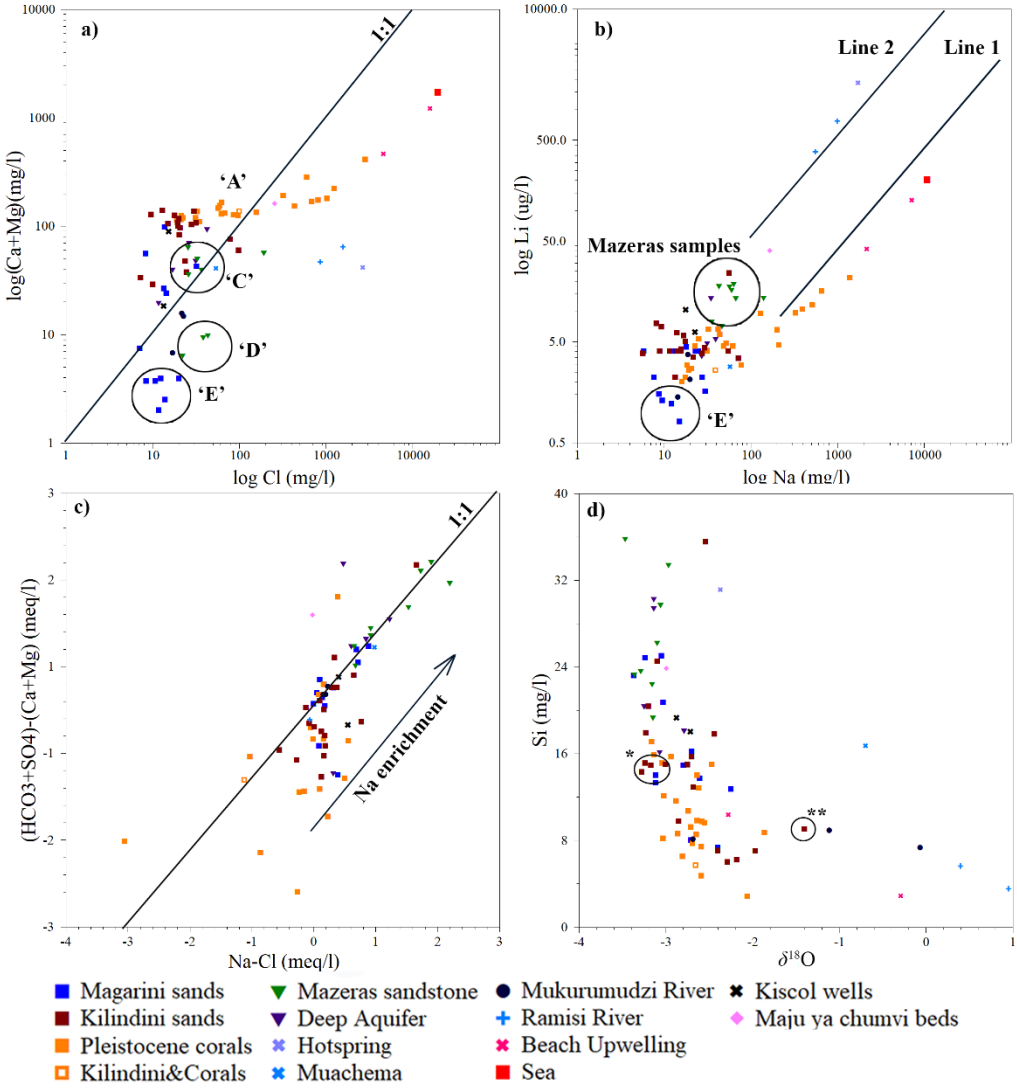

Figure 2.9. a) Cl^- vs. Ca+Mg in mg/L; b) Li concentration (µg/L) vs. Na in mg/L; c) ($Na\text{-}Cl^-$) vs. [($HCO_3^-+SO_4^{2-}$)-(Ca+Mg)] in meq/L; d) Si vs. $\delta^{18}O$. * It is referred to the samples in zone 4 that present $\delta^{18}O$ <-3. ** It is referred to samples D/16/10.

2.5.5. Water environmental isotopes

There is a relatively small change in altitude in the study area with a maximum elevation of 454 m a.s.l. at the Shimba Hills. Most of the samples follow the African Meteoric Water Line (AMWL) (Mckenzie et al., 2010). Relative to the Global Meteoric Water Line (GMWL) the samples present a deuterium excess between 8 and 13 ‰ (Fig. 2.10a), which is the same deuterium excess obtained in Levin et al., 2009 for the coast of Kenya and Ethiopia. It may

be indicative of precipitation formed from water vapor from an oceanic environment with less than average air humidity conditions, or alternatively from water evaporated near the land surface, either as a product of evaporated rainfall that recondenses or evaporation from surface water (Levin et al., 2009).

All samples from Shimba Hills (group 'D') and those of group 'E' in the Magarini sands have the lightest isotopic signal with $\delta^{18}O$ equal to -3.15 ‰ ±0.21 ‰ and -3.07 ‰ ±0.25 ‰ respectively. Most samples of the deep aquifer have the same isotopic composition as the samples from Shimba Hills (Fig. 2.10b).

The shallow aquifer has a higher water isotopic composition due to its proximity to the coast and the lower altitude. Nevertheless, the shallow wells located in Kilindini formation in the north area present lower isotopic values, similar to the samples from the deep aquifer. In addition, sample D/16/10 has a higher isotopic value ($\delta^{18}O$ = -1.4 ‰) and could be on a line of slope 4 (Fig. 2.10) corresponding to evaporation from a free water surface. This isotopic enrichment in ^{18}O suggests the influence of water infiltrated from the seasonal Lake Nimbodze near the sampled point (Fig. 2.10b).

The isotopic composition of the samples from the rivers in the study area (Ramisi, Mkurumudzi and Mwachema Rivers) show evaporation effect, except the sample upstream of Mkurumudzi, located at the Shimba Hills (Fig. 2.10a).

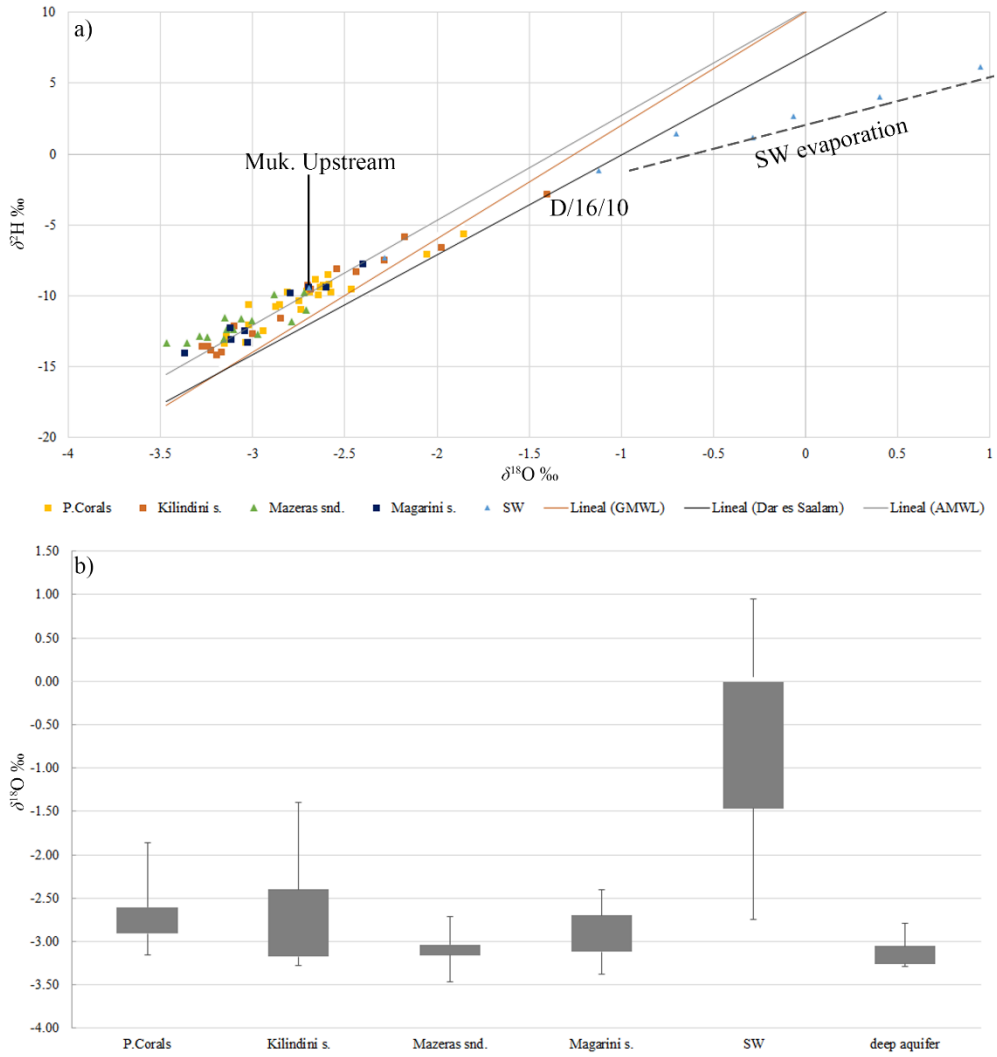

Figure 2.10. a) $\delta^{18}O$ vs. $\delta^{2}H$ of water samples and the Global Meteoric Water Line (GMWL) $\delta^{2}H=8*\ \delta^{18}O+10$ ‰ (orange line), Dar es Salaam local meteoric water line $7.05*\ \delta^{18}O+7$ ‰ (black line) and African Meteoric Water Line (AMWL) $7.4*\ \delta^{18}O+10.1$ ‰ (grey line). The dotted line refers to surface water evaporation; b) Box plot that shows the maximum, minimum and median of $\delta^{18}O$ for each geological formation.

2.5.6. Nitrogen pollution

One of the most common groundwater quality problems worldwide is nitrate pollution (Custodio, 2013). Typically, nitrate pollution in Africa comes from nitrogen compounds in wastewater and sewage (e.g. leakage from latrines into the aquifer), and from fertilizers applied in agriculture (Ouedraogo and Vanclooster, 2016); soil degradation and faecal contamination from extensive animal raising can also be factors. Most samples in the study

area show low nitrate concentrations, under 5-10 mg/L NO_3^- (Table 3, Appendix A), which may approach the chemical groundwater base-line. During March 2014 (dry season), only 2 out of 32 samples had nitrate concentration over the drinking water level limit of 50 mg/L: Z3-98 (63 mg/L) and Z4-78 (113 mg/L). During the wet season in the same year, only point Z3-98 (48 mg/L) had relatively high nitrate concentration, just below the drinking water limit. In 2016, when 75 (March) and 80 (June) groundwater points were sampled across the study area, samples with higher nitrate concentrations were also uncommon (Figure 1, Appendix A). In March, samples with nitrate over or approaching 50 mg/L were located as follows: UK-WL (58 mg/L) (a hand-dug well near Ukunda village), A/06/13 (48 mg/L) and Z3-98, to the east of the KISCOL sugar plantation (41.7 mg/L). In June 2016, only 20 samples presented a nitrate concentration over 10 mg/L and only 4 were above the drinking water limit: the same one near Ukunda village (UK-WL: 55.0 mg/L), one sample from Gazi village (A/01/11: 64.7 mg/L); one from Msambweni village (C/05/09: 51.8 mg/L) and Z3-98. Indeed, in June 2016 one deep monitoring borehole located in KISCOL's Milalani (southern fields) was measured and it had (73.1 mg/L). This high concentration could come from the fertilizers added in the sugar fields. Therefore, the small amount points which show nitrate contamination are located in the main villages of Msambweni, Gazi and Ukunda, except point Z3-98 located east of the KISCOL sugar fields around Kinondo (Table 3, Appendix A). In village areas, the source of nitrate pollution in the samples could be latrines or animal faeces. In the sugarcane plantation, nitrate pollution could be associated with fertilizer use. Overall, despite the potential for nitrate pollution due to poorly managed sewage/wastewater and growing agricultural activity in the study area, nitrate pollution seems so far to be locally confined. In 2014 and 2016 nitrate concentration was higher during the dry season than during the wet season, likely due to the lower rate of recharge in the dry season (see Folch et al., 2011; Menció et al., 2016). Recharge dilutes and pushes local contamination down flow, while higher rates of nitrogen uptake as plants grow following precipitation also reduces nitrate concentration in the soil (Wick et al., 2012).

Some samples show significant concentrations of ammonia. During the dry season of 2016, 6 points had ammonia between 0.2 and >8 mg/L NH_4^+ and during the wet season, only 4 points presented ammonia of between 0.2 and 5 mg/L. Furthermore, there are points in several geological areas with values of Eh in the range of iron reduction by nitrate (Table 3, Appendix A) (Faulwetter et al., 2009). The most reducing waters are those located in the middle area, in the Pleistocene corals and in the deep aquifer. Some of these points also have a high concentration of dissolved manganese and iron. Therefore, although there is no clear trend or distribution, hydrochemical data seems to indicate potential reducing

conditions across the study area which could affect nitrate concentrations as ammonia is oxidized.

This assumption may be confirmed by the iron stability diagram (Figure 2, Appendix A). All samples are located between the Fe^{+2} and $Fe_2O_3.nH_2O$ stability fields. The samples on the Fe^{+2} field are located on Mazeras sandstone and Magarini sands, i.e. in facies 'C', 'D' and 'E'. These facies present lower pH due to the absence of carbonates in the terrain and thus, boreholes in these areas produce more corrosive water, which has been seen to affect borehole/handpump functionality in these areas. The fact that significant DO concentrations were measured in many of these points (Table 3, Appendix A) indicates that there is no chemical equilibrium between dissolved oxygen, pH and Eh, but a kinetic situation.

Redox conditions could be influenced by the presence of organic matter. High concentration of dissolved organic carbon, measured as total organic carbon (TOC), was observed. Notably, the TOC value tends to increase towards the coast, with lower values inland. The samples with the highest TOC are located in Pleistocene corals (Table 3, Appendix A). It is possible that TOC is an input from the soil/surface since the high PCO_2 values match those expected from degradation of soil organic matter, which could be affecting the redox conditions in the aquifer (Table 3, Appendix A). In order to understand potential natural attenuation processes, it is important to define first the baseline composition of the aquifer system as Manzano et al. (2007b) did, and then apply other sources of information, such as nitrate isotope measurement or organic matter data.

2.5.7. Hydrochemical changes between seasons in 2014 (wet) and 2016 (La Niña) years

Comparing the 24 samples from March and June 2014 (wet year) field surveys, most fresh water samples (around 60 %) were more saline during June than in March (Table 4 and 5, Appendix A). However, the samples in the lower part of zone 4 do not present any variation between the two field campaigns. In contrast with 2014, in 2016 the fresh groundwater samples from the dry and wet seasons (March and June 2016 respectively) show similar salinities (Table 6, Appendix A). However, there is an increase in salinity in the samples from groundwater affected by saline intrusion along the coastline, mainly on the north coast around Ukunda and Diani (Fig. 1.1).

Comparing hydrochemical data for the 22 points sampled in both wet seasons (June 2014 and June 2016 – La Niña year of low rainfall), most of the fresh groundwater samples (around 60 %) showed higher salinity during June 2014. The samples in zone 4 have the

same hydrochemical composition in both years, with less than 2.4 % average difference when comparing the concentration of the major ions between years and less than 6.3 % average difference when comparing the EC values. However, the samples affected by saline intrusion (group 'B') present a 20 % increment in salinization during La Niña year compared to that measured in June 2014.

2.6. Discussion

2.6.1. Conceptual flow model

The geophysical profiles allow a comprehensive three-dimensional understanding of the aquifer geometry of the study area and of vertical and lateral relationships through the geological formations. The groundwater level time series, hydrochemistry and water isotopes have helped to determine the main recharge areas, the connectivity between the geological formations and the consequences of drought on the groundwater system.

According to the stability diagrams of silicates (Figure 3, Appendix A), weathering produces kaolinite as the main clay mineral in equilibrium with primary silicates for all the points sampled in the study area. This weathering product is preferentially formed under the climatic conditions dominating in the study area. Kaolinite is formed in rainy areas with intense rainfall and well-drained conditions (Appelo and Postma, 2005). Hydrochemical and isotopic data allow the definition of groundwater flow paths and main recharge areas, as in other studies under similar conditions (Anglés et al., 2017; Edmunds et al., 2003; Manzano et al., 2007a; Menció et al., 2012). Different hydrochemical data facies illustrate the hydrochemical sequence that takes place within the system (Fig. 2.8).

Up to the Shimba Hills, it is possible to distinguish two types of processes affecting deep wells located and screened only in the Mazeras sandstone (Fig. 2.8). The samples of group 'D' located in this geological formation present high silica concentration and are saturated with respect to quartz. Based on the Ca - HCO_3^- and Na – Cl^- relationships the samples are enriched in HCO_3^- and Na, resulting from silicate weathering, mainly-feldspar (Appelo and Postma, 2005). For this reason, these samples are unsaturated with respect to calcite (Table 2, Appendix A). The EC range of these samples is between 260 and 313 µS/cm. However, the rest of the samples in Mazeras sandstone formation, north of the mining site are of the hydrochemical group 'C'. These samples, compared to group 'D', have lower silica concentration but despite this, they are also unsaturated with respect to calcite, and the saturation index is less negative than in group 'D' (Table 2, Appendix A). Silicate weathering in this facies is less significant compared to that in group 'D', even though they are more

enriched in Na (Fig. 2.9c) and present higher values of EC (from 499 to 666 µS/cm). This may be due to increased evapotranspiration.

The same range of Li (8-35µg/L) in the deep aquifer samples and the samples of the group 'C and D' seems to indicate that recharge of the deep aquifer originates in the Shimba Hills range (Table 3, Appendix A).

The hydraulic continuity of Shimba Hills aquifer and the Mazeras Fm. deep aquifer is also confirmed by the water isotopic data since the composition of most samples of the deep aquifer is in the same isotopic interval as the samples from Shimba Hills (Fig. 2. 10a). Some samples located in the deep aquifer in zone 2 have the same hydrochemical facies (group 'C') as the samples located in the Shimba Hills. These samples are from some Base Titanium boreholes screened in Jurassic materials (Kambe, Mtomkuu and Mazeras Fm.). In addition, the EC values of these samples are in the same range (370 µS/cm) as results from the samples of group 'C'. This suggests hydraulic continuity along the Mazeras sandstone, which is also confirmed by seasonal changes in deep groundwater level (Fig. 2.6). The time lag between a rainfall event and the groundwater level peak smothered indicates hydraulic connection throughout the Mazeras Fm. and the recharge area of the deep aquifer. This is also confirmed by artesian (flowing) behaviour during the drilling of some of Base Titanium's wells that are only screened in the deep aquifer.

The redox values (Eh from +94 to +191 mV) and dissolved oxygen (DO from 0.8 to 4 mg/L) found in the Base Titanium boreholes tapping the deep aquifer are higher than those of the samples of group 'D' located in the Shimba Hills, and show that there is no significant inflow of shallow groundwater induced by the abstractions. This points to semi-confined conditions suggesting the presence of a semi-confining layer (data not shown) (Fig. 2.11). Indeed, the artesian flow in two Base Titanium boreholes indicates the presence of this confining and/or semi-confining layer (Fig. 2.1). The permeability of this aquitard varies across the study area depending on geological formation and is affected by the palaeochannels and also by some deep wells with screens in both the shallow and deep aquifer. The presence of a semi-confining layer dividing a formation into two aquifer units has been observed elsewhere (Manzano et al., 2013). The identification of this layer and detailed characterization of the groundwater system modifies the former conceptual model of a single coastal aquifer into a more complex but still hydrogeologically simple system consisting of two separate layers with an aquitard in between. Other deep well samples present facies typical of group 'A', due to the screened sections of these boreholes being in multiple geological materials, taking water from Pleistocene corals, Kambe limestone, Mtomkuu Fm. and probably Mazeras Fm. as well. These wells show higher values of EC (590

µS/cm) and higher pH values (6.9 and 7.2 respectively) than the wells screened only in the Mazeras sandstone. Some KISCOL wells also screened in both shallow and deep geological formations show hydrochemical facies of group 'A' and a similar range of EC and pH.

The KISCOL boreholes (BH302 and BH310) located in the sugar fields in zone 1 have a higher isotopic composition than boreholes screened only in the deep aquifer, and also differ in terms of hydrochemical composition. This isotopic range would appear to be due to the multiple screened intervals in the KISCOL wells, presumably aimed at maximizing groundwater abstraction by capturing water from different aquifer units. Water from both boreholes show silicate weathering, but whilst BH310 has a Ca-HCO_3^- facies with $\delta^{18}O$ = -2.72 ‰, borehole BH302 presents a Na-Ca-HCO_3^- facies with lower water isotopic composition ($\delta^{18}O$ = -2.88 ‰). Considering that the average error for $\delta^{18}O$ is ± 0.05, the two samples appear to be slightly different suggesting that BH310 has a greater proportion of water from the shallow aquifer which has higher isotopic composition compared to BH302. This supposition is backed up by a comparison of Li concentrations (Fig. 2.9b), as BH302 with a hydrochemical facies typical of the deep aquifer has higher Li concentration (10-20 µg/L) than BH310 (1-8 µg/L) with hydrochemical facies typical of the shallow aquifer. In addition, the BH310 $\delta^{18}O$ change from March (-2.94 ‰) to June (-2.72 ‰) may indicate that during the dry season a higher proportion of the groundwater being abstracted is from the deep aquifer. Moreover, the facies of this point changes from Ca-Na-HCO_3^- in March, incorporating Na from the deep aquifer to Ca-HCO_3^- in June, which points to recharge from the shallow aquifer.

Regarding the shallow aquifer formations, the hydrochemical signal of group 'E', all points located in Magarini sands, indicate that this geological formation acts as the recharge area for the shallow groundwater system. Infiltration through the sand is accompanied by silicate weathering, forming a local hydrochemical system. Low pH (average of 5.6) and EC (between 50 and 170 µS/cm) compared with the samples located in other geological formations indicate the absence of soluble carbonate minerals and suggest less interaction with the soil and the unsaturated zone (Table 3, Appendix A).

The different composition of the samples located in the Mazeras sandstone and in the Magarini sands, with lower salinity and Cl^- and higher Si concentrations in samples from the second geological formation, indicate that there is no hydraulic connection between these two geological formations. However, the groundwater contour map (Fig. 2.4) indicates the possibility of deep groundwater flow from the Shimba Hills to the sea. These two factors indicate that the fault located East of the Shimba Hills (Fault 2 of Fig. 2.1) acts as a low permeability boundary, forcing recharge from the Shimba Hills to the deep aquifer located

under the shallow geological formations (Magarini sands, Pleistocene sands and corals) (Fig. 2.11).

Groundwater flowing through the shallow groundwater system becomes enriched in Ca and HCO_3^-, (Group 'A' samples), due to the geology (carbonate, mainly limestone - Pleistocene materials) of the southern area. The modified Stiff diagrams show how this enrichment in Ca and HCO_3^- going from inland (Magarini sands) toward the coast point to connection through the geological formation. The relatively high Si concentration in Pleistocene formations and in samples taken from an upwelling/spring located on the tidal Msambweni beach in zone 1 (over 10 mg/L Si) confirms the connection between all the shallow aquifer systems (Magarini sands, Kilindini sands and Pleistocene corals) (Table 3, Appendix A). On the other hand, samples with low Si concentration located in zone 1 and 2 along the Pleistocene materials indicate a possible dilution of Si concentration due to local recharge through these geological formations. Indeed, the wells located along the coast which are not affected by saline intrusion show a slight EC decrease during rainy periods, indicating shallow local recharge in the Pleistocene corals. Some samples near the south coast present lower isotopic composition, more similar to the samples from the deep aquifer. This further confirms the connectivity between diverse geological materials in the palaeochannel areas due to the process of erosion and deposition during the original formation of the channels (Fig. 2.11).

Furthermore, considering the change in isotopic composition across the field surveys, the samples showing the greater percentage change in water isotopic composition when comparing March and June field surveys are the samples with Na-Cl^- facies (group 'B'). This is due to the isotopic mixing produced by seawater intrusion. Seawater intrusion is also confirmed by the high Li concentration (9-22 µg/L) (Fontes and Matray, 1993) following the mixing seawater line (Line 1 Fig. 2.9b). However, samples from the shallow aquifer located in Magarini sands with Na-HCO_3^--Cl^- facies (group 'E') also present higher isotopic change between seasons due to the influence of local rainfall during the wet season. On the contrary, samples in the deep aquifer (group 'D') present little isotope variation (Fig. 2.10b), suggesting a uniform and constant recharge in the deep aquifer throughout the seasons. Samples located in the Magarini sands and the Mazeras sandstone (group 'E' and 'D' respectively) present low values but a high variation of EC between seasons providing further evidence of their role as recharge areas.

There is a negative correlation ($P < 0.01$) between Si concentration and water isotope composition ($\delta^{18}O$), except for in surface water samples and those allowing evaporation from a free surface (Fig. 2.9d). This confirms the main recharge areas previously mentioned:

the Mazeras sandstone and Magarini sands, and the two main flow paths: one from the Mazeras sandstone to the deep aquifer and a second from the Magarini sands to the coral limestone. The change in isotopic composition and Si concentration (among others) along the flow path of the shallow aquifer formation shows that besides the Magarini sands, significant recharge of the shallow aquifer is also occurring on the Pleistocene formations. Finally, the fact that significant DO concentrations were measured in many wells (Table 3, Appendix A) indicates that dissolved oxygen, pH and Eh are not in chemical equilibrium. This observation may suggest that the water under more reducing conditions coming from the Magarini sands is mixing with more oxygenated water from recharge through the Pleistocene materials as the shallow aquifer is recharged across the study area. That said, DO values in zone 4, which range from 3.1 to 5.7 mg/L, are lower, suggesting other processes may be taking place in this area (Table 3, Appendix A).

Seasonal variation in groundwater level in wells in zone 4, along with lower DO values and the isotopic composition of samples from this area may indicate the existence of a clay layer associated with the marine sediments of the Kambe and Mtomkuu Fm. The low permeability of this layer would limit local recharge to the deep aquifer in the lower part of the basin, explaining the relatively lower isotopic composition of groundwater recharged in the higher areas. This explanation is in agreement with observed groundwater level variation after extreme rainfall events in which the limited change in groundwater level after rainfall indicates the absence of direct recharge (Fig. 2.5b).

Regarding surface water-groundwater interaction, although it cannot be defined along all rivers with the potentiometric data (Fig. 2.4), the hydrochemical results indicate that the slightly brackish Ramisi River is being fed by the aquifer as the point sampled downstream has lower salinity than the sample from upstream (Fig. 2.8), which can be explained by dilution as lower salinity groundwater flows into the river. The Li concentration in the samples from Ramisi River comes from the hot springs at Mwananyamala (Tole, 1990) (Line 2 Fig 2.9b). The potentiometric map shows that the Mkurumudzi River is also effluent (gaining), which agrees with the composition of point S1-3KD06 ($\delta^{18}O$ = -2.6 ‰) being in the same range as groundwater. However, river-aquifer interactions are difficult to ascertain with this kind of data as the sampling points may be affected by water released at dams and subject to other hydrochemical processes.

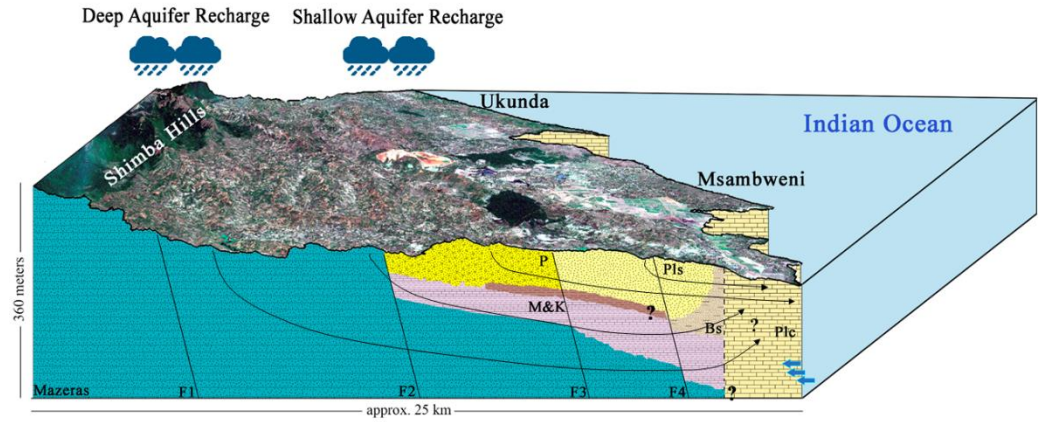

Figure 2.11. Schematic conceptual model of the aquifer. The flow lines indicate flow direction and connectivity through the geological formations from the recharge areas for the shallow and deep aquifer. The question marks indicate the existence of a clay layer, the connectivity between the Mazeras Fm. and Pleistocene corals and the discharge of the deep aquifer. Mazeras (Mazeras Fm.), M&K (Mtonkuu and Kambe Fm.), P (Magarini sands), Pls (Kilindini sands), Bs (Bioclastic sands with clay lenses), Plc (Pleistocene corals), and in brown color the clay layer acting as an intercalated aquitard. F1 to F4 indicates the main fault in the study area.

2.6.2. Effects of La Niña drought on the groundwater system and its hydrochemistry

There is insufficient groundwater level data to evaluate the effect of La Niña in the shallow aquifer as data in most points starts in 2016. However, during La Niña event, the wells located on the Kilindini sands (except in zone 4) and Magarini sands present higher groundwater drawdown (3.4 to 1.4 m) compared to the wells located on Pleistocene corals. In the deep aquifer, with data available since 2012 in the Zone 2, it is possible to observe a larger recession in groundwater level during La Niña event compared to that seen in 2012, possibly caused by increased abstraction rates during the drought period.

The behaviour of the system in 2014 is the one expected for an area affected by the monsoon in a tropical area (Isa et al., 2014). The recharge volume difference in 2014 between seasons produces an ionic differentiation of the composition of the sample. During the post-monsoon (wet season-June 2014) inland samples display an elevated concentration of mineral ions (Ca and Mg). This increment during the wet season could be explained by the associated reversible cation exchange. Oppositely, during La Niña event, there are not fresh water salinity differences between campaigns in 2016 due to the low recharge caused by the low rainfall in the wet season. Zone 4 is an exception to this pattern, as there is no hydrochemical variation between field surveys in 2014 and 2016 confirming the existence of a clay layer in this area.

In the coastal area, during the pre-monsoon (dry season-March 2014), there is a higher concentration of (Na and Cl^-) due to an increase of seawater intrusion caused by lower recharge. As expected, samples affected by saline intrusion shows higher salinity during the dry season due to lower recharge. The EC values during the dry season are around 22 % on average higher than the wet season. On the contrary, during La Niña, this increment on saline intrusion on the coastal samples during the dry season is lees compared to 2014. The increment on CE values during the dry season is only 12 % on average compared to the wet season. Therefore, during La Niña drought the whole year behaves as a "dry season" causing its main impact in the coastal area.

2.7. Limitations of the groundwater conceptual model and implications

In this study, a groundwater conceptual model of the Kwale aquifer has been defined and the effects of La Niña on the hydrodynamics of the system have been assessed. However, it should be noted that the research here presented has some limitations and uncertainties.

One important limitation is that the effect of "La Niña" in 2016 on the shallow aquifer is based only on groundwater level data from the same year which limits the understanding of the effect of this drought on the shallow aquifer system. Moreover, the hydrodynamics of the shallow aquifer in some areas are not yet completely understood. Wells located in zone 4 did not seem to be affected by La Niña event. However, the behaviour of the system under longer drought periods is unknown. In the same way, hydrochemical and isotopic data from wells located in the Kilindini sands in zone 2 indicate different aquifer hydrodynamics in this area.

Another important issue is incomplete knowledge of the full extent of the aquitard, which separates the groundwater system into the shallow and deep aquifer levels. While this layer is clearly identified in Zone 2 in the area of Base Titanium boreholes, its presence or absence in zones 1, 3 and 4 not affected by the palaeochannels is unknown due to the lack of deep boreholes in those areas. Potential connectivity between the aquifer units must be taken into account in terms of groundwater exploitation since intense abstraction in the deep aquifer could affect the shallow aquifer levels. The connectivity between the shallow and deep aquifer levels in the Pleistocene corals is also not well understood Whilst it is thought that the Pleistocene corals overlay the Mazeras Fm. in depth near the coast, there is a lack of knowledge about how the deep aquifer connects with the sea and thus the potential for salinization of both aquifer levels.

It was possible to identify two palaeochannels located in zone 1 and 3. However, the full extent and continuity of these sedimentary layers are not completely understood which in turn limits understanding of the hydraulic properties of the formation and the potential hydraulic connectivity with surrounding formations. In addition, the exact borders of the paleochannels and their connectivity with the sea are undetermined. Therefore, although water level and quality in the area of the paleochannels did not appear to be affected by La Niña 2016, the behavior of the system under longer drought periods and the effect of the palaeochannels at a regional scale cannot be defined. For example, in a prolonged drought it is possible that the palaeochannels could act as preferential zones of saline intrusion.

The hydrochemical data from the Ramisi River suggests that the aquifer feeds water into the middle reaches of the river. However, the river-aquifer relation along the river length and the effect of the drought period in the river is not fully understood due to the lack of groundwater data from areas bordering the stream.

The drought that occurred in 2016 did not have dramatic effects on water level and. However, due to the above-mentioned limitations and uncertainties, the consequences of a future longer drought period cannot be predicted.

2.8. Summary and conclusions

Drought provoked by La Niña and IOD conditions harassed the Greater Horn of Africa region in 2016. One of the affected areas was the coastal county of Kwale (Kenya), a rural area, where the effects of drought on the aquifer system can be used as an indication of likely effects throughout the coastal strip sharing similar geology.

Before analysing the effect of La Niña 2016 event on the groundwater system, a conceptual model of the hydrogeological system was defined. By means of a geophysical approach, it was possible to define the aquifer geometry and its limits. The studied aquifer system is formed by two hydrogeological systems: one shallow aquifer composed of younger geological materials (Pliocene and Pleistocene formations) and a deep aquifer composed of older materials (Jurassic and Triassic) which outcrops inlandwards, in the Shimba Hills Range. In the middle part of the area, the deep aquifer acts as a confined aquifer due to the presence of an aquitard with very low permeability located between the younger and the older materials. However, the confined behaviour of the deep aquifer changes along the study area, becoming less confined such that connectivity between the shallow and deep aquifer increases. This is due to the presence of palaeochannels, one in the northern area (zone 3) and another in the southern area (zone 1). The shallow unconfined aquifer is

recharged directly by local rainfall across the area, except in the lower part of zone 4, where the shallow aquifer behaves as semiconfined/confined due to the heterogeneity of geological materials and the presence of clay/low permeability materials. The deep aquifer is recharged in the Shimba Hills area by preferential flow though faults and joints. The discharge of both hydrogeological systems is littoral to the Indian Ocean, through abstraction by the different water users of the region (communities, agriculture, mining) and through direct evaporation and evapotranspiration, etc.

One of the effects of La Niña drought of 16/17 was the reduction in the recharge during this event. In 2016 recharge was reduced by 78 % compared to the wet year of 2014 and reduced by 69 % compared to a year with normal annual rainfall (2013). In effect, the wet season of 2016 behaved like a continuation of the dry season.

The change in recharge caused by La Niña drought meant that groundwater quality remained constant in the samples located inland throughout the year, compared to the seasonal differences observed in 2014. On the other hand, due to a reduction in recharge attributed to La Niña drought, salinity in the coastal wells increased between March and June instead of being reduced, as occurs in normal years.

Regarding groundwater quality beyond the coast, results seem to indicate that nitrate pollution is not a significant problem in the study area, and what exists is mainly linked to urban areas.

The effect of La Niña 2016/17 event on the aquifer system in Kwale County has important implications for groundwater management, as the “recovery” of groundwater levels and quality is damaged in the absence of normal wet season rainfall. Effectively, this region experienced an extended dry season from the end of 2015 to the middle of 2017, with a consequent decrease in aquifer water levels and an increase in the saline intrusion. For successful long-term management of water resources, the effects of long drought periods must be considered together with impacts associated with increased groundwater demand throughout Africa. Intensification of agriculture, industrialization and population growth along with the effects of extended droughts may act in damaging synergy on Africa’s groundwater systems.

The author gratefully acknowledge the support of Kenya's Water Resource Authority (formerly WRA), the Kwale Country Government, Base Titanium Ltd., Kwale International Sugar Company Ltd. and Rural Focus Ltd. This research was funded by the UK Government via NERC, ESRC and DFID as part of the Gro for GooD project (UPGro Consortium Grant: NE/M008894/1). I appreciate the constructive comments and English reviewer to Nancy Gladstone.

Chapter 3

Hydrogeological and non-hydrogeological parameters affecting the presence of faecal bacteria

Ferrer, N., Folch, A., Masó, G., Sanchez, S., Sanchez-Vila, X. 2019. What are the main factors influencing the presence of faecal bacteria pollution in groundwater systems in developing countries? Manuscript submitted.

3.1. Introduction

Worldwide, human populations rely heavily on groundwater as a source. This situation is even more significant in Asia and Africa, where groundwater is the major source of drinking water and has an important role in improving health and sustaining urban livelihoods (Adelana and MacDonald, 2008; MacDonald et al., 2012). Although groundwater has been historically assumed to be free of bacterial pathogens, surveys carried out during the last decades indicate that a significant fraction of groundwater supply sources are responsible for water-borne diseases outbreaks around the world (Bhattacharjee et al., 2002). Globally, 25 % of people lack access to water free from microbial contamination (Nowicki et al., 2019). In Africa, this figure doubles, to a value above 50 % (Bain et al., 2014), far from compliance with the Sustainable Development Goal number 6 of the United Nations.

Hand-pumped tube-wells, being low-cost and low-tech efficient solutions, offer affordable access to shallow aquifers in many developing countries across Africa, Asia and the Pacific. These type of wells, most generally operated by families or small rural communities, are a valid alternative to private or governmentally-operated deep boreholes (Ferguson et al., 2012). However, they are susceptible to faecal contamination due to the introduction of bacterial pathogens into the subsoil, arising from a variety of sources, such as septic tank infiltration, improper disposal of solid urban waste, leachate from landfills, anthropogenic controlled water recharge, or crop excess irrigation with untreated or insufficiently treated sewage effluent (Charles et al., 2008; Goyal et al., 1984; Matthess et al., 1988; Oteng-Peprah et al., 2018; Yates et al., 1985). Once bacteria reach the groundwater, and under very favourable conditions with respect to flow, geochemistry and lack of competing indigenous biomass, bacterial pathogens can eventually travel considerably long distances (Sharma and Srivastava, 2011). Groundwater transport in shallow aquifers is primarily a function of the hydrogeological setting and climate conditions (Macler and Merkle, 2000). It is known that the transport, rate of survival and fate of microbes in the subsurface environment are directly influenced by the microbial population (both diversity and individual characteristics and concentrations, e.g., (Barba et al., 2019a)), the microbes physical state (dead or alive), the type and characteristics of the subsurface soil and aquifer sediment, as well as water temperature, quality and hydrological conditions (Rao et al., 1986). Therefore, in order to protect drinking water wells against microbial contamination, safe setback distances are essential between wastewater disposal services and water supply wells (Blaschke et al., 2016).

Understanding the mechanisms of bacterial fate and transport in the subsurface is of great importance to control soil and groundwater pollution (e.g., Sepehrnia et al., 2018). Some

recent studies focus in understanding the role of the vadose zone in the flow and transport of Escherichia coli (*E. coli*) through the soil until reaching the shallow water table in unconfined aquifers (Sepehrnia et al., 2018; Weldeyohannes et al., 2018). Yet, this should be completed with the detailed analysis of the impact of design, construction and maintenance of individual wells. As an example, Kilungo et al., (2018) compares the water quality of samples from wells of different designs, in order to help guiding future efforts in providing affordable and sustainable interventions to improve access to clean and safe water in rural communities without centralized supply and sewage networks. Other authors (e.g., Olajuyigbe et al., 2017) examine some relevant socio-economic characteristics of population, such as gender, age, household size, family size, employment, and average income, in order to capture information about the exposure of hand-dug wells to pollution and contamination. Moreover, some authors (e.g., Devane et al., (2018) review the different faecal tracking tools to recommend the suitable method to determine faecal sources in rural areas. Furthermore, some studies try to correlate the temporal variation in the concentrations of *E. coli* as a function of seasonal rainfall characteristics (Elangovan et al., 2018; Howard et al., 2003; Kayembe et al., 2018), well depths, distance to a septic tank, and population density (Dayanti et al., 2018; Martínez-Santos et al., 2017; Rohmah et al., 2018).

Despite some authors try to correlate the presence of faecal bacteria to diverse sanitary risk factors in order to assess the microbiological risk posed by groundwater sources (Ercumen et al., 2017; Godfrey et al., 2006; Lin et al., 2018), to our knowledge, there are no studies which combine both hydrogeological and non-hydrogeological variables within the same study, with the goal to somehow assess the variables that are actually correlated, and also their relative ranking to evaluate and eventually predict faecal pollution.

Therefore, the main goal of this chapter is to discern what are the hydrological, geochemical, physical and sanitary variables potentially influencing the presence of faecal bacterial pollution in groundwater sources in rural areas. The method proposed is based on performing a number of multivariate statistics evaluations, being tested in the study area, one of the multiple zones along the African continent heavily affected by bacterial pollution (Mzuga et al., 1998; Nowicki et al., 2019; Tole, 1997) in shallow aquifers of very different geologies and hydrochemical facies, as well as different types of waterpoints in terms of construction and maintenance. Understanding which variables are affecting, and to what degree, the presence of *E. coli* in the groundwater sources, could provide significant knowledge for an accurate management of the waterpoints, land use and water resources to avoid faecal contamination to population, being the cause of a combination of sanitary and educational problems that are perpetuating gender inequality and poverty in rural areas in developing countries.

3.2. Methods

3.2.1. Study area

The study area is defined in Section 1.3 (Fig. 1.1 and 3.1). Adding that the economy of these communities is mainly based in self-consumption livestock. There is not wastewater treatment, and the basic sanitation facilities in the area are pit latrines. The communities are supplied by diverse type of groundwater points (WP) such as hand-dug wells (large-diameter wells, less than 30 meter deep, and frequently uncovered), hand-dug wells with handpumps (similar to the previous ones, but covered by the presence of hadpumps), handpump boreholes (small diameter boreholes, less than 30 meter deep, fully covered on the surface by concrete) and deep boreholes (small diameter boreholes, with depths exceeding 30 m).

The area, as well as the location of the waterpoints, span the geological units defined in Section 2.3.

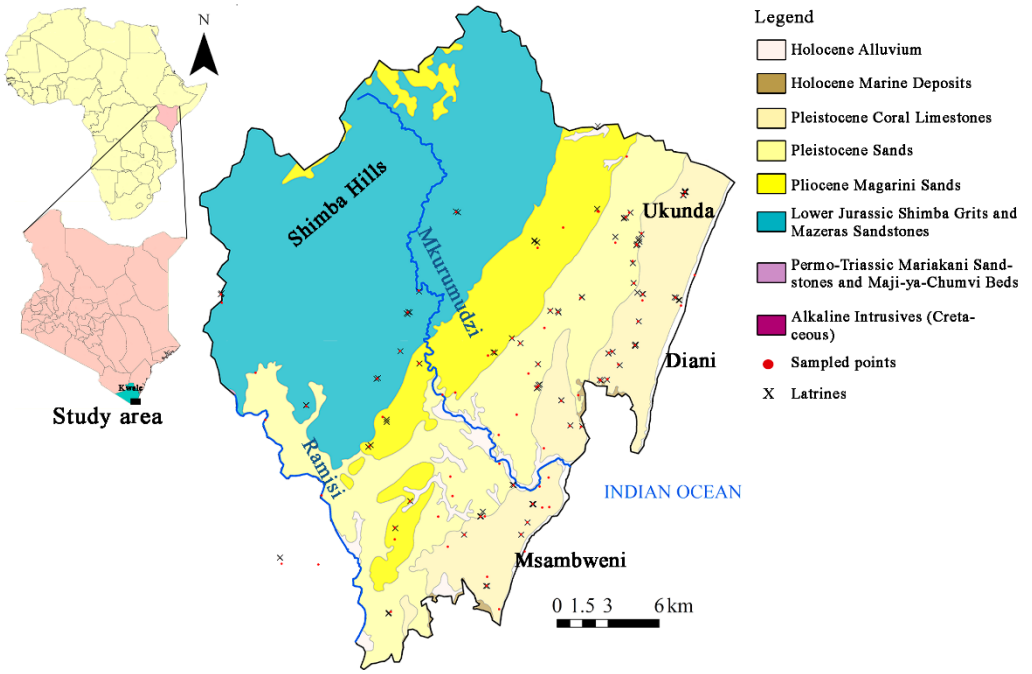

Figure 3.1. Study area with the geological units. The location of the sampled points and the latrines are displayed.

3.2.2. Water sampling

Two sampling campaigns were carried out in March 2016 (end of the dry season) and June 2016 (end of the wet season) to measure several hydrochemical and bacteriological parameters under different climate conditions. During the field surveys, the number of sampling points were 78 (March) and 77 (June), here including different sources: large diameter hand-dug wells, either uncovered or covered wells with or without a placed handpump, boreholes with handpumps, and deep boreholes, and all on the range of 30 to 80 meters depth. In addition, the main rivers in the study area, Mkurumudzi and Ramisi (Fig. 3.1), were also sampled.

Samples for hydrochemical analysis were taken from wells used daily by the population, explained in detail in Section 2.4.4. Bacteriological samples were taken using the same methodology just explained, except in those points in which a bucket was needed. In those cases, a stainless bucket previously sterilized with ethanol was used. In the waterpoints with handpumps, samples were taken at the outlet point, cleaned with ethanol before sampling was performed.

3.2.3. Physicochemical parameters and ion analyses

The methodology to measure the physicochemical parameters and the diverse ion analyses is described in detail in Section 2.4.4.

3.2.4. Bacteria concentration determination

Concentrations of *E. coli* were determined using Aquagenx Compartment Bag Test (CBT) (Aquagenx, 2015). CBTs allow for a quantitative assessment of *E. coli* concentration based on a most probable number (MPN) along with an upper 95 % confidence interval (Foster and Willetts, 2018; Gronewold et al., 2017; Stauber et al., 2014). MPN testing involves multiple presence/absence tests on different volumes of the same sample. Samples were collected in sterile purpose-made bags stored in a fridge during their transport and processed within 24h, 30h or 48h of collection, depending on temperature recommendations by the manufacturer (Stauber et al., 2014). MPN was calculated with data supplied by the manufacturer, here enclosed as Table 3.1, and based on the World Health Organization “Guidelines for Drinking Water Quality” 4th Edition, assigning risk categories of drinking water to *E. coli* levels ranges.

Table 3.1. E. coli risk categories of drinking water (modified from Aquagenx, 2015), and values assigned for the statistical analysis.

Sampled volume with colour changed	*Risk categories*	*Value assigned for the statistical analysis*
0/100 ml	Safe	0
1-10/100ml	Intermediate risk	1
11-100/100 ml	High risk	2
>100/100 ml	Very High risk/Unsafe	3

3.2.5. Sanitary risk inspections

A questionnaire comprised of 13 questions (Table 3.2), involving sanitary risk factors, was carried out based on Wright et al., (2013). Sanitary risk inspections were undertaken at each groundwater point. The first 10 questions were answered for all points, and the last 3 for hand-dug wells only. The questions were related to physical and sanitary conditions of all analysed wells and the presence of latrines according to different distances (<10, <30 or >30m.). Questions related to animal presence around the well or any important damage that could influence bacterial contamination were also included.

Table 3.2. Questions related to value the sanitary risk factors according to Wright et al. 2013.

Question 1	Does the cement floor extend more than 1.5 m from the well?
Question 2	Is there any ponding of water on the cement floor?
Question 3	Are there cracks in the cement floor which could permit water to enter the well?
Question 4	Is the pump loose where attached to the base, allowing water to enter the casing?
Question 5	Is the drainage channel cracked, broken or in need of cleaning?
Question 6	Do animals have access to within 10 m of the well?
Question 7	Are there any latrines within 10 m of the well?
Question 8	Are there any additional latrines within 30 m of the well?
Question 9	Are there any open water sources within 20 m of the borehole?
Question 10	Are there any uncapped wells within 30 m of the borehole?
Question 11	Is there any scattered waste within 30 m of the well?
Question 12	Is the cover of the well unsanitary?
Question 13	Is there any scattered waste inside the well?

3.2.6. Data analysis

Multivariate statistics is a suitable technique to treat big datasets involving different sorts of variables, from quantitative to categorical, and thus amenable to be used to combine biochemical, hydraulic, geological and external conditions (such as design, drilling characteristics. and maintenance) of groundwater points (Barba et al., 2019b). Principal Component Analysis (PCA) is a multivariate statistics method which involves the analysis of a number of parameters or variables, revealing associations between them, known as (vario)factors or components. Analyses were performed using the IBM-SPSS software.

The PCA analyses were subjected to Orthogonal Varimax rotation, first developed by Thompson (2004). This implies the rotation of the original system corresponding to the directions of largest variance in the dataset. Variables with loadings closer to ±1 indicate the strongest degree of linear correlations between variables, while values within the interval [-0.5, 0.5] indicate weak correlations. Prior to the extraction of the factors, the Kaiser-Meyer-Olkin (KMO) and the Bartlett sphericity tests were conducted to assess the suitability of the existing data for factor analysis. KMO returns values between 0 and 1, and values >0.50 are considered suitable for factor analysis (Hair et al., 1995; Tabachnik and Fidell, 2007). The Bartlett sphericity test checks if the observed correlation matrix diverges significantly from the identity matrix. It should be significant ($p<0.05$) for factor analysis to be suitable.

To assess which variables influence significantly the presence of *E. coli*, generalized mixed models with Poisson error distribution (Bates et al., 2015) were used. *E. coli* was included as a dependent variable, and covariates included correspond to the main principal component variofactors of the final PCA. Because of repeated measures were taken on the same waterpoint, "Sample ID" was modelled as a random factor. For all tests, the significance level was set at $\alpha = 0.05$ (two-tailed test). Overdispersion was tested and corrected if necessary by means of including the number of observation as a random factor (Broström and Holmberg, 2011). All analyses were run using R 3.5.1 (Team, 2018).

3.3.7. Selecting variables for the statistical analyses

Statistical parametric methods accomplish best when data follows a unimodal symmetric distribution (Paliy and Shankar, 2016). Therefore, in order to follow better with the assumption of PCA analysis, some variables from the initial dataset were grouped, transformed and/or eliminated. Following Barba et al., (2019b), non-Gaussian hydrochemical variables were transformed to log concentrations, these being Alkalinity, Eh (a proxy for redox conditions), and the concentrations of SO_4^{2-}, Na^+, Cl^-, and SiO_2. On the

other hand, TOC (Total Organic Carbon), DO (Dissolved Oxygen), and the concentrations of NO_3^- and NH_4^+, were added to the analysis as raw data without any transformation. Since the aim of the statistical analysis was to emphasize the correlations with the *E. coli* data, most redundant geochemical variables, such as Mg^{2+}, Ca^{2+} and K^+ were disregarded due to the strong correlation with other hydrochemical elements. The discrete (also termed categorical) variables were transformed to continuous ones based on a logical structure, as indicated in Table 3.3. Due to the cero variability in the response in the questions 4 and 5 of the questionnaire (Table 3.2), these two questions were not included in the analysis.

The variables included in the first sets of PCAs to value to correlation of *E. coli* with all type of water points were: geology; aquifer unit; type of well; sanitary risk factors (Questions 1, 2, 6, 7, 8, 9, 10); field parameters (conductivity, pH, TOC, alkalinity, DO, Eh); and hydrochemical parameters (NH_4^+, Cl^-, SO_4^{2-}, NO_3^-, Na, Si). The closest latrine was considered for every waterpoint, even if several were found nearby. The two field surveys were considered, using the date of each field campaign as a variable of seasonality.

The variables included in the second sets of PCAs, targeting to the correlation of the presence of *E. coli* with a subset of waterpoints, here only hand-dug wells and hand-dug wells with handpumps, were: the same as the previous mentioned, adding the variables (both expressed in m) water column as ($well\ depth - piezometric\ level$) and depth to groundwater level (GWL), which were only measured in these type of waterpoints. Furthermore, the questions related to sanitary risk factor included in the analysis were 1, 2, 3, 6, 7, 8, 10, 11, 12 and 13.

Table 3.3. Assigning categorical data to quantitative values to be included in the statistical analysis.

Variable	***Weights***	***Value assigned***	***Justification***
Geology	Pliocene sands	1	According to the aquifer units composition based on the conceptual model described in Chapter 2.
	Pleistocene sands	2	
	Pleistocene sands /corals	3	
	Pleistocene corals	4	
	Sandstones.	5	
Aquifer unit	Shallow aquifer	0	
	Deep aquifer	1	
Type of well	Hand-dug well	1	Increasing from the simplest structure to the most complex one.
	Hand-dug wells w/handpump	2	
	Handpump	3	
	Deep borehole	4	
Sanitary risk factors from questionnaire (Table 2)	No	0	
	Yes	1	

3.3. Results

3.3.1. E. coli quantification

33 of the 78 waterpoints sampled in March 2016 showed low-risk, meaning no *E. coli* colonies were detected; 5 waterpoints were classified as intermediate-risk, 12 as high-risk and 28 were in the range very high-risk/unsafe (Table 1, Appendix B). Samples from surface bodies (rivers) were classified as very high risk. In the June 2016 campaign, *E. coli* risk was measured in 77 waterpoints; 34 showed low-risk, (no *E. coli* colonies), 3 intermediate-risk, 15 high-risk, and 25 very high-risk/unsafe (Table 2, Appendix B).

72 samples were measured in both campaigns in which 13 % of the waterpoints reduced the *E. coli* risk from March to June, while 7 % of the points incremented the risk factor in the latter campaign with respect to the March one.

3.3.2. PCA results

Five different PCAs were carried out to evaluate all the information available and considering all type of wells/boreholes present in the study area (Table 3.4). Data from both sampling campaigns were included, and the samples for the surface water were not considered. We indicate, in the same table and for each statistical analysis performed, the extracted components and their variables, as well as the proportion of variance represented by each component. The measure of sampling adequacy (KMO test value) is reported. Furthermore, a brief explanation about the indication of each component is included for later discussion.

All type of groundwater points (wells/boreholes)

A first PCA_1 (Table 3.4) was conducted in order to observe which physicochemical variables displayed high correlation and to exclude those which would make the subsequent PCAs (3 to 5) redundant or masked (thus reducing reliability). The component four indicated that oxygen changes with seasonality, could be attributed to a slight increment in recharge of oxygenated water during the wet season (high DO values). PCA_2 (Table 3.4) was conducted in order to exclude the sanitary risk factors (Table 3.2) that do not add significant information in the subsequent analyses. Once the two firsts PCAs were conducted, the most redundant variables were detected, then removed from the list of variables, and additional PCAs were performed adding the variable representing the concentration of *E. coli*. PCA_3 (Table 3.4) thus contains the six most relevant hydrochemical variables from the first PCA_1 plus *E. coli* concentrations.

E. coli concentration was also added to seven selected variables from PCA_2 to perform PCA_4 (Table 3.4). Here, the first component shows a negative correlation between *E. coli* concentrations, Q1 "*Does the cement floor extend more than 1.5 m from the* well?", but positive correlation with Q8 *"Are there any additional latrines within 30 m of the well?"*, suggesting faecal bacterial pollution in wells located near latrines, and for not properly constructed wells. Notice that type of well and presence of cement floor (Q1) were positively correlated, as virtually all handpumps are cemented.

After conducting PCA_3 and PCA_4, the variables most correlated with the presence of *E. coli* were selected to conduct the final PCA_5 (Table 3.4), here including hydrochemical parameters, sanitary risk factors, latrine data and *E. coli* quantification, for a total of ten variables. Altogether, this indicates that all deep boreholes have handpumps (or pumps), and that the probability of faecal bacterial pollution increased with the presence of nearby latrines and with uncapped wells. The second component indicated a correlation between

Na concentration and the presence of cemented floor around the well, as the latter is common in waterpoints situated near the coast line, with seawater intrusion influence. The results of the PCA_5 are represented in Figure 3.2 in a projection on the plane corresponding to variofactors 1 and 2.

Once the final correlation between hydrogeological and non-hydrogeological parameters with the presence of *E. coli* was obtained, a new and final $PCA_{5.1}$ (Table 3.4) was performed including the same variables as PCA_5, but now removing *E. coli* from the set, thus in order to assess which variables influence most significantly the presence of *E. coli*. Based on the results of the $PCA_{5.1}$ a generalised mixed model with Poisson error distribution was performed, including principal components variofactors as covariates. The covariates affecting significantly the presence of *E. coli* were only C1 (Figure 3.3a; χ^2_1= 63.379; p < 0.001) and C2 (Figure 3.3b; χ^2_1= 3.852; p = 0.049), while C3 (χ^2_1= 2.655; p = 0.103) and C4 (χ^2_1= 0.199; p = 0.655) were not significant (p values exceeded 0.05), thus making the conclusions of PCA_5 even more robust.

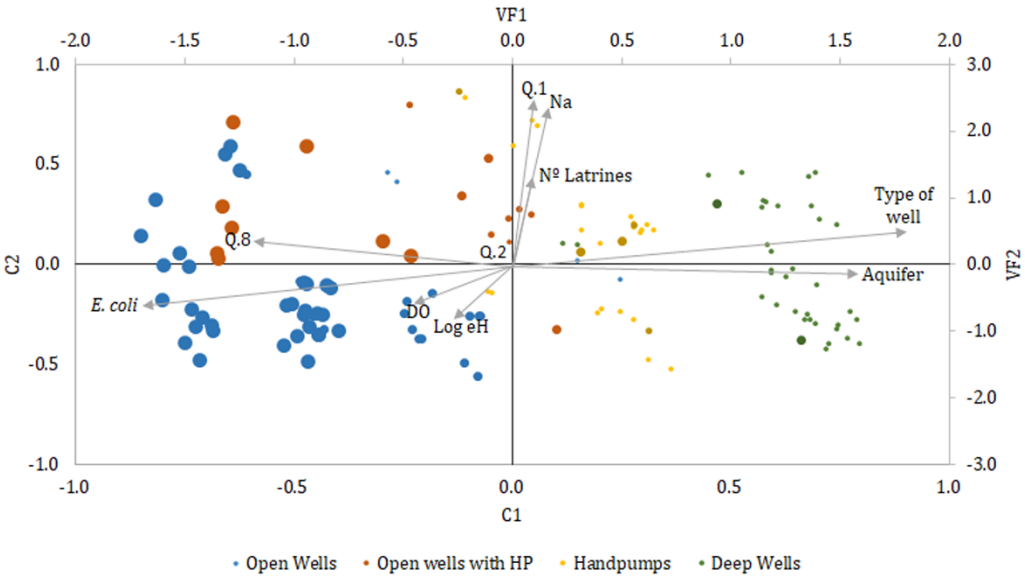

Figure 3.2. Main results of PCA_5. Samples are projected to variofactor space (VF1 and VF2 axes), and position of samples is scaled for visualization purposes. Size of the points increase with E. coli measurements. Grey arrows represent the contribution of each variable projected into the variofactor plane, so that components can be easily identified.

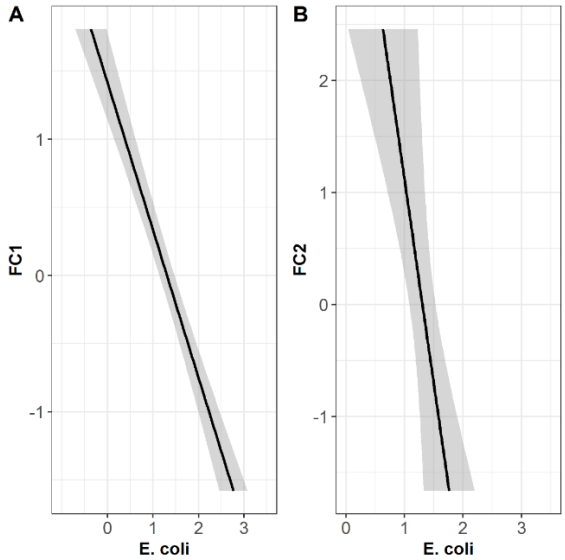

Figure 3.3. Significant relation between E. coli and variofactors 1 (A) and variofactors 2 (B) from $PCA_{5.1}$ considering all types of wells. E. coli ranges from safe (0) to unsafe (3) (Table 2.1).

Table 3.4. First components extracted from PCA analyses (bold indicates that the correlation is inverse);–log in geochemical variables indicates that log transformation was performed; Q indicates "question" (from Table 3.2.). For all PCA's the Bartlett sphericity test was significant ($p<0.001$).

Type of variables	***# of variables***	***PCA number***	***Extracted components***	***% of variance***	***Total of variance***	***KMO Test Value***	***Indication of each component***
Physicochemical parameters	14	PCA_1	C1: Geology, Log Cl^-, Log EC, Log Na, Log SO_4^{2-}	25.65	72.74	0,69	Major ions and geological setup
			C2: Aquifer unit, Geology, Log Si	15.18			Aquifer unit
			C3:NH_4^+, **Log Eh,** Log Alkalinity	11.38			Redox state
			C4: Date, DO	11.07			Oxygen as function of seasonality
			C5: NO_3^-, TOC	9.46			Nitrate correlated with TOC
Sanitary risk factor+latrine data	12	PCA_2	C1: Q6, **Type of well**	17.41	63.62	0,51	Deep boreholes mainly from the industries have a fence
			C2: Q1, Q9, Q10	13.34			Unknown explanation
			C3: **Num. Latrines,** distance latrines	12.44			Presence and distance from latrines
			C4: **Q7**	10.49			Isolated variable representing a statistical component
			C5: Q2	9.94			Isolated variable representing a statistical component
Physicochemical + E. coli	7	PCA_3	C1: **Aquifer unit**, *E. coli*	21.32	62.44	0,50	Highest presence of *E. coli* in the shallow aquifer
			C2: Date, DO	21.18			Oxygen as function of seasonality
			C3: **log Eh**, Na	19.94			Redox state
	8	PCA_4	C1: Q1, **Q8**, Type of well, ***E. coli***	26.31	59.55	0,60	Latrines nearby and bad well properties construction more *E. coli*

Sanitary risk + E. coli +latrine data			C2: Q10, Distance latrines	17.5			Unknown explanation
			C3:Q2, **Q7**	15.74			Unknown explanation
Physicochemical data + E. coli+Sanitary risk factor +latrine data	10	PCA_5	C1: Type of well, Aquifer unit, **Q8, *E. coli***	25.39	69.05	0,63	Main variables related to presence of *E. coli*
			C2: Log Na, Q1	15.74			Waterpoints located in the coastline (more Na+) have cemented floor
			C3: DO, log Eh, Num. Latrines	15.08			Eh partially depends on DO content
			C4: Q2	12.84			Isolated variable representing a statistical component
PCA_5 without E. coli	9	$PCA_{5.1}$	C1: Type of well, Aquifer unit, **Q8**	23.32	69.99	0,61	Main variables related to presence of *E. coli*
			C2: Log Na, Q1	17.49			Waterpoints located in the coastline (more Na+) have cemented floor
			C3: DO, log Eh, Num. Latrines	15.26			Eh partially depends on DO content
			C4: Q2	13.92			Isolated variable representing a statistical component

Hand-dug wells and Hand-dug wells with handpumps

Another way of reading Figure 3.3a is by noticing that hand-dug wells (either with or without handpumps) are the most polluted well types, with significantly high presence of *E. coli* in agreement with previous studies (Dayanti et al., 2018; Kilungo et al., 2018; Mzuga et al., 1998; Ugochukwu and Ojike, 2019). In order to find which variables are affecting the presence of *E. coli* in these most polluted points. Five new PCAs were performed now only including data from hand-dug wells. Therefore, we included here the variables only measured in this type of wells such as groundwater depth (GWL), groundwater column height within the well, and some specific sanitary risk factors related only to this type of waterpoints. Like the previous sets of PCAs both sampling surveys were included (Table 3.5).

As in the previous section, the first PCA_a (Table 3.5) was a preliminary screening of variables to select the ones providing information, thus allowing eliminating those that were redundant or irrelevant for the information point of view. A second analysis was conducted (PCA_b) (Table 3.5), considering only the sanitary risk factors from the questionnaire in Table 2 for this particular subset of waterpoints (thus, without the need to include here the variable "type of well"). Following the same scheme as in the previous set, these two PCAs were followed by two more where the variable *E. coli* is added. PCA_c included selected hydrochemical variable and *E. coli*. PCA_d included sanitary risk factors (selected from the results of PCA_b) and the variable *E. coli*, for a total of nine variables.

PCA_e involved nine variables including hydrochemical, risk factor variables and presence of *E. coli* in the same subset of waterpoints. In component two, *E. coli* showed inverse correlation with depth to groundwater level, water column and Eh. In general, despite the uniformity in the physical and chemical properties in the water column, a prominent stratification of microbial groups was observed (consisted with Karlov et al., (2008). The inverse correlation between *E. coli* and the water column suggested preferential presence of faecal bacteria when the water column was low. Results of PCA_e are represented in Figure 3.4 in a projection on the plane corresponding to variofactors 1 and 2.

Finally, $PCA_{e.1}$ was performed including the same variables as PCA_e, just excluding *E. coli*. In short, the components obtained were very similar to those from PCA_e, thus indicating robustness in the previous analysis. From the results of $PCA_{e.1}$, a generalised mixed model with Poisson error distribution was performed including principal components variofactors as covariates. The analysis indicates that the covariates affecting significantly the presence of *E. coli* only in hand-dug well and hand-dug well with handpumps were C1 (Figure 3.5a; $\chi^2_1 = 7.399$; $p = 0.006$) -sanitary issues- and C2 (Figure 3.5b; $\chi^2_1 = 4.496$; $p =$

0.033) -redox state related to GW levels-, while C3 (χ^2_1= 1.388; p = 0.238), as well as subsequent components, were not found significant.

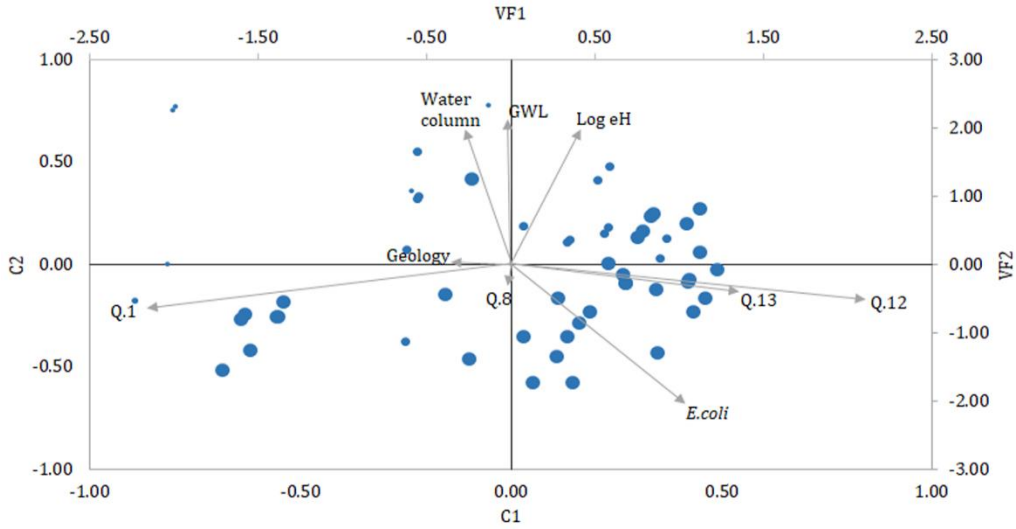

Figure 3.4. Main results of PCA$_e$. Samples are projected to variofactor space (VF1 and VF2 axes), and position of samples is scaled for visualization purposes. Size of the points is according to E. coli measurements. Grey arrows represent the contribution of each variable projected into the variofactor plane, so that components can be easily identified.

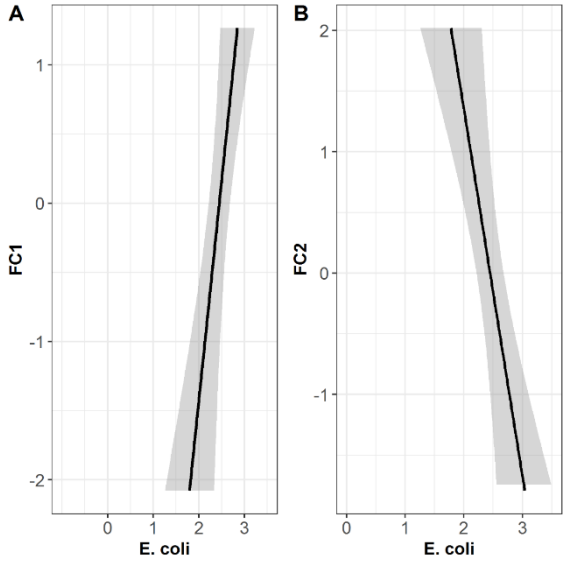

Figure 3.5. Significant relation between E. coli and variofactors V1 (A) and V2 (B) from PCAe.1 considering only hand-dug wells and hand-dug wells with handpumps. E. coli ranges from safe (0) to Unsafe (3).

Table 3.5. Relation to main correlations among variables obtained by PCA analysis. Negative correlations displayed in bold); –log in geochemical variables indicates that log transformation was performed; each PCA includes. For all PCA's the Bartlett sphericity test was significant ($p<0.001$).

Type of variables	***#of variables***	***PCA number***	***Extracted components***	***% of variance***	***Total of variance***	***KMO Test Value***	***Indication of each component***
Physicochemical parameters	15	PCA_a	C1: Geology, Log EC, Log Na, Log Cl^-, Log SO_4^{2-}	23.02	86.72	0,540	Major ions and geological setup
			C2:Geology, Log EC, Log Alkalinity, GWL	15.32			GWL in function of geology and chemical properties
			C3:Date, DO	11.57			Oxygen as function of seasonality
			C4:**NO_3^-**, Log Si	10.42			Flux indicators
			C5: GWL, Water Column	9.86			Water levels
			C6: Log Eh, **NH_4^+**	8.96			Redox state
			C7: TOC	7.57			Isolated variable representing a statistical component
Sanitary risk data	12	PCA_b	C1:Q6, **Num. Latrines**	23.02	71.13	0,564	Latrines located inside the main villages in the coast, where animals have no physical access
			C2:Q1, Q3, Q10	15.32			Well construction and maintenance parameters
			C3: Q8, Q12, Q13	11.57			Pollution and sanitary conditions that is presence of latrines
			C4: Q11	11.04			Isolated variable representing a statistical component
			C5: Q2, **Distance Latrines**	10.18			Unknown explanation
Physicochemical + E. coli	8	PCA_c	C1: Log Eh, ***E. coli,*** Water Column, DO, TOC, Geology	55.09	72.16	0,805	Higher *E. coli* concentrations as the water columns decrease; also *E. coli* correlates to redox potential (Eh, DO) and presence of organic carbon

			C2: NO_3^-, GWL	17.07			The largest villages with NO_3^- pollution are located near the coast where the groundwater level is shallow
Sanitary risk + E. coli	9	PCA_d	C1: **Q1**, Q12, Q13, *E. coli*	26.97	69.2	0,573	*E. coli* positively correlated with that of unsanitary well cover, and waste inside the well , and inversely with the present of cement floor
			C2: Q6, **Q8**	14.4			Latrines located inside the main villages in the coast, where animals have no physical access
			C3: Q11	13.97			Isolated variable representing a statistical component
			C4: Q2, Q3	13.86			Potential sanitary conditions caused by direct water infiltration
Physicochemical + E. coli+*Sanitary risk data*	9	PCA_e	C1: **Q1**, Q12, Q13	20.64	68.91	0,517	Unsanitary well cover, and waste inside the well , and inversely with the present of cement floor
			C2:Log Eh, ***E. coli,*** Water column, GWL	19.45			*E. coli* inverse correlated with depth to groundwater level, water column and Eh
			C3:Q8, Q13, Water column	15.93			Latrines and scattered waste inside open well
			C4: Geology	12.89			Isolated variable representing a statistical component
PCA_e without E. coli	8	$PCA_{e.1}$	C1: **Q1**, Q12, Q13	24.41	60.71	0,497	Unsanitary well cover, and waste inside the well , and inversely with the present of cement floor
			C2:Log Eh, Water column, GWL	18.71			*E. coli* inverse correlated with depth to groundwater level, water column and Eh
			C3:Q8, Water column	17.59			Latrines and scattered waste inside open well

3.4. Discussion

In the study area, a coastal rural area in South-East Kenia, it was observed that microbiological pollution levels exceeded the WHO drinking water quality recommendations in almost all the waterpoints analysed. We could not find any direct relation of geology to *E. coli* pollution, although in other cases we believe that geology could be a significant factor, as it might drive fast/slow recharge.

Most bacteriological problems in supply waterpoints can be associated to improper well design, bad construction, and/or insufficient maintenance practices. (Lutterodt et al., (2018) already points out that shallow hand-dug wells have more pollution and sanitary issues as compared to boreholes. In this study, well type (or design) is the variable most controlling the presence of *E. coli.* Inadequate maintenance of hand pumps, improper sanitation and unhygienic conditions around the waterpoints, are factors that may contribute to faecal contamination. Our results are in line with those of several authors (Lin et al., 2018; Nkini et al., 2006; Sukumaran et al., 2015), since unsanitary covers and litter scattered inside (or around) the well strongly result in the presence of *E. coli* in hand-dug wells, regardless of the presence of handpumps. Furthermore, the extension of the cement floor around the waterpoints, is found to be an important factor affecting *E. coli* presence, since a smaller protection by cementation could imply short transit times (direct injection of bacteria) through the non-saturated zones.

The highest counts of faecal bacteria were observed near human settlements. Unlike other studies that suggest that groundwater faecal pollution is influenced by seasonal changes (Howard et al., 2003) and is significantly higher during the wet season compared to the dry season (Kayembe et al., 2018), the present study does not show any difference in *E. coli* quantification between seasons. This could be explained due to the low precipitation during the wet season in 2016, when the study area was affected by La Niña event, with an estimated 69 % reduction in recharge compared to average values as stated in Chapter 2. Actually, in the study area, it was observed that *E. Coli* concentration values increased during low groundwater levels mostly in dry season, related most probably to direct input of bacteria (either for well construction or maintenance conditions) into small volumes of water. Future research is needed to understand the actual causality of this correlation, since longer and more recurrent droughts will be expected under future climate change conditions that in sub-Saharan Africa might imply the lowering of groundwater levels, causing a potential cascading effect on water availability and quality.

Some geochemical variables displayed a strong correlation with the registered concentrations of *E. coli.* Yet, in some cases it is only due to some external factor that

explains both variables together. An example, is Na^+ concentrations. In the study area, Na^+ and *E. coli* concentrations display a significant negative correlation; low Na^+ and high *E. coli* concentration values were found in the wells located in the Magarini and Kilindini sands. This geological formation shows low transit time through the unsaturated zone (recall Chapter 2) and thus less attenuation capacity of the soil. Therefore, high *E. coli* counts reach the shallow aquifer. These observations are in line with Howard et al., (2003), who suggested that fast recharge is the major cause of microbiological contamination, and underpins that the use of hydrochemical and isotopical data, routinely used to evaluate transit times in aquifer systems, might also be used as indicators of the presence or absence of faecal pollution in other study areas in similar realities.

Regarding the risk factors affecting all type of waterpoints, this study confirms that the presence of leaching pit latrines in the vicinity of supply wells is a clear driver of faecal pollution, causing serious concerns for the public, as already shown in Howard et al., 2003; Graham and Polizzotto, 2013; Martínez-Santos et al., 2017; Prüss-Ustün et al., 2016; Schmoll et al., 2006. This effect increases whenever there is a general lack of physical barriers (e.g., concrete) in the latrines between stored excreta and soil and/or groundwater (Van Ryneveld and Fourie, 1997). Despite the presence of *E. coli* in the study area is correlated to the presence of pit latrines within 30 m from the well, it is not correlated to the actual number of latrines in the vicinity; this could indicate that one latrine is enough to cause pollution at the well, becoming irrelevant the actual number of them.

Redox condition shows a positive correlation with dissolved oxygen, number of latrines and *E. coli* concentration. The latter are an obvious source of oxygenated water with a large organic matter and bacteria loads. Low values of Eh results in enhanced transport of bacteria in groundwater. *E. coli* is also correlated again to water levels; thick non-saturated zones increase water transit times from the surface to the aquifer, reducing aquifer vulnerability to pollution. As Weldeyohannes et al. (2018) show, the levels of *E. coli* decrease dramatically (below detection limits) when the vadose zone is more than 0.9 m thick. This could be due to the additional mechanisms in the unsaturated zone favouring colloid/bacterial retention at the solid-water interfaces (Sepehrnia et al., 2018a). This effect might counteract that of bacteria increasing with reducing water levels mentioned before; a reduction of the saturated thickness also results in an increase in the unsaturated area that can allow a greater retention of faecal bacteria in the unsaturated zone.

A management strategy to reduce sanitary risks related with groundwater supply should focus on the correct construction of the wells to improve the isolation of the waterpoints to possible external contaminants. One possible solution should imply drilling of shallow

boreholes with handpumps totally protected. Furthermore, despite they are less affordable, drilling deep boreholes seem to be the safest solution, but could result in groundwater that are in anaerobic conditions, with the need for additional treatment. Well maintenance, protection of waterpoints (preventing water ponding around, and with sanitation coverage implementation), and sanitary practices are a must, and should be emphasized; as a consequence, awareness and sensitization campaigns to eradicate malpractices should be carried out.

3.5. Conclusions

While the presence of faecal bacteria in domestic supply wells has been acknowledged for decades, no study until the present discriminate and quantify how the combination of hydrogeological and non-hydrogeological parameters correlate with the presence of *E. coli* as a proxy of faecal pollution. Therefore, a number of qualitative and quantitative variables combining geological, hydrological, geochemical, sanitary risk factors, well types, and maintenance variables have been statistical analysed for correlations with *E. coli* concentrations in a coastal area of Sub-Saharan Africa, with high presence of faecal bacteria in the groundwater used to supply the population.

This study demonstrates that including in a PCA different type of variables, such as cited previously, is a useful methodology to obtain precise information of the relations between all those variables, most times separated in analysis (e.g., in modelling efforts). Furthermore, this study goes a step forward when trying to assess which variables are related to faecal bacteria pollution by providing reliable information on which of these variable significantly influence the presence of *E. coli*. Thus, including PCA variofactors as a covariate in mixed models might become a useful tool when working regions in order to compare different areas, as well as to assess the main factors influencing *E. coli* and/or the presence of other pathogens.

Despite the geological formation itself has not shown a direct relation to *E. coli* pollution, different certain hydrogeological properties (capacity of colloids retention, flow velocity, redox condition, etc) could be related. Therefore, the way to include geology when the risk pollution is evaluated should be according to hydrogeological properties more than just the geological formation where the waterpoints are located.

This methodology has confirmed in a quantitative way that the well constructive characteristics are most important to avoid bacteria presence in groundwater in the field. Extended cement floor would reduce the presence of faecal bacteria pollution, being more

important in those areas where the water infiltrates fast through the unsaturated zone. Furthermore, knowing the geochemical elements, indicators of transit time, and groundwater depth, could be a good indicative of faecal bacteria presence. Hence, easy hydrogeological and geochemical measurements such as Eh and water column, easy to identify and measure, can help identifying the presence of faecal bacteria. The former can be related to the presence of input water with high organic matter load (indicating the presence of nearby latrines), while the latter is related to climate and to well operation conditions.

The authors gratefully acknowledge the support of Kenya's Water Resource Authority (formerly WRA), the Kwale Country Government, Base Titanium Ltd., Kwale International Sugar Company Ltd. and Rural Focus Ltd (RFL). This research was funded by the UK Government via NERC, ESRC and DFID as part of the Gro for GooD project (UPGro Consortium Grant: NE/M008894/1).

Chapter 4

Sustainability of the aquifer system under new abstraction rate by water-reliant industries

Ferrer, N., Folch, A., Lane, M., Olago, D., Katuva, J.,Thomson, P., Jou, S., Hope, R., Custodio, E., 2019. How does water-reliant industries affect groundwater systems in coastal Kenya? Manuscript submitted.

4.1. Introduction

The exploitation of groundwater generates different types of negative externalities (Giannoccaro et al., 2017): (i) reduced availability of the resource for other current or future uses; (ii) increase in extraction costs; (iii) possible risk of water quality degradation; and (iv) damage to groundwater dependent ecosystems. If the exploitation of groundwater occurs close to the coastline, other negative externalities and costs are generated: (i) reduction of groundwater supply due to enhanced corrosion and well failure; (ii) health problems; (iii) negative effects on agriculture, since crop, land quality and cropping area potentially decrease (SASMIE, 2017).

The expected increase in abstraction must be considered together with the expected increase in droughts in dry periods and precipitation in wet periods (Solomon and Qin, 2013; Stocker et al., 2013). Climate change will affect hydrogeological system dynamics and their water resources quality (Mas-Pla and Menció, 2018). For example, aquifer recharge reduction caused by climate changes is an important factor in aquifer salinization (Oiro and Comte, 2019). The increased abstraction is poorly compatible with the sustainable use of coastal aquifers where there is a high population density and where tourism is concentrated (Dhar and Datta, 2009; Mantoglou, 2003; Okello et al., 2015b), since the use of coastal groundwater is compromised by salinization (Michael et al., 2017). Many coastal aquifers in the world are currently experiencing intensive saltwater intrusion (SWI) caused by both natural and man-induced processes (Custodio, 2010; De Filippis et al., 2016a, 2016b; SASMIE, 2017; Adrian D. Werner et al., 2013).

In the last couple of decades many African countries have seen unprecedented economic growth rates, and this has drawn the region into the global limelight (World Bank, 2013). This industrialization process has led to an overall increase in groundwater abstraction in most African countries (Adelana and MacDonald, 2008). The drilling of new deep boreholes with higher abstraction rates than traditional dug wells or shallow borehole handpumps has increased in many areas to meet the water demands of these new economic activities (Comte et al., 2016).

The high socio-economic and ecological importance of groundwater and the fact that groundwater is an important strategic resource are recognised throughout developing countries. However, data on groundwater systems are sparse and the current state of knowledge is poor (Pavelic et al., 2012). Most of the time the data that are available are often spatially and temporally inconsistent (Candela et al., 2014) These are serious limitations for the sustainable development of groundwater resources (Gaye and Tindimugaya, 2018). Key aquifers need urgent characterization to change the current

situation, in which development proceeds with insufficient aquifer knowledge (Olago, 2018). One of the main challenges when studying these aspects is the lack of information, especially with respect to abstraction data and the location of abstraction well fields, in order to determine the possible future impacts at the local and/or regional scale on groundwater systems.

A study by Pavelic et al. (2012) emphasizes that data on groundwater systems throughout Sub-Saharan Africa SSA is sparse, so the current state of knowledge creates a barrier to sustainable groundwater development. In order to define realistic local management policy it is essential to understand groundwater use and users. One of the major challenges to proper governance is lack of scientific and technical knowledge about aquifers. Without adequate technical understanding of aquifers, actors may not properly identify the source of aquifer pollution or depletion and may be prone to blaming each other for mismanagement (IGRAC, 2019). Thus, in the absence of coordinated efforts to manage aquifers, it is unlikely that any advanced technical understanding will be achieved. This paradox is the crux of the groundwater governance challenge and perhaps explains why effective groundwater governance regimes are still elusive today.

Therefore, the aim of this study is to assess how increased competition for water may be affecting groundwater systems by analysing the sustainability of new abstraction regimes in the study area. Kenya is examined, where new water-reliant industries have been established since 2012. This should avoid repeating the errors made in many areas worldwide, such as in the Mediterranean basin, where some coastal aquifers were salinized decades ago by tourism, industrial and agricultural groundwater abstraction and where local economies suffered the consequences, costs and expenses of developing the new water sources that were required (SASMIE, 2017). Aquifer sustainability has been assessed during a drought period caused by the 2016 La Niña event (Uhe et al., 2018), and during the following recovery period after the significant rains of 2017. Knowing the aquifer behavior under different climatic conditions can help decision making in the future, and assist in ensuring sustainable use of the groundwater system.

4.2. Study area

The study site is defined in Section 1.3 of the present document. From what is said before adding that there are around 300 handpumps providing drinking water to local communities, schools and healthcare centres scattered across the study area. These handpumps are used daily by the population to fill buckets for different purposes, such as drinking and domestic water uses. The coastal strip has a long established coastal tourism

industry at Diani. Most of the hotels are located in the coastal area in the north of the study area. Furthermore, Ukunda area has many private homes that have their own shallow well or borehole. In the last two decades, the acquisition of small parcels of land has increased in this area to build bungalows/maisonettes for which the source of water for construction and supply is often groundwater.

The two major economic activities established in the study area are defined below: The Special Mining Lease operated by Base Titanium cover 1661 ha. The Project resource comprises two dunes that contain economically viable concentrations of heavy minerals. These two areas are separated by the Mkurumudzi River (Fig. 1.1). Mine construction was completed at the end of 2013 and the first bulk shipment of mineral departed from Mombasa in February 2014. Projected 2019 production is up to 450,000 tonnes of ilmenite; 93,000 tonnes of rutile (14 % of the world's rutile output); and 37,000 tonnes of zircon. The total mineral resource on 30th June 2018 were estimated to be 134 million tonnes.

Currently KISCOL's sugarcane fields occupy a total area of 5500 ha, of which 4100 ha have been put to cultivation of sugarcane since 2008; 800 ha are currently under sub-surface drip irrigation. The fields are located in the Kinondo, Milalani/Shirazi and Nikaphu areas, the last one being located south of the study area (Fig. 1.1). The factory has the capacity to crush 3000 tonnes of cane per day and it is projected to produce 3500 tonnes/day of sugar at full capacity, self-generating 18 MW of electricity in a bagasse-fired power plant, and producing around 50,000 L/day of ethanol (http://www.kwale-group.com). The planned area for irrigated (not rain-fed) sugar at KISCOL is 3000 ha, to be achieved when all dams and the bulk water system (BWS) is completed in the coming years.

4.2.1. Climate

The area experiences a bimodal rainfall pattern: 1) From May 2016 to early 2017, the study area experienced unusually dry conditions. Local weather data (Kwale Agricultural Department Station KMD 9439001 in Kwale) suggest that this period represents one of the most extreme droughts since 1974 in this area (recall Section 2.2).

4.2.2. Hydrogeology

The conceptual model of the groundwater system has been defined in detail in Chapter 2.

4.3. Methodology

4.3.1. Recharge estimation

In order to assess the sustainability of the aquifer system during the 2016 La Niña drought, the total recharge to the aquifers of the study area has to be known, which is the main input of the system as stated in Section 2.5.2. The recharge was calculated following the methodology, based on the soil water balance for the period 2010-2017 (recall Section 2.4).

In that study, groundwater recharge was calculated for each land cover type and each soil type, following the process presented in the Figure 1, Appendix C. Rainfall data and meteorological parameters were obtained from three different stations for the period 2010-2015. At the end of 2015, 11 manual rain gauge stations were established, spread around the study area. These new data improved the accuracy of recharge estimation. During 2016-2017, temperature data were obtained from the Trans-African HydroMeteorological Observatory (TAHMO) stations (www.tahmo.org) (Fig. 4.1).

Table 4.1. Rainfall and temperature data from different meteorological stations used to calculate groundwater recharge. The location of each station is shown in Figure 4.2.

Rainfall & Temperature 2010-2015	***Rainfall from manual rain gauge station 2016-2017***	***Temperature 2016-2017***
SWAT Nº 45395	Boyani station	TAHMO Kidongo gate
	Footprints	
	Kidongo gate	
	KISCOL	
	Muhaka ICIPE	
SWAT Nº45394	Mwachande	TAHMO Msambweni SACO
	KISCOL	
	Muhaka	
SWAT Nº42397	Hobo Msambweni	TAHMO Msambweni SACO
	Jabalini	
	KISCOL	
	Mwachande	

4.3.2. Hydrochemical data

In order to assess the possible effects of the water-reliant industries on the groundwater system, hydrochemical field data obtained during La Niña event in 2016 were used (recall Chapter 2).

In order to study the aquifer recovery after La Niña event, hitherto not studied, the groundwater level and electrical conductivity (EC) of 23 points were measured in Magarini sands, Kilindini sands and the Pleistocene corals every two weeks from 4 m bgl to 27 m bgl (below ground level) after La Niña event, until December 2017. These points are part of a monitoring network in which groundwater levels and physicochemical parameters were measured every two weeks. Fortnightly groundwater levels (2012-2017) measured by Base Titanium in its monitoring network have also been used to study the aquifer evolution as well as the potential interaction between the shallow and the deep aquifer during the study period.

To represent EC evolution in the study area, this information was mapped for each of the seven field surveys using ArcGis 10.0 software, and the hydrogeochemical analysis tool QUIMET (Velasco et al., 2014). To represent the spatial distribution of the variables, the Inverse Distance Weighting (IDW) method was used, which is a deterministic method that allows multivariate interpolation from a set of known scattered points. The EC data were obtained from different wells measured during the field surveys carried out in the study area in September 2013, March 2014, June 2014, March-May 2015, and September 2015. The physiochemical parameters measured in situ were temperature, pH and EC_{25} (electric conductivity at 25 ºC) by means of a Hanna Instruments meter.

In order to understand the geochemical processes occurring in the area affected by seawater intrusion (SWI), a geochemical modelling exercise was carried out to understand the long-term evolution in this geological context and the potential impacts of SWI dynamics. Given the composition of the Pleistocene corals, different geochemical models considering several conceptual hydrogeological models were generated to understand which reactions are taking place, to what extent, under which conditions, and how water quality and aquifer mineralogy could change due to SWI.

PHREEQC software was used to simulate the mixing between fresh groundwater located inland in the Pleistocene formation with EC < 1000 µS/cm and one sample from the saline water upwelling on the beach (Diani), which is 83 % seawater according to chloride concentration (Table 1, Appendix C). A total of 20 mixed waters were simulated, each under 5 different conceptual hydrogeological scenarios: 1) initial and mixing solutions in

equilibrium with calcite; 2) initial and mixing solutions in equilibrium with calcite and dolomite; 3) none of the samples in equilibrium with calcite or with dolomite; 4) only the initial solution in equilibrium with calcite; and 5) both end member solutions in equilibrium with calcite and dolomite, but not the mixed waters.

4.4. Abstraction data and future estimation

One of the main challenges when studying this kind of area is the lack of information, especially abstraction data and the location of production boreholes. It proved very helpful to integrate information from the Water Resources Authority (WRA) and from groundwater users in the area (particularly the mining and sugar companies). The abstraction permits for each economic activity were obtained from the Water Resources Authority (WRA). The WRA data comprised the permitted daily well/borehole abstraction volumes for individual consumers and companies, such as Base, KISCOL, the hotels in the South Coast, and community boreholes. However, not all the abstraction data from the different water users have the same accuracy.

Base Titanium provided daily abstraction data from the end of 2013 to 2017. These actual abstraction estimates are very accurate. Unlike Base Titanium, KISCOL's actual abstraction rates were not available. However, the company report that they control drip irrigation by means of soil humidity sensors to conserve water. Therefore, KISCOL's estimated monthly abstraction is based on soil evaporation deficit (ETD). The ETD is the difference between potential evapotranspiration and actual evapotranspiration under natural conditions, which gives the minimum amount of irrigation water required to maintain the soil moisture that allows the crop to get the water it needs. Multiplying the ETD by the KISCOL irrigation area, the minimum crop water requirement (MCWR) is obtained.

Observed groundwater abstraction was available for only one hotel located at the coast in Zone 4. Therefore, a complementary estimate of hotel abstractions using other data sources was made. Hotel locations, both those with and without WRA permit data, were obtained from Google Earth. The number of rooms for each hotel and the hotels' class were collected from the TripAdvisor webpage. Total groundwater volume consumed by hotels was estimated using the consumptions specified in the Practice Manual for Water Supply Services in Kenya (2005) for each type of hotel, assuming a water use of 600 L/day per bed for high class hotels and 300 L/day per bed for medium class. For 35 % of the hotels identified from Google Earth, interviews with hotel managers validated consumption data. The Kenya National Bureau of Statistics (KNBS) provided bed occupancy data for the South Coast 2015 to 2017. Despite hotel abstraction data does not present the same degree of

accuracy as Base Titanium data, using this methodology it is possible to estimate the order of magnitude of hotel abstraction.

The average abstraction of the community handpumps was obtained from Water point Data Transmitters (WDTs), which provide reliable real-time data on handpump usage (Thomson et al., 2012). Using a low cost integrated circuit (IC) based accelerometer, the WDT automatically monitors the number of strokes made in operating a handpump and then transmits this information to a computer over the GSM network. Volumetric abstraction was calculated from the accelerometer data for the period 2014-2015. These data provide information on hourly pump use.

The abstraction of the water-reliant industries will increase in the near future; Base Titanium planned to drill more boreholes within the same wellfield, thus increasing the total groundwater abstracted. In the absence of any better estimates, we arbitrarily assumed a 20 % increase in groundwater abstraction for irrigated sugar. The Draft Kwale Water Master Plan has assumed a 1 % growth per year in water demand for the tourism sector over the next 20 years. In order to supply more water to the population, the Water Supply Master Plan (2018) for Mombasa and other towns within the Coast Province (CWSB, 2016) has proposed developing the Msambweni wellfield to meet future demand for the middle and south coast zones. This is the considered future scenario for groundwater abstraction.

4.5. Results

This section presents all the results analysed in order to determine the sustainability of the groundwater system. First of all, the recharge from 2010-2017 and its change is assessed, since it is the main water input of the system and key to understanding the water budget. Secondly, abstraction for each groundwater use is estimated and used as outputs from the groundwater system. In the third component, the groundwater level evolution is analysed as the main indicator of storage changes in the system, showing the relationship between system inputs and outputs. To evaluate the system in the coastal zone, where groundwater quality plays an important role in the sustainability of the system, the evolution of electrical conductivity (as a proxy for salinity) is analysed. Finally, the results of the geochemical models, which are needed to understand the geochemical processes occurring in the area affected by seawater intrusion, are also presented.

4.5.1. Recharge

Total recharge volume was calculated for an area of 660 km^2. This area is bigger than the four study Zones (Fig. 1.1), covering the recharge area of the shallow and deep aquifers from the sea to the Shimba Hills. While the shallow aquifer is recharged directly from the surface, the underlying deep aquifer is recharged from the Shimba Hills. To estimate recharge across the study area, 123 soil water balances were calculated (Fig. 4.1).

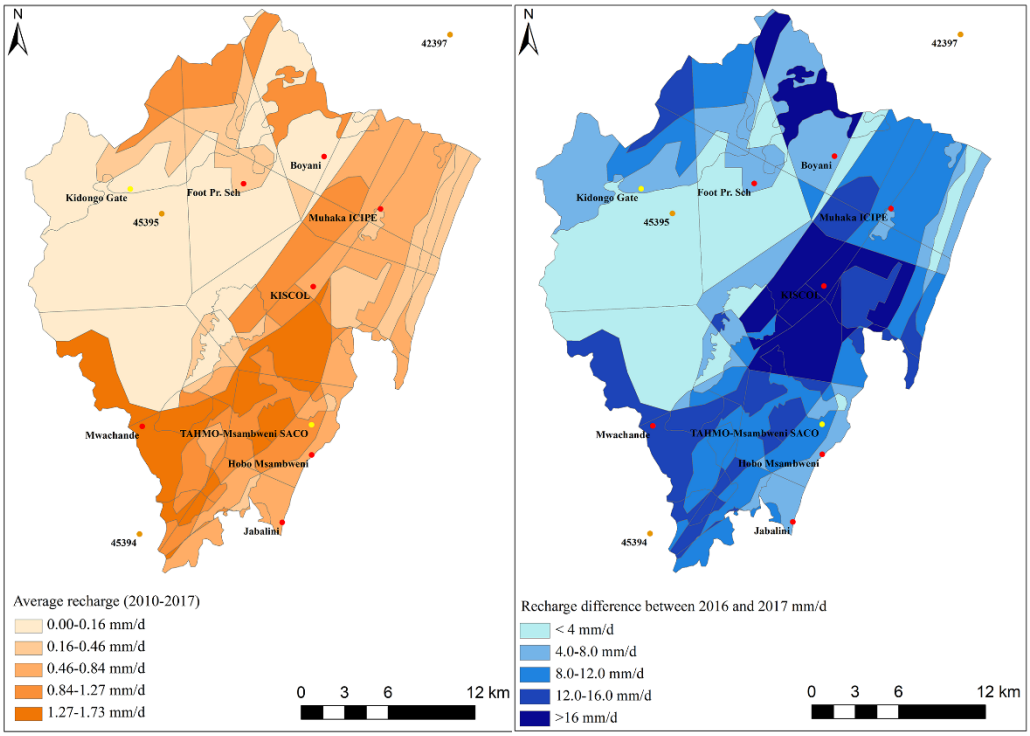

Figure 4.1. (Left) Average recharge from 2010 to 2017 in mm/d. (Right) Recharge difference between La Niña (2016) and a normal climatic year (2017). The coloured dots are the meteorological stations used to calculate the net recharge.

The spatial distribution of recharge follows the rainfall spatial pattern. Higher recharge occurs near the coast and decreases inland, west of Shimba Hills. However, in the eastern Shimba Hills (around 450 m a.s.l., see Fig. 1.1) recharge is higher. The highest average recharge volume for the period 2010-2017 occurred in areas underlain by ferralic arenosols, which have low usable soil water reserves (UR). Some areas overlying the shallow aquifer in the Kilindini and Magarini sands also have this type of soil. On the contrary, lower average recharge occurs in areas with high UR ferric acrisols. These soils are mainly located on the Mazeras sandstone, in the Shimba Hills.

The total recharge during La Niña in 2016 was 58 MCM/year, 74 % less compared to 2017 (224 MCM/year). A comparison of recharge during La Niña with previous years (Table 4.2) shows that there is minimal correlation between total annual rainfall and total annual recharge. This is because the rainfall intensity and distribution through the year influences net recharge, rather than the total annual volume of rainfall. High rainfall peaks produced by intense but short storms are more effective in driving recharge than lower, more continuous rainfall. An intense rainfall event (>100mm) on a saturated catchment leads to intense and significant recharge. This is consistent with other studies on the phenomenon (Taylor et al., 2012; Taylor and Jasechko, 2015). The recharge volume represents 7 % of the annual rainfall in the driest years, but up to 23 % in 2017.

Table 4.2. Annual precipitation in mm/year obtained from the different meteorological stations located in the study area (Table 1) and the annual recharge volume in MCM/year.

Year	**Precipitation** *(mm/year)*	**Recharge** *(MCM/year)*
2010	1022	71
2011	1406	160
2012	987	50
2013	1154	86
2014	1715	156
2015	1757	169
2016	867	58
2017	1442	224

4.5.2. Groundwater use by water-reliant industry

In this sub-section we present a detailed description of each water-reliant user in the area and its abstraction rate estimate.

Base Titanium Ltd

The mining company constructed and commissioned an 8.4 MCM water supply dam on the Mkurumudzi River to meet most of its water requirements for mining. This supply is backed up by a wellfield comprising four, 95-105 meter deep boreholes. At the end of 2013, both surface and groundwater were abstracted to start the mine. The average abstraction for a

"normal climate year" such as 2014 and 2015 was 1449 and 1806 m^3/day, respectively. However, during the 2016 La Niña event, this abstraction increased by around 66 % to 4272 m^3/day on average (Table 4.3). After La Niña event, the daily average abstraction fell by around 26 % (3370 m^3/d) in 2017, compared to 2016 (Fig. 4.2). It should be pointed out that Base Titanium recycles a considerable proportion of process water: in 2016, it recycled >70 % of the total daily water use. It improved in 2017, recycling around 78 %.

The mine site is located on the Pliocene formation but the Base wellfield is on the Kilindini sands (Pleistocene) east of the mine. These production wells are screened in the deep aquifer, to ensure that groundwater is pumped only from the Jurassic and Triassic formations. This was a deliberate design philosophy to reduce as much as possible adverse effects to the shallow aquifer that local communities use for water supply.

Adjacent to each operational borehole a shallow and deep monitoring piezometer measures the groundwater level fluctuations under baseline conditions and due to subsequent abstraction. Under natural conditions before abstraction started in 2013, the deep groundwater levels were higher than the shallow groundwater levels as the piezometric control area of the confined deep aquifer is at a higher elevation, in the Shimba Hills. Once abstraction started at the end of 2013, the shallow piezometric trend shows a limited effect of pumping from the deep aquifer, maintaining the hydraulic relationship between the shallow and deep aquifer, except sporadically due to occasionally higher abstraction rates, as in April 2014 (Fig. 4.2). However, during the dry year of 2016 (La Niña event), some deep boreholes had a piezometric level below the shallow aquifer groundwater level.

Since 2013, Base Titanium has also monitored the groundwater quality in its production boreholes and some shallow and deep community wells spread around the mine. The hydrochemical composition of the pumped water from 2013 to the present (data not shown) indicates that there is no significant change in groundwater quality in the groundwater pumped from the deep aquifer, even during La Niña event. The EC values measured in the inland deep community wells monitored by Base Titanium have been <1500 µS/cm from 2012 until the present.

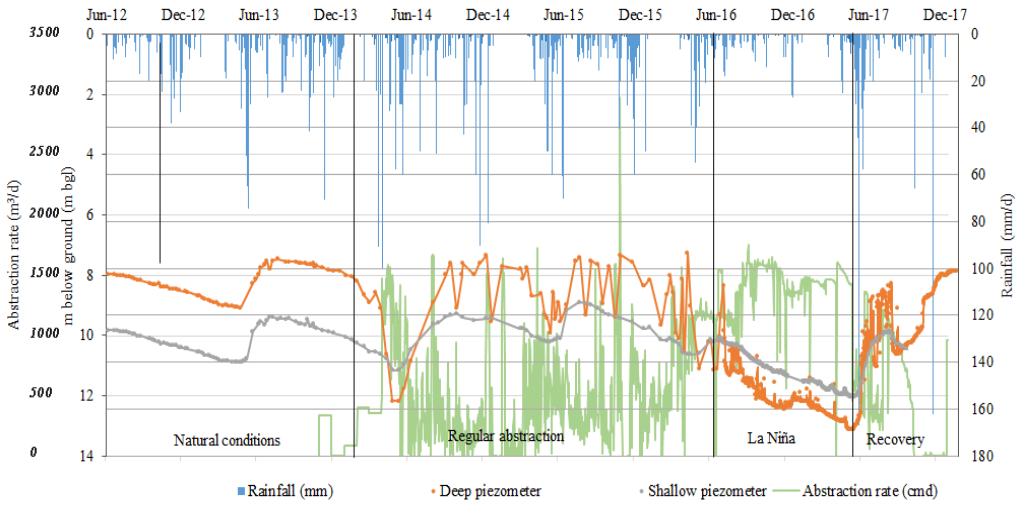

Figure 4.2. Comparison between shallow and deep groundwater levels of piezometers located near a production borehole recorded by Base Titanium. Black vertical lines indicate the hydraulic relationship between the shallow and the deep aquifer under different conditions: 1) "Natural conditions" refers to groundwater levels when the wellfield was not intensively pumped before October 2013; 2) "regular abstraction" shows the shallow and deep groundwater levels once the deep aquifer exploitation started; 3) "La Niña" shows the groundwater levels during the drought period caused by La Niña event in 2016/2017 and 4) "Recovery" refers to the recovery of the aquifer hydraulic relationship after the rains of April 2017. Rainfall volume data is from Kwale Agricultural Department station (Kenya Meteorological Department) (mm/d). The green line shows Base Titanium abstraction as m^3/d.

KISCOL sugar fields

KISCOL uses different water sources to meet sugarcane water demand. Its water demand depends on the crop water requirements of the sugar plant. As expected, the minimum crop water requirement (MCWR) is higher during the driest months, with an average of 40,784 m^3/day from January to March and 28,349 m^3/day for the wet period (April to June).

Groundwater is obtained from up to 17 boreholes, 60-100 meters deep, drilled in and spread across the sugar fields. According to WRA, KISCOL has been allocated a total of 10535 m^3/day from 12 production boreholes. However, information available indicates that only eight boreholes are currently operational, so actual groundwater abstraction is probably lower than the WRA allocation. These eight boreholes are operational (since mid-2015), and are located in the Milalani fields (Zone 1, Fig. 1.1). The Kinondo fields are irrigated by surface water (Zone 3, Fig. 1.1) as the borehole pumps are not connected to power lines and electrical generators have been vandalized. Pumped groundwater is stored in one-day storage lagoons, together with water coming from the dams, which is the other water source for sugar irrigation. Groundwater acts as a strategic water reserve; volumes used are small compared with water from dams. According to current WRA rules, the

maximum volume that may be pumped is 60 % of the well test discharge rate over a ten-hour pumping day. It means that the mean estimated abstraction rate for the eight KISCOL boreholes is 2088 m^3/day (Table 4.2). This value is in accordance with the KISCOL test yields for these eight boreholes and it is in the same range as other unpublished data from KISCOL.

KISCOL wells are multi-screened, taking water from multiple water-bearing zones in the shallow and deep aquifer units. This well design increases the yield but produces a mix of groundwater from different origins, as shown by the isotopic and hydrochemical composition (Ferrer et al., 2019) and may facilitate the entrance of contaminated water from the shallow aquifer towards the deep one. This screen configuration is different from the Base Titanium boreholes, which are only screened in the deep aquifer.

Water quality was measured within KISCOL's Milalani plantation in a monitored borehole at different depths in the June 2016 field survey (Ferrer et al., 2019). The most significant result was the measured nitrate concentration in this borehole: 48 mg/L at 21 m bgl and 31 mg/L at 65 m bgl, as NO_3^-. Furthermore, a well located at Nikaphu, south of the study area, had 1.2 mg/L of ammonia, as NH_4^+, during the March 2016 field campaign. Taking into account that groundwater has an Eh of +239.4 mV and dissolved oxygen of 1.42 mg/L, the relatively high ammonia content indicates that the sample is not in chemical equilibrium. This shows a relatively fast recirculation of shallow groundwater around the pumping well. Currently, there are no nitrate polluted shallow wells around the KISCOL Mililani fields. Conversely, in the Kinondo fields (Zone 3), where sugar is irrigated only with surface water, there is only one point at the outflow from the end of the fields that is polluted by nitrates, at 73 mg/L NO_3^- in June 2016.

Table 4.3. The allocated and the actual or estimated groundwater abstraction for each water user. *Hotel groundwater use is based on Table 4.4.

Period	***Recharge (m^3/d)***	***Groundwater abstraction (m^3/d)***				
		Base Titanium	*KISCOL*	*Hotels*	*Handpumps*	*Community boreholes*
Dry year: La Niña 2016	158,602	**Current: 4272** Allocated: 5280	**Current: 2088**	**3272***	**450**	**991**
Recovery/ average year: 2017	613,890	**Current: 3370** Allocated: 5280	Allocated: 2528			
Future abstraction		8800	9504	3926	540	11500

Tourism

From the data obtained from Google Earth, 85 % of the hotels located on the coast are located in Zone 3 and 4 on the Diani coast, with only a few situated on the Msambweni coast in Zone 1 and 2 (Fig. 1.1).

The highest tourism season is from October to March and the lowest from April to July. Hotel water use is closely associated with the number of tourists, so both intra- and inter-annual abstraction varies considerably. Most hotels use water from private boreholes, from which large volumes of water are withdrawn using electrical and/or diesel driven pumps. The groundwater abstraction points that support this economic activity are located near the coast, mainly exploiting the shallow aquifer located in the Pleistocene corals formation. Using both Google Earth and Trip Advisor, it was possible to identify 109 hotels and obtain the number of rooms for 91 hotels. Personal interviews with hotel managers improved the understanding of water use and water source for each hotel. Around 40 % of the hotels were unwilling to answer the questions and the remaining 60 % of hotels at least revealed the water source. Of the 60 % of the hotels that answered, 72 % are only supplied by private boreholes while the remaining 28 % supplement groundwater with municipal piped water from the Tiwi aquifer, located 6-12 km north of Ukunda and covering an area of approximately 30 km^2.

We estimated hotel groundwater abstraction according to the different type of data source (WRA allocations and hotel interviews). We also estimated hotel groundwater abstraction using the number of rooms and the hotel class type (Table 4.4).

Table 4.4. Hotel groundwater abstraction (m^3/d) based on different information sources.

Source	*Kind of data*	*Number of points with available data*	*Abstraction (m^3/day)*
WRA	WRA allocation permits	29	2760
Hotels	Answer direct from the Hotels	38	1809
Estimate	Google Earth + Trip Advisor + Manual for Water Supply Services	91	3272

The total number of beds available on the south coast has decreased around 40 % from 2015 to 2017, since some hotels closed during this period. However, the percentage of beds occupied has increased, maintaining an occupancy rate of around a million bed-nights/year for the period 2015-2017 (Fig. 4.3). The Draft Kwale Water Master Plan assumed a 1 %/year growth in water demand for the tourism sector over the next 20 years.

Hotel groundwater use varies through an order of magnitude across the months of the year, based on bed occupancy. Water consumption is lower during the wet season, since it coincides with the months with lowest tourism activity. However, the water consumption in the rest of the year is significant. It is worth emphasising that the highest bed occupancy rate and thus the highest water consumption occur from October to December, just before the dry season.

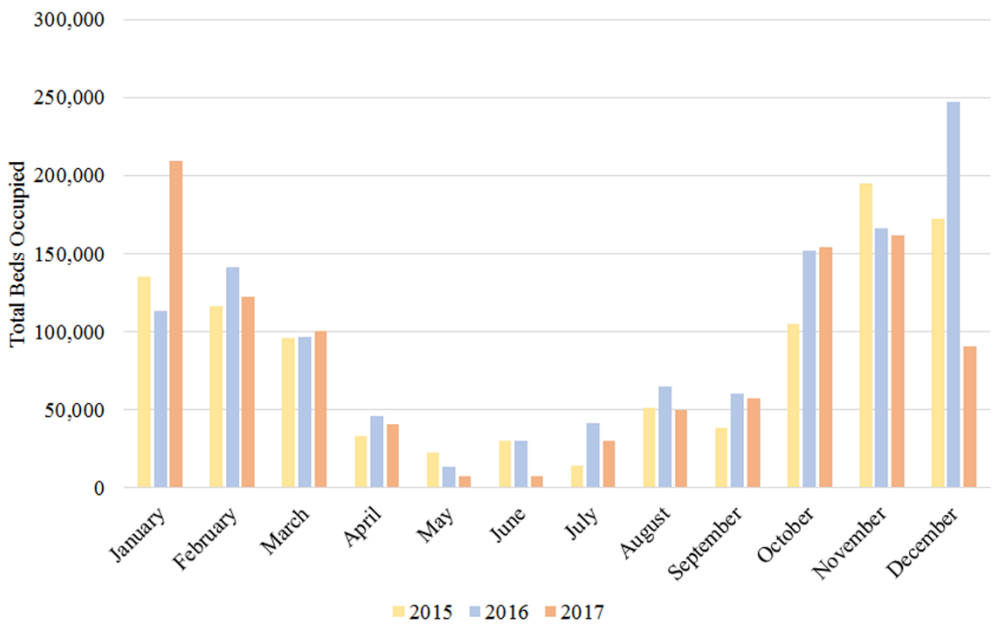

Figure 4.3. Total bed occupancy for the South Coast hotels from 2015 to 2017 obtained from the Kenya National Bureau of Statistics (KNBS).

Community abstraction

Groundwater abstraction from commercial activities takes place alongside the traditional dispersed 300 functional handpump-equipped shallow wells and boreholes, and 22 community boreholes (some with solar pumps put in by Base Titanium), that provide drinking water to communities and institutions. The WRA allocation for 22 community boreholes within the study area is 991 m^3/day (Table 3.3). There are also some open wells operated with buckets within the study area for which no abstraction data exist; however, anticipated abstraction rates are much lower than in handpump-equipped boreholes.

Weekly data obtained from the transmitters (WDT) from the 300 handpumps during 2014 and 2015 gave a mean daily abstraction of approximately 1.5 m^3/day per pump. Water pumped from community handpumps also depends on rainfall (Thomson et al., 2019). Abstraction varied from 0.71 m^3/day per pump in the wet season to 2.05 m^3/day per pump in the dry season, with monthly variation shown in Figure 4.4. They operate under different dynamics, according to the economic activities in the area. The monthly average volume pumped is lower than the annual average abstractions from May to December. This shows that communities use other water sources during wet periods, such as rainwater collection (Thomson et al., 2019).

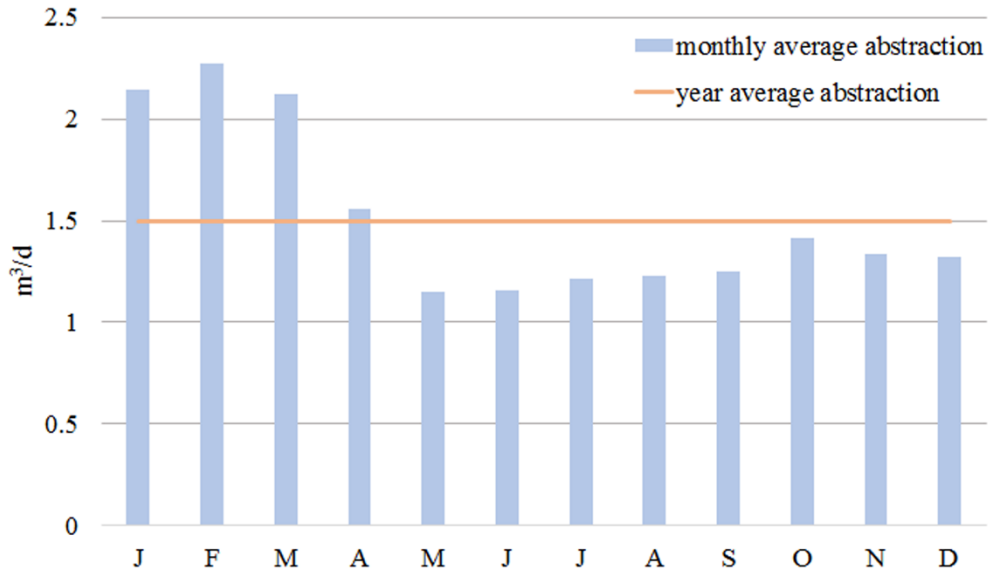

Figure 4.4. Monthly average abstraction variation for handpumps during 2014 and 2015.

4.5.3. Groundwater level evolution

In order to determine the sustainability of the groundwater system under different abstraction regimes, it is important not only to consider how abstraction could affect aquifers during a drought, but also how the systems recover after such climatic events. Therefore, the present study goes beyond that of Ferrer et al., (2019), as it focuses on the recovery of groundwater levels during 2017 after La Niña event and especially on shallow aquifer recovery. The shallow aquifer is the source of water for most communities in the study area.

During La Niña event, there was a groundwater level decline in 86 % of the measured shallow wells. In the remaining wells, the groundwater levels were nearly constant. However, levels in 95 % of the wells affected by La Niña drawdown recovered after the first rainy season (AMJ) in 2017 (Table 2, Appendix C). In this regard, the first rainy season (AMJ) is more effective in the recovery of the groundwater system than the short rains (OND).

Regarding groundwater level recovery after La Niña event in the deep aquifer, there are only data from Zone 2 (from the Base Titanium monitoring network). Figure 4.2 shows the effects of recharge and abstraction on deep piezometer water levels; this shows that groundwater levels recovered after the first rainfall event in April 2017, to values close to those observed in previous wet years.

4.5.4. Groundwater quality on the coastal strip

Sea water intrusion (SWI) in aquifers occurs naturally in coastal areas around the world (Custodio, 2010; SASMIE, 2017). The position of the seawater/fresh water-mixing zone is influenced by groundwater discharge into the sea and aquifer thickness, as well as aquifer hydraulic conductivity. The natural discharge rate could be affected by groundwater abstraction, reducing diffuse discharge into the sea. In order to study short-term salinity changes, we carried out a spatial analysis of groundwater EC (electrical conductivity) between 2013 between 2016.

The evolution of EC since 2013 (Fig. 4.5) shows that salinity increased, mainly in 2016. This illustrates the relationship between EC increase and decreasing rainfall, since the total rainfall during 2016 (when La Niña event occurred), was 49 % less compared to the 2014 total (Table 2, Appendix C). The highest EC values in June 2016 correspond to the wells located in Zones 3 and 4 (except for a point in Zone 1), with an EC mean value of 2814 µS/cm and a maximum of 3793 µS/cm (Table 3, Appendix C). Looking at the EC variation across 2016-2017 for the wells located near the coast, around 88 % of the sampled sites show an EC increase across the period. The wells that do not show any EC increase are mainly located inland in Zone 4, and in some wells in the Magarini sands in Zone 1 (Table 2, Appendix C).

We compared hydrogeochemical modelling results with the samples from wells/boreholes affected by SWI in the shallow aquifer to understand the importance of the SWI change. Field samples contain between 0 % and 30 % of seawater (Fig. 4.6a), except for the sample taken from a beach upwelling, which had 83 % seawater. Of the conceptual models tested (data not shown), the one that gives results closest to the observed field samples is the mixing of fresh and saline water, both in equilibrium with calcite (i.e. Fig. 4.6a).

Looking at the delta ion evolution for calcite (total quantity of precipitated/dissolved calcite mineral) in this conceptual model, during mixing between fresh groundwater and saline water (Fig. 4.6b) the increase in salinity tends to dissolve calcite, with 30-40 % maximum dissolution in a water mixture containing 50 % of seawater.

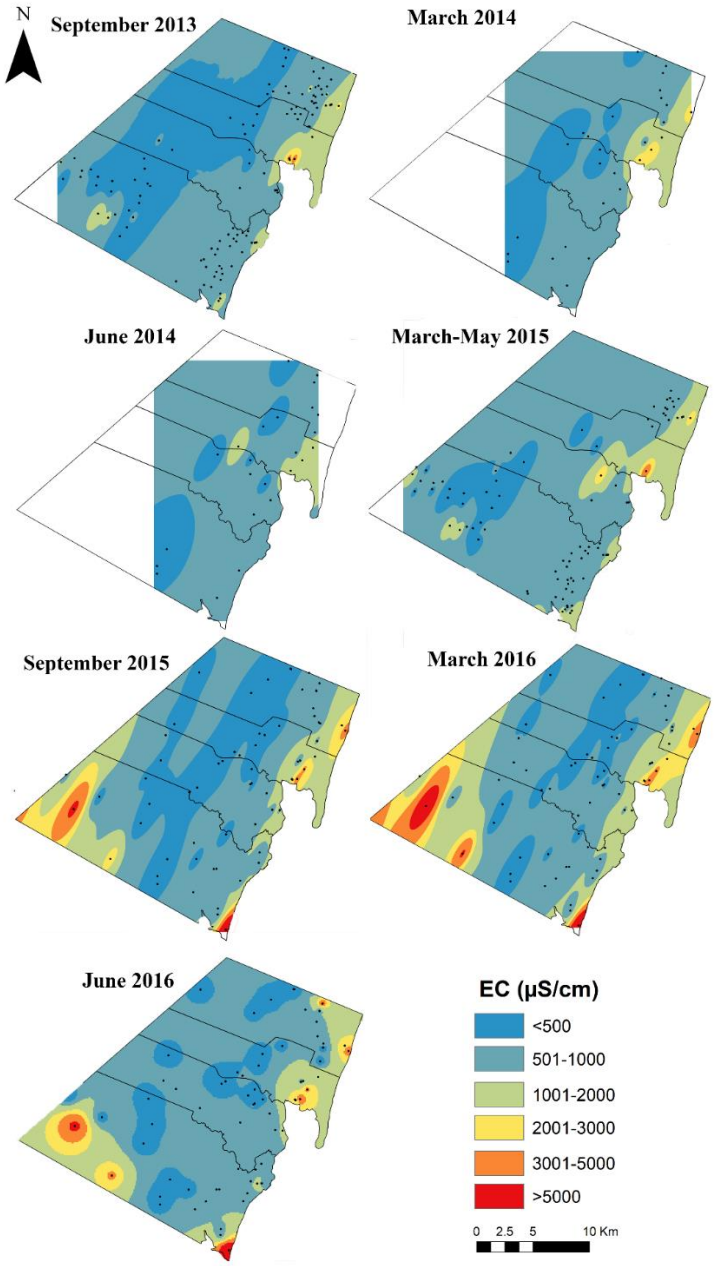

Figure 4.5. EC spatial distribution along time after the different field surveys from 2013 to 2016. The inland white areas mean that no data is available. The high EC values located inland in from September 2015 to June 2016 correspond to a saline geological formation, the Maji ya Chumvi beds (Caswell, 1953).

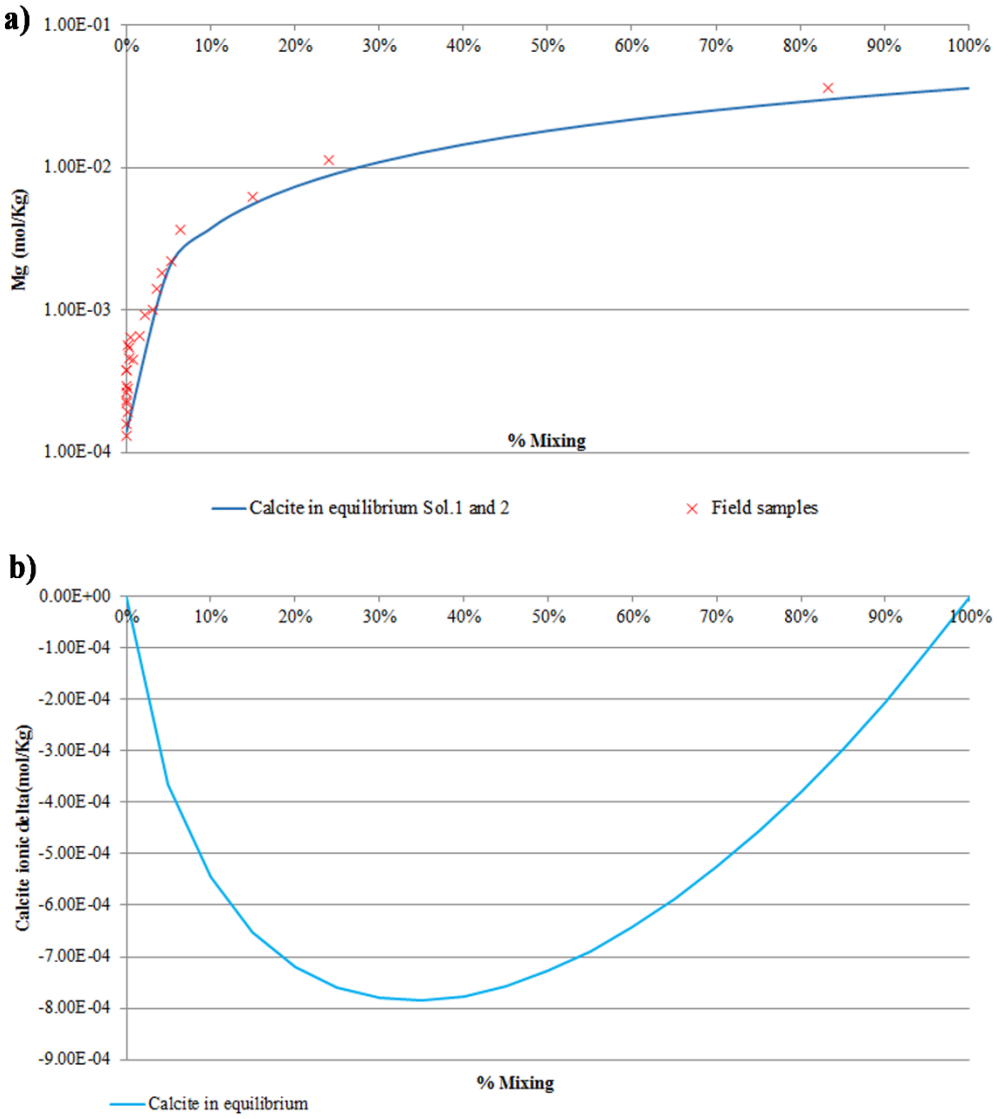

Figure 4.6. a) Mg vs. percentage of mixing. The red crosses represent sampled waters near the coast. The X-axis shows the percentage of mixing from 0 % to 100 % of fresh water in the coast samples and the upwelling. The light blue line represents the best-fitting conceptual model (water solutions in equilibrium with calcite). 4.6.b) Calcite ion delta (change) vs. percentage of mixing of the model in equilibrium with calcite. The Y-axis represents the calcite saturation index and the X-axis shows percent mixing.

4.6. Discussion

Current situation

The total groundwater abstraction represented 6 % of the recharge during La Niña and 1.3 % of recharge during a normal climatic year, such as 2017. The recharge volume is an important component of the aquifer system dynamics, responsible for groundwater level variation in both the shallow and deep aquifers.

Not all water users exploit the same aquifers (formations). The community wells, handpumps and hotels mainly abstract groundwater from the shallow aquifer. The recharge areas of this aquifer unit are those exhibiting more volume variation between drought and a normal climatic year (i.e. 2017) (Fig. 4.1). The shallow aquifer unit is less resilient to climate variation than the deep one. This explains why some wells located in the Kilindini and Magarini sands became dry during La Niña drought. The aquifer system exhibited swift recovery after the first normal rainy season in 2017. This allowed the system to return to the average groundwater budget and to face the next drought period.

One consequence of wells becoming dry is the increase in walking distance to collect water. As reported during fieldwork in June 2016, during La Niña event, some communities stated that they had to walk longer distances to collect water because the nearest borehole or well was dry. Amongst other impacts, Demie et al. (2016) found that spending more time searching for water had a negative impact on girls and women, since this forces them to stop investing time in their education and other important activities. Furthermore, the reduction in groundwater availability leads to an increase in the price of the water sold to local residents. The Gro for Good research team found that during the drought event of 2016/2017, some areas having very limited access to drinking water suffered a peak in the price of vended water, with charges ranging from 20 to 50 Ksh per 20 litres reported west of the Shimba Hills. Such costs are an order of magnitude higher than the usual price for vended water, which is 2 to 3 Ksh per 20 litres. This price increase has a huge impact on families is an area where the average household income is about 330 Ksh/day, about the cost of 2.5 kg of rice. This price increase will either result in households having reduced funds for other needs because of the drought, or reducing their water use, or a combination of both. This may cause adverse health impacts from compromised hygiene behaviour.

Unlike communities and hotels, Base Titanium exploits the deep aquifer and KISCOL both aquifer units. The fact that the recharge variation is less in the Shimba Hills than in the lowland means that the deep aquifer is more resilient to drought events. This favours groundwater abstraction by these users, since they can continue to exploit the deep aquifer

during periods of drought without impacting the shallow aquifer exploited by the communities and hotels lasting at least as long as the last La Niña event.

Focusing on mining, the abstraction rate depends on rainfall patterns, increasing during the dry period in 2016, and reducing during wet years, such as in 2017. The influence of abstraction on the shallow aquifer is insignificant up to the present, according to observation piezometer water level data in the shallow and deep aquifer in the Base Titanium wellfield. This is due to the presence of an aquitard between the two aquifers. Groundwater abstraction only quantitatively affected the deep aquifer system to a significant degree during the 2016 drought. This groundwater level decline could be due to the combination of abstraction from the deep aquifer and the reduced recharge during the drought in the Shimba Hills (Fig. 4.2). Unlike in other areas, like Italy, Tunisia, Mediterranean Spain and the Canary Islands (La Vigna et al., 2013; Maliki et al., 2000; SAMIE, 2017), where intensive exploitation permanently affects the relationships between aquifer units, after La Niña event the hydraulic relationship between the shallow and deep aquifer recovered following the rains in April 2017, showing that the impact on the deep aquifer in 2016 was attribute to the recharge.

Like Base, KISCOL water use changes over time, as their principal use is for irrigation: less water is consumed during the wet season and more during the dry season and droughts. At present, current KISCOL abstraction has a dual effect on groundwater quality, as the potential pollutants related to fertilizers used in the sugarcane fields are present in the deep pumping wells but do not spread beyond the sugar fields due to the recharge of irrigation return flow (Fig. 4.7). The presence of a high NO_3^- concentration (31 mg/L) at 65 meters depth in a KISCOL control piezometer located in Milalani (in the southern fields), confirms the aquifer unit's connection through the well due to the long screened sections. The northern fields (Kinondo), which are irrigated with surface water, shows how the pollutants may move following groundwater flow, as a well located down flow of the fields is one of the few in the area with elevated nitrate (recall Section 2.5.6).

The relationship between the shallow and deep aquifer at the coast itself is unknown. Furthermore, as there are no data on the deep aquifer in the area between the coast on the one hand and the sugar fields and the mine on the other, it is not possible to determine the effects of sugarcane irrigation and mining abstraction on saline intrusion in the deep aquifer. However, none of the deep boreholes sampled during this study (up to 100 m depth, data not shown) shows SWI influence. Moreover, it is unknown how water abstraction from boreholes located within or near the palaeochannel could increase the SWI, mainly around the Msambweni area, in Zone 1 (Fig. 1.1).

In the coastal areas with major tourism concentrations, recent years' data seem to show a local salinization effect in the shallow aquifer due to the higher abstraction induced by tourism and associated activities. However, a longer period of observation is needed to determine the saline water intrusion dynamics in order to consider rainfall fluctuations and to differentiate between seasonal effects (still unclear but possible) and long-term trends. As the zone with most of the hotels is also the area with the highest population density, it is not possible to differentiate between saline intrusion caused by the hotel sector itself and that caused by wells and boreholes serving private dwellings or used by local communities.

EC in most measured shallow wells remained high after the drought period, even after the important rains of early 2017, indicating that groundwater quality in the coastal zone did not fully recover. This behaviour is in agreement with the well-studied Llobregat Delta aquifers, near Barcelona (Custodio, 2002; SASMIE, 2017), which show that salinity takes much longer than groundwater level to change and to recover once the aquifer is salinized.

Future situation

Total groundwater abstraction is expected to increase by a factor of four over the current rate (see Table 4.3). This level of abstraction would represent 22 % of the total recharge occurring during La Niña event. Currently, the existing water-reliant industries are exploiting the aquifer without significantly affecting groundwater levels. However, the possible local effect of pumping wells on the aquifer system and the consequences of future increased groundwater abstraction during long drought periods should be evaluated. The number of dry shallow wells could increase in the future due to more frequent and longer droughts, but also due to augmented abstraction.

Considering the groundwater level difference between aquifer units during La Niña in the 14 m-thick aquitard (the minimum aquitard thickness reported by Base) and the estimated vertical hydraulic conductivity, Darcy's Law shows that the vertical water downward displacement through the aquitard is of the order of 2 m/year, penetrating much less than the aquitard thickness in one year. Consequently, pollution from the upper aquifer level cannot reach the deep aquifer except due to poor well construction. However, in a future scenario with a four-fold increase in groundwater abstraction rate and/or longer droughts, a longer and possibly permanent shift in the difference in piezometric levels between the aquifer units may occur, increasing the risk of contamination from vertical drainage through the aquitard.

A future increase in groundwater abstraction by the sugar company during a drought period may affect both the shallow and the deep aquifer, as those wells are screened in both

aquifers (for maximum borehole yield). A potential reduction in groundwater level in the shallow aquifer in Zone 1 may affect the Ramisi River-aquifer relationship in that area. A fall in the shallow aquifer level would decrease aquifer discharge to the river and at some point could induce river water infiltration into the aquifer. The infiltration of naturally saline water from the Ramisi River could affect the groundwater quality in shallow wells adjacent to the river by increasing its salinity, thus limiting their use. The maximum EC upstream in the Ramisi River was 5594 µS/cm (Table 3, Appendix A). In extreme cases, the EC could limit the use of groundwater from the shallow aquifer. This does not only apply to domestic uses but also to sugar irrigation, as the threshold EC for sugarcane is 1700 µS/cm (FAO, 2018), if some of abstraction wells were located close to the river. In order to prevent this occurring, KISCOL might consider irrigating the south sugar fields with surface water from dams located in the Mkurumudzi catchment. Furthermore, it is expected that in periods when the groundwater level in the deep aquifer stays lower than in the shallow aquifer, pollution of the deep aquifer can be induced in the wells, as has occurred in other areas (Menció et al., 2011) and is a common occurrence in coastal areas.

SWI is an important issue in coastal aquifers, and has already been observed in Kwale County (Oiro and Comte, 2019). A reduction in groundwater flow would lead to a slow penetration of the saltwater wedge inland, increasing the percentage of saline water in shallow wells already affected by SWI and affecting new areas. The significance of SWI is that only 2 to 3 % of seawater mixed with fresh water is enough to make the resulting water useless for most purposes.

The calculation of the freshwater-saltwater mixing zone is a complex task, but an approximation can be obtained assuming a sharp freshwater-saline water interface and comparing the results with the final equilibrium state. The steady state penetration of the sea water wedge in the case of an homogeneous aquifer can be easily calculated from aquifer thickness and hydraulic conductivity for a given groundwater flow discharging at the coast (see Section 13, (Custodio and Bruggeman, 1986; Custodio and Llamas, 1976). We calculated seawater wedge growth from the coastline for the shallow aquifer, under the future increased abstraction scenario with the same net recharge as during La Niña event (Table 1, Appendix C). Increasing groundwater abstraction from 9535 m^3/d to 34270 m^3/d will move the steady state saline water wedge from 232 m inland up to 280 m in the final equilibrium state. This advance of the saline wedge could affect hotel groundwater supply and community handpumps located near the coast.

We also calculated the saline wedge depth for different distances from the coast and for the different geologies near the coast, i.e. the Pleistocene corals and Kilindini sands (Table 1,

Appendix C). The results show that even during the future abstraction scenario during a drought year like the 2016 La Niña, the saline wedge will not affect the Kilindini sands. Under the future scenario, the saline wedge in the Kilindini sands (around six kilometres inland from the coast) would be around 400 m deep, so the shallow aquifer would not be affected. Only the coral formation is affected by SWI in the present and future scenarios. The saline wedge depth in the coral formation ranges from two meters deep at one meter inland from the coastline, to 100 m deep at the geological contact between the corals and the Kilindini sands, located around four kilometres inland.

The future consequences of borehole salinization would be an increasingly salty taste and at some point unsuitability of the water for human consumption. This would increase costs, due to corrosion of domestic appliances, hotel facilities, pipes, and pumps, besides the cost of providing drinking water by other means, and the early abandonment of wells and associated facilities. Furthermore, as shown by Foster et al., (2018), handpump failure risks are higher and lifespans are shorter when groundwater is more saline and the static water level is deeper.

The increase in salinity, as observed in 2016, and the dynamics of the SWI will tend to increase calcite dissolution (Fig. 4.6b). The related increase in karstification would have a number of potential long-term effects: 1) induced hydraulic conductivity rise will hasten further aquifer salinization and; 2) would increase the creation of sinkholes already observed in parts of the coral limestone during fieldwork. New sinkholes may be caused when caverns or channels in the coral limestone collapse due to groundwater overexploitation (Alfarrah et al., 2017; Jakemann et al., 2016; Khanlari et al., 2012). Occurrences of land subsidence in limestone have been globally reported, such as in Spain (Molina et al., 2009), India (Sahu and Sikdar, 2011), Mexico (Ortiz-Zamora and Ortega-Guerrero, 2010) and the United States (Holzer and Galloway, 2005). This has implications for the stability of buildings and other structures constructed on the limestone.

Despite the uncertainty of the impacts caused by the future abstraction scenario and longer forecast drought periods (Stocker et al., 2013), aquifer management decisions regarding the potential impacts on the aquifer system and the linked communities and economic activities are needed. Private sector and public participation in water resources management should be enhanced through decentralised management approaches. In this way, stakeholders, including the Water Resources Authority, private water users and communities in the study area, should carry out decision-making. Water infrastructure and technologies should be fit-for-purpose in application and scale, and the pro-poor focus should be underpinned by appropriately focused management regimes (Olago, 2018).

This decision-making must focus on managing the aquifer system in a sustainable way in order to protect the communities. These are the most vulnerable stakeholders, since they rely on the less resilient aquifer for water supply. Therefore, alternative, secure water resources must be developed to supply vulnerable communities before community wells become dry or salinize. One potential solution could be to supply the communities from deep boreholes, since this aquifer unit is more resilient in the face of adverse climate events. Base Titanium is already working together with Kwale County government to install community water sources into the deep aquifer to provide water security to communities, with a number of Base-drilled boreholes originally with handpumps installed planned to be converted to solar or mains-powered pumps. Other possible actions to ensure community well sustainability would comprise taking measures to protect the main recharge areas as is being done by the Kenya Wildlife Service supported by Base Titanium together with conservation organisations in the Shimba Hills National Reserve – the Water Tower for the Mkurumudzi catchment; managing land use to ensure high infiltration rates; promoting managed artificial recharge; and conjunctive water use. A common conjunctive management strategy is the recharge and storage of surface water in aquifers when it is available in excess of demand, for withdrawal later when surface supplies are reduced, as during drought (Foster and van Steenbergen, 2011). Furthermore, private companies should strive to manage their groundwater resources sustainably, minimising the impact on community well water quality and availability. For example, Base Titanium adopts recycling and conjunctive use, combining surface and groundwater during drought periods as a management strategy.

This study uses simple calculations to illustrate the possible future risks of increased abstraction under climate stress to an aquifer system in Kwale County. At present, under 'normal' climatic conditions, we have observed no adverse consequences in the aquifer system since major abstraction started in 2012. However, the study underlines the importance of evaluating all risks to any aquifer system prior to major groundwater abstraction.

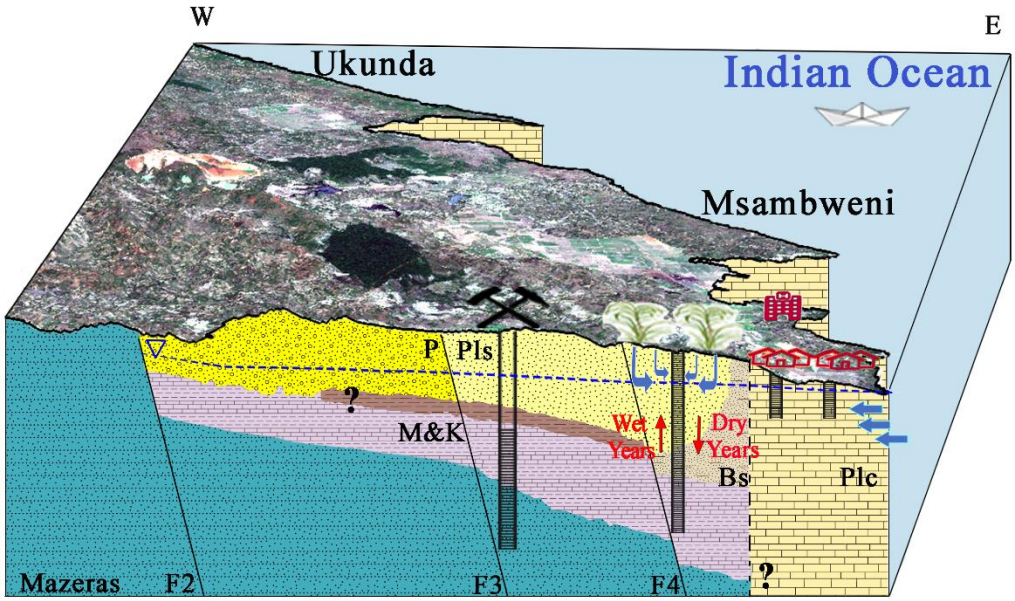

Figure 4.7. Schematic hydrogeological conceptual model of the aquifer system with the main economic activities in the area and the location in the geology of the abstraction boreholes for each activity. The question marks indicate the unknown extension of the clay layer (in brown) acting as an intercalated aquitard that reduces the connectivity between the Mazeras Fm. and Pleistocene corals and sands, and the discharge of the deep aquifer. Mazeras (Mazeras Fm.), M&K (Mtomkuu and Kambe Fm.), P (Magarini sands), Pls (Kilindini sands), Bs (Bioclastic sands with clay lenses), Plc (Pleistocene corals). F2 to F4 indicate the main faults in the study area.

4.7. Conclusions

Water-reliant growth in Africa needs to manage multiple risks for sustainable management of strategic groundwater resources. Securing new investors in rural areas where poverty is high and environmental regulation is weak may focus on the former at the cost of the latter. Lack of historical data such as water level, abstraction and quality data is typically the norm and challenge objective decision-making in the face of urgent development priorities. Government and enterprises may find environmental sustainability of secondary importance to advancing economic production, creating local jobs and new sources of taxation. This may translate into unknown risks to local, vulnerable populations and future generations who rely on shallow groundwater for water supply. Droughts compound this risk, with multiple and competing bulk water users abstracting from the same aquifer system without any shared understanding of impacts, including short and long-term damage from saline intrusion in coastal aquifers. As in most aquifers, water quality does not recover in all wells after wet season recharge, and significant amounts of data are needed to evaluate future aquifer response. Furthermore, in areas of the continent with lower

precipitation and consequently lower recharge, a lower level of abstraction could be harmful to aquifers. Future risk should therefore be predicted under different abstraction future scenarios, before major abstraction takes place.

While gambling with groundwater may be common in Africa and globally, this study shows that groundwater resources can be significant and resilient to unpredictable but recurrent drought events. Given over half a billion dollars in capital investment in the two water-reliant industries in Kwale, in addition to tourism and related investment, understanding investor risk and liability from groundwater sustainability would seem prudent, if not a legal obligation, before major abstraction starts. Government leadership is essential to manage the aquifer as a system for all, including environmental services, rather than for the powerful few. Without technical, material and political support, water resource management agencies face stark choices in Africa, as limited staff and capacity are unable to ensure that adequate monitoring systems exist to guide regulations that manage water resources in the public interest. Governance failure can promote market failure, by mismanaging groundwater, by design or by accident. However, this is not inevitable and we see evidence of good corporate water management as a catalyst for providing critical deep aquifer data to inform a credible model for future groundwater management and resource allocation in Kwale. Furthermore, using often simple information sources (interviews, Google Earth, Trip Advisor, basic analytical methods, etc.), enables groundwater abstraction to be estimated, allowing potential future risks to be assessed as has been shown by this study.

We strongly recommend compliance with existing regulations and codes of practice and strengthening of the capacity of the Water Resources Authority to monitor such compliance. Further, in line with the current updating of the national water policy, we advocate for improvement of the application of the legal framework and regulatory reach so as to encompass the notion of shared risks and responsibilities among the government and the private sector, and creation of a business climate that espouses resource protection for growth and promotion of sustainable development.

The authors gratefully acknowledge the collaboration and key data shared by Base Titanium Ltd., and the support of Kenya's Water Resource Authority, the Kwale Country Government, Kwale International Sugar Company Ltd., and Rural Focus Ltd. This research was funded by the UK Government via NERC, ESRC and DFID as part of the Gro for GooD project (UPGro Consortium Grant: NE/M008894/1).

Chapter 5

Evidence of groundwater vulnerability to climate variability and economic growth

5.1. Introduction

Climate change and future changes in abstraction effect groundwater resources. The uncertainty of possible future impacts is a major challenge nowadays, given the urgency of adopting measures required to secure drinking water supplies (Van Engelenburg et al., 2018). Global change and climate evolution seem to have modified the hydrologic cycle and resulted in changes in precipitation pattern by increasing the frequency of extreme events, such as droughts and floods, accelerating the melting of glaciers and icecaps, and modifying soil moisture and river runoff (Bates et al., 2008). Forecasted spatial and temporal changes in mean annual rainfall (Stocker et al., 2013) are known to influence the water balance as a whole, and groundwater recharge in particular (Carter and Parker, 2009).

The effects of climate change will be even more serious in countries with high population growth, which will generate an increasing demand of water resources (Carter and Parker, 2009). This increased water demand will strain local water supply, limiting the amount of water available per person. The growth in urban populations is accompanied by significant food production increases in both rural and peri-urban areas. Water resources will be further stressed by an increase in groundwater abstraction. Drilling deeper boreholes with higher intended abstraction rates than those traditionally obtained with dug wells or shallow boreholes equipped with handpumps, will increase in many areas to meet the water demand of new economic activities that are taking place across developing countries (Comte et al., 2016).

During the past 40 years or more, numerical groundwater flow models have been proved suitable for evaluating groundwater resources and testing alternative approaches for aquifer management (Howard and Griffith, 2009). They are becoming increasingly useful and reliable tools when it comes to addressing the principal challenges involved in planning and managing water resources, and are being widely applied (Barthel et al., 2005; Feng et al., 2018; Folch and Ferrer, 2015; Mas-Pla et al., 2012; Urrutia et al., 2018; Vázquez-Suñé et al., 2006; Vižintin et al., 2017, among others). Moreover, these models have been shown to constitute an important tool for predicting the effects of climate change on aquifer behaviour (Kopytkovskiya et al., 2015; Levison et al., 2014; Taylor et al., 2013; Adrian D Werner et al., 2013) and for investigating mitigation measures (Howard and Griffith, 2009). Despite their importance, developing climate change scenarios in groundwater models is difficult because the scale of global climate models is too large and the local historical data needed to predict future trends is typically lacking. Most of these global climatic models are unable to accurately reproduce local historical climate conditions, since they suffer

systematic bias in the simulated variables (e.g., precipitation and temperature); a correction is therefore needed to obtain reliable local scale results (D'Oria et al., 2018).

Africa is considered the most vulnerable continent to climate change, with one-third of the population living in drought-prone areas, with the highest rate of population increase in the world (Meigh et al., 1999), with high industrialization increase based on different economic activities (mining, agriculture, tourism…). One of the key uncertainties surrounding the impacts of climate change in Africa is the effect on the sustainability of rural water supplies (MacDonald et al., 2009). In East Africa, impacts on agriculture caused by climate change will translate into impacts on livelihoods for the majority of people, as almost 80 % of the population depends on agriculture, which contributes 40 % of the national gross domestic product (Adhikari et al., 2015). Within this context, it is clear that it is necessary to develop long-term water management plans in Africa, to address the consequences of the joint effect of climate change, population growth and increase of water abstraction in a continent where most people depend on groundwater for a range of different purposes (Abiye, 2016; Kahsay et al., 2018; Taylor and Howard, 1996).

Despite the importance of numerical flow models, they are rarely developed in sub-Saharan Africa, as the data describing groundwater systems are often sparse and the current state of aquifer understanding is poor. Furthermore, data related to economic growth that is suffering the continent is in most of the cases unknown. Candela et al. (2014) evaluated the effects of dry and wet periods on groundwater recharge in the Lake Chad Basin, a data scarce area, while Yihdego et al. (2017) estimated seasonal variability of groundwater-surface water exchange fluxes on the water balance of Lake Naivasha, in Kenya. Despite the fact that hydrological processes in coastal areas will be profoundly affected by climate change (Stefanova et al., 2015), there are only a few groundwater models developed for the East Coast of sub-Saharan Africa so far. Kamermans et al., (2002) developed a numerical groundwater flow model to study the effects of groundwater discharge on the diversity and abundance of lagoon seagrasses, from the coast of Kenya to northern Tanzania, including Zanzibar.

The aim of this chapter is to extend the emerging evidence of the implications of climate variability on recharge in Africa by including impacts of economic development and associated abstraction. The contributions to the literature are methodological and empirical in developing future scenarios using numerical groundwater flow models with observed data on abstraction and historical rainfall data. Furthermore, the analysis of the groundwater level variation of the aquifer units of the study area, provides insights into the potential vulnerability of rural communities who largely depend on shallow aquifer.

5.2. Methodology

5.2.1. Future scenarios

In order to build future groundwater flow model scenarios to study which variables (rainfall, temperature, and/or abstraction) are the priority concern in aespecific location, firstly solving the 3D partial differential equation of groundwater flow is needed. The governing equation for groundwater flow is:

$$\frac{\partial}{\partial \mathrm{x}}\left(K_{xx}\frac{\partial \mathrm{h}}{\partial \mathrm{x}}\right)+\frac{\partial}{\partial \mathrm{y}}\left(K_{yy}\frac{\partial \mathrm{h}}{\partial \mathrm{y}}\right)+\frac{\partial}{\partial \mathrm{z}}\left(K_{zz}\frac{\partial \mathrm{h}}{\partial \mathrm{z}}\right)+W=S_s\frac{\partial \mathrm{h}}{\partial \mathrm{t}}$$

where K_{xx}, K_{yy}, K_{zz} are the values of hydraulic conductivity along the *x, y, z* coordinate axes, which are assumed to be parallel to the major axes of hydraulic conductivity [L T^{-1}]; *h* is the groundwater level [L]; *W* are the source/sink terms, with $W < 0$ for flow out of the groundwater system and $W > 0$ for flow into the system [T^{-1}]; *Ss* is the specific storage of the porous material [L^{-1}]; and *t* is time [T]. The source code of MODFLOW is open and easily accessible.

The numerical model is used as a tool to study the future scenarios which are calculated uploading a new period of data for some of the boundary conditions. In order to study the effects of climate variables new rainfall and temperature time series are used to estimate the corresponding groundwater recharge for each land use, using the soil water balance approach. Results of the soil water balance are introduced into the modelled period as a recharge boundary condition for six hypothetical years. The process followed is that detailed in Figure C.

The rainfall serie was calculated based on the Standardized Precipitation Index (SPI) method (Guttman, 1999, 1998; Mckee et al., 1993). The SPI index was developed as a versatile tool in drought assessment, analysis and monitoring to represent both short timescales (e.g., soil moisture status) and long timescales (e.g., reservoir and groundwater storage). The SPI can be seen as the standard deviation of observed anomalies with respect to the long-term average for the same period (month, season or year). The expected total rainfall depth is described in terms of terciles: “below normal” is rainfall less than the 33rd percentile, “above normal” is rainfall greater than the 67th percentile and “normal” is in between the 33rd and 67th percentiles. Each scenario describes a sequence of rainfall seasons that reflect a specific stress condition.

The SPI method has been used to characterize meteorological droughts over a wide range of timescales and areas (Mckee et al., 1993). Values and their interpretation are

summarized in Table 5.1. For the purposes of this analysis, the SPI categories were lumped together into three categories that distinguish “below normal”, “normal” and “above normal conditions”.

Table 5.1. SPI classification.

SPI Values	*Classification*	*Lumped categories*
2.00 and above	Extremely wet	Above Normal
1.50 to 1.99	Very wet	
1.00 to 1.49	Moderately wet	
-0.99 to 0.99	Near Normal	Normal
-1.00 to -1.49	Moderate dry	Below Normal
-1.50 to -1.99	Severely dry	
-2.00 and less	Extremely dry	

The method requires the selection of a “primary” rainfall record to select specific seasons based on the SPI. The seasonal rainfall total depths and the SPI were calculated for each season. The mean monthly rainfall measured indicates the seasons for specific area. Four different rainfall scenarios were developed to reflect different degrees of deviation from a 3-year “normal” rainfall pattern. The “normal” scenario is compiled exclusively from seasons which fall in the normal category (i.e. -1.0<SPI<+1.0). The “wet” scenario is compiled using rainfall seasons which fall in the “above normal” category (i.e. SPI>+1.0) and the “dry” and “very dry” scenarios compiled using dry seasons that fall in the “below normal” category (i.e. SPI<-1.0 and SPI<-2.0 respectively). After applying this methodology, rainfall data was spliced to form a synthetic time series of daily rainfall that reflects the rainfall conditions for each scenario.

The temperature time series was generated using the same approach as for the rainfall. The daily temperature data for selected seasons were spliced together to obtain a synthetic time series. Once the temperature baseline time series was built, two plausible temperature scenarios for the selected rainfall stations were defined: TC_0 (Baseline temperature) and TC_2 (Baseline temperature +2ºC).

In order to study the economic growth in an area, the abstraction boundary condition needs to be uploaded with future abstraction data. Firstly, the groundwater demand was

disaggregated across different users and aquifers. In the absence of actual measured abstraction data, the water permit allocation was used. Groundwater permits ascribe a maximum daily abstraction rate for each borehole (m^3/day). One plausible abstraction scenario (referred to as D0) assumes that the total abstraction is equal to the daily allocated amount for 365 days per year. A second scenario assumes that groundwater demand has increased (Scenario D2). This second future estimation considers implicitly the future population and economic growth, since more people would imply more groundwater consumption.

5.2.2. Field application

The groundwater model and the futures scenarios have been tested in the study area presented in Section 1.3 (Fig. 5.1).

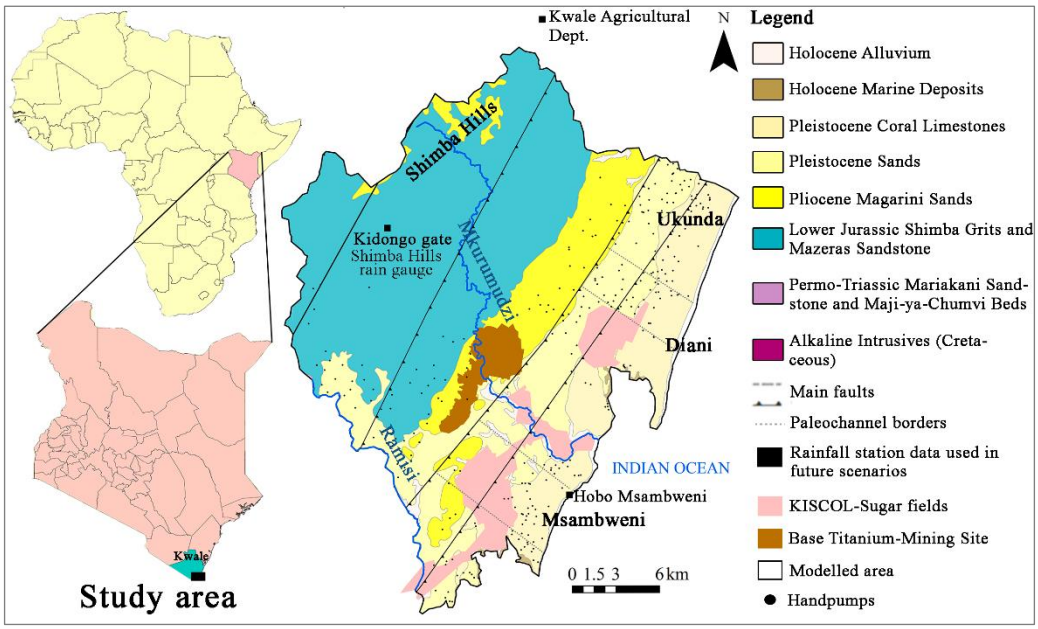

5.1. Study area with the main geological units and formations. The squares are the rainfall stations used to calculate the recharge in the future scenarios.

5.3. Groundwater model setup

The groundwater flow model has been constructed using the MODFLOW-2005 Package and the graphical interface ModelMuse (Winston, 2009). MODFLOW is a 3D code that solves the finite-difference method and includes modules to simulate steady-state or transient groundwater flow in confined/unconfined aquifers (Harbaugh, 2005). A steady-state

simulation has been conducted to set up initial conditions, as compared with field data. The transient simulation covers an eight year period from from 2010 until November 2017. Monthly stress periods with 3 time steps in each have been adopted in the model simulation.

Model grid and boundary conditions

The uniform finite difference mesh of the study area has been discretized in 120 columns and 99 rows, with a size of 300 m x 300 m per cell; thus, the model includes 11,880 cells and represents an area of 665.5 km^2. The vertical discretization extends from the ground surface, determined from a Digital Elevation Model with a resolution of 90 m x 90 m. Geophysical surveys at large scale using ERT (electro-resistivity tomography) helped to define layer thicknesses and to improve the understanding of the geological structure.

The three aquifer units have been discretised in 16 horizontal layers. The first two layers represent the shallow aquifer unit (Pliocene-Pleistocene Fm.). The next 10 layers represent the middle aquifer (Kambe and Mtomkuu Fm.). This layer is discretized in several layers to represent the two palaeochannels present in the study area, one in the north and another in the south. The last four layers represent the deep aquifer (Mazeras sandstone) (Fig. 5.2).

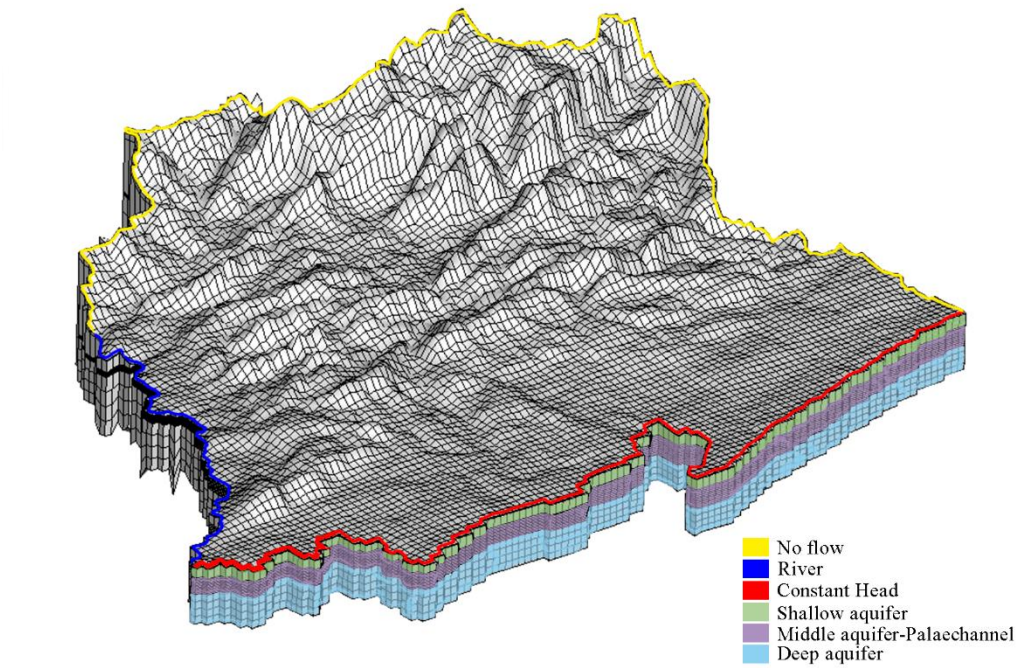

Figure 5.2. Modelled domain gridded with the boundary conditions to limit the model area. The cross section colours indicate the discretization for the main aquifer units; shallow aquifer (green), middle aquifer/aquitard/palaeochannels (red) and deep aquifer (blue).

The model limits have been defined by lateral boundary conditions and include the following two natural boundaries: the coastline of the Indian Ocean to the east and the Ramisi River to the south. The sea level has been defined by a Dirichlet condition with the MODFLOW package CHD (Time-Variant Specific Head). The Ramisi River has been defined as a river condition. The other model boundaries have been defined as no flow (Fig. 5.2).

Other defining conditions are used in the model:

Recharge from precipitation. Groundwater recharge has been estimated for the modelled period (2010-2017), for each land use. This recharge has been calculated by soil water balance and the result has been introduced into the model as the main input. The process followed and the data used to calculate the recharge is detailed in Section 4.3.1. In order to define accurately recharge values, field experiments were carried out to verify that the soil properties data base (KENSOTER, cited in Section 2.4.2) was correct. In addition, historic rainfall data from an established climate station was used, as well as rainfall data from new manual rainfall stations established by the study.

Groundwater abstraction. A large number of pumping wells were defined to describe the groundwater abstraction using the WEL package. The main groundwater abstraction is carried out by the main economic activities in the study area: mining, irrigated sugarcane and factory, and hotels. The abstraction rate for each economic activity, plus the community boreholes and handpumps, are detailed in Section 4.4.

Surface/groundwater interaction. The perennial rivers in the study area (the Ramisi and Mkurumudzi Rivers) have been defined using the RIV package, which calculates water exchange between the rivers and groundwater. The river bed conductance has been defined by calibration and was set at 12 m/d. Small ephemeral surface water flows were defined using the DRAIN package, since flows only occur during intense rainfall events. This type of boundary condition only allows groundwater discharge to rivers when groundwater level is higher than the river channel. The drain conductance has been defined by calibration and was set at 55 m/d for all drains.

The hydraulic parameters have been divided into zones, based on geological formation. Due to the lack of hydrogeological parameters, the transmissivities for the main geological formation were obtained from boreholes drilled during the 1980s to the mid-1990s (thanks to the first-large scale deployment of the Afridev handpump). The Afridev is a lever-action reciprocating handpump, originally designed to be maintained at the village-level and capable of a pumping lift of up to 45 m (Baumann and Furey, 2013). The Swedish International Development Cooperation Agency (SIDA) played a critical role in financing the programme. The transmissivity for each borehole was calculated from specific capacity, using the Galofré equation (1966) (Custodio and Llamas, 1976) taking the LPS (litre per second) test data and calculating the difference between the static and dynamic groundwater level obtained during the borehole construction. The transmissivities have been complemented with hydrogeological data obtained during Base Titanium borehole drilling and pumping tests in the deep aquifer system. Horizontal hydraulic conductivities (*Ky* and *Kx*) were set, while the vertical component (*Kz*) was fixed as 10 % of the horizontal hydraulic conductivities. In order to simulate the effect of the low permeability barrier behind the indurated corals located adjacent to Kilindini Sands, a HFB (Horizontal Flow Barrier) package was used. This package simulates thin, vertical low-permeability geological features that impede horizontal groundwater flow. Given that changes in hydraulic heads are negligible compared to the saturated thickness, all model layers are assumed to behave as confined units (constant transmissivity).

A steady-state simulation was used to conduct a first calibration of hydrogeological parameters and determine the initial heads of the transient simulations. The transient

simulation covers the period 2010 to 2017, though the period most representative of the mass balance is from 2014 to 2017; from 2010 to 2013 the water balance is based on simulated heads affected by unknown initial heads. Fortnightly groundwater head data from 34 observation shallow wells measured from 2016 to 2017 and groundwater heads measured in Base's water resources monitoring network (ten deep boreholes and 18 shallow boreholes) from 2012 to 2017 were used to calibrate the model (Table 1, Appendix A). The hydraulic conductivity and the specific yield values were calibrated manually. The root mean squared error (RMSE) has been selected as an indicator of goodness of fit.

Due to the uncertainty of some GWL measurements in some hand-dug wells, different weights have been defined by type of water point: lower weights were applied to hand-dug wells and higher weights to piezometer wells installed by Base Titanium, as the screened sections are well-defined. Results show that the simulated GWLs match most observed GWLs, with a R^2=0.89. The main calibrated hydrogeological parameters (i.e., *Kx* and *Ss*) are presented in Table 5.2.

Simulated GWLs fit the observed GWLs fluctuations in most of the observation wells (Fig. 5.3). The middle zone of the study area, mainly wells located in the Kilindini sands, are the wells with the best-fitting. Regarding the fluctuations through the model period, the drawdown slope of the simulated values is better adjusted than the recovery slope of GWLs. However, there are some simulations of wells located to the north and south, mainly in the Magarini sands, where simulations need a better adjustment.

Table 5.2. Obtained hydraulic conductivity and specific storage for the entire model domain after calibration processes with observed data.

Geological formation	***Hydraulic conductivity (K) in m/day***	***Specific storage (Ss) in m^{-1}***
Alluvial	50	0.001
Corals Fm.	between 100 and 300	between 1E-5 to 0.001
Kilindini sands	between 1 and 40	0.008
Pliocene Fm.	between 0.1 and 3	0.0007 to 0.01
Mazeras Fm. outcrop	1	1.00E-05
Mkomtuu and Kambe Fm.	between 0.1 and 1	0.0001
Palaeochannels	0.6 to 1.1	0.01

Regarding the tendencies of GWLs in each geological formation, the coastal wells located in the corals show fast but small GWL variations. The water level decline variation of these wells is less than two meters, being the maximum peak of GWL increase after the rainfall event of April 2016 (model time 2708). The simulated GWLs of the wells located in Kilindini and Magarini sands show a different pattern compared with the wells located in Pleistocene corals; GWL variation through the model period is smoother, with a maximum water level decline of around two meters (Fig. 5.3). These wells show GWL recovery after the drought period in the wake of the long rains wet season of 2017. The wells located in the deep aquifer show more pronounced GWL variations than GWLs in the shallow aquifer units, with a maximum water level decline of four meters (Fig. 5.3).

The groundwater balance was also analysed during the 2010-17 simulation period (Table 5.3). From 2014 to 2017, the results show that the recharge term in the groundwater balance is the main input of the system and represents 80 % of the total input, which comprises the recharge and river inflow to the aquifer. Groundwater discharge includes groundwater abstraction from the shallow and deep aquifers, lateral aquifer discharge to the sea and groundwater flow from the aquifer to the rivers. In dry years, like 2016, there is 75 % less recharge compared with 2017. This can be attributed to last La Niña event. Around 20 % of aquifer recharge comes from the main river channels (Table 5.3).

The main output of the system is groundwater discharge to the ocean, which represents around 46 % of total outputs. This output is constant throughout the modelled period, with only 8 % less outflow to the sea in the year of least recharge (2016) compared to 2017. Another important output of the model is the flow coming from drains, which is also nearly constant throughout the model period, even during the years of least recharge. Total groundwater abstraction only represents 0.44 % of total outputs (Table 5.3).

This net balance is almost constant along the modelled period. Based on the potentiometric map (data not shown), most recharge from surface water infiltrates in the downstream reach of the Mkurumudzi River, where river to aquifer inflow is 52 % higher than the aquifer to river outflow. In contrast, the Ramisi River receives around 67 % more water from the aquifer than the aquifer gets from the river. This is in agreement with the hydrochemistry of samples of the river presented in Chapter 2, where a sample upstream was more saline than a downstream sample, showing surface water dilution with groundwater outflow.

The model shows some of the limitations of the conceptual model. The northern area appears to be less influenced by La Niña event than the central area (see Ferrer et al. 2019). The calibrated model shows different hydrodynamic behaviour in this area. However, there

is no objective geological or hydrogeological evidence that the northern area is significantly different to the central area, particularly with respect to the shallow aquifer system.

Table 5.3. Water balance results in hm3/year for the transient simulation. Note: Mku is the Mkurumudzi River. The * in 2017 means that the total water balance for that year is from January to November.

Modflow terminology	***Real terminology***	***2010***	***2011***	***2012***	***2013***	***2014***	***2015***	***2016***	***2017****
Recharge in	***Recharge***	71.44	160.60	50.05	86.13	156.93	169.42	57.89	224.07
River	***Mku. Stream losing***	25.21	25.35	25.95	26.39	26.62	26.67	27.64	24.99
Leakage in	***Ramisi Stream losing***	4.86	5.16	5.55	5.35	4.89	4.73	5.14	4.33
Constant Head in	***Inflow from the sea***	0.00	0.00	0.00	0.00	0.00	0.00	0.00	0.00
TOTAL IN	***Total inflow***	101.52	191.10	81.55	117.87	188.43	200.83	90.67	253.40
Wells out	***GW abstraction***	0.30	0.31	0.40	0.45	0.95	1.01	1.97	1.58
Constant Head out	***GW discharge to the sea***	88.51	103.73	84.53	84.69	93.51	99.59	81.41	88.89
River Leakage out	***Mku. Stream gaining***	13.71	12.69	10.80	9.98	9.88	10.11	8.63	8.79
	Ramisi Stream gaining	15.43	15.83	14.24	14.28	15.36	16.55	14.50	14.20
Drains out	**Drains**	94.13	85.54	77.23	73.50	76.42	82.06	73.27	79.22
TOTAL OUT	**Total outflow**	212.08	218.11	187.20	182.90	196.12	209.33	179.78	192.68
IN-OUT	**Change in storage**	-110.56	-27.00	-105.65	-65.04	-7.68	-8.50	-89.12	60.71

Simulated GWLs in wells located in the Magarini sands also show a poor fit to observed values. Again, this could be due to conceptual model limitations, such as an incomplete understanding of the full extent and continuity of the palaeochannels; or the potential hydraulic continuity with surrounding formations. Finally, it could also be due to an incomplete understanding of the full extent of the aquitard, which separates the groundwater system into the shallow and deep aquifers.

However, the model is reasonably effective in simulating the groundwater dynamics of the aquifer. Therefore, it has been used as a tool to analyze the complicated groundwater behavior of the aquifer system under future scenarios.

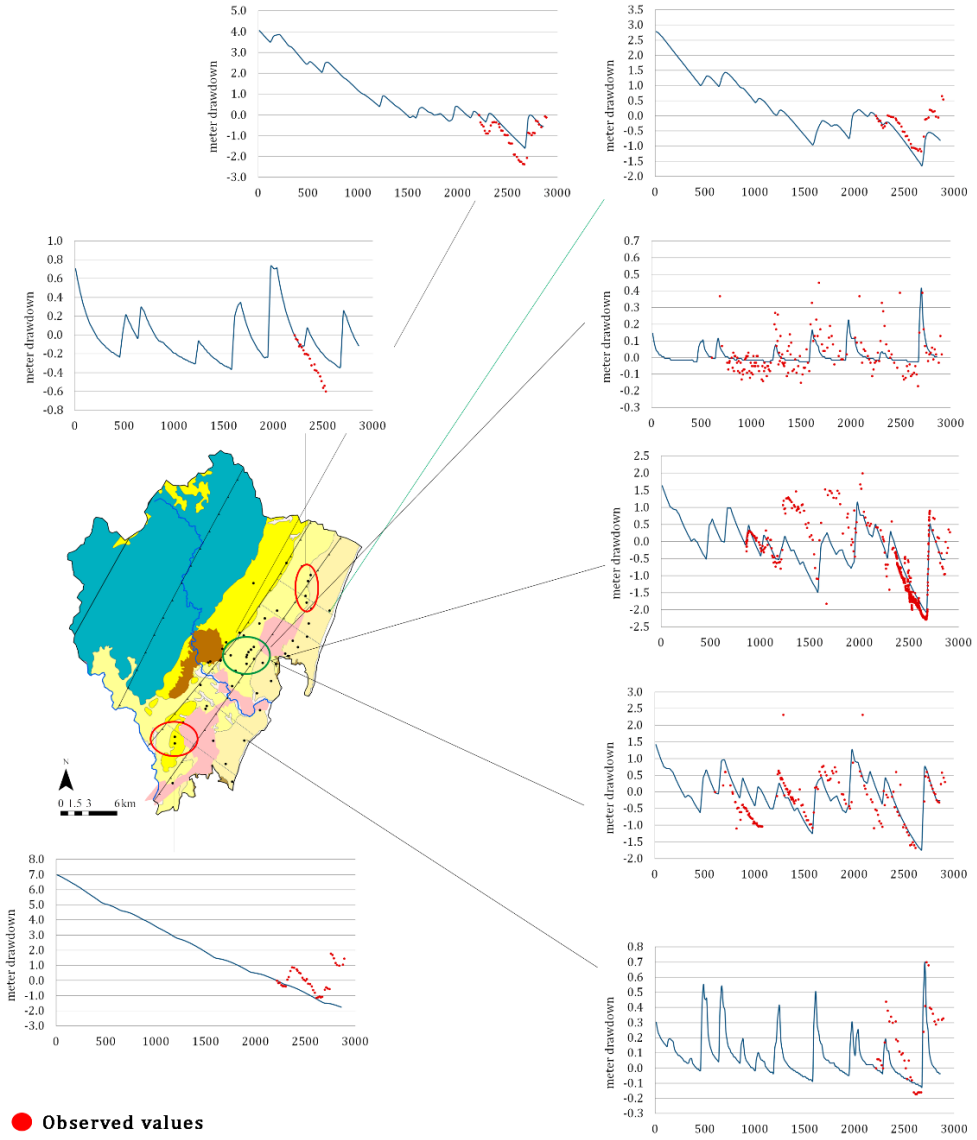

Figure 5.3. Observed values (red dots) versus calibrated values (blue line) of some representative wells for each geological formation. The red circles are the areas with less effectively calibrated groundwater drawdowns. The green circles are the Base Titanium shallow piezometers with good fitting.

5.4. Future scenarios

To simulate the future groundwater resource availability under global change, eight scenarios encompassing the rainfall, temperature, and groundwater demand variables have been considered (Table 5.3), in order to understand the sensivity of the system to a combination of different changes; the simulation period covers the hypothetical six year period. The first three years simulate the possible drought periods with low and very low rainfall (1st rain cycle). The persistence within the system of impacts induced under the change scenario is tested under different recovery scenarios that are defined by the characteristics of the rainfall in the recovery phase (2nd rain cycle). Therefore, the last three years of the future simulations take into account a normal and an above normal precipitation, which is responsible for the recovery of the aquifer system. All the scenarios, except one, are calculated without a temperature increase, since these were considered the most realistic short-term scenarios. A scenario with a 2 °C temperature increase was generated to study the impact of increased temperature on the aquifer system. Finally, all the scenarios were run for current abstraction volumes and future increased abstraction to study the effect of abstraction on the system. These eight model scenarios are summarised in Table 5.4.

Table 5.4. Combinations of variables used to simulate the eight numerical flow models to represent different future climate change scenarios.

Variable of future scenario	***Dry_ Normal_0 _Current***	***Dry_ Normal_0_ Increase***	***VDry_ Normal_0 _Current***	***VDry_ Normal_0 _Increase***	***VDry_ Normal_2 _Current***	***VDry_ Normal_ 2_ Increase***	***VDry_ Wet_0_ Current***	***VDry_ Wet_0_ Increase***
1st rain cycle	Dry	Dry	Very dry	Very dry	Very dry	Very dry	Very dry	Very dry
2nd rain cycle	Normal	Normal	Normal	Normal	Normal	Normal	Wet	Wet
Temp.	0ºC	0ºC	0ºC	0ºC	2ºC	2ºC	0ºC	0ºC
GW Demand	Current (D0)	Increase (D2)	Current (D0)	Increase (D2)	Current (D0)	Increase (D2)	Current (D0)	Increase (D2)

5.4.1. Data used in field application

The Shimba Hills (Kidongo Gate) record has been the most appropriate "primary" station to apply SPI, as it is located centrally within the study area (Fig. 5.1). The time data and daily data set records range between 1959 and 2017, with data gaps between 1989 and 99, and in 2002. The mean monthly rainfall measured in Shimba Hills indicates that the seasons for this area are best defined as January-March (JFM), April-June (AMJ), July-September (JAS) and October-December (OND). In order to develop rainfall surfaces that reflect the natural spatial variability of rainfall, the Msambweni DO and Kwale Agricultural Department station records were used for matching the time periods defined previously (JFM, AMJ, JAS and OND), as selected for Shimba Hills (Fig. 5.1).

In order to create the temperature time series, two SWAT Global Weather (Soil and Water Assessment Tool) stations have been used to represent the rainfall time series between 1979 and 2015. The TAHMO stations (Trans-African HydroMeteorological Observatory) for Msambweni and Kidongo Gate have been selected, based on proximity, to extend the SWAT data to cover the period 2016 – 2017. The net result has been a synthetic temperature time series for each of the three rainfall stations (Shimba Hills, Kwale Agric. and Msambweni DO) used as the temperature input data for the simulation of the rainfall scenarios.

Groundwater abstraction is controlled by the total amount of water allocated to the user by the Water Resources Authority (WRA) through water permits. Groundwater permits ascribe a maximum daily abstraction rate for each borehole (m^3/day). This may vary season to season. Here, in the absence of actual measured abstraction data, the water permit allocation was used. Four different types of users were identified, namely: (I) mining, with abstraction from the deep aquifer; (II) irrigated sugar farming, with abstraction from both the shallow and deep aquifers; (III) tourism enterprises, with abstraction from the shallow coastal aquifer; and (IV) medium-scale public water supplies and rural communities, with abstraction from the shallow aquifer. The future abstraction rate for each activity and information sources are detailed in Table 4.3.

5.5. Results and discussion

5.5.1. Effects of climate variability on recharge

The possible future temperature increase of 2°C implies a 7 % reduction in recharge when the same future climate and abstraction variables are compared under the scenario with three very dry years followed by three years of normal rainfall. The recharge reduction due to increased temperature is lower than 7 % in the wet scenarios compared with the driest scenarios (Table 1, Appendix D). The groundwater model balance confirms that rainfall is the key climatic variable responsible for the main input of water into the aquifer system, as suggested previously in Chapter 2. Considering future estimation in Kenya, where climate projection estimates that rainfall intensities and total rainfall will increase, but wet seasons will be shortened, and droughts will be deeper and last longer (Herrero et al., 2010), the scenarios considered are plausible and would have an important impact on groundwater resources in the study area.

The recharge volume for the future scenarios has been calculated based on future rainfall patterns for the three rainfall stations (Fig. 5.1). Table 5.5 shows that the correlation between the rainfall and the recharge is not linear, confirming that there is no simple direct relationship between average annual rainfall and recharge (Butterworth et al., 1999). This is especially significant for the normal scenario in which the two years show a total precipitation slightly above 1200 mm, but a range of recharge between 51 and 160 mm. In particular, rainfall during intense but short storms is more effective in driving recharge than lower intensity, more continuous rainfall. The rainfall intensity and distribution through the year influences net recharge, rather than simply the total annual volume of rainfall. Therefore, an intense rainfall event (>100mm) on a saturated catchment leads to intense and significant recharge. This is consistent with other studies of the phenomenon (Carter and Parker, 2009; Taylor et al., 2012; Taylor and Jasechko, 2015). Recharge differences across different climate scenarios can be explained by antecedent soil moisture. When the field capacity of the soil is empty (i.e. at the end of a drought period), rain is retained in the soil until the soil moisture deficit is satisfied, so less recharge reaches the aquifer. The opposite happens in wet soils (i.e. during wet periods), where the soil field capacity is full, so more net recharge reaches the aquifer. The normal rainfall annual mean of this area is greater than 500 mm per year, indicating an area where the results show that the population relies on regular recharge (MacDonald et al., 2009). Current recharge meets demand, but if climate change were to induce a reduction in recharge, either from a decline in total rainfall or in the intensity of individual rainfall events or periods which disproportionately contribute to recharge, would represent a risk to the population.

Table 5.5. Rainfall at Kidongo Gate (Shimba Hills), in mm/year versus recharge in hm3/year for the 3 -year future scenarios.

Station Shimba Hills*		***Year 1***	***Year 2***	***Year 3***
	Rainfall (mm/year)	432	392	461
Very Dry	Recharge (hm^3/year)	12	12	9
	Rainfall (mm/year)	578	698	694
Dry	Recharge (hm^3/year)	11	17	12
	Rainfall (mm/year)	1245	1157	1209
Normal	Recharge (hm^3/year)	160	72	51
	Rainfall (mm/year)	2226	2005	2336
Wet	Recharge (hm^3/year)	305	272	340

5.5.2. Effects of rainfall variability

In this aquifer system, despite reduced recharge under drought conditions, the discharge from the system through the different boundaries is nearly constant. The reduction of the water stored is reflected by the GWLs across the entire system, which decline during all drought periods. The aquifer system is significantly affected by three years of dry conditions, and needs a wet period in order to recover to the initial state (Figure 5.4). The GWL decline over a three year drought period is not reversed when followed by three normal climatic years. The general patterns of GWLs in wells located in the shallow aquifer for different future scenarios is similar. It shows that there is little difference in water level decline in the 3-year dry or very dry scenarios. The main difference in the GWL patterns comparing the different scenarios is the 3-year wet scenario, which is the period required for the aquifer system to recover (Fig. 5.4).

These GWL declines are not the same in all geological formations, so the possible effects are also not the same. In the deep aquifer, GWL decline is higher compared to levels in the shallow aquifer, with a maximum of 10 meters after a three drought year. This decline could affect abstraction by the main water-intensive industries in the area supplied from deep boreholes. The cost of pumping groundwater increases approximately linearly with changes in water table depth in groundwater-fed irrigation systems, where energy cost is the main component of water price (Foster et al., 2015). This increased energy cost could increase the sugar and by extension Base Titanium operating costs and consequently product prices.

The shallow wells located in the Kilindini and Magarini sands are the most susceptible to desiccation. The GWL decline in these geological formations will be around 5 meters after a three year drought scenario. This will materially influence community well-being, since these communities are largely supplied by handpumps exploiting the shallow aquifer. Of the observation wells used to calibrate the model, the depths of 26 of them are known; 60 % of these wells would become dry after a long dry period. In fact, 29 % of these wells were dry at the end of the 2016 drought. In prolonged drought periods, shallow wells often fail. Those result indicates only deeper hand-dug wells and boreholes are reliable across all seasons and in drought periods. Long drought periods would also influence community economies in the study area which are based mainly on subsistence farming and small-scale livestock-raising. Even though water level decline in wells located in the corals near the coast will not be as significant as in other geological formations, small GWL declines could be sufficient to increase the risk of saline intrusion; climate change, particularly long drought periods, favours increased saline intrusion (Kumar, 2012; Okello et al., 2015b).

Rainfall variability will also influence the river-aquifer relationship, reducing river flows as outflow from the aquifer to rivers during drought periods declines. The reduction of flow from aquifer to river in a dry year will be 20% less compared to a normal climatic year. During prolonged drought periods, this could then affect the dams used for water supply by the main industries (Base Titanium and KISCOL). The use of dams to store surface water by the water-reliant industries, along with the pumping of groundwater illustrates the importance of conjunctive use of water resources in the study area. In conjunctive water resources management, groundwater resources are used in dry periods in anticipation of wet season recharge. Recharge is made more effective if groundwater abstraction is reduced during recharge periods, when water demand can be met by surface water sources. Therefore, conjunctive water management is the optimum way to use water sources when seasonal variations in water availability are taken into account. The climatic conditions in Kwale mean that surface water resource availability is strongly seasonal, following a bimodal rainfall year. Dams are constructed to store wet season water for use at other times. Groundwater, on the other hand, constitutes a water resource that is available throughout the year, but is subject to certain constraints. The most significant of these are the effective groundwater recharge and actual abstraction.

Rainfall variability could not only produce drought periods. but also wet periods where rainfalls will be above average. These wet periods are needed for aquifer systems to recover after a long drought period, since average rainfall after a drought is insufficient to lead to full groundwater level recovery. Thus, if a drought period lasts longer than one year and the

annual recharge is 70% less than an average year, as occurred during the 2016 La Niña event, a long wet period is need for the aquifer system to recover. This GWL increase would occur in both aquifer systems and in all geological formations, with higher GWL increase in the Kilindini and Magarini sands. The GWL level increment in these shallow aquifers could have negative impacts on groundwater quality in the area. This could be explained as major increases in GWLs in the shallow aquifer could reach the bottom level of pit latrines, the most common human excreta disposal systems in the study area, enabling pathogens and other contaminants to directly enter shallow groundwater. Furthermore, wet periods imply an increase in groundwater discharged to the sea (Supplementary material wet scenario). Although increased discharge to the sea may reduce the saline wedge penetration, it has a negative effect on seagrass diversity (Kamermans et al., 2002). This study found that groundwater outflow influences seagrass species diversity along the East African coast, with less species diversity observed in lagoons with high groundwater outflow.

5.5.2.1Progression of the saline wedge

This sub-section discusses the movement of the saline wedge based on the equation presented in Ferrer et al. (2019a). In this case, reduced recharge caused by a drought period (29,863 m^3/d) and increased abstraction from 3,616 m^3/d to 23,589 m^3/d would move the saline wedge 0.5 km inland, where it is located under current abstraction, reaching 2 km inland under these conditions in the future. At 6 km inland, the top of the saline water wedge is calculated to be located at 93 m bgl under current abstraction, but would rise to 29 m bgl under the future abstraction scenario, affecting the shallow aquifer. The progression of the saline wedge under the future drought scenario is higher compared to the hypothetical scenario with the same increased abstraction scenario and the recharge produced during La Niña event presented in Ferrer et al, (2019). These calculations indicates that in other coastal regions with higher abstraction rates and higher hydraulic conductivities, the saline wedge would penetrate further inland and produce negative impacts for groundwater users.

Since most of the population lives near the coast (Carter and Parker, 2009; Nlend et al., 2018), aquifer salinization near the coast will affect groundwater quality and reduce the availability for a large proportion of the population of Kwale. This will also affect coast hotel water supply and so will impact the country's economy. According to the Kenya Tourist Board (KTB), about 65% of the tourists coming to Kenya visit the Coast. People living along the Kenyan Coast depend extensively on tourism, which is already being affected by changes in weather and climate (Ongoma and Onyango, 2014). Anecdotally salinization is already affecting the drinking water of hotels in this area.

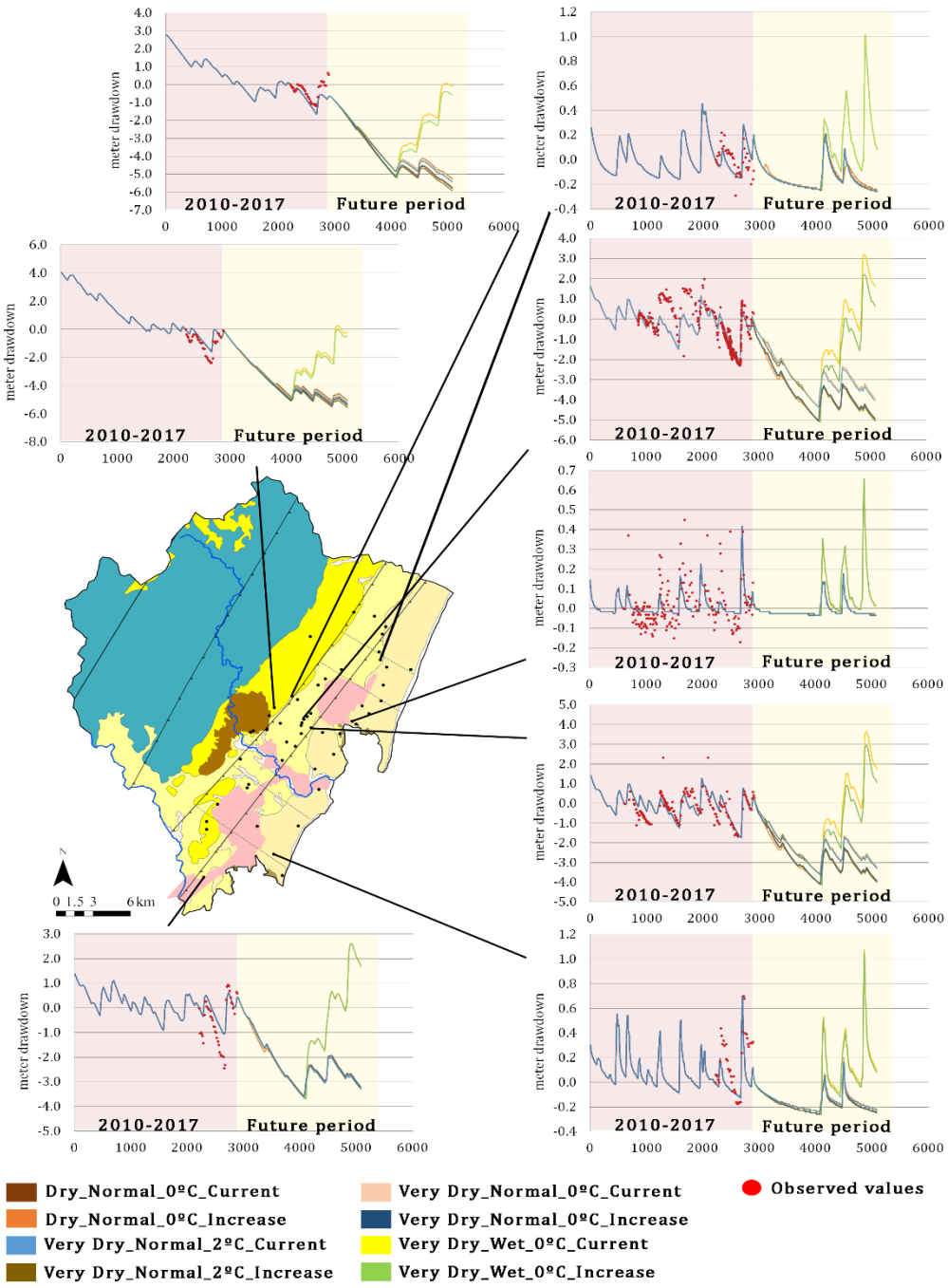

Figure 5.4. Observed versus simulated groundwater drawdowns, calibrated for different geological formations from 2010-2017 (pink shading) and for simulated future scenarios (yellow shading).

5.5.3. Effects of temperature increment

The 2 °C temperature increase under the wet scenario cannot be observed in GWL evolution as the effect of increased temperature on GWLs is less than 0.05 meters. Increasing temperature will produce an increase in PET, which in turn will lead to reduced recharge. However, the effect of increased PET is limited, leading to a water level decrease of around 0.05 meters. Despite the temperature increase not significantly affecting the GWL decline during drought periods, the increased temperature will affect agriculture. Serdeczny et al. (2015) show that each day during the growing season with a temperature above 30 °C reduces yields by 1% compared to optimal, drought-free, rain-fed conditions. Maize, for example, one of the commonest crops in Sub-Saharan Africa and in the study area, has been found to have a particularly high sensitivity to temperatures above 30 ˚C during the growing season. In addition to this, the rainfall reduction during drought periods presented here will affect crop productivity, which will need irrigation, or more irrigation in order to mitigate yield losses.

5.5.4. Effects of socio-economic growth

The total anticipated volume abstracted will increase by around 85 % compared with current abstraction (Supplementary material). The percentage of this increment will affect the aquifer storage in each of the future scenarios, reducing the aquifer storage around 1% in the dry/normal scenario and 2 % in the very dry/normal and the very dry/wet scenarios.

Focusing only on increased groundwater pumping rates, abstraction would reduce the volume of groundwater in storage and increase the rate of water level decline across the system. Increased abstraction also has a local effect on water levels in shallow and deep wells located near intensively-pumped boreholes. The future GWL patterns in wells located in the middle zone near the Base Titanium well field, show the effect of the increased abstraction scenario, compared with the current abstraction scenarios. Water level decline in the deep aquifer in the middle area may produce a water level decline in shallow wells in the middle area that would be around 0.6 meters, rising to a maximum of 1 meter compared with wells located far from the well field in the same geological formation. In addition (and as with shallow wells located near the well field), there are differences in the GWL response in the deep aquifer under both current and increased abstraction scenarios, depending on the distance of the observation piezometer from the production well. Piezometers located near production wells show a higher water level decline under future increased abstraction, which would be between 3 and 5 meters. This could be due to the affect of the drawdown cone produced in the pumping well. The only scenario which leads to full deep aquifer GWL

recovery is the three wet year scenario under the current pumping regime. On the contrary, under the three wet year scenario under increased abstraction, the GWLs do not fully recover (Fig. 5.5). This shows that increased abstraction will affect the shallow aquifer in the middle part of the study area, worsening the situation already produced by climate change.

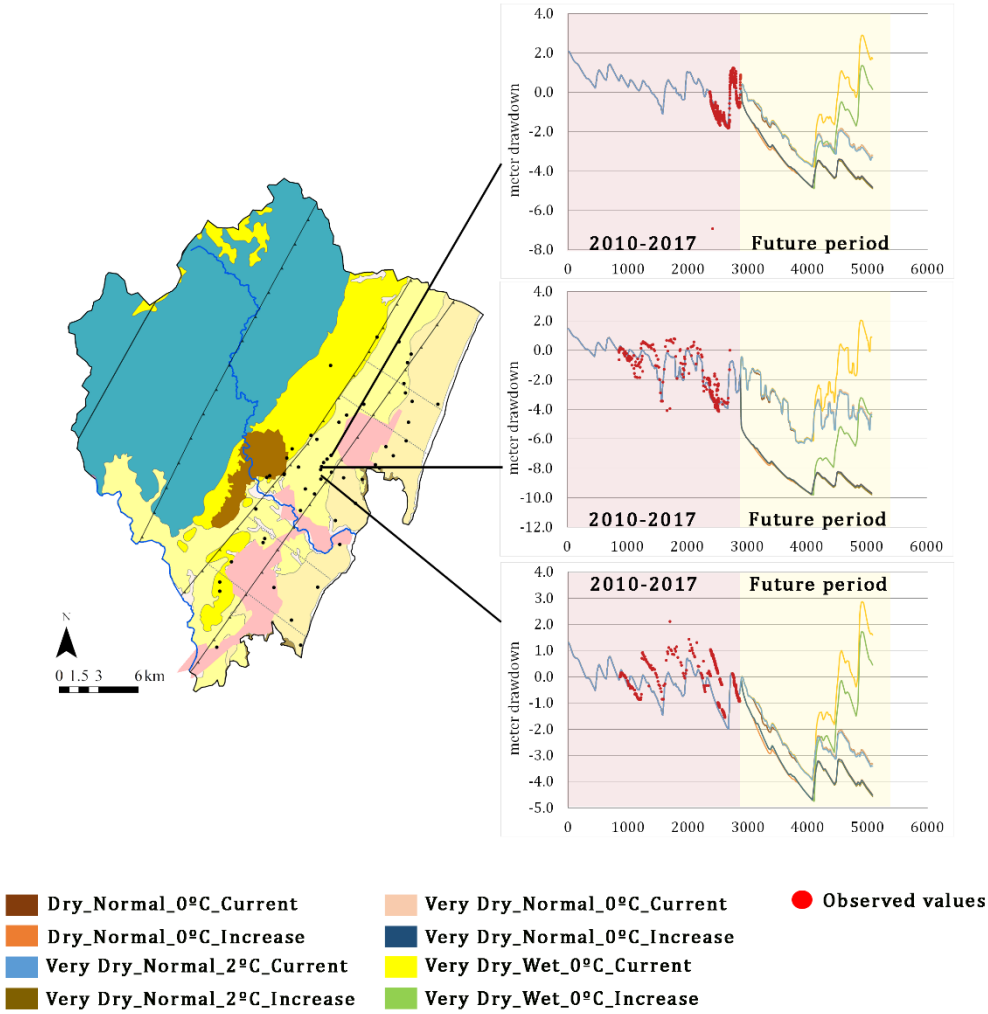

Figure 5.5. Observed versus simulated groundwater drawdowns, calibrated for wells drilled in the deep aquifer unit from 2010-2017 (pink background) and GWLs for the simulated future scenarios with yellow background.

5.6. Conclusions

This study presents the first numerical groundwater flow model of an aquifer located on the East African coast, based on a conceptual model developed previously. The conceptual model helped to build the numerical model, which was subsequently calibrated against known groundwater level and abstraction data; it also shows the limitations already defined in the conceptual model. The numerical model confirms the current sustainability of the aquifer system and the capability of water levels in the system to recover after drought events, like La Niña event of 2016.

This model has been used as a tool to test empirically how rainfall and temperature variability could affect recharge in Africa and in aquifer system by including also the increment of abstraction due to the future socio-economic growth. The future scenario models show the importance of recharge in maintaining the volume of water in aquifer storage. Recharge is not linearly correlated with rainfall in 'normal' and 'dry' rainfall scenarios. Rainfall distribution and intensity are more important in producing effective recharge than the total annual rainfall. GWL patterns show that the aquifer needs a rainfall period above 'average' in order to recover GWLs after a long drought period. The impact of increased abstraction is not equal across the study area. Wells near the Base Titanium well field show greater drawdown in GWLs under increased abstraction future scenarios. Finally, deep piezometers located near the Base Titanium production boreholes show GWLs drawdown that do not fully recover, even during wet periods under the projected increased abstraction rates. The future scenarios show the possible impacts on the groundwater system, such as movement of the saltwater wedge, desiccation of community shallow wells and increased cost of deep groundwater abstraction. These would affect both the large-scale and community users of groundwater, of particular concern being the impact on the latter, who—absent other sources of supply—will struggle to get access to reliable potable water.

This future groundwater depletion will not only be related to the consequence of drought periods or the future abstraction increase, but also is related to the economic and social policies of the study area. A well management should involve the stakeholder and all the water-reliant users of the area in the process of decision making. These results, which are a long term approach, should help to make management policies and practices that improve human-water relationships by harmonizing the equilibrium between humans and natural water resources, mainly when they are under pressure, such as during a drought period. Furthermore, this chapter emphasises the minimum data of an aquifer system needed to make sustainable management of groundwater resources.

Chapter 6

Safety, Closeness and Reliability-SCR Index

6.1. Introduction

Almost one-fifth of the world's population, live in areas of water scarcity. Another almost one quarter of the world's population, face economic water shortage, meaning areas lacking the necessary infrastructures to take water from rivers or aquifers (UN, 2016). Two thirds of the world's population currently live in areas that experience water scarcity for at least one month a year (Mekonnen and Hoekstra, 2016).

Inadequate sanitation is also a problem for 2.1 billion people, being exposed to diseases such as cholera, typhoid fever, and other water-borne illnesses. Two million people, mostly children, die every year from diarrheal diseases alone. Another 844 million people do not have even a basic drinking water service. This includes 263 million people who have to spend over 30 minutes to arrive to a drinking water supply source, and about 159 million still drinking untreated water from surface water sources, such as streams or lakes (www.unicef.org).

With the existing climate change scenario, it is expected that by 2030 water scarcity in some arid and semi-arid areas in the planet will displace between 24 million and 700 million people (UNDP, 2006). Furthermore, population growth is creating an increasing demand for water, and due to the rising of living standards, water consumption per capita is also likely to increase (Sullivan, 2002). This means that water resource availability is linked to economic and social progress, suggesting that development is likely to be influence by the combination of water availability and how water resources are managed (Sullivan, 2002).

Provision of a reliable, sustained, and safe water supply worldwide has become a top priority on the international agenda, being one of the UN Sustainable Development Goals. Water managers are often faced with an increasing and competing demand, but with limited resources to manage it (Giné Garriga and Pérez Foguet, 2011). Therefore, good information supported by appropriate indicators is required to determine how a populated area is faring, whether it is on-track to meet its objectives of full safe supply and what decisions need to be made to maximize performance. A key prerequisite to support effective planning is to access consistent information through accurate monitoring, backed up by rigorous interdisciplinary science. Thus, it is needed to develop an index that can offer policy planners an appropriate tool for performance monitoring, benchmarking comparisons, policy progress evaluation, public information, and decision making. Simple aggregated indices can encapsulate more than one measure of progress in a single number, and allow quantitative and qualitative elements to be combined (Sullivan et al., 2003). However, indices are incomplete and imperfect tools, and caution is required when using them for supporting poverty alleviation (Giné Garriga and Pérez Foguet, 2010).

One such index is the Water Poverty Index (WPI), developed by Sullivan (2002). WPI has been recognized as a useful and holistic tool in policy analysis, and specifically designed to contribute to effective water management (Sullivan et al., 2003). It was created as an interdisciplinary indicator to assess water stress and scarcity, linking estimates of water availability with the socioeconomic drivers of poverty (Giné Garriga and Pérez Foguet, 2010). The WPI has been applied in different areas in the World, such as Java, Mexico, and North Kenya (Giné Garriga and Pérez Foguet, 2011; López Álvarez et al., 2015; Perera and Muttil, 2009), both at the local and national scales (Giné Garriga and Pérez Foguet, 2010; Lawrence and Meigh, 2003; Sullivan and Meigh, 2007; Sullivan et al., 2003).

The WPI was developed in a participatory manner, through consultation with a wide range of stakeholders, policy makers, and scientists. Despite all the studies are based on five key components (Resources, Access, Capacity, Use, and Environment), every study case is based on specific variables or subcomponents. WPI combines the information from local authorities, field investigation and household surveys to assess an integrated indicator of water poverty at some specific time ("steady state conditions"). Due to the correlation between the variables and the subjectivity of the response of the surveys completed by users, it is difficult to predict how some of these variables might change in the future.

Therefore, it is relevant to find a tool that could help evaluating the future groundwater availability in areas based on a simplistic and fast way, since in low-income areas, any solution to improve water poverty assessment needs to be efficient and cost-effective. The successful and sustainable development of groundwater resources in these areas is critical for future safe water supplies, economic growth and food security in the continent. Regional assessment of the impacts of climate change indicates that future changes in rainfall patterns including large drought periods and concentrated precipitation events with very large variability will reduce recharge. This, coupled with increasing population growth (both in urban and in rural areas), will reduce population access to drinking water resources

Therefore, the goal of this chapter is to go an step forward to build an index to assess the risk for a given household to have no access to drinking water (in terms of either quantity or quality) under "transient" conditions and incorporating data from groundwater models, the "management tool" for groundwater managers and planners. The index developed is based upon the already existing WPI, but focused on hydrogeological data that could be provided by numerical groundwater models outputs (piezometric level and drawdowns) and household fields (households geographical location). Therefore, the index intends to be objective, yet due to the difficulty to obtain reliable information related to the water use in

developed countries, this new index is based only on 3 simple variables: Safe to drink, Closeness to the supply source, and Reliability (thus, the name SCR). One of the advantages of using numerical models as inputs of the index is the potential of evaluating the effects of different future scenarios related either to climate change or to future water management realities (e.g., groundwater abstraction in time and the spatial distribution). Finally, showing the changes in this new index spatially by mapping could help water managers to define the potential riskier areas to suffer scarcity in terms of the fraction of affected households in some given area. The index SCR has been tested in the study area.

6.2. Development of the SCR index

The idea of obtaining an "ideal index" that perfectly captures and aggregates variables of very interdisciplinary nature is quite challenging. Yet, many such indices have been developed and are widely used. We intend to present an index based only on elements supported by groundwater numerical models, thus avoiding both the inclusion of non-quantitative index or based on surveys or public perception. This does not preclude any problem on existing indices, but it expresses the need for getting fast quantitative results that could be translated efficiently into one index that relies only on groundwater aspects to map the areas prone to suffer water scarcity.

6.2.1. Regional approach

As cited before, the SCR index is a local index applied at a household scale. However, it is recommended to calculate first the availability of groundwater as a resource at the aquifer (regional) level in order to frame the development of the SCR index. The term "Availability" in this study is the equivalent to the term Resources (R) used in the WPI. This indicator looks at how much groundwater is available per unit of time for each person in a particular area, and it is defined as (López Álvarez et al., 2015):

$$A = \frac{Recharge - Abstraction}{Recharge} \qquad \text{(eq. 2.1)}$$

A negative value of index A points to groundwater mining, defined as the withdrawal of groundwater over a sustained period of time that exceeds the natural recharge rate of the aquifer. An area with low (or negative) availability might need to find other sources of water, which most of the time is less safe. Notice that both recharge and abstraction as a function of space and time are inputs to regional numerical groundwater models, the former usually obtained from a soil water balance, while the latter is directly related to groundwater use for population supply, industry and agricultural needs.

6.2.2. Local approach

The SCR index is composed by 3 variables:

Safety (S, component X_1): this parameter of the index is related to the groundwater quality. Groundwater quality is an important issue when assessing the risk of water resources, due to the fact that poor quality of groundwater can affect social, health and economic aspects, clearly influencing household poverty. A conservative transport model is an option to assess the groundwater quality evolution. Many numerical models are available to simulate the contaminant flow path in the aquifer. The partial differential equation describing the transport of contaminants in 3D transient groundwater flow systems can be written as:

$$\frac{\partial(\mathrm{nC})}{\partial \mathrm{t}} = \sum_{i,j} \frac{\partial}{\partial \mathrm{x}_i}\left(nD_{ij}\frac{\partial \mathrm{C}}{\partial \mathrm{x}_j}\right) - \sum_i \frac{\partial}{\partial x_i}(nv_i C) + q_s C_s + \sum_n R_n \qquad \text{(eq. 2.2)}$$

where C is dissolved concentration of contaminant (mol/L), n is porosity of the medium, D_{ij} is hydrodynamic dispersion coefficient tensor (m^2/s), C_s is the external concentration (mol/L) of the source or sink flux being q_s (L/s), R_n are sink/source terms driven by geochemical reactions (mol\L-s), and v_i is the seepage or linear pore water velocity (m/s), calculated as $v_i = -\frac{K_i}{n}\frac{\partial \mathrm{h}}{\partial \mathrm{x}_i}$. The external source can be used in model predictions, being obtained from numerical codes used externally (e.g., coupled climate-recharge codes).

The concentration range at the point of interest (supply well or small defined area, defined from the numerical model, either at the cell size or downscaled) will be normalized (range [0,1]), where 1 means no pollution and 0 means that the contaminant concentration is over the limit established by the WHO. The quality problem is composed by multiples components, such as chemical elements, trace metals, organic compounds, or pathogens. Therefore, this parameter will be quantified as follows: if only one compound of the total number analyzed exceeds the limit defined by the WHO, the quality index assigned to a well will set equal to 0; otherwise, a linear or non-linear relationship can be stablished to assign the index value to a given value of concentration. We suggest

$$X_1 = \begin{cases} 1 - C/C_t & if\ C < C_t \\ 0 & if\ C \geq C_t \end{cases}$$

In the case of lack of data to build a full transport flow model, a vulnerability map (based on semiquantitative indices) can give a reasonable delineation of the areas where households are at risk due to a potential reduction of the groundwater quality. This step outlines the use of two tools: GIS and expert judgment, which are often used in conjunction with each

other to produce vulnerability maps. As in the previous methodology, the concentration of a given contaminant will be normalized from 0 to 1 based on expert judgment.

In some cases, the index X_1 could be based on only one specific quality problem. For example, in the case of a coastal aquifer, the evaluation of Safety could be based on the potential salinization of wells caused by the seawater wedge progress. In this case, the full numerical model can be replaced by a simple evaluation of the length of the toe of the saline wedge, given analytically by

$$L = \frac{K*\beta(1+\beta)*b^2}{2q_t} \qquad \text{(eq. 2.3)}$$

where L is the length of the saline wedge; K means the arithmetic average of the horizontal hydraulic conductivity; b is the aquifer thickness; β is the ratio of the difference between saltwater and fresh water densities to fresh water density, being approximately equal to 0.03 for the Western Indic Ocean (Poisson et al., 1981); and $q_t = \frac{W-Q}{coast\ length}$ where W is regional freshwater flow and Q is groundwater abstraction, so that the difference, $W - Q$, is the net discharge of freshwater to the sea. This equation can be used to delineate in plain view a boundary line separating fully penetrating wells that are located in the intrusion area or not. Additional equations can be used for partially penetrated wells to evaluate upconing.

Closeness (C, component X_2): this parameter considers whether a groundwater source is available near a given household. Collecting water is often the most time-consuming and most important daily activity for women and young girls in developing countries (www.unicef.org). The average distance that women and children walk for water in Africa and Asia is 6 km. It has been estimated that women in sub-Saharan Africa spend 40 billion hours annually fetching and carrying water from sources (that not always even provide clean water) far from home. The time spent collecting water makes it difficult for women to focus on other economic activities and for young girls to attend school. The weight of the water they carry also exposes them to a greater risk of malnutrition, back problems, and anaemia. The combination of illiteracy, malnutrition and recurrent sickness combine to perpetuate poverty and gender inequality in some rural areas.

Sometimes this term of closeness to a water resource is determined by a socio-politic geographic distances. This means that a household can be supplied by a given well despite having another one closer, just based on own or family (inherited) decisions. However, using an objective approach in order to define the SCR index under future scenarios, we assume an acceptable maximum distance of 15 minutes walking or 1 km distance, based on Giné Garriga and Pérez Foguet (2010) and (MacDonald et al., 2012).

A simple way to assign this index is based on calculating the distances between a given household and all available supply points (not necessarily the Euclidean one, as elements such as existing paths, orography, property issues, can be significant). Using a GIS platform is most convenient. Notice that during a certain period of time one well can become dry, polluted, or just deactivated due to malfunctioning of the pump or political issues. In such a case, distances should be recalculated to find the next available source. To give a quantitative value to this parameter, we assume that a distance equal or higher than a predefined distance L_t (by default we stablish 1 km) leads to a value of 0, while shorter distances are quantified using a linear formulation expressed as

$$X_2 = \begin{cases} 1 - L/L_t & if\ L < L_t \\ 0 & if\ L \geq L_t \end{cases}$$

Reliability (R, component X_3): this parameter is defined as household access to a drinking water source sustained in time. In many countries, the water supply is only reliable during the wet season, since during the dry season most wells become dry. Therefore, reliability should mostly be assessed during the dry season. From a groundwater model, reliability is governed by the difference between groundwater heads (in unconfined aquifers) and the bottom of the well. This difference is termed "water column (H)"; it is location-specific, and evolves with time. The minimum value of H that can sustain pumping depends on the pump (existence, type) and on drilling boreholes characteristics.

Another point is to define for how long a well has to remain dry (H below the minimum value) to consider a well as non-reliable. This can be assessed through an initial survey in households, or from expert judgement based on climate conditions, average size of a family, household water use, and other local conditions, that would be used to estimate the amount of days that a given family could survive without fetching clean water. An option to calculate the risk related to the water scarcity could be defined as 1 meaning that the water column does not decline below the predefined value in a given period, while 0 indicates the opposite. Thus, in principle this value is binary at a given time, yet it can take any value between [0,1] if a probabilistic approach is adopted so that water column becomes uncertain in predictive scenarios.

6.3. Structure of the Index

The SCR index has a similar structure to that of the WPI and aquifer vulnerability index (DRASTIC). The three key components are combined using the following general expression:

$$SCR = \sum_{i=1}^{3} w_i X_i \qquad \text{(eq. 3.1)}$$

Where X_i refers to component i of the SCR structure (S=1, C=2, R=3) and w_i is the weight applied to that component. The weights are constrained to be nonnegative and to add up to one, thus implying that SCR lies also in the range [0,1].

In any composite index, the choice of weights is aimed at reflecting the relative importance given to the variable comprising the index. Despite weight selection based on consultation with experts is a quite a subjective method, it is a conventional practice in most existing indices that combine multidisciplinary data, regardless whether parameters are treated as deterministic or uncertain (DRASTIC is a well-known example, see, e.g., Armengol et al., (2014). Alternatively, multivariate techniques, such as principal component analysis or factor analysis, present an empirical and objective option for weight assignment. No weighting system is beyond criticism.

Each term composing the SCR index is a function of time, and so does the full SCR index. This time should be defined by the experts or could be an outcome of the numerical model, thus calculating the SCR index for all predefined times.

The scores obtained from the SCR index will be distributed in order to provide a qualitative indicator of risk, from "high risk" ($SCR \in [0,0.25]$), "medium risk" ($SCR \in (0.25,0.5]$), "low risk" ($SCR \in (0.5,0.75]$), or "no risk" ($SCR \in (0.75,1.0]$).

6.4. Development and application at the household scale

6.4.1. Case study

To illustrate the application of this index, and to study how it changes under future climate scenarios, a real application was explored. The study area is defined in Section 1.3 of this document. Complementary to the information already presented, in August 2013, a waterpoint survey identified 571 handpumps (all Afridev model, see Section 5.2) in the study area of which 45 % were non-functioning. A sample of 531 handpump locations were used as a framework for two rounds of household surveys in 2013/14 (Nov-Jan) and 2015 (March-May). In 2014-2015, multidimensional poverty indices (MPIs) were mapped, interviewing around 3500 households. This study showed that groundwater and welfare can be conceptualized together merging information on water resources, drinking water, productive systems, and welfare status (Katuva et al., 2019). Some of these variables are clearly related to the components of the SCR index.

In 2019, a numerical groundwater flow model of the studied aquifer was built using Modflow-2005 code presented in Chapter 5. The outputs of these flow model scenarios have been used to delineate the SCR index for future scenarios.

6.4.2. Data available and methodological application of SCR to the study area

The three components of the SCR index were calculated for the case study based on the characteristics of the boreholes and the data available:

Safety: Kwale is a coastal area with salinity problems due to seawater intrusion (recall Section 4.5.4). Therefore, the X_1 component was only based on EC (electrical conductivity) measurements. EC was measured in 2014 during the corresponding household field survey, and these point values were used to delineate the map of estimated EC concentrations based using kriging as the interpolation method. In those areas with estimated values higher than 1000 μS/cm, a value of 0 was assigned to X_1. For the years modelled years (2015-2017 plus 6-future simulated years), the salinity progress was defined from equation 2.3, using the groundwater flux from the numerical model in a deterministic way. In dried wells, the values were also assigned to 0. Those wells with the EC values under 1000 μS/cm the safety value was 1.

Closeness: the term closeness was inferred from questions asked in the 2013/2014 field survey, where components of each household were requested to answer whether they thought that the community handpump was close. The Euclidian distance was measured between each household and the handpumps reported. From the results of the survey, a distance of L_t = 400 m was assigned as the value indicated in average by the households to declare that a supply point was considered far. Therefore, we assigned a value of $X_2 = 0$ when $L > 400$ m, and $X_2 = 1$ when $L < 400$ m. When a community well was dry, the distance from the household to the closest handpump was recalculated to the next well in terms of component values.

Reliability: Available data includes the depth of boreholes and the topographic elevation obtained from a Digital Elevation Model. The numerical model provides drawdown values every 15 days and we calculated the annual mean decline for each borehole and for each simulated year. Taking as reference piezometric map, the one corresponding to 2014, the drawdown in each well and construction data allowed mapping the water column at each pumping well and for the different simulated years. The Afridev handpump devices stop working when the water column is zero. If there is no groundwater decline $X_3 = 1$, when the water column is zero $X_3 = 0$, and a weighting between 0 and 1 if

there was some groundwater column decline always having groundwater column value above zero.

6.4.3 SCR Index maps.

The household surveys in 2013/14 and 2015 carried in the study case were used to obtain the georeferenced location of the boreholes and the households interviewed in the welfare field survey. Boreholes locations were introduced in the existing numerical flow model to get the groundwater head decline at each borehole under different global scenarios. Each parameter has the same weight (0.33).

First of all the Availability term has calculated for each year to have a regional view of the aquifer system and its evolution under different global scenarios. The availability value range from 0.19 during the drought period to 0.96 during the wet scenarios both with the future increase of abstraction. Looking in detail the SCR evolution using the modelled data from 2015 to 2017, the figure 6.1 captures the effect of the drought year caused by La Niña event that triggered a severe drought in East Africa in 2016 (recall the model presented in Chapter 2). The figure 6.2 shows the evolution for each individual parameter. In the case of La Niña event the X_2 and X_3 are the parameters that changes more from 2015 to 2017.

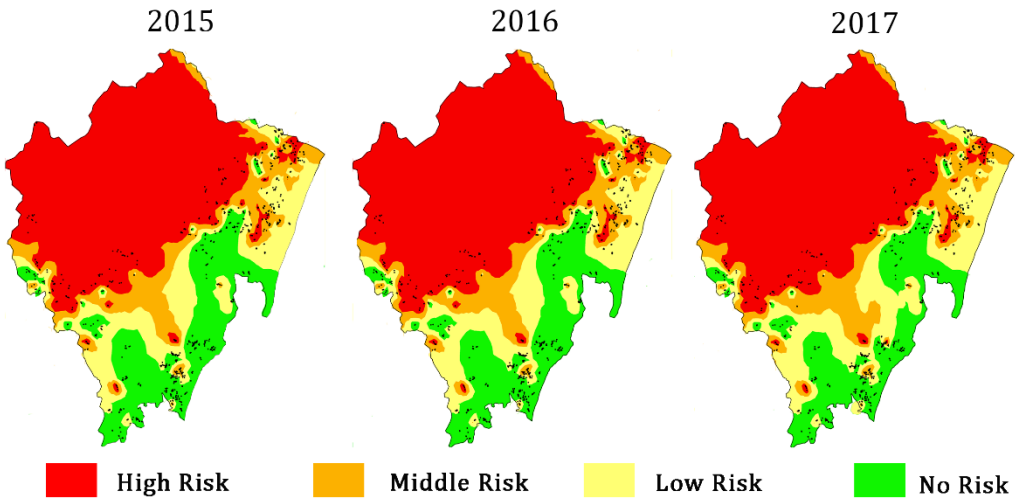

Figure 6.1. SCR index from 2015 to 2017. Red colour means values from 0 to 0.25 (high risk), Orange colour means values from 0.25 to 0.5 (middle risk), green colour from 0.5 to 0.75 (low risk) and blue colour from 0.75 to 1 (no risk).

6.4.4. SCR maps – Predictive scenarios

The impact of future climate scenarios (6 simulated future years) is displayed in Fig. 6.3. It represents a 3-year long drought period, with the rainfall volume 90 % less compared to an average year, followed by a 3-year long wet period, with the rainfall annual volume 70 % more compared to the average. During all the simulation period, we considered an increment of groundwater abstraction with respect to the present value, following the scenarios presented in Chapter 4.4.

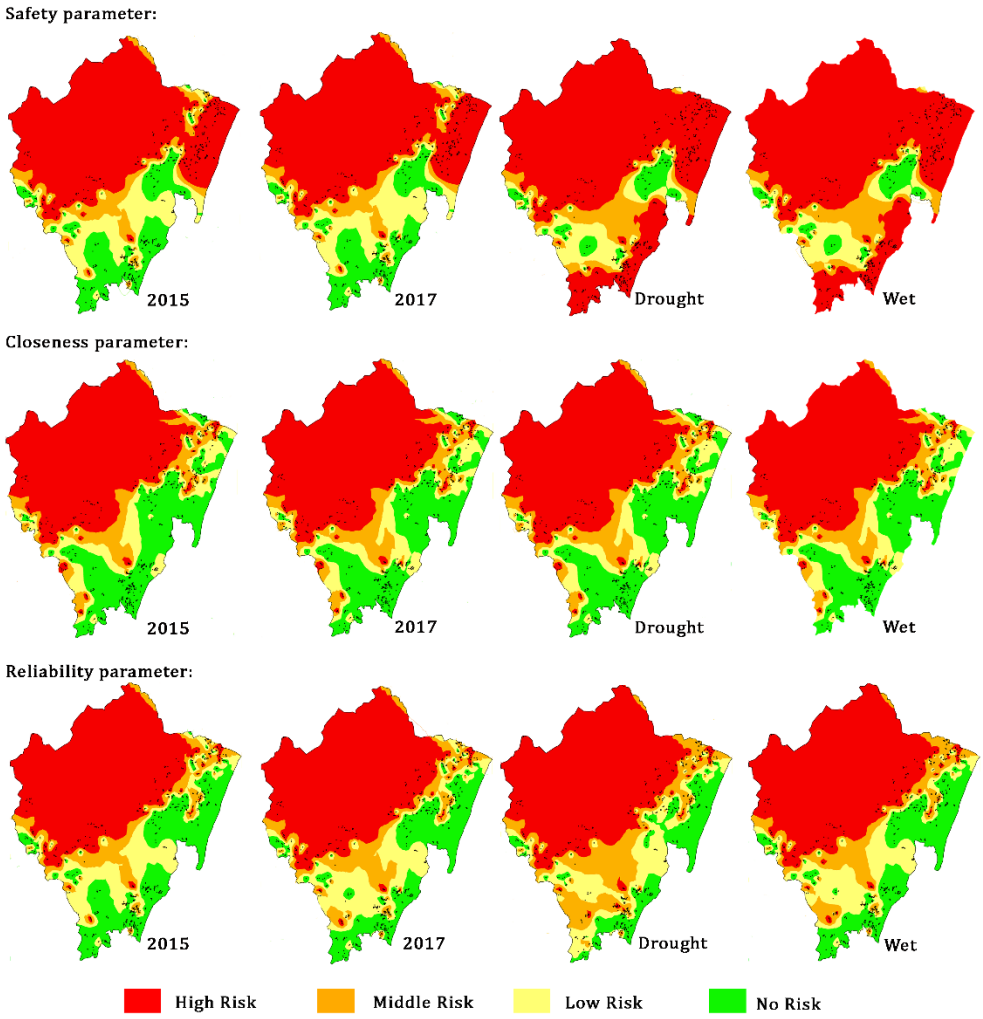

Figure 6.2. SCR index values for each parameter, Safety, Closeness and Reliability.

6.5. Discussion

Figure 6.2 displays the S,C,R terms for three representative years: 2015 and 2017, affected by (hypothetical dry year), and (hypothetical wet year). The spatial patterns of all components are quite different. The one displaying the lower values is X_1, with high-risk values in the north coast, and in the inland area due to some of the wells located in the Magarini sands were dry. Low values of Safety appear in the drought year, indicating the effect of seawater intrusion in the south coast, due to the reduction in recharge. In order to value the salinity changes thought the time, a variable-density flow model should be run, since the eq. 2.3 only works for steady state situation. However, the salinity variable during the wet year shows that this effect does not get reverted as stated in the Chapter 2 and 4, since the salinization process takes years to revert its effects on the handpumps/ wells.

The closeness parameter is quite constant throughout the simulated years. This parameter presents lowest values inland where there is less handpump density and thus, there is more distance between them.

Reliability is the parameter that changes more as a function of climate conditions showing the effects of the variability in recharge. The reliability value decreases during the drought period, and increases during the wet period in the wells located on the coast, as recharge is the main driving factor controlling water column.

Overlapping the three maps for the S, C, R indices we obtain the areas that are most vulnerable to suffer groundwater supply shortages under different scenarios. Here we separate the effects of periods with existing data (2015-2017, see Fig. 6.1), from predictions based on the outputs of the numerical model (Fig. 6.3). In 2014, the central study area displayed very low values of SCR, since most of the wells in this area were reported dry. There is some uncertainty in these result, as it could be an error associated with the topographic data (elevation was extracted from a 90m x 90m DEM map) with the respectively associated error that could provide huge errors in the initial conditions input in the model.

The SCR index decreased widespread during La Niña episode that started in 2016 and lasted until April 2017. The effects of this drought period made that some handpumps became dry, mainly in wells located some km inland from the coast.

Maps corresponding to the 3-years of drought were based on predictions considering a three-year drought period caused by climate change (see Chapter 5). The effects of drought seem to be translated to the SCR Index mostly for the first two years. The lowering in the index, and therefore the increase in the perception of risk, is mainly due to the enhancement

of the saline wedge progress due to the reduction of recharge and the increase in abstraction and, consequently, the reduction in net discharge to the sea. Indices slightly (not fully) recover after 3 wet years where some wells located inland and not affected by saline intrusion see an increase in SCR, changing from “low risk” to “no risk”.

Due to the lack of data related to the household located on the northern area in the mountainous range, it is not possible to define reliable SCR indices in this area. The value depicted in the maps are thus just extrapolations.

We can also state the relevance of location in the relevance of the individual components of the SCR Index. Inland, Reliability is the most significant variable. However, on the coast, Safety becomes key. Furthermore, Closeness is more significant inland as compared to the households located at the coast, since the latter location concentrates most of the population, and thus they are the areas with the highest concentration of wells.

The SCR index is a simple tool for the water manager in order to be able to take decisions regarding water supply to rural areas with simple, yet quantifiable, data. The advantages of using only three variables are clear. But the simplicity is also one of the drawbacks. We know that more parameters would be needed to incorporate additional information that could result in informed decisions, but here we consider that the three components selected: distance, groundwater quality, and quantity, encompass enough relevant information to make first decisions in complex areas. It is an easy index that can help to define the first maps that show the areas of highest risk to suffer a reduction of good water supply. Then, these maps could be used as a baseline tool to study in detail the areas where higher budget should be devoted in order to obtain additional data that could be included in different, more sophisticated, indices, such as the WPI.

Despite the simplicity of the components, there are also prone to errors. In the study case, one such error was caused by the resolution to the DEM map, leading to erroneous values of the initial water column, so that some wells were assumed as dry. A more accurate technique, such as a DGPS could have been used (difference in elevation between a DEM map and DGPS can range 5 m of difference). Furthermore, detailed information of each borehole depth is a must, while this information is rarely available in developing countries. In addition, in the study case we fixed a zero value for Reliability is zero when the water column was zero, but this can be different depending on the waterpoint and pump characteristics. Furthermore, the perception of Reliability can be somewhat subjective for every household, with a strong local variability even for neighbouring households. Moreover, in the study case, we calculated the average annual groundwater decline, but it should be more specific to calculate the SCR index for each climatic season. So, it is

important to know the climate of the studied area to define the correct time index, also a challenging problem as most climate change scenarios provide data in a very coarse grid that should then be downscaled to the elements in the study area.

Regarding Closeness, this is a relative parameter linked to socio-topography barriers. In this study case, we used as the maximum acceptable distance once taken from a survey, plus we computed distances based on Eucledian distance. These two elements could be challenged, and assigned differently in other realities. For example, acceptable distance (here 400 m) could change in the future, due to unforeseen social and cultural decisions.

Finally, the component Safety defines the quality of the system which is always composed of many parameters. In any given site, we should first screen as many parameters as possible to decide the really stringent ones, but this means money and time to make the analysis. In Kwale County, we based the S component in just one parameter that was easy to measure during the field survey, the EC. Despite EC is always a relevant parameter, mostly in coastal areas, it is not necessarily the most critical one in other realities, where the presence of pathogens could be the limiting element for water quality.

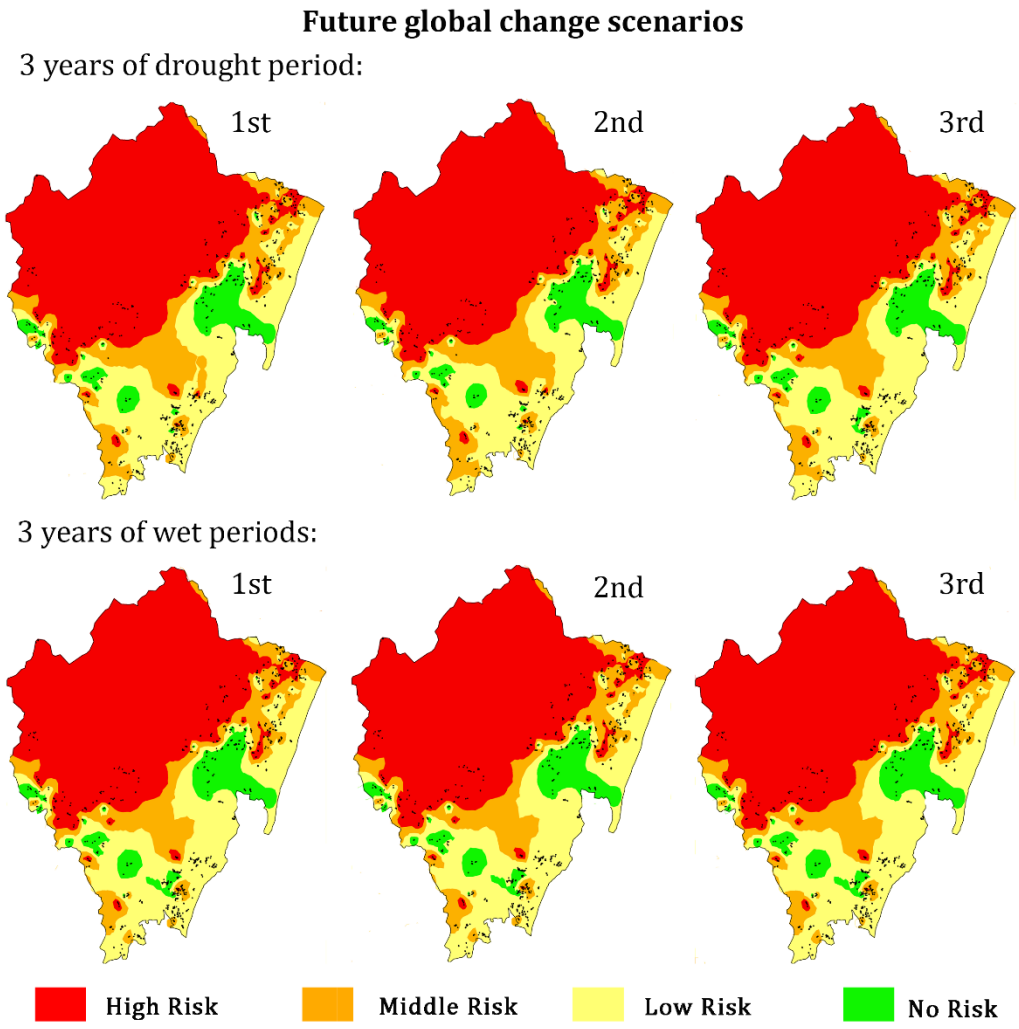

Figure 6.3. SCR index for under future scenarios.

6.6. Conclusions

This chapter presents a new methodology based on an index that measure the risk to run out with groundwater due to scarcity and/or quality reduction for each household. The SCR index has been applied in the study area of Kwale, where the communities are mainly supplied by handpumps. This index is an easy index only composed of three variables that encompass distance between the household and the waterpoint, groundwater quality and, quantity.

The novelty of the index relays in the combination of groundwater model outputs with household data, which allow generating a "transient" risk index that can be calculated for several scenarios depending of the data available to run the initial groundwater model. Its application to the studied area has given consistent results with the current knowledge of the Kwale coast. As this index allows running different potential future scenarios, it helps to understand better the effect of the global change at household scale. Therefore, it is a predictive tool that allows evaluate future potential groundwater risks in time and space, being very useful for water authorities and stakeholders, who will be able to take action before groundwater availability reduction takes place. At the same time, this new index is a step forward to use the real potential of groundwater models for water resources management.

Chapter 7

General conclusions

In the context of Africa, groundwater management is hampered by a lack of information on aquifer characteristics. The data describing groundwater systems is often sparse and so, the current state of aquifer understanding is poor. Furthermore, African nations are the most vulnerable to the effects of climate change due to the slow pace of economic development and inadequate institutional capacity. Plus to climate change, the population growth and the continent industrialization will produce an effect on groundwater systems, reducing its availability and quality. Therefore, more research is needed to understand how all these future changes will affect the groundwater resources and supply, in order to improve and adapt the management of these resources to future global change.

In this dissertation, the aquifer system located in Kwale County (Kenya) has been studied as a paradigmatic case of what is happening in the African continent under socio-economic development. Interestingly, this aquifer is exploited by different water-reliant industries of different kinds (mining, agriculture, tourism), which share groundwater supply with the rural communities. Furthermore, the groundwater system has a geological structure that is representative of an important portion of the East Coast of Africa. The research conducted in this area provides various insights into the problem of aquifer management in the continent under different global scenarios. First, the aquifer has been characterized using physicochemical data, groundwater level measurements, environmental isotopes, and geophysics transects. The main quality problems have been also approached being the most important the anthropogenic pollution of faecal bacteria presence and the induced pollution problem of saline intrusion. Furthermore, the impacts on groundwater availability has been assessed studying the sustainability of the aquifer system under new pump rate by the water-reliant users in the area. The availability of groundwater resources under future climate change has been valued also through the evaluation of the produced by La Niña event 2016/17, a severe drought that affected the aquifer system. All this previous knowledge has helped to build a numerical groundwater flow model in order to integrate all the information available, define the relationship between surface and groundwater and to use it as a tool to study how the climate change and the future increased abstraction rate will affect groundwater vulnerability and how to manage this resource under global change. Finally, a new index has been defined and tested in the study area to define the risk for a given household to have no access to drinking water (in terms of either quantity or quality). Overall, these results are a contribution to the knowledge of how to face the groundwater resource management in this continent under future global scenarios.

The geophysical and geological data point out that the aquifer system is composed by a shallow aquifer composed of young geological materials, including silicate sands (Pliocene Fm.) and carbonates, corals and sands (Pleistocene Fm.), and a deep aquifer composed of

older materials, mainly sandstones (Jurassic and Triassic) which crop out in the western part of the area in the Shimba Hills range. The hydrochemical facies and the water isotopic composition indicate that there is hydraulic connectivity across the materials that comprise the shallow aquifer. The same data show that the Mazeras sandstones in the Shimba Hills are hydraulically connected with the deep aquifer. These two aquifer units are separated by the presence of a middle/low permeability aquitard emplaced between the young and old materials. Furthermore, the geophysical data points that the confined aquifer is disrupted across the area by two in-filled palaeochannels (filled with sedimentary and re-worked fluvio-deltaic materials) perpendicular to the coast (in Zone 1 and 3) that enhance the connectivity between the shallow and deep aquifer in each of these zones. Equipotential lines of the shallow aquifer show that the groundwater flow direction is from the Shimba Hills to the Indian Ocean. The potentiometric map and the hydrochemistry indicate that the Ramisi (Zone 1) and Mkurumudzi (Zone 2) Rivers are gaining streams, receiving water from the aquifer, at least in their middle parts. The hydrochemical data and environmental isotope data shows that the shallow aquifer is directly recharged by local rain through the ground surface and the deep aquifer is recharged laterally from the Shimba Hills where it outcrops. The discharge of both hydrogeological systems is along the littoral to the Indian Ocean, through abstraction by the different water users of the region (communities, agriculture, mining and tourism), through direct and evapotranspiration. This aquifer characterization takes place during the extreme climatic event caused by La Niña event in 2016/2017. La Niña drought affected the groundwater system inducing and important decrease of groundwater recharge reducing it by 78 % compared to the wet year of 2014 and reduced by 69 % compared to a year with normal annual rainfall (2013). During La Niña event, there was a groundwater level decline in 86 % of the measured shallow wells.

During the aquifer characterization different contaminant were analyzed such as trace metals, nitrates and faecal bacteria in 75 and 80 waterpoints, in March and June 2016 respectively. The studied aquifer does not present any trace metal that overtake the health threshold define by the WHO. The nitrates pollution is a localized problem, since most samples in the study area show low nitrate concentrations, under 5–10 mg/L NO_3^-. The small amount of points showing nitrate contamination are located in the main villages of Msambweni, Gazi and Ukunda, except one point located east of the KISCOL sugar fields around Kinondo. The main anthropogenic pollution found in the study area is faecal bacteria (*E. coli*), found in 60 % of the water points. The statistical analysis (PCA and mixed models) have allowed to elucidate which hydrogeological and non-hydrogeological parameter drive this kind of pollution. Opposite to previous studies, recharge/seasonality does not seem to be an important factor influencing the presence of *E. coli* in groundwater.

However, the study case has been performed during La Niña event with nil wet season. Agree with other studies, the well constructive characteristics are the most important factors affecting bacteria presence, having higher concentration in hand dug wells, a common type of well in developing countries. Analysing in detail this type of waterpoints, results indicate that the factors of low Eh and small water column are correlated with higher faecal bacteria pollution.

The other important quality problem in the aquifer area, is the saline intrusion. In the coastal areas with major tourism concentrations, recent years' data show a local salinization effect in the shallow aquifer due to the higher abstraction induced by tourism and associated activities (localized population). Furthermore, due to a reduction in recharge attributed to La Niña drought, salinity in the coastal wells increased between the dry and wet season instead of being reduced, as occurs in normal years. Despite groundwater levels are recovered after the drought period, EC in most shallow wells, remain high even after the important rains of early 2017, indicating that groundwater quality in the coastal zone is not fully recovered. The increase in salinity, as observed in 2016, and the dynamics of the SWI will trend to increase calcite dissolution which could induce other potential risks as increase the creation of sinkholes already observed in parts of the coral limestone during fieldwork and, the rise of hydraulic conductivity induced that could hasten further aquifer salinization.

A part from groundwater quality, the groundwater abstraction by water-reliant users and its impact have been also evaluated by different methods despite the lack of data concerning to abstractions in these areas. In the studied case, recharge term in the groundwater balance is the main input of the system and represents 80 % of the total input. The total groundwater abstraction represents only 1.3 % of recharge during a normal climatic year, such as 2017, pointing out the limited effect of abstraction in normal years. However, in areas of the continent with lower precipitation and consequently lower recharge, a lower level of abstraction could be harmful to aquifers. The obtained results highlight that the lack of historical data such as water level, abstraction, and quality parameters is typically the norm and challenge objective decision-making to face urgent development priorities. This may translate into unknown risks to local, vulnerable populations and future generations who rely on shallow groundwater for water supply. The integration of hydrogeological data from water-reliant industries and/or stakeholders as Base Titanium as well as, the creation of a simple but effective monitoring groundwater network in order to define the sustainability of the aquifer system, can help to overcome these problems. In the case of abstraction data, most of the time unknown in developing countries, simple information

sources (interviews, Google Earth, Trip Advisor, basic analytical methods, etc.) can enable groundwater abstraction to be estimated, allowing potential future risks to be assessed.

The numerical groundwater model built has helped to integrate all the hydrogeological information available in the study area and check the reliability of the conceptual model. The numerical model has defined the surface-groundwater relationship confirming the previously established by the hydrochemical and isotopic data. The limitations detected during the definition of the aquifer characterization has reproduced in the numerical groundwater model mainly in zone 1 and 4. Furthermore, the numerical groundwater flow model has used as a tool to asses the groundwater vulnerability under climate variability and under future increment of groundwater abstraction caused by the socio-economic growth through numerical groundwater flow scenarios. A long drought period caused by rainfall variability causes a GWL decrease in all aquifer units. However, the effect of temperature increment has a low effect on GWL since only implies a 7 % reduction in recharge. The impact of increased abstraction is not equal across the study area since the wells near the Base Titanium well field show greater drawdown in GWLs in increased abstraction future scenarios. After the groundwater level decline during La Niña event and during prolonged dry periods, the aquifer system can recover followed by a humid period. Levels in 95 % of the shallow wells affected by La Niña drawdown recover after the first rainy season (AMJ) in 2017. This allows the system to return to the average groundwater budget and to face the next drought period.

This thesis presents an index which allows incorporating the hydrodynamical function of an aquifer. This allows to study the risk under a “transient time” instead of “steady state”, as most of the current indexes do. Furthermore, the SCR index defines the risk at household level pointing the importance of the groundwater quality, the distribution and density of the waterpoints in the space, and the groundwater availability in order to do good management at long-term. Incorporating the results of future modelled scenarios makes that the index can be used as a predictive, management and plan tool since the most vulnerable areas could be defined and in which households. In this way, different and accurate solutions could be planned to face this risk.

In conclusion, this dissertation shows the reality of the changes that the African continent is suffering. This dissertation contributes to the hydrogeological knowledge in a context that represents much of East Africa. Different tools have been presented in order to study these systems in a hydrogeological context characterized by limited understanding and lack of data. It shows the importance of integrating the hydrogeological data of stakeholders, such as Base Titanium monitoring data in the presented case, and the alternative sources of

information used (Google Earth, Trip Advisor…) to advance the knowledge in areas with lack of data. Furthermore, this dissertation presents how to use different tools and kinds of data to study the sustainability of the aquifer system, focusing on the groundwater availability as well as its quality. This sustainability has been studied not only during the present time but also under different future scenarios affected by global change. Furthermore, integrating hydrogeological and social household data let a bigger understanding of how the groundwater system changes, naturally or induced, can affect the groundwater availability to the water-reliant users. Furthermore, the integration of this information can serve as a reference for water managers and stakeholders in the future.

.

References

A Prüss-Ustün, J Wolf, C Corvalán, R.B. and M.N., 2016. Global Burden of Diseases From Environmental Risks.

Abiye, T., 2016. Synthesis on groundwater recharge in Southern Africa: A supporting tool for groundwater users.

Adelana, S.M.A., MacDonald, A.M., 2008. Groundwater research issues in Africa. IAH Sel. Pap. Hydrogeol. 13, 1–7.

Adhikari, U., Nejadhashemi, A.P., Herman, M.R., 2015. A Review of Climate Change Impacts on Water Resources in East Africa. Trans. ASABE 58, 1493–1507.

Alfarrah, N., Berhane, G., Hweesh, A., Walraevens, K., 2017. Sinkholes Due to Groundwater Withdrawal in Tazerbo Wellfield, SE Libya.

Allan, R.P., Soden, B.J., 2008. Atmospheric warming and the amplification of precipitation extremes. Science (80-.). 321, 1481–1484.

Anglés, M., Folch, A., Oms, O., Maestro, E., Mas-Pla, J., 2017. Stratigraphic and structural controls on groundwater flow in an outcropping fossil fan delta: the case of Sant Llorenç del Munt range (NE Spain). Hydrogeol. J. 25, 2467–2487.

Appelo, C.A.J., Postma, D., 2005. Geochemistry, groundwater and pollution. A.A. Balkema Publishers.

Aquagenx, 2015. Compartment Bag Test (CBT) Instructions for Use: Drinking Water. URL www.aquagenx.com

Armengol, S., Manzano, M., Bea, S.A., Martínez, S., 2017. Identifying and quantifying geochemical and mixing processes in the Matanza-Riachuelo Aquifer System, Argentina. Sci. Total Environ. 599–600, 1417–1432.

Armengol, S., Sanchez-Vila, X., Folch, A., 2014. An approach to aquifer vulnerability including uncertainty in a spatial random function framework. J. Hydrol. 517, 889–900.

Arnell, N.W., 1999. Climate change and global water resources. Glob. Environ. Chang. 9: S31--S49.

Bain, R., Cronk, R., Hossain, R., Bonjour, S., Onda, K., Wright, J., Yang, H., Slaymaker, T., Hunter, P., Prüss-Ustün, A., Bartram, J., 2014. Global assessment of exposure to faecal contamination through drinking water based on a systematic review. Trop. Med. Int. Heal. 19, 917–927.

Bakari, S.S., Aagaard, P., Vogt, R.D., Ruden, F., Brennwald, M.S., Johansen, I., Gulliksen, S., 2012. Groundwater residence time and paleorecharge conditions in the deep confined

aquifers of the coastal watershed, South-East Tanzania. J. Hydrol. 466–467, 127–140.

Barba, C., Folch, A., Gaju, N., Sanchez-Vila, X., Carrasquilla, M., Grau-Martínez, A., Martínez-Alonso, M., 2019a. Microbial community changes induced by Managed Aquifer Recharge activities: linking hydrogeological and biological processes. Hydrol. Earth Syst. Sci 23, 139–154.

Barba, C., Folch, A., Sanchez-Vila, X., Martínez-Alonso, M., Gaju, N., 2019b. Are dominant microbial sub-surface communities affected by water quality and soil characteristics? J. Environ. Manage. 237, 332–343.

Barnett, T.P., Adam, J.C., Lettenmaier, D.P., 2005. Potential impacts of a warming climate on water availability in snow-dominated regions. Nature 438, 303–309.

Barthel, R., Rojanschi, V., Wolf, J., Braun, J., 2005. Large-scale water resources management within the framework of GLOWA-Danube. Part A: The groundwater model. Phys. Chem. Earth 30, 372–382.

Bates, B.C., Kundzewicz, Z.W., Wu, S., Palutikof, J.P., 2008. Climate change and water-Technical Paper of the Intergovernmental Panel on Climate Change. Geneva.

Bates, D., Mächler, M., Bolker, B., Walker, S., 2015. Fitting Linear Mixed-Effects Models Using **lme4**. J. Stat. Softw. 67, 1–48.

Baudoin, M.A., Vogel, C., Nortje, K., Naik, M., 2017. Living with drought in South Africa: lessons learnt from the recent El Niño drought period. Int. J. Disaster Risk Reduct. 23, 128–137.

Baumann, E., Furey, S., 2013. How three handpumps revolutionised rural water supplies: A brief history of the India Mark II/III, Afridev and the Zimbabwe bush pump.

Behera, S.K., Luo, J.J., Masson, S., Delecluse, P., Gual- di, S., Navarra, A., Yamagata, T., 2005. Paramount Impact of the Indian Ocean Dipole on the East Af- rican Short Rains: A CGCM Study. J. Clim. 18, 4514–4530.

Bhattacharjee, S., Ryan, J.N., Elimelech, M., 2002. Virus transport in physically and geochemically heterogeneous subsurface porous media. J. Contam. Hydrol. 57, 161–187.

Bin Hu, Yanguo Teng, Yilun Zhang, Chen Zhu, 2019. Review: The projected hydrologic cycle under the scenario of 936 ppm CO2 in 2100. Hydrogeol. J. 27, 31–53.

Blaschke, A.P., Derx, J., Zessner, M., Kirnbauer, R., Kavka, G., Strelec, H., Farnleitner, A.H., Pang, L., 2016. Setback distances between small biological wastewater treatment systems and drinking water wells against virus contamination in alluvial aquifers. Sci. Total Environ. 573, 278–289.

Broström, G., Holmberg, H., 2011. Generalized linear models with clustered data: Fixed and random effects models. Comput. Stat. Data Anal. 55, 3123–3134.

Buckley, B.S., 1981. Report on a visit to assess Groundwater Potential of the Kenya Coast of Malindi (including proposals for the South Coast Groundwater Resources Project).

Institute of Geological Sciences (IGS), Wallingford, UK.

Butterworth, J.A., Macdonald, D.M.J., Bromley, J., Simmonds, L.P., Lovell, C.J., Mugabe, F., 1999. Hydrological processes and water resources management in a dryland environment III: Groundwater recharge and recession in a shallow weathered aquifer. Hydrol. Earth Syst. Sci. 3, 345–351.

Candela, L., Elorza, F.J., Tamoh, K., Jiménez-Martínez, J., Aureli, A., 2014. Groundwater modelling with limited data sets: The Chari-Logone area (Lake Chad Basin, Chad). Hydrol. Process. 28, 3714–3727.

Cannon, R.T., Simiyu Siambi, W.M.N., Karanja, F.M., 1981. The Proto-Indian Ocean and a probable paleozoic/mesozoic triradial rift system in East Africa. Earth Planet. Sci. Lett. 52, 419–426.

Carter, R.C., Parker, A., 2009. Climate change, population trends and groundwater in Africa. Hydrol. Sci. Sci. Hydrol. 54, 676–689.

Carvalho Resende, T., Longuevergne, L., Gurdak, J.J., Leblanc, M., Favreau, G., Ansems, N., Van der Gun, J., Gaye, C.B., Aureli, A., 2018. Assessment of the impacts of climate variability on total water storage across Africa: implications for groundwater resources management. Hydrogeol. J.

Caswell, P.V., 1953. Geology of the mombasa-Kwale area. Geological Survey of Kenya.

Charles, K.J., Souter, F.C., Baker, D.L., Davies, C.M., Schijven, J.F., Roser, D.J., Deere, D.A., Priscott, P.K., Ashbolt, N.J., 2008. Fate and transport of viruses during sewage treatment in a mound system. Water Res. 42, 3047–3056.

Commission on Revenue Allocation, 2013. . Kenya Ctry. Fact Sheets, Second ed. Comm. Revenue Alloc. Nairobi.

Comte, J.C., Cassidy, R., Obando, J., Robins, N., Ibrahim, K., Melchioly, S., Mjemah, I., Shauri, H., Bourhane, A., Mohamed, I., Noe, C., Mwega, B., Makokha, M., Join, J.L., Banton, O., Davies, J., 2016. Challenges in groundwater resource management in coastal aquifers of East Africa: Investigations and lessons learnt in the Comoros Islands, Kenya and Tanzania. J. Hydrol. Reg. Stud. 5, 179–199.

County Government of Kwale, 2013. First County Integrated Development Plan.

Custodio, E., 2013. Trends in groundwater pollution: loss of groundwater quality & related Action., Groundwater Governance: A global Framework for CountryTrends in groundwater pollution: loss of groundwater quality & related Action., Groundwater Governance: A global Framewor.

Custodio, E., 2010. Coastal aquifers of Europe: an overview. Hydrogeol. J. 18, 269–280.

Custodio, E., 2002. Low Llobregat aquifers: intensive development, salinization, contamination and management, in: Sabater, S., Ginebreda, A., Barceló, D. (Eds.), The Story of a Polluted Mediterranean River. The Handbook of Environmental Chemistry. pp. 27–50.

Custodio, E., Bruggeman, G.., 1986. Groundwater problems in coastal areas. Studies and Reports in Hydrology, in: UNESCO. pp. 1–596.

Custodio, E., Llamas, M., 1976. Hidrología Subterránea, Omega. ed. Barcelona.

Custodio, E., Llamas, M.., Samper, J., 1997. La evaluación de la recarga a los acuíferos en la planificación hidrológica. International Association of Hydrogeologists- Spanish Group. MAdrid.

CWSB, 2016. Services Coast Water Board. URL https://www.cwsb.go.ke/ (accessed 8.20.11).

D'Oria, M., Tanda, M.G., Todaro, V., 2018. Assessment of local climate change: Historical trends and RCM multi-model projections over the Salento Area (Italy). Water (Switzerland) 10.

Dai, A., 2011. Drought under global warming: A review. Wiley Interdiscip. Rev. Clim. Chang. 2, 45–65.

Day, J.A., 1993. The major ion chemistry of some southern African saline systems. Hydrobiologia 267, 37–59.

Dayanti, M.P., Fachrul, M.F., Wijayanti, A., 2018. Escherichia coli as bioindicator of the groundwater quality in Palmerah District, West Jakarta, Indonesia, in: IOP Conference Series: Earth and Environmental Science.

De Filippis, G., Foglia, L., Giudici, M., Mehl, S., Margiotta, S., Negri, S.L., 2016a. Seawater intrusion in karstic, coastal aquifers: Current challenges and future scenarios in the Taranto area (southern Italy). Sci. Total Environ. 573, 1340–1351.

De Filippis, G., Giudici, M., Margiotta, S., Negri, S., 2016b. Conceptualization and characterization of a coastal multi-layered aquifer system in the Taranto Gulf (southern Italy). Environ. Earth Sci. 75, 686.

Demlie, M., Titus, R., 2015. Hydrogeological and hydrochemical characteristics of the natal group sanstone, South Africa. South African J. Geol. 118, 33–44.

Devane, M.L., Weaver, L., Singh, S.K., Gilpin, B.J., 2018. Fecal source tracking methods to elucidate critical sources of pathogens and contaminant microbial transport through New Zealand agricultural watersheds – A review. J. Environ. Manage. 222, 293–303.

Dhar, A., Datta, B., 2009. Saltwater Intrusion Management of Coastal Aquifers. I: Linked Simulation-Optimization. J. Hydrol. Eng. 14, 1263–1272.

DiGregorio, A., 2002. Multipurpose Landcover Database for Kenya – Africover. FAO. URL http://www.fao.org/geonetwork/srv/en/metadata.show?id=38098&currTab=simple

Easterling, D.R., Meehl, G.A., Parmesan, C., Changnon, S.A., Karl, T.R., Mearns, L.O., 2000. Climate extremes: Observations, modeling, and impacts. Science (80-.). 289, 2068–2074.

Edmunds, W.M., Guendouz, A.H., Mamou, A., Moulla, A., Shand, P., Zouari, K., 2003. Groundwater evolution in the Continental Intercalaire aquifer of southern Algeria and Tunisia: trace element and isotopic indicators. Appl. Geochemistry 18, 805–822.

Elangovan, N.S., Lavanya, V., Arunthathi, S., 2018. Assessment of groundwater contamination in a suburban area of Chennai, Tamil Nadu, India. Environ. Dev. Sustain. 20, 2609–2621.

Ercumen, A., Mohd Naser, A., Arnold, B.F., Unicomb, L., Colford, J.M., Luby, S.P., 2017. Can Sanitary Inspection Surveys Predict Risk of Microbiological Contamination of Groundwater Sources? Evidence from Shallow Tubewells in Rural Bangladesh. Am. J. Trop. Med. Hyg 96, 561–568.

Ezekiel, I.T., Maurice, N., Maurice, K. 'orowe, 2016. Seawater Intrusion Vulnerability Assessment of a Coastal Aquifer: North Coast Of Mombasa, Kenya as a Case Study. J. Eng. Res. Appl. www.ijera.com ISSN 6, 2248–962237.

Falkenmark, M., 2013. Adapting to climate change: towards societal water security in dry-climate countries. Int. J. Water Resour. Dev. 29, 123–136.

FAO, 2018. Food and Agriculture Organization of the United Nations (FAO). URL www.fao.org

FAO, 2011. The State of the World's land and water resources for Food and Agriculture, Managing systems at risk, Food and Agriculture Organization.

Faulwetter, J.L., Gagnon, V., Sundberg, C., Chazarenc, F., Burr, M.D., Brisson, J., Camper, A.K., Stein, O.R., 2009. Microbial processes influencing performance of treatment wetlands: A review. Ecol. Eng. 35, 987–1004.

Feng, D., Zheng, Y., Mao, Y., Zhang, A., Wu, B., Li, J., Tian, Y., Wu, X., 2018. An integrated hydrological modeling approach for detection and attribution of climatic and human impacts on coastal water resources. J. Hydrol. 557, 305–320.

Ferguson, A.S., Layton, A.C., Mailloux, B.J., Culligan, P.J., Williams, D.E., Smartt, A.E., Sayler, G.S., Feighery, J., McKay, L.D., Knappett, P.S.K., Alexandrova, E., Arbit, T., Emch, M., Escamilla, V., Ahmed, K.M., Alam, M.J., Streatfield, P.K., Yunus, M., van Geen, A., 2012. Comparison of fecal indicators with pathogenic bacteria and rotavirus in groundwater. Sci. Total Environ. 431, 314–322.

Ferrer, N., Folch, A., Lane, M., Olago, D., Odida, J., Custodio, E., 2019. Groundwater hydrodynamics of an Eastern Africa coastal aquifer, including La Niña 2016–17 drought. Sci. Total Environ. 661, 575–597.

Folch, A., Ferrer, N., 2015. The impact of poplar tree plantations for biomass production on the aquifer water budget and base flow in a Mediterranean basin. Sci. Total Environ. 524–525, 213–224.

Folch, A., Menció, A., Puig, R., Soler, A., Mas-Pla, J., 2011. Groundwater development effects on different scale hydrogeological systems using head, hydrochemical and isotopic data and implications for water resources management: The Selva basin (NE Spain).

J. Hydrol. 403, 83–102.

Fontes, J., Matray, J., 1993. Geochemistry and origin of formation brines associated with triassic salts. Chem Geol 109, 149–175.

Foster, S., van Steenbergen, F., 2011. Conjunctive groundwater use: a `lost opportunity' for water management in the developing world? Hydrogeol. J. 19, 959–962.

Foster, T., Willetts, J., 2018. Multiple water source use in rural Vanuatu: are households choosing the safest option for drinking? Int. J. Environ. Health Res. 28, 579–589.

Foster, T., Willetts, J., Lane, M., Thomson, P., Katuva, J., Hope, R., 2018. Risk factors associated with rural water supply failure: A 30-year retrospective study of handpumps on the south coast of Kenya. Sci. Total Environ. 626, 156–164.

Fulazzaky, M.A., 2014. Challenges of integrated water resources management in Indonesia. Water (Switzerland) 6, 2000–2020.

Gaye, C.B., Tindimugaya, C., 2018. Review: Challenges and opportunities for sustainable groundwater management in Africa. Hydrogeol. J. 28, 1–12.

Giannoccaro, G., Scardigno, A., Prosperi, M., 2017. Economic analysis of the long-term effects of groundwater salinity: bringing the farmer's perspectives into policy. J. Integr. Environ. Sci. 14, 59–72.

Giné Garriga, R., Pérez Foguet, A., 2011. Application of a revised Water Poverty Index to target the water poor. Water Sci. Technol. 63, 1099–1110.

Giné Garriga, R., Pérez Foguet, A., 2010. Improved Method to Calculate a Water Poverty Index at Local Scale. J. Environ. Eng. 136, 1287–1298.

Godfrey, S., Timo, F., Smith, M., 2006. Microbiological risk assessment and management of shallow groundwater sources in Lichinga, Mozambique. Water Environ. J. 20, 194–202.

GoK, 2013. Kenya Country Fact Sheets, 2nd Ed. Government of Kenya, Commission on Revenue Allocation, Nairobi.

Goyal, S.M., Keswick, B.H., Gerba, C.P., 1984. Viruses in groundwater beneath sewage irrigated cropland. Water Res. 18, 299–302.

Graham, J.P., Polizzotto, M.L., 2013. Pit Latrines and Their Impacts on Groundwater Quality: A Systematic Review. Environ. Health Perspect. 121, 521–530.

Green, T.R., Taniguchi, M., Kooi, H., Gurdak, J.J., Allen, D.M., Hiscock, K.M., Treidel, H., Aureli, A., 2011. Beneath the surface of global change: Impacts of climate change on groundwater.

Gronewold, A.D., Sobsey, M.D., Mcmahan, L., 2017. The compartment bag test (CBT) for enumerating fecal indicator bacteria: Basis for design and interpretation of results. Sci. Total Environ. 587–588, 102–107.

Guttman, N.B., 1999. Accepting the standardized precipitation index, Journal Of The

American Water Resources Association.

Guttman, N.B., 1998. Comparing the Palmer Drought Index and the Standardized Precipitation Index', Journal of the American Water Resources Association.

Hair, J., Anderson, R., Tatham, R., Black, W., 1995. Multivariate Data Analysis, 4th ed, Technometrics. Prentice-Hall Inc, New Jersey.

Hansen, J., Sato, M., Hearty, P., Ruedy, R., Kelley, M., Masson-Delmotte, V., Russell, G., Tselioudis, G., Cao, J., Rignot, E., Velicogna, I., Tormey, B., Donovan, B., Kandiano, E., Von Schuckmann, K., Kharecha, P., Legrande, A.N., Bauer, M., 2016. Ice melt, sea level rise and superstorms: Evidence from paleoclimate data, climate modeling, and modern observations that 2 °c global warming could be dangerous. Atmos. Chem. Phys. 16, 3761–3812.

Harbaugh, A.W., 2005. MODFLOW-2005, The U. S. Geological Survey Modular Ground-Water Model—the Ground-Water Flow Process.

Hargreaves, G., Samani, Z., 1982. Estimating potential evapotranspiration. J. Irrig. Drain. Div. - ASCE 108, 225–230.

Herrero, M., Ringler, C., Steeg, J. van de, Thornton, P., Zhu, T., Bryan, E., Omolo, A., Koo, J., Notenbaert, A., 2010. Climate variability and climate change and their impacts on Kenya's agricultural sector. Sci. Bridg. 2000 beyond, a virtual colloqium by Elf-Aquitaine Profr. Académie des Sci.

Holzer, T.L., Galloway, D.L., 2005. Impacts of land subsidence caused by withdrawal of underground fl uids in the United States. Eng. Geol. 16, 87–99.

Howard, G., Pedley, S., Barrett, M., Nalubega, M., Johal, K., 2003. Risk factors contributing to microbiological contamination of shallow groundwater in Kampala, Uganda. Water Res. 37, 3421–3429.

Howard, G., Pedley, S., Barrett, M., Nalubega, M., Johal, K., 2003. Risk factors contributing to microbiological contamination of shallow groundwater in Kampala, Uganda. Water Res. 37, 3421–3429.

Howard, K., Griffith, A., 2009. Can the impacts of climate change on groundwater resources be studied without the use of transient models? Hydrol. Sci. Sci. Hydrol. 54.

IGRAC, 2019. Groundwater Governance | IGRAC. URL https://www.un-igrac.org/areas-expertise/groundwater-governance (accessed 1.29.19).

Isa, N.M., Aris, A.Z., Sulaiman, W.N.A.W., Lim, A.P., Looi, L.J., 2014. Comparison of monsoon variations over groundwater hydrochemistry changes in small Tropical Island and its repercussion on quality. Hydrol. Earth Syst. Sci. Discuss 11, 6405–6440.

Jakemann, A., Randall, O., Huntt, J., Andrewwross, J.-D., 2016. Integrated Groundwater Management Concepts, Approaches and Challenges.

Kahsay, K.D., Pingale, S.M., Hatiye, S.D., 2018. Impact of climate change on groundwater recharge and base flow in the sub- catchment of Tekeze basin, Ethiopia.

Kamermans, P., Hemminga, M.A., Tack, J.F., Mateo, M.A., Marbà, N., Mtolera, M., Stapel, J., Verheyden, A., Van Daele, T., 2002. Groundwater effects on diversity and abundance of lagoonal seagrasses in Kenya and on Zanzibar Island (East Africa). Mar. Ecol. Prog. Ser. 231, 75–83.

Karlov, D.S., Marie, D., Danil, •, Sumbatyan, A., Chuvochina, M.S., Kulichevskaya, I.S., Alekhina, I.A., Sergey, •, Bulat, A., 2008. Microbial communities within the water column of freshwater Lake Radok, East Antarctica: predominant 16S rDNA phylotypes and bacterial cultures. Polar Biol. 40.

Katuva, J., Hope, R., Foster, T., Koehler, J., Thomson, P., 2019. Groundwater and Welfare: A conceptual framework applied to Coastal Kenya. (Accepted). J. Groundw. Sustain. Dev.

Kayembe, J.M., Thevenon, F., Laffite, A., Sivalingam, P., Ngelinkoto, P., Mulaji, C.K., Otamonga, J.P., Mubedi, J.I., Poté, J., 2018. High levels of faecal contamination in drinking groundwater and recreational water due to poor sanitation, in the sub-rural neighbourhoods of Kinshasa, Democratic Republic of the Congo. Int. J. Hyg. Environ. Health 221, 400–408.

Kelbe, B.E., Grundling, A.T., Price, J.S., 2016. Modelling water-table depth in a primary aquifer to identify potential wetland hydrogeomorphic settings on the northern Maputaland Coastal Plain, KwaZulu-Natal, South Africa. Hydrogeol. J. 24, 249–265.

Kempen, B., 2007. Soil and terrain database for Kenya (ver.2) (KENSOTER).

Khanlari, G., Heidari, M., Momeni, A.A., Ahmadi, M., Taleb Beydokhti, A., 2012. The effect of groundwater overexploitation on land subsidence and sinkhole occurrences, western Iran. Q. J. Eng. Geol. Hydrogeol. 45, 447–456.

Kilungo, A., Powers, L., Arnold, N., Whelan, K., Paterson, K., Young, D., 2018. Evaluation of well designs to improve access to safe and clean water in rural Tanzania. Int. J. Environ. Res. Public Health 15, 1–11.

Kopytkovskiya, M., Geza, M., McCray, J.E., 2015. Climate-change impacts on water resources and hydropower potential in the Upper Colorado River Basin. J. Hydrol. 3, 473–493.

Kumar, C.., 2012. Climate Change and Its Impact on Groundwater Resources. Int. J. Eng. Sci. 1, 43–60.

Kusangaya, S., Warburton, M.L., Archer van Garderen, E., Jewitt, G.P.W., 2014. Impacts of climate change on water resources in southern Africa: A review. Phys. Chem. Earth 67–69, 47–54.

Lawrence, P., Meigh, J., 2003. The Water Poverty Index : an International Comparison Keele Economics Research Papers 2002.

Levin, N.E., Zipser, E.J., Ceding, T.E., 2009. Isotopic composition of waters from Ethiopia and Kenya: Insights into moisture sources for eastern Africa. J. Geophys. Res. Atmos. 114, 1–13.

Levison, J., Larocque, M., Ouellet, M.A., 2014. Modeling low-flow bedrock springs providing ecological habitats with climate change scenarios.

Lichter, M., Vafeidis, A.T., Nicholls, R.J., Kaiser, G., 2011. Exploring Data-Related Uncertainties in Analyses of Land Area and Population in the "Low-Elevation Coastal Zone" (LECZ). J. Coast. Res. 274, 757–768.

Lin, A., Ercumen, A., Benjamin-Chung, J., Arnold, B.F., Das, S., Haque, R., Ashraf, S., Parvez, S.M., Unicomb, L., Rahman, M., Hubbard, A.E., Stewart, C.P., Colford, J.M., Luby, S.P., 2018. Effects of Water, Sanitation, Handwashing, and Nutritional Interventions on Child Enteric Protozoan Infections in Rural Bangladesh: A Cluster-Randomized Controlled Trial. Clin. Infect. Dis. 67, 1515–1522.

López Álvarez, B., Santacruz de León, G., Ramos Leal, J.A., Morán Ramírez, J., 2015. Water Poverty Index in subtropical zones:the case of Huasteca Potosina, México. Rev. Int. Contam. Ambient. 31, 173–184.

Lutterodt, G., van de Vossenberg, J., Hoiting, Y., Kamara, A.K., Oduro-Kwarteng, S., Foppen, J.W.A., 2018. Microbial groundwater quality status of hand-dug wells and boreholes in the Dodowa area of Ghana. Int. J. Environ. Res. Public Health 15, 1–12.

MacDonald, A.M., Bonsor, H.C., Dochartaigh, B.É.Ó., Taylor, R.G., 2012. Quantitative maps of groundwater resources in Africa. Environ. Res. Lett. 7, 24009.

MacDonald, A.M., Calow, R.C., MacDonald, D.M.J., Darling, W.G., Dochartaigh, B.E.O., 2009. What impact will climate change have on rural groundwater supplies in Africa? Hydrol. Sci. Journal-Journal Des Sci. Hydrol. 54, 690–703.

Macler, B.A., Merkle, J.C., 2000. Current knowledge on groundwater microbial pathogens and their control, Hydrogeology Journal.

Mantoglou, A., 2003. Pumping management of coastal aquifers using analytical models of saltwater intrusion. Water Resour. Res. 39, 1–12.

Manzano, M., Custodio, E., Higueras, H., 2007a. Groundwater and its functioning at the Doñana RAMSAR site wetlands (SW Spain): role of environmental isotopes to define the flow system. Advances in Isotope Hydrology and its Role in Sustainable Water Resources Management, in: IHS–2007, Proc. Symp. Viena. International Atomic Energy Agency. Wien, pp. 149–160.

Manzano, M., Custodio, E., Iglesias, M., Lozano, E., 2007b. Groundwater baseline composition and geochemical controls in the Doñana aquifer system, SW Spain., in: W.M. Edmunds & P. Shand (Ed.), The Natural Baseline Quality of Groundwater. Blackwell Publ., Oxford., pp. 216–232.

Manzano, M., Custodio, E., Lozano, E., Higueras, H., 2013. Relationships between wetlands and the Doñana coastal aquifer (SW Spain)., in: Taylor & Francis (Ed.), Groundwater and Ecosystems. pp. 169–182.

Martínez-Santos, P., Martín-Loeches, M., García-Castro, N., Solera, D., Díaz-Alcaide, S., Montero, E., García-Rincón, J., 2017. A survey of domestic wells and pit latrines in rural settlements of Mali: Implications of on-site sanitation on the quality of water supplies. Int. J. Hyg. Environ. Health 220, 1179–1189.

Mas-Pla, J., Font, E., Astui, O., Menció, A., Rodríguez-Florit, A., Folch, A., Brusi, D., Pérez-Paricio, A., 2012. Development of a stream-aquifer numerical flow model to assess river water management under water scarcity in a Mediterranean basin. Sci. Total Environ. 440, 204–18.

Mas-Pla, J., Menció, A., 2018. Groundwater nitrate pollution and climate change: learnings from a water balance-based analysis of several aquifers in a western Mediterranean region (Catalonia). Environ. Sci. Pollut. Res. 1–19.

Matthess, G., Pekdeger, A., Schroeter, J., 1988. Persistence and transport of bacteria and viruses in groundwater - a conceptual evaluation. J. Contam. Hydrol. 2, 171–188.

Mckee, T.B., Doesken, N.J., Kleist, J., 1993. The relationship of drough frequency and duration to time scales, Eighth Conference on Applied Climatology.

Mckenzie, J.M., Mark, B.G., Thompson, L.G., Schotterer, U., Lin, P.-N., 2010. A hydrogeochemical survey of Kilimanjaro (Tanzania): implications for water sources and ages. Hydrogeol. J. 18, 985–995.

Meigh, J.R., Mckenzie, A.A., Sene, K.J., 1999. A Grid-Based Approach to Water Scarcity Estimates for Eastern and Southern Africa. Water Resour. Manag. 13, 85–115.

Mekonnen, M., Hoekstra, Y.A., 2016. Four Billion People Facing Severe Water Scarcity. Am. Assoc. Adv. Sci. 2, 1–7.

Menció, A., Folch, A., Mas-Pla, J., 2012. Identifying key parameters to differentiate groundwater flow systems using multifactorial analysis. J. Hydrol. 472–473, 301–313.

Menció, A., Mas-Pla, J., Otero, N., Regàs, O., Boy-Roura, M., Puig, R., Bach, J., Domènech, C., Zamorano, M., Brusi, D., Folch, A., 2016. Nitrate pollution of groundwater; all right…, but nothing else? Sci. Total Environ. 539, 241–251.

Menció, A., Mas-Pla, J., Otero, N., Soler, A., 2011. Nitrate as a tracer of groundwater flow in a fractured multilayered aquifer. Hydrol. Sci. J. 56, 108–122.

Michael, H.A., Post, V.E.A., Wilson, A.M., Werner, A.D., 2017. Science, society, and the coastal groundwater squeeze. Water Resour. Res. 53, 2610–2617.

Miller, S., 1994. Handbook for agrohydrology. Natural Resources Institute.

Molina, J.L., García Aróstegui, J.L., Benavente, J., Varela, C., de la Hera, A., López Geta, J.A., 2009. Aquifers overexploitation in SE Spain: A proposal for the integrated analysis of water management. Water Resour. Manag. 23, 2737–2760.

Mpelasoka, F., Awange, J.L., Zerihun, A., 2017. Influence of coupled ocean-atmosphere phenomena on the Greater Horn of Africa droughts and their implications. Sci. Total Environ. 610611, 691–702.

Mtoni, Y., Mjemah, I.C., Bakundukize, C., Van Camp, M., Martens, K., Walraevens, K., 2013. Saltwater intrusion and nitrate pollution in the coastal aquifer of Dar es Salaam, Tanzania. Environ. Earth Sci. 70, 1091–1111.

Mumma, A., Lane, M., Kairu, E., Tuinhof, A., Hirji, R., 2011. Kenya Groundwater Governance Case Study. URL https://openknowledge.worldbank.org/handle/10986/17227 (accessed 5.11.17).

Mutemi, J.., 2003. Climate anomalies over eastern Africa associated with various ENSO evolution phases. University of Nairobi, Kenya.

Mzuga, J.M., Tole, M.P., Ucakuwun, E.K., 1998. The impact of geology and pit latrines on groundwater quality in Kwale District, Dunes, groundwater, mangroves and birdlife in coastal Kenya.

Ndlovu, M., Demlie, M., 2016. Hydrogeological characterization of the Kosi Bay Lakes system, north-eastern South Africa. Environ. Earth Sci. 75:, 1334.

Neumann, B., Vafeidis, A., Zimmermann, J., Nicholls, R., 2015. Future Coastal Population Growth and Exposure to Sea-Level Rise and Coastal Flooding - A Global Assessment. PLoS ONE 10(3).

Nkini, G.R.L., Kimaro, E.C., Moshi, L., 2006. Southern and eastern african mineral centre. South. East. african Miner. Cent. 1, 28.

Nlend, B., Celle-Jeanton, H., Huneau, F., Ketchemen-Tandia, B., Fantong, W.Y., Ngo Boum-Nkot, S., Etame, J., 2018. The impact of urban development on aquifers in large coastal cities of West Africa: Present status and future challenges.

Nowicki, S., Lapworth, D.J., Ward, J.S.T., Thomson, P., Charles, K., 2019. Tryptophan-like fluorescence as a measure of microbial contamination risk in groundwater. Sci. Total Environ. 646, 782–791.

Obura, D.O., 2001. The Coastal and Marine Environment. Mar. Pollut. Bull. 42, 1264–1278.

Ogwang, B.A., Ongoma, V., Li Xing, F., Ogou, F.K., 2015. Influence of Mascarene High and Indian Ocean Dipole on East African Extreme Weather Events. Geogr. Pannonica 19, 64–72.

Oiro, S., Comte, J.C., 2019. Drivers, patterns and velocity of saltwater intrusion in a stressed aquifer of the East African coast: Joint analysis of groundwater and geophysical data in southern Kenya. J. African Earth Sci. 149, 334–347.

Oke, S.A., Fourie, F., 2017. Guidelines to groundwater vulnerability mapping for Sub-Saharan Africa. Groundw. Sustain. Dev. 5, 168–177.

Okello, C., Antonellini, M., Greggio, N., Wambiji, N., 2015a. Freshwater resource characterization and vulnerability to climate change of the Shela aquifer in Lamu , Kenya 3801–3817.

Okello, C., Tomasello, B., Greggio, N., Wambiji, N., Antonellini, M., 2015b. Impact of population growth and climate change on the freshwater resources of Lamu Island, Kenya. Water (Switzerland) 7, 1264–1290.

Olago, D.O., 2018. Constraints and solutions for groundwater development , supply and governance in urban areas in Kenya.

Olajuyigbe, A.E., Olamiju, I.O., Ola-Omole, C.M., 2017. Vulnerability of hand-dug wells in the core area of Akure, Nigeria. Urban Water J. 14, 797–803.

Ongoma, V., Onyango, O., 2014. A Review of the Future of Tourism in Coastal Kenya: The Challenges and Opportunities Posed by Climate Change. Earth Sci. Clim. Chang.

Ortiz-Zamora, D., Ortega-Guerrero, A., 2010. Evolution of long-term land subsidence near Mexico City: Review, field investigations, and predictive simulations. Water Resour. Res. 46, 1–15.

Oteng-Peprah, M., de Vries, N.K., Acheampong, M.A., 2018. Greywater characterization and generation rates in a peri urban municipality of a developing country. J. Environ. Manage. 206, 498–506.

Ouedraogo, I., Vanclooster, M., 2016. A meta-analysis of groundwater contamination by nitrates at the African scale. Hydrol. Earth Syst. Sci. Discuss. 1–43.

Paliy, O., Shankar, V., 2016. Application of multivariate statistical techniques in microbial ecology. Mol. Ecol. 25, 1032–1057.

Pavelic, P., Giordano, M., Keraita, B., Ramesh, V., Rao, T., 2012. Groundwater availability and use in sub-Saharan Africa: A review of 15 countries. Colombo, Sri Lanka.

Perera, B.J.C., Muttil, N., 2009. Conceptual framework for the development of West Java water sustainability index 3343–3349.

Poisson, A., Lebel, J., Brunet, C., 1981. The densitites of western Indian Ocean, Red Sea and eastern Mediterranean surface waters. Deep. Res. 28, 1161–1172.

Rais-Assa, R., 1988. Stratigraphy and geodynamics of the Mombasa Basin (Kenya) in relation to the genesis of the proto-Indian Ocean. Geol. Mag. 125, 141–147.

Rao, V.C., Metcalf, T.G., Melnick3, J.L., 1986. Articles in the Update series Human viruses in sediments, sludges, and soils*, Bulletin of the World Health Organization.

Richey, A.S., Thomas, B.F., Lo, M.-H., Famiglietti, J.S., Swenson, S., Rodell, M., 2015a. Uncertainty in global groundwater storage estimates in a total groundwater stress framework. Water Resour. Res. 51, 5198–5216.

Richey, A.S., Thomas, B.F., Lo, M.-H., Reager, J.T., Famiglietti, J.S., Voss, K., Swenson, S., Rodell, M., 2015b. Quantifying renewable groundwater stress with GRACE. Water Resour. Res. 51, 5217–5238.

Rohmah, Y., Rinanti, A., Hendrawan, D.I., 2018. The determination of ground water quality based on the presence of Escherichia coli on populated area (a case study: Pasar Minggu, South Jakarta). IOP Conf. Ser. Earth Environ. Sci. 106.

Sahu, P., Sikdar, P.K., 2011. Threat of land subsidence in and around Kolkata City and East Kolkata Wetlands, West Bengal, India. J. Earth Syst. Sci. 120, 435–446.

Sappa, G., Ergul, S., Ferranti, F., Sweya, L.N., Luciani, G., 2015. Effects of seasonal change and seawater intrusion on water quality for drinking and irrigation purposes, in coastal

aquifers of Dar es Salaam, Tanzania. J. African Earth Sci. 105, 64–84.

SASMIE, 2017. Salinización de las aguas subterráneas en los acuíferos costeros mediterráneos e insulares españoles [Groundwater salinization in Mediterranean and island coastal aquifers in Spain].

Schmoll, O., Howard, G., Chilton, J., Chorus, I., 2006. Protecting Groundwater for Health: Managing the Quality of Drinking-water Sources, Protecting Groundwater for Health: Managing the Quality of Drinking-water Sources.

Schuol, J., Abbaspour, K.C., Srinivasan, R., Yang, H., 2008. Estimation of freshwater availability in the West African sub-continent using the SWAT hydrologic model. J. Hydrol. 352, 30–49.

Sepehrnia, N., Bachmann, J., Hajabbasi, M., Afyuni, M., Horn, M., 2018a. Modeling Escherichia coli and Rhodococcus erythropolis transport through wettable and water repellent porous media. Colloids Surfaces B Biointerfaces 172, 280–287.

Sepehrnia, N., Memarianfard, L., Moosavi, A.A., Bachmann, J., Rezanezhad, F., Sepehri, M., 2018b. Retention modes of manure-fecal coliforms in soil under saturated hydraulic condition. J. Environ. Manage. 227, 209–215.

Sharma, P.K., Srivastava, R., 2011. Numerical analysis of virus transport through heterogeneous porous media. J. Hydro-Environment Res. 5, 93–99.

Solomon, S., Qin, D., 2013. Climate Change 2007 The Physical Science Basis The, Journal of Chemical Information and Modeling.

Stauber, C., Miller, C., Cantrell, B., Kroell, K., 2014. Evaluation of the compartment bag test for the detection of Escherichia coli in water. J. Microbiol. Methods 99, 66–70.

Stefanova, A., Krysanova, V., Hesse, C., Lillebø, A.I., 2015. Climate change impact assessment on water inflow to a coastal lagoon: the Ria de Aveiro watershed, Portugal. Hydrol. Sci. J. 60, 1–20.

Steyl, G., Dennis, I., 2010. Review of coastal-area aquifers in Africa. Hydrogeol. J. 18, 217–225.

Stocker, T.F., Qin, D., Plattner, G.-K., Tignor, M.M.B., Allen, S.K., Boschung, J., Nauels, A., Xia, Y., Bex, V., Midgley, P.M., 2013. Climate Change 2013. The Physical Science Basis Working Group I Contribution to the Fifth Assessment Report of the Intergovernmental Panel on Climate Change.

Sukumaran, D., Sengrupta, C., Saha, R., Rakesh, C., 2015. Ground Water Quality Index of Howrah, the Heritage City of West Bengal, India. Appl. Ecol. Environ. Sci. 3, 5–10.

Sullivan, C., 2002. Calculating a Water Poverty Index. World Dev. 30, 1195–1210.

Sullivan, C.A., Meigh, J., 2007. Integration of the biophysical and social sciences using an indicator approach: Addressing water problems at different scales. Integr. Assess. Water Resour. Glob. Chang. A North-South Anal. 111–128.

Sullivan, C. a, Meigh, J.R., Giacomello, a M., Fediw, T., Lawrence, P., Samad, M., Mlote, S., Hutton, C., Allan, J. a, Schulze, R.E., Dlamini, D.J.M., Cosgrove, W., Delli Priscoli, J., Gleick, P., Smout, I., Cobbing, J., Calow, R., Hunt, C., Hussain, A., Acreman, M.C., King, J., Malomo, S., Tate, E.L., Regan, D.O., Milner, S., Steyl, I., 2003. The water poverty index: Development and application at the community scale. Nat. Resour. Forum 27, 189–199.

Tabachnik, B., Fidell, L., 2007. Using multivariate statistics. Pearson Education Inc, Boston, MC.

Taylor, R.G., Howard, K.W.F., 1996. Groundwater recharge in the Victoria Nile basin of east Africa: support for the soil moisture balance approach using stable isotope tracers and flow modelling. J. Hydrol. 180, 31–53.

Taylor, R.G., Jasechko, S., 2015. Intensive rainfall recharges tropical groundwaters. Environ. Res. Lett. 10, 124015.

Taylor, R.G., Scanlon, B., Döll, P., Rodell, M., van Beek, R., Wada, Y., Longuevergne, L., Leblanc, M., Famiglietti, J.S., Edmunds, M., Konikow, L., Green, T.R., Chen, J., Taniguchi, M., Bierkens, M.F.P., MacDonald, A., Fan, Y., Maxwell, R.M., Yechieli, Y., Gurdak, J.J., Allen, D.M., Shamsudduha, M., Hiscock, K., Yeh, P.J.-F., Holman, I., Treidel, H., 2013. Ground water and climate change. Nat. Clim. Chang. 3, 322–329.

Taylor, R.G., Todd, M.C., Kongola, L., Maurice, L., Nahozya, E., Sanga, H., MacDonald, A.M., 2012. Evidence of the dependence of groundwater resources on extreme rainfall in East Africa. Nat. Clim. Chang. 3, 374–378.

Team, 2018. R: A Language and Environment for Statistical Computing.

Thompson, B., 2004. Exploratory and Confirmatory Factor Analysis: Understanding Concepts and Applications.

Thomson, P., Bradley, D., Katilu, A., Katuva, J., Lanzoni, M., Koehler, J., Hope, R., 2019. Rainfall and groundwater use in rural Kenya. Sci. Total Environ. 649, 722–730.

Thomson, P., Hope, R., Foster, T., 2012. GSM-enabled remote monitoring of rural handpumps: a proof-of-concept study. J. Hydroinformatics 14, 829–839.

Tole, M.P., 1997. Pollution of groundwater in the coastal Kwale Distric, Kenya. Sustain. Water Resour. under Increasing Uncertain. 287–297.

Tole, M.P., 1990. Chemical geothermometry and resource potential of low enthalpy geothermal systems in Kenya. Geotherm. Resour. Counc. Trans. 14, 187–193.

Treidel, H., Aureli, A., Taniguchi, M., Kooi, H., Green, T.R., Gurdak, J.J., Allen, D.M., Hiscock, K.M., 2011. Beneath the surface of global change: Impacts of climate change on groundwater. J. Hydrol. 405, 532–560.

Ugochukwu, U.C., Ojike, C., 2019. Assessment of the groundwater quality of a highly populated district in Enugu State of Nigeria. Environ. Dev. Sustain.

Uhe, P., Philip, S., Kew, S., Shah, K., Kimutai, J., Mwangi, E., van Oldenborgh, G.J., Singh, R.,

Arrighi, J., Jjemba, E., Cullen, H., Otto, F., 2018. Attributing drivers of the 2016 Kenyan drought. Int. J. Climatol. 38, e554–e568.

Uhe, P., Philip, S., Shah, K., Kimutai, J., Otto, F., Van Oldenborgh, G.J., Singh, R., Arrighi, J., Cullen, H., 2017. Climate and Development Knowledge Network and World Weather Attribution Initiative Raising Risk Awareness.

UN, 2016. Water Scarcity Report.

UN, 2015. Population 2030: Demographic challenges and opportunities for sustainable development planning, United Nations.

UNDP, 2006. Human Development Report.

UNEP, 2011. Annual Report 2010: United Nations Environment Programme, United Nations Environment Programme.

UNESCO-IHP, 2015. Graphic. Groundwaer and climate change. Mitigating the Global Groundwater Crisis and Adapting to Climate Change.

Urrutia, J., Jódar, J., Medina, A., Herrera, C., Chong, G., Urqueta, H., Luque, J.A., 2018. Hydrogeology and sustainable future groundwater abstraction from the Agua Verde aquifer in the Atacama Desert, northern Chile. Hydrogeol. J.

Van Camp, M., Chikira Mjemah, I., Al Farrah, N., Walraevens, K., 2013. Modeling approaches and strategies for data-scarce aquifers: example of the Dar es Salaam aquifer in Tanzania. Hydrogeol. J. 21, 341–356.

Van der Gun, J., 2012. Groundwater and Global Change: Trends, Opportunities and Challenges, United Nations World Water Assessment Programme.

Van Engelenburg, J., Hueting, R., Rijpkema, S., Teuling, A.J., Uijlenhoet, R., Ludwig, F., 2018. Impact of Changes in Groundwater Extractions and Climate Change on Groundwater-Dependent Ecosystems in a Complex Hydrogeological Setting. Water Resour Manag. 32, 259–272.

Van Ryneveld, M., Fourie, A., 1997. A strategy for evaluating the environmental impact of on-site sanitation systems. Water SA 23, 279–291.

Vázquez-Suñé, E., Abarca, E., Carrera, J., Capino, B., Gámez, D., Pool, M., Simó, T., Batlle, F., Niñerola, J.M., Ibáñez, X., 2006. Groundwater modelling as a tool for the European Water Framework Directive (WFD) application: The Llobregat case. Phys. Chem. Earth 31, 1015–1029.

Velasco, V., Tubau, I., Vázquez-Suñé, E., Gogu, R., Gaitanaru, D., Alcaraz, M., Serrano-Juan, A., Fernàndez-Garcia, D., Garrido, T., Fraile, J., Sanchez-Vila, X., 2014. GIS - based hydrogeochemical analysis tools (QUIMET). Comput. Geosci. 70.

Vižintin, G., Ravbar, N., Janež, J., Koren, E., Janež, N., Zini, L., Treu, F., Petrič, M., 2017. Integration of models of various types of aquifers for water quality management in the transboundary area of the Soča/Isonzo river basin (Slovenia/Italy). Sci. Total Environ. 619–620, 1214–1225.

Wada, Y., Van Beek, L.P.H., Van Kempen, C.M., Reckman, J.W.T.M., Vasak, S., Bierkens, M.F.P., 2010. Global depletion of groundwater resources. Geophys. Res. Lett. 37, 1–5.

Weldeyohannes, A.O., Kachanoski, G., Dyck, M., 2018. Wastewater Flow and Pathogen Transport from At-Grade Line Sources to Shallow Groundwater. J. Environ. Qual. 47, 1051.

Werner, A.D., Bakker, M., Post, V.E.A., Vandenbohede, A., Lu, C., Ataie-Ashtiani, B., Simmons, C.T., Barry, D.A., 2013. Seawater intrusion processes, investigation and management: Recent advances and future challenges. Adv. Water Resour. 51, 3–26.

Werner, A.D., Bakker, M., Post, V.E.A., Vandenbohede, A., Lu, C., Ataie-Ashtiani, B., Simmons, C.T., Barry, D.A., 2013. Seawater intrusion processes, investigation and management: Recent advances and future challenges.

Wick, K., Heumesser, C., Schmid, E., 2012. Groundwater nitrate contamination: Factors and indicators. J. Environ. Manage. 111, 178–186.

Winston, R.., 2009. ModelMuse-A graphical user interface for MODFLOW-2005 and PHAST: U.S.Geological Survey Techniques and Methods.

World Bank, 2013. An Analysis of Issues Shaping Africa's Economic Future. Africa's Pulse. Washington, DC: TheWorld Bank.

World Tourism Organization, 2013. Sustainable Tourism Governance and Management in Coastal Areas of Africa, UNWTO,Madrid. Madrid.

Wright, J.A., Cronin, A., Okotto-Okotto, J., Yang, H., Pedley, S., Gundry, S.W., 2013. A spatial analysis of pit latrine density and groundwater source contamination. Environ. Monit. Assess. 185, 4261–4272.

Yates, M. V, Gerba, C.P., Kelley, L.M., 1985. Virus persistence in groundwater. Appl. Environ. Microbiol. 49, 778–781.

Yihdego, Y., Reta, G., Becht, R., 2017. Human impact assessment through a transient numerical modeling on the UNESCO World Heritage Site, Lake Naivasha, Kenya. Environ. Earth Sci. 76.

.

Supporting information

This section comprises supporting information for Chapters 2, 3,4 and 5.

Appendix A. Supplementary information of Chapter 2: Field data for each sampling campaign.

Appendix B. Supplementary information of Chapter 3: *E. coli* presence in each samples for March and June field campaigns.

Appendix C. Supplementary information of Chapter 4: Information used in the mixing model and equation applied to calculate the saline intrusion wedge.

Appendix D. Supplementary information of Chapter 5: Groundwater mass balance for each scenario.

Appendix A. Supplementary information of Chapter 2: Field data for each sampling campaign

Figure 1, Appendix A: Nitrate concentration in mg/l during dry season (March 2016) and wet season (June 2016).

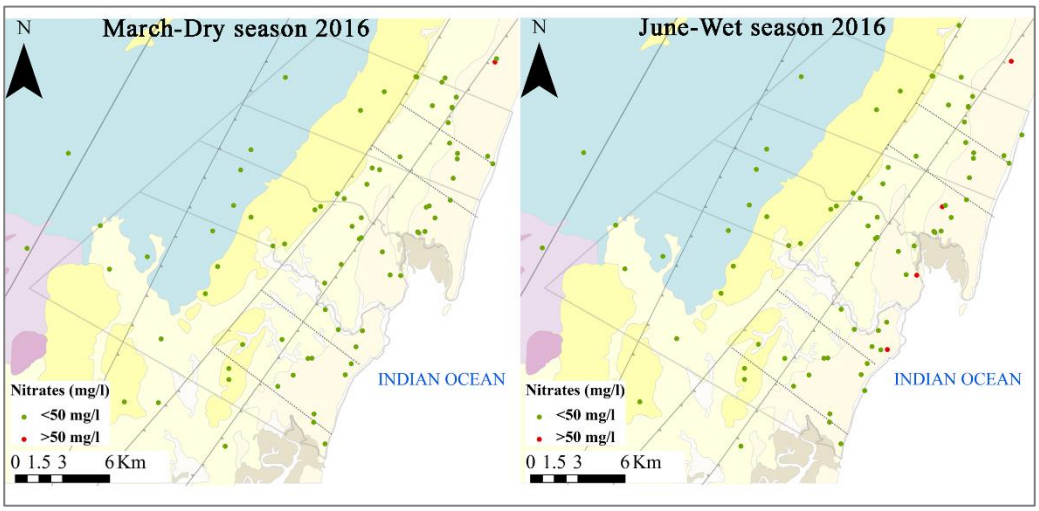

Figure 2, Appendix A: Iron stability diagram for June 2016 field samples.

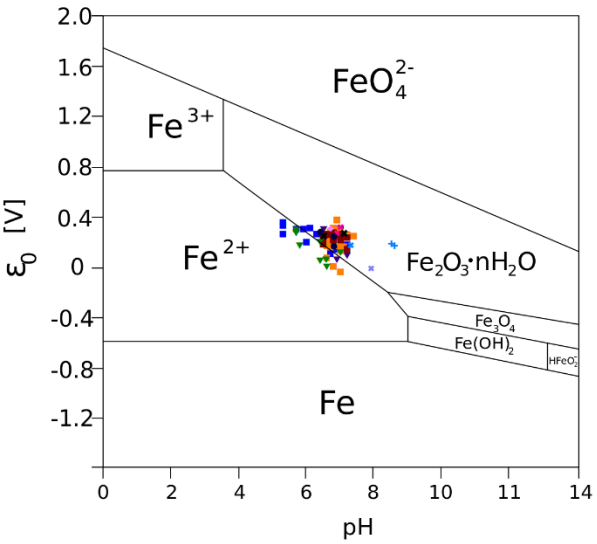

Figure 3, Appendix A: Stability relations for gibbsite for June 2016 field samples.

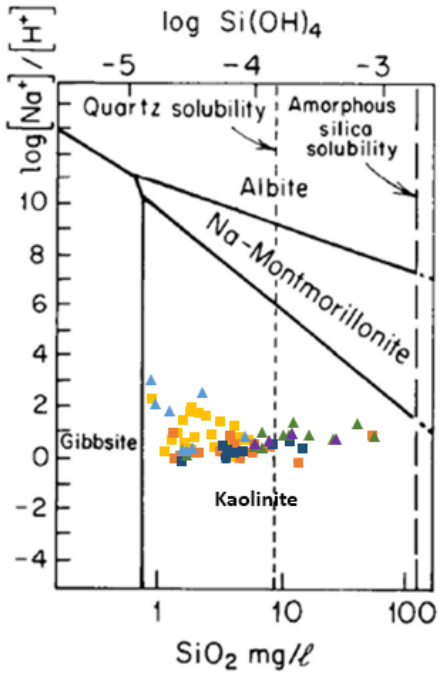

Table 1, Appendix A: Drawdown range for shallow and deep boreholes monitored by Base Titanium.

Code	*Dates*	*Aquifer*	*Geology*	*Zone*	*Drawdown from 01/2016 to 12/2016 maximum -minimum level of these period*	*Lack between rain event and maximum groundwater level recorded after (days)*	*Base of screen (m bgl)*
GS1	02/2008-12/2016	Shallow Aquifer	Kilindini s.	2	2.89	12	>8.63
GS2	02/2008-12/2016	Shallow Aquifer	Kilindini s.	1	2.65	13	8.2
GS5	11/2011-09/2016	Shallow Aquifer	Kilindini s.	1	0.83	13	5.4
GS3	12/2011-10/2013	Shallow Aquifer	P. Corals	2	no data	26	11.2
GS4	11/2011-10/2013	Shallow Aquifer	P. Corals	1	no data	13	5.6
GS6	02/2008-12/2016	Shallow Aquifer	Kilindini s.	2	1.38	6	5.2
GS7	11/2011-12/2016	Shallow Aquifer	Kilindini s.	3	0.45	13	7.2
GS9	11/2011-12/2016	Shallow Aquifer	Kilindini s.	2	1.9	20	>6.44
GS20	06/2012-12/2016	Shallow Aquifer	Kilindini s.	2	4.289	32	18.3
GD8	06/2012-12/2016	Deep Aquifer	Mazeras snd.	2	5.19	pump affected	54.0
GS21	05/2012-09/2016	Shallow Aquifer	Kilindini s.	2	1.68	6	5.7
GD9	05/2012-09/2016	Deep Aquifer	Mazeras snd.	2	3	pump affected	34.1
GS22	05/2012-09/2016	Shallow Aquifer	Magarini s.	2	2.47	13	14.0
GD10	05/2012-09/2016	Deep Aquifer	Mazeras snd.	2	2.2?	20	54.0
GS23	02/2013-09/2013	Shallow Aquifer	Kilindini s.	2	3.13	13	12.0
GD11	11/2012-12/2016	Deep Aquifer	Mazeras snd.	2	2.8	13	36.0

GS24	05/2012-12/2016	Shallow Aquifer	Kilindini s.	2	2.5	13	14.2
GD12	05/2012-12/2016	Deep Aquifer	Mazeras snd.	2	5.11	pump affected	60.9
GS25	05/2012-12/2016	Shallow Aquifer	Kilindini s.	2	1.48	6	11.6
GD13	05/2012-12/2016	Deep Aquifer	Mazeras snd.	2	2.24	13	64.1
GD7	06/2016-12/2016	Deep Aquifer	Mazeras snd.	2	1.6	no data	100.2
GI21	05/2012-12/2016	Shallow Aquifer	Magarini s.	2	1.75	13	18.3
GS26	06/2016-12/2016	Shallow Aquifer	P. Corals	2	0.36	no data	8.6
GS28	07/2016-12/2016	Shallow Aquifer	Magarini s.	2	0.334	no data	2.1
GS29	07/2016-12/2016	Shallow Aquifer	Magarini s.	2	1.02	no data	16.1
GD22	06/2016-12/2016	Deep Aquifer	Mazeras snd.	2	2.08	no data	14.0
GS30	07/2016-12/2016	Shallow Aquifer	Magarini s.	2	0.77	no data	21
GD23	06/2016-12/2016	Deep Aquifer	Mazeras snd.	2	0.57	no data	52.0
GS31	07/2016-12/2016	Shallow Aquifer	Magarini s.	2	0.332	no data	9.9
GS36	03/2016-12/2016	Shallow Aquifer	Kilindini s.	2	0.1	not affected	9.0
GS37	03/2016-12/2016	Shallow Aquifer	Kilindini s.	2	0.64	54	9.0
GS42	03/2016-12/2016	Shallow Aquifer	Magarini s.	2	0.11	38	10.0
GS45	07/2016-12/2016	Shallow Aquifer	Kilindini s.	2	0.39	no data	8.8
GS47	07/2016-09/2016	Shallow Aquifer	Magarini s.	2	0.4	no data	3.0
GD24	06/2016-12/2016	Deep Aquifer	Mazeras snd.	2	0.1	no data	38.0

Table 2, Appendix A: Isotopic data from March and June 2016 field survey; Saturation Index of Calcite and Quartz for June 2016 field samples and ionic relation for June 2016 field survey.

CODE	*DATA*	*$\delta^{18}O$*	*$\delta^{2}H$*	*DATA*	*$\delta^{18}O$*	*$\delta^{2}H$*	*SI CALCITE*	*SI QUARTZ*	*NA/CL^{-}*	*CA/HCO_3^{-}*
FOOTPRINTS SCHOOL	06/06/2016	-3.47	-13.35	01/03/2016	-3.43	-13.51	-3.34	0.72	1.54	0.16
Z4-11	06/06/2016	-2.80	-9.79	01/03/2016	-2.87	-10.13	-1.40	0.32	1.46	0.98
Z4-09	-	-	-	02/03/2016	-3.14	-12.88	-	-	-	-
Z4-01	07/06/2016	-3.24	-13.56	02/03/2016	-3.50	-13.72	0.10	0.32	1.30	1.03
A/04/12	07/06/2016	-3.16	-13.30	06/03/2016	-3.30	-13.77	0.00	0.37	1.04	0.88
Z4-18	07/06/2016	-3.14	-12.87	06/03/2016	-2.98	-12.70	0.18	0.34	0.99	0.97
A/06/12	07/06/2016	-2.74	-10.92	06/03/2016	-2.66	-11.30	0.16	0.17	0.73	1.31
Z4-78B	07/06/2016	-2.65	-9.94	06/03/2016	-2.39	-10.01	0.28	0.09	0.77	1.49
Z4-08	06/06/2016	-3.17	-14.02	02/03/2016	-3.47	-13.89	-0.07	0.31	2.19	0.76
Z4-06	06/06/2016	-3.23	-13.84	02/03/2016	-3.42	-13.50	-0.01	0.40	2.53	0.84
D/100/16	06/06/2016	-3.28	-13.58	02/03/2016	-3.52	-13.59	-0.01	0.30	3.10	0.37
Z4-04	07/06/2016	-3.00	-12.67	02/03/2016	-3.15	-13.41	0.17	0.33	1.30	0.88
Z4-MS	06/06/2016	-3.12	-13.03	01/03/2016	-3.34	-13.56	-1.37	0.28	1.10	1.31
D/82/14	06/06/2016	-3.05	-12.46	01/03/2016	-3.31	-13.24	-4.60	0.56	1.98	0.22
Z4-85	07/06/2016	-2.94	-12.46	06/03/2016	-2.83	-11.82	0.12	0.33	0.94	1.11
Z4-24	08/06/2016	-2.44	-8.31	05/03/2016	-2.49	-8.07	-0.87	0.40	0.90	1.05
Z3-25	-	-	-	05/03/2016	-2.31	-7.85	-	-	-	-
D/63/13	08/06/2016	-3.37	-14.04	05/03/2016	-3.42	-14.73	-3.46	0.51	2.28	0.23
D/68/13	08/06/2016	-3.24	-14.06	05/03/2016	-3.37	-14.49	-3.09	0.54	3.90	0.16
Z3-30	08/06/2016	-2.54	-8.11	03/03/2016	-2.54	-7.75	-0.54	0.69	1.08	1.04

Z3-29	08/06/2016	-2.68	-9.52	03/03/2016	-2.83	-9.32	-0.95	0.27	1.01	1.18
DB/BM/HP	08/06/2016	-3.14	-12.22	03/03/2016	-3.25	-11.09	-1.62	0.62	3.57	0.42
BH310	23/06/2016	-2.72	-9.80	04/03/2016	-2.94	-11.64	0.03	0.40	2.27	0.97
BH402	-	-	-	04/03/2016	-2.78	-10.67	-	-	-	-
NK-03	-	-	-	04/03/2016	-2.86	-10.84	-	-	-	-
Z1-70	13/06/2016	-2.29	-7.52	11/03/2016	-2.42	-7.14	-0.91	-0.07	1.12	0.84
Z1-33	13/06/2016	-2.64	-9.28	11/03/2016	-2.72	-10.02	0.21	0.16	1.38	1.32
A/14/10	13/06/2016	-2.86	-10.59	11/03/2016	-2.90	-10.69	0.09	0.08	1.26	1.04
Z3-87	07/06/2016	-2.59	-9.17	06/03/2016	-2.78	-9.29	0.01	0.01	0.75	1.18
Z3-98	11/06/2016	-2.59	-8.46	08/03/2016	-2.72	-9.69	0.10	-0.18	0.75	1.16
Z3-90	14/06/2016	-2.62	-9.24	08/03/2016	-2.78	-10.37	0.06	0.27	0.51	1.81
A/05/11	14/06/2016	-2.47	-9.48	01/03/2016	-3.16	-11.69	0.03	0.30	0.63	1.75
HOTSPRING	09/06/2016	-2.37	-9.64	10/03/2016	-2.24	-8.94	0.97	0.24	1.00	0.10
C108HWL	09/06/2016	0.95	6.13	10/03/2016	1.85	7.66	0.98	-0.38	0.99	0.22
3KD01	09/06/2016	0.40	4.04	10/03/2016	2.78	11.48	0.62	-0.16	1.00	0.49
TIWI 8.2	18/06/2016	-2.94	-13.04	15/03/2016	-3.12	-13.98	-0.74	0.50	0.94	0.86
TIWI 1	14/06/2016	-2.24	-9.69	15/03/2016	-2.38	-10.30	0.06	0.37	1.49	0.93
MUACHEMA TRIB	11/06/2016	-0.70	1.41	-	-	-	-0.35	0.42	1.65	0.52
S1-3KD06	15/06/2016	-2.69	-9.45	09/03/2016	-2.78	-10.77	-2.87	0.15	1.31	0.41
GD31	15/06/2016	-3.36	-13.36	09/03/2016	-3.45	-13.72	-0.61	0.53	2.65	0.47
MUK DAM	15/06/2016	-0.07	2.66	09/03/2016	0.30	5.72	-1.68	0.04	1.32	0.59
MUK DWS	15/06/2016	-1.12	-1.15	09/03/2016	-0.86	1.14	-1.66	0.13	1.35	0.51
KINGOMBERO	25/06/2016	-3.03	-11.29	11/03/2016	-3.06	-11.46	-4.17	0.30	-	0.35
Z1-122	10/06/2016	-2.25	-6.65	04/03/2016	-2.18	-5.83	-1.80	0.26	1.01	0.82
Z1-125	10/06/2016	-2.70	-9.39	04/03/2016	-2.73	-10.24	-4.09	0.37	1.48	0.26

Z1-124	10/06/2016	-2.61	-9.37	04/03/2016	-2.87	-9.12	-0.86	0.28	1.42	0.87
D/16/10	10/06/2016	-1.40	-2.81	04/03/2016	-1.30	-2.39	-0.36	0.10	1.45	1.07
Z1-121B	10/06/2016	-3.10	-12.13	05/03/2016	-2.92	-11.47	-0.18	0.54	0.68	0.96
Z1-116	15/06/2016	-3.02	-12.04	11/03/2016	-2.83	-11.69	-0.11	0.21	1.12	1.13
C/07/09	10/06/2016	-2.55	-9.71	11/03/2016	-2.40	-9.58	-0.19	0.11	0.51	1.26
A/01/11	14/06/2016	-2.71	-9.67	05/03/2016	-2.49	-8.93	-0.08	0.11	1.31	1.18
Z2-103	11/06/2016	-2.69	-9.74	05/03/2016	-2.79	-10.35	0.16	0.03	1.40	0.80
D/203/27	14/06/2016	-2.70	-9.26	08/03/2016	-2.64	-9.71	-0.22	0.32	0.39	1.07
DB/MS/LST	13/06/2016	-2.88	-10.71	05/03/2016	-2.82	-10.20	-0.05	0.20	0.98	0.88
Z1-135	08/06/2016	-1.97	-6.63	02/03/2016	-2.15	-7.47	-0.58	0.01	2.45	0.76
Z2-112	08/06/2016	-2.40	-7.71	03/03/2016	-2.45	-8.44	-2.80	0.03	1.25	0.55
Z1-140	15/06/2016	-3.12	-12.26	09/03/2016	-3.11	-12.14	-0.41	0.30	2.02	0.96
Z2-104	16/06/2016	-2.64	-9.35	03/03/2016	-2.56	-9.59	-0.19	0.29	2.05	1.04
Z1-110	16/06/2016	-2.18	-5.85	03/03/2016	-1.90	-4.86	-0.73	-0.09	1.36	1.00
DB/FI/HP	16/06/2016	-3.07	-12.39	03/03/2016	-2.96	-11.37	-0.19	0.33	1.54	0.49
Z3-96	11/06/2016	-2.58	-9.70	08/03/2016	-2.55	-8.64	-0.02	0.14	0.75	1.33
E/29/01	11/06/2016	-2.66	-8.83	08/03/2016	-2.55	-8.78	-0.08	-0.10	0.60	1.10
A/09/11	14/06/2016	-1.86	-5.61	08/03/2016	-1.68	-5.03	-0.01	0.07	0.81	1.24
MIVUMONI	15/06/2016	-3.06	-11.60	09/03/2016	-3.02	-12.12	-3.39	0.62	2.47	0.14
C/15/10	09/06/2016	-3.15	-11.56	09/03/2016	-2.97	-11.72	-1.33	0.45	4.02	0.33
C/109/21	15/06/2016	-3.16	-13.07	09/03/2016	no data	no data	-0.66	0.52	3.63	0.47
C/12/12	09/06/2016	-2.97	-12.71	10/03/2016	-2.93	-12.47	-1.25	0.67	1.12	0.50
C/06/12	09/06/2016	-3.10	-12.40	10/03/2016	-3.20	-9.94	-3.11	0.58	1.85	0.15
C/19/10	09/06/2016	-2.71	-11.00	10/03/2016	-3.04	-10.20	-4.41	0.06	1.59	0.33
D/129/19	06/06/2016	-3.03	-13.27	01/03/2016	-3.08	-13.27	-3.45	0.48	2.77	0.11

DB/MH/CO	07/06/2016	-2.79	-11.82	02/03/2016	-2.75	-11.77	0.04	0.40	1.83	0.72
Z1-141	13/06/2016	-2.06	-7.02	13/03/2016	-2.05	-7.34	0.04	-0.38	0.75	2.38
UK-WL	11/06/2016	-3.04	-13.27	06/03/2016	-2.99	-12.77	-0.12	0.32	0.85	1.21
D/103/16	06/06/2016	-3.20	-14.18	08/03/2016	-3.16	-13.74	-0.08	0.46	1.66	0.78
LUKORE-SEC. SCHOOL	09/06/2016	-3.00	-11.74	10/03/2016	-3.06	-11.77	-0.14	0.54	1.00	0.56
Z1-118	10/06/2016	-2.75	-10.36	11/03/2016	-2.89	-10.57	-0.31	0.32	1.50	1.13
VIN-WL	13/06/2016	-2.85	-11.61	11/03/2016	-3.27	-8.99	-0.04	0.13	0.69	1.06
BASE_BH_3	17/06/2016	-3.25	-12.93	16/03/2016	-3.20	-13.12	-0.24	0.47	1.27	1.22
BASE_BH_7	17/06/2016	-3.14	-12.39	16/03/2016	-3.23	-12.70	-0.90	0.63	3.55	0.55
DB/KI/ST	18/06/2016	-3.29	-12.84	16/03/2016	-3.34	-11.15	-1.13	0.54	2.67	0.28
Z3-102B	16/06/2016	-2.40	-8.88	-	-	-	0.04	-0.02	1.23	0.95
BH302	23/06/2016	-2.88	-9.89	-	-	-	-1.76	0.42	2.05	0.55
DIANI	22/06/2016	-0.29	1.19	-	-	-	-0.30	-0.34	0.70	5.77
MSW BEACH	22/06/2016	-2.28	-7.34	-	-	-	-0.03	0.18	0.73	1.30
KIS_21	23/06/2016	-2.62	-8.27	-	-	-	-2.21	0.22	1.61	0.72
KIS_65	23/06/2016	-	-	-	-	-	-2.84	0.35	2.11	0.66
GD14_5	17/06/2016	-2.78	-10.72	-	-	-	-0.14	-0.14	0.54	2.70
GD14_ 35	17/06/2016	-2.90	-10.95	-	-	-	0.36	-0.02	0.81	0.90
C/05/09	24/06/2016	-3.03	-10.62	-	-	-	0.20	0.07	1.26	0.91
C/03/09	24/06/2016	-2.81	-9.69				0.05	-0.04	0.77	1.06

Table 3, Appendix A: Physico-chemical parameters measured in the field and hydrochemical data for June 2016 field survey.

CODE	GEOLOGY	COND.	Tª	PH	TOC	ALKALINITY	HCO3	DO	ORP	EH	NH4	CL
		(µS/cm)	°C		(mg/L)	as mg/L HCO3		(mg/L)	mV	mV	(mg/L)	(mg/L)
FOOTPRINTS SCHOOL	Mazeras snd.	311,7	27,5	5,8	0,9	54,9	54,9	2,2	-26,5	193,5	0,0	43,3
Z4-11	Magarini s.	205	29,0	6,6	0,9	79,3	79,3	7,9	38,4	258,4	0,0	13,5
Z4-01	Kilindini s.	671	29,2	7,0	0,9	317,3	317,3	5,4	71,2	291,2	0,0	20,0
A/04/12	P.Corals	64,5	29,6	6,8	0,7	396,6	396,6	5,8	93,5	313,5	0,0	62,3
Z4-18	P.Corals	881,0	29,3	7,0	1,1	366,1	366,1	6,5	33,0	253,0	0,0	68,3
A/06/12	P.Corals	2743	29,5	7,1	1,0	311,2	311,2	7,1	-39,6	180,4	0,0	690,1
Z4-78B	P.Corals	3793	28,1	7,4	1,5	256,3	256,3	6,1	34,9	254,9	0,0	1025,2
Z4-08	Kilindini s.	406,1	29,6	6,8	1,8	378,3	378,3	4,5	7,9	227,9	0,0	19,4
Z4-06	Kilindini s.	769	28,9	6,8	0,5	396,6	396,6	3,7	61,5	281,5	0,0	17,9
D/100/16	Kilindini s.	875	29,1	7,0	0,6	488,2	488,2	3,1	50,4	270,4	0,0	28,0
Z4-04	Kilindini s.	592	28,6	7,2	0,9	292,9	292,9	5,7	25,5	245,5	0,0	20,9
Z4-MS	Magarini s.	364,1	28,4	6,5	0,7	85,4	85,4	5,8	44,8	264,8	0,0	32,2
D/82/14	Magarini s.	91,9	27,7	5,3	0,8	18,3	18,3	7,9	136,2	356,2	0,0	11,7
Z4-85	P.Corals	64,5	29,9	7,0	1,0	317,3	317,3	6,1	65,8	285,8	0,0	85,6
Z4-24	Kilindini s.	282,6	28,4	6,9	1,6	103,7	103,7	3,5	-58,0	162,0	0,0	24,6
D/63/13	Magarini s.	170,2	28,8	5,7	1,5	42,7	42,7	2,9	88,3	308,3	0,0	20,0
D/68/13	Magarini s.	51,4	29,0	6,0	1,1	54,9	54,9	3,0	-5,8	214,2	0,0	10,8
Z3-30	Kilindini s.	735	29,2	6,8		189,2	189,2	3,9	52,5	272,5	0,0	78,3
Z3-29	Kilindini s.	342,2	28,1	6,7	1,4	115,9	115,9	4,3	45,6	265,6	0,0	23,9
DB/BM/HP	Kambe	256,4	28,7	6,5	1,4	109,8	109,8	5,3	91,0	311,0	0,0	11,8
BH310	Mazeras snd.	510	28,8	7,1	2,0	262,4	262,4	3,8	56,8	276,8	0,0	15,4
Z1-70	Kilindini s.	820	28,2	6,6	3,9	177,0	177,0	5,4	-120,8	99,2	0,0	98,7
A/14/10	P.Corals	667	28,9	6,9	3,4	353,9	353,9	3,9	80,0	300,0	0,0	21,6
Z3-87	P.Corals	2011,0	29,2	6,9	1,0	335,6	335,6	5,5	47,1	267,1	0,0	433,2

Z3-98	P.Corals	830	28,8	6,9	2,9	347,8	347,8	7,2	40,7	260,7	0,0	33,0
Z3-90	P.Corals	2360	28,2	6,6	1,2	433,2	433,2	5,5	-33,3	186,7	0,0	602,5
A/05/11	P.Corals	1750	30,3	6,8	1,7	305,1	305,1	3,3	-32,0	188,0	0,0	320,8
HOTSPRING	Spring	15792,0	58,8	7,9	1,7	976,3	976,3	0,9	-197,0	23,0	5,0	2642,7
C108HWL	SW	5594,0	32,1	8,5	7,6	445,4	445,4	11,6	-18,3	201,7	1,2	1561,9
3KD01	SW	3211	30,6	8,6	9,4	158,7	158,7	8,9	-32,5	187,5	0,0	858,9
MUACHEMA TRIB	SW	505	25,0	7,3	14,9	189,2	189,2	5,1	-30,6	189,4	0,0	53,5
S1-3KD06	SW	140	22,6	6,4	3,0	30,5	30,5	8,6	66,8	286,8	0,0	16,9
GD31	Mazeras snd.	290	28,0	7,0	1,4	207,5	207,5	4,3	-77,9	142,1	0,0	32,8
MUK DAM	SW	230	26,9	6,8	4,0	61,0	61,0	7,4	-36,3	183,7	0,0	21,6
MUK DWS	SW	210	26,3	6,8	5,5	67,1	67,1	8,2	32,3	252,3	0,0	22,4
Z1-122	Magarini s.	210	27,9	6,3	1,5	79,3	79,3	7,6	51,2	271,2	0,0	14,4
Z1-125	Magarini s.	112	27,6	5,3	1,2	30,5	30,5	5,4	111,9	331,9	0,0	12,5
Z1-124	Magarini s.	325,3	28,9	6,5	1,7	189,2	189,2	2,2	23,3	243,3	0,5	8,3
D/16/10	Kilindini s.	592	28,7	6,6	1,5	286,8	286,8	3,4	52,8	272,8	0,0	15,0
Z1-121B	Kilindini s.	589	28,4	6,5	1,6	433,2	433,2	5,2	25,5	245,5	0,0	13,0
Z1-116	P.Corals	740	30,0	6,8	2,0	292,9	292,9	3,2	58,7	278,7	0,0	31,4
C/07/09	P.Corals	666	30,1	6,6	1,9	378,3	378,3	3,4	-9,1	210,9	0,0	22,4
A/01/11	P.Corals	1040,0	29,1	6,7	1,4	360,0	360,0	1,1	31,2	251,2	1,2	57,3
Z2-103	P.Corals	890	28,8	7,0	3,8	396,6	396,6	5,6	-69,4	150,6	0,0	34,9
D/203/27	Kilindini s.	610	30,7	6,7	1,4	292,9	292,9	3,3	-3,3	216,7	0,0	31,9
DB/MS/LST	P.Corals	1010	29,8	6,8	4,1	372,2	372,2	1,4	-180,9	39,1	0,8	97,4
Z1-135	Kilindini s.	253,9	27,6	7,2	1,4	122,0	122,0	7,1	-25,8	194,2	0,0	7,3
Z2-112	Magarini s.	41,3	27,6	6,1	1,4	36,6	36,6	5,6	93,8	313,8	0,0	7,1
Z1-140	Magarini s.	650,0	28,3	6,7	1,8	256,3	256,3	1,0	-92,0	128,0	0,0	13,8
Z2-104	P.Corals	610	29,2	6,7	2,1	317,3	317,3	2,1	-42,6	177,4	0,0	19,0
Z1-110	Kilindini s.	180	30,5	7,2	2,6	85,4	85,4	3,0	-56,8	163,2	0,0	10,1
DB/FI/HP	Kambe	590,0	30,6	7,2	2,0	244,1	244,1	0,8	-96,7	123,3	0,0	31,4

Z3-96	P.Corals	3300	28,9	7,0	173,3	292,9	292,9	3,6	-221,0	-1,0	0,0	810,8
E/29/01	Pls-Plc	980	29,2	6,7	3,2	360,0	360,0	3,7	-9,4	210,6	0,0	99,9
A/09/11	P.Corals	475	30,1	7,0	1,2	323,4	323,4	1,8	-21,1	198,9	0,0	1241,2
MIVUMONI	Mazeras snd.	260	29,1	5,7	1,9	61,0	61,0	1,8	64,2	284,2	0,0	22,2
C/15/10	Mazeras snd.	66,4	27,8	6,4	1,5	207,5	207,5	1,7	-134,3	85,7	0,2	25,9
C/109/21	Mazeras snd.	630	27,2	6,6	1,4	317,3	317,3	1,1	-178,7	41,3	0,0	25,6
C/12/12	Mazeras snd.	65,7	29,1	6,4		195,3	195,3	1,6	0,7	220,7	0,0	192,4
C/06/12	Mazeras snd.	313	27,8	5,7	1,6	85,4	85,4	2,5	87,7	307,7	0,0	38,5
C/19/10	Magarini s.	42,7	28,0	5,3	1,6	18,3	18,3	2,6	52,6	272,6	0,0	8,4
D/129/19	Magarini s.	49,2	27,9	5,9	0,4	48,8	48,8	4,1	87,5	307,5	0,0	13,9
DB/MH/CO	Mazeras snd.	516	29,3	7,2	0,4	268,5	268,5	5,2	48,7	268,7	0,0	26,2
Z1-141	P.Corals	9440	28,0	6,9	4,4	329,5	329,5	3,8	32,2	252,2	0,0	2852,4
UK-WL	P.Corals	1040	29,2	6,7	2,6	335,6	335,6	6,6	70,3	290,3	0,0	59,7
D/103/16	Kilindini s.	539,0	28,7	7,0	0,7	286,8	286,8	4,3	90,6	310,6	0,0	20,3
LUKORE-SEC. SCHOOL	Mazeras snd.	70,0	27,7	6,7	1,5	543,1	543,1	1,6	90,5	310,5	0,0	253,8
Z1-118	P.Corals	710,0	28,7	6,5	1,6	335,6	335,6	3,4	-21,5	198,5	0,0	9,6
VIN-WL	Kilindini s.	780,0	29,6	6,7	4,4	378,3	378,3	5,7	45,9	265,9	0,0	30,2
BASE_BH_3	Mazeras snd.	590,0	28,1	6,9	3,0	219,7	219,7	0,8	-126,3	93,7	0,0	42,5
BASE_BH_7	Mazeras snd.	370,0	28,6	6,7	3,3	183,1	183,1	4,1	-28,8	191,2	0,0	17,0
DB/KI/ST	Mazeras snd.	500	27,5	6,58	2,375	238,0	238,0	3,3	-127,0	93,0	0,0	36,8
Z3-102B	P.Corals	540,0	29,6	7,0	2,8	299,0	299,0	7,0	5,8	225,8	0,0	19,7
BH302	Mazeras snd.	200,0	29,6	6,5	1,8	79,3	79,3	2,7	40,3	260,3	0,0	13,4
DIANI	SW	46750,0	27,3	7,0	3,7	177,0	177,0	4,4	101,6	321,6	0,0	15844,0
MSW BEACH	SW	12250,0	29,1	6,9	3,7	439,3	439,3	4,7	58,0	278,0	0,0	4570,0
C/05/09	P.Corals	894,0	28,3	6,9	1,9	384,4	384,4	2,7	40,3	260,3	0,0	62,7

C/03/09	P.Corals	1435,0	28,5	6,9	2,1	353,9	353,9	4,2	154,2	374,2	0,0	157,1		

CODE	***SO4***	***NO3***	***PO4***	***BR***	***F***	***CA***	***MG***	***NA***	***K***	***FE***	***SI***	***AL***	***LI***	***MN***
	(mg/L)	*(mg/L)*	*(mg/L)*	*(mg/L)*	*(mg/L)*	*(mg/L)*	*(mg/L)*	*(mg/L)*	*(mg/L)*	*(mg/L)*	*(mg/L)*	*(mg/L)*	*ppb*	*ppb*
FOOTPRINTS SCHOOL	33,2	0,3	0,1	0,3	0,1	3,0	6,8	43,2	4,4	2,27	35,8	0,00	17,8	144,5
Z4-11	4,5	1,0	0,0	0,1	0,0	25,6	0,8	12,9	0,6	0,00	14,9	-0,04	<0,8	11,5
Z4-01	13,0	2,0	0,0	0,1	0,2	107,1	9,3	16,8	2,6	0,04	15,1	-0,08	5,7	4,4
A/04/12	27,5	2,1	0,0	0,5	0,2	114,4	13,9	42,2	4,2	0,05	17,1	-0,08	6,6	0,8
Z4-18	24,9	3,6	0,0	0,4	0,2	117,0	13,2	43,9	3,5	0,03	15,9	-0,03	5,9	2,1
A/06/12	86,1	6,1	0,0	5,7	0,2	133,5	34,0	327,4	8,6	0,18	10,7	-0,06	9,6	5,8
Z4-78B	132,6	11,8	0,0	4,1	0,2	125,0	54,1	510,8	16,6	0,03	8,5	-0,04	11,5	12,5
Z4-08	3,8	1,8	0,1	0,2	0,1	94,7	12,9	27,5	2,5	0,01	14,9	-0,09	3,8	14,2
Z4-06	3,3	0,5	0,0	0,2	0,2	108,6	15,9	29,3	2,7	0,04	17,9	-0,03	4,3	12,6
D/100/16	26,6	0,1	0,0	0,5	0,7	58,6	44,0	56,4	2,4	0,00	14,3	-0,02	23,8	3,3
Z4-04	15,6	1,2	0,0	0,2	0,1	84,5	11,0	17,5	3,5	0,04	15,0	-0,09	5,0	8,5
Z4-MS	19,5	6,9	0,0	0,2	0,0	36,8	5,7	23,0	1,8	0,03	13,3	-0,14	<0,8	16,6
D/82/14	6,0	0,9	0,0	0,1	0,0	1,3	0,7	15,1	2,0	0,03	25,0	-0,06	0,8	10,3
Z4-85	16,1	3,1	0,0	1,2	0,1	115,0	11,1	51,9	2,5	0,00	15,7	-0,06	4,8	2,6
Z4-24	2,2	0,8	0,0	0,1	0,1	35,7	1,8	14,3	1,3	0,02	17,8	-0,05	<0,8	102,5
D/63/13	8,2	4,5	0,0	0,1	0,0	3,2	0,7	29,6	1,6	0,03	23,2	-0,06	1,6	12,8
D/68/13	9,3	2,6	0,0	0,1	0,0	2,9	0,8	27,4	1,6	0,45	24,8	-0,13	2,2	8,8

Z3-30	30,8	37,3	0,1	0,3	0,1	64,7	10,5	54,9	8,4	-0,02	35,5	-0,09	<0,8	90,2
Z3-29	14,8	2,1	0,0	0,1	0,0	44,7	2,7	15,7	2,6	0,13	12,9	-0,02	4,2	7,3
DB/BM/HP	14,6	0,3	0,3	0,1	0,1	15,0	4,5	27,3	2,3	0,05	29,4	-0,08	3,6	2,3
BH310	4,8	9,4	0,1	0,1	0,2	83,2	5,5	22,6	2,2	0,03	18,0	0,03	6,2	2,0
Z1-70	54,0	41,4	0,0	0,2	0,0	49,0	10,4	71,8	28,2	0,03	6,0	-0,04	3,4	43,7
A/14/10	6,0	6,1	0,0	0,1	0,1	120,3	3,8	17,6	1,4	0,02	8,6	0,02	2,2	1,1
Z3-87	49,7	17,2	0,0	2,1	0,1	130,2	22,5	210,7	5,9	0,03	7,4	-0,09	4,6	0,8
Z3-98	2,1	73,1	<LOQ	3,8	0,1	132,4	3,2	16,1	0,4	0,00	4,7	-0,02	2,0	2,6
Z3-90	41,8	1,6	0,0	2,1	0,1	257,7	24,5	200,9	5,9	0,18	12,8	0,20	6,5	14,1
A/05/11	29,0	5,5	0,0	1,0	0,1	174,6	16,1	130,0	5,6	0,07	15,0	0,17	9,5	21,8
HOTSPRING	<LOQ	0,2	0,1	8,5	8,9	32,9	8,2	1715,3	61,0	0,07	31,1	-0,02	1832,0	48,3
C108HWL	16,7	0,3	<LOQ	5,7	4,1	32,1	31,6	997,5	30,1	-0,01	3,5	-0,07	764,8	55,3
3KD01	11,9	0,2	0,0	4,6	2,1	25,3	21,0	555,3	15,4	0,18	5,6	0,03	379,0	212,4
MUACHEMA TRIB	2,6	0,3	0,0	0,2	0,1	32,3	8,2	57,2	5,9	0,08	16,7	-0,09	2,8	312,0
S1-3KD06	6,3	1,5	0,0	0,1	0,0	4,1	2,6	14,3	2,2	0,02	8,1	-0,12	1,4	68,6
GD31	51,7	1,2	0,1	0,2	0,2	31,7	17,9	56,5	5,7	0,85	23,3	-0,06	17,5	836,5
MUK DAM	5,2	0,9	0,0	0,1	0,1	11,8	3,8	18,5	3,5	0,06	7,3	-0,01	3,7	155,8
MUK DWS	2,8	0,5	0,0	0,1	0,1	11,2	3,4	19,6	2,0	0,23	8,9	0,00	2,1	231,7
Z1-122	2,3	20,8	0,0	0,1	0,0	21,5	2,4	9,5	0,5	0,03	12,7	-0,11	1,3	9,1
Z1-125	4,3	6,6	0,0	0,1	0,0	2,6	1,3	12,1	1,3	0,03	16,2	-0,10	1,2	34,3
Z1-124	6,5	9,9	0,0	0,1	0,0	54,1	1,5	7,6	1,8	0,01	13,7	-0,05	2,2	16,5

D/16/10	6,5	4,5	0,0	0,0	0,1	100,9	3,5	14,1	4,7	-0,04	9,0	-0,08	6,1	0,9
Z1-121B	0,3	1,4	0,0	0,1	0,1	136,0	3,4	5,7	0,5	0,00	24,5	-0,03	3,8	1,8
Z1-116	14,6	3,5	0,0	0,1	0,2	109,0	9,2	22,7	2,5	0,04	12,1	0,04	4,5	4,5
C/07/09	10,8	4,5	0,0	0,2	0,2	112,3	5,7	18,3	1,5	0,01	9,6	-0,04	2,9	0,9
A/01/11	31,3	64,7	0,0	0,2	0,1	138,8	6,8	48,7	10,1	0,02	9,2	0,06	4,5	1,7
Z2-103	31,8	6,1	0,0	0,2	0,1	104,5	4,7	31,6	48,6	0,06	7,7	-0,01	4,0	9,2
D/203/27	2,1	18,2	0,0	0,1	0,1	102,9	3,1	8,1	1,3	0,06	15,7	0,07	7,5	4,0
DB/MS/LST	15,9	0,3	0,0	0,3	0,2	107,9	15,6	62,0	6,1	2,12	11,6	-0,04	4,5	467,4
Z1-135	3,1	3,1	0,0	0,1	0,1	30,4	2,9	11,6	7,2	0,05	7,0	-0,13	<0,8	16,6
Z2-112	1,6	0,8	<LOQ	0,0	0,0	6,6	0,8	5,8	0,8	0,00	7,3	-0,10	<0,8	7,0
Z1-140	15,0	0,2	0,0	0,1	0,2	80,3	17,0	18,0	9,1	0,16	14,0	0,08	4,4	110,6
Z2-104	13,8	2,1	0,0	0,1	0,1	107,7	6,5	25,2	2,0	0,08	14,0	0,08	5,3	3,7
Z1-110	9,2	3,7	<LOQ	0,1	0,1	27,9	0,9	8,9	1,1	0,04	6,2	0,02	<0,8	9,1
DB/FI/HP	32,0	0,2	0,1	0,1	0,2	39,3	8,2	31,4	2,0	0,03	16,1	-0,06	4,8	41,8
Z3-96	110,6	5,7	0,0	3,4	0,1	127,6	44,6	391,6	11,7	0,03	9,7	-0,06	10,4	11,6
E/29/01	8,6	1,7	<LOQ	0,5	0,1	130,2	6,6	39,0	1,6	0,00	5,7	-0,07	2,6	2,4
A/09/11	166,7	0,0	0,0	4,7	0,2	131,6	89,3	655,5	28,6	0,05	8,7	0,02	15,8	2,6
MIVUMONI	22,6	9,2	0,1	0,1	0,1	2,8	3,6	35,5	2,8	0,07	29,7	-0,06	7,9	93,0
C/15/10	27,0	0,4	0,3	0,6	0,2	22,6	13,2	67,4	3,9	0,78	19,3	-0,09	13,4	186,7
C/109/21	24,5	0,3	0,0	0,1	0,1	48,5	15,1	60,2	4,7	5,70	22,4	0,01	16,3	73,6
C/12/12	50,0	4,9	0,2	0,8	0,2	31,9	24,7	140,3	4,6	0,07	33,4	-0,12	13,6	267,5

C/06/12	18,1	8,3	0,2	0,3	0,1	4,1	5,3	46,2	5,0	0,02	26,2	-0,12	7,1	6,8
C/19/10	5,4	4,1	0,0	0,1	0,0	2,0	1,7	8,7	1,5	2,82	8,0	-0,10	1,5	52,7
D/129/19	8,5	1,0	0,0	0,1	0,1	1,8	0,7	25,0	0,8	0,12	20,7	-0,03	<0,8	5,9
DB/MH/CO	9,2	3,4	0,1	0,1	0,1	63,5	6,5	31,0	2,7	-0,01	18,1	-0,10	4,1	<0,8
Z1-141	359,6	1,5	<LOQ	10,3	0,1	257,5	151,9	1393,2	40,0	0,01	2,8	0,13	21,4	12,8
UK-WL	14,4	55,0	0,0	0,9	0,2	133,4	20,0	32,7	3,5	0,03	15,1	-0,01	6,6	3,4
D/103/16	2,3	1,1	0,1	0,2	0,1	73,32	9,37	21,77	3,45	0,05	20,34	-0,05	3,5	1,6
LUKORE-SEC. SCHOOL	114,8	3,4	0,1	1,3	0,1	98,96	61,21	164,12	10,33	0,20	23,86	-0,07	39,7	68,2
Z1-118	1,1	3,7	0,0	0,0	0,1	124,75	2,59	9,28	1,07	0,04	14,94	-0,02	7,0	5,9
VIN-WL	5,6	14,4	0,0	0,1	0,1	131,41	5,43	13,40	1,46	0,01	9,77	0,02	2,2	6,7
BASE_BH_3	15,9	0,4	0,1	0,2	0,1	88,12	4,98	34,91	3,87	0,13	20,34	-0,06	13,4	112,1
BASE_BH_7	21,4	1,8	0,1	0,1	0,2	32,80	6,79	39,20	3,03	0,08	30,24	-0,01	5,3	12,3
DB/KI/ST	26,8	0,8	0,0	0,3	<LOQ	21,60	17,73	63,71	3,27	0,84	23,61	-0,01	18,6	225,4
Z3-102B	2,1	10,7	0,0	0,1	0,1	93,23	7,14	15,72	3,65	0,02	7,04	-0,01	<0,8	<0,8
BH302	8,9	6,3	0,0	0,1	0,1	14,33	3,92	17,79	2,17	0,11	19,27	0,09	10,3	4,9
DIANI	2208,2	0,8	0,0	58,7	0,7	334,91	878,22	7138,30	268,35	0,08	2,84	0,23	126,1	16,0
MSW BEACH	651,6	1,1	0,0	16,5	0,3	186,98	271,84	2167,80	81,47	0,01	10,34	0,07	41,3	3,4
C/05/09	9,2	51,8	0,03	0,2	0,1	158,58	6,58	20,90	1,64	0,05	8,18	0,15	2,7	5,4
C/03/09	27,5	16,4	0,03	0,5	0,1	122,60	10,90	78,08	2,89	0,07	6,49	0,19	2,9	1,6

Table 4, Appendix A: Physico-chemical parameters measured in the field and hydrochemical data for March 2014 field survey.

Code	*Localization*	*Data*	*Cond.*	*T*ª	*pH*	*HCO_3*	*Cl*	*SO_4*	*NO_3*	*Ca*	*Mg*	*Na*	*K*
			(µS/cm)	*°C*		*(mg/L)*	*(mg/L)*	*(mg/L)*	*(mg/L)*	*(mg/L)*	*(mg/L)*	*(mg/L)*	*(mg/L)*
Z1-140	Vumbu Shallow Well	25/03/2014	420	27.8	6.42	94	14	7.21	2.83	68.5	3.67	13.8	9.27
Z1-116	Mwaembe, Msambweni	26/03/2014	670	29.5	6.64	112	35.2	16.1	1.77	107	9.13	26.1	2.81
Z1-121	Alternate to Milalani Mosque	26/03/2014	624	28.7	6.62	136	22.6	6.37	6.58	110	3.81	17.1	4.84
Z1-122	Kidzumbani Mosque (Buda Rd)	26/03/2014	143.1	28.1	6.52	40.5	14.5	1.1	12.9	16.1	1.9	9.06	0.54
Z1-124	Gongonda South	26/03/2014	157.2	28.6	5.85	55	10	4.28	1.77	20	1.4	8.97	1.53
Z1-125	Gongonda North	26/03/2014	91.8	27.8	5.26	31.8	12.5	5.48	7.96	2.93	1.27	13	1.41
Z1-33	Munje Mosque	26/03/2014	596	28.2	7.05	190	19.5	7.09	3.04	108	3.89	19.5	1.61
Z1-70	Darigube Mosque, Ramisi	26/03/2014	705	29.4	5.94	57	136	41.8	11.8	37.6	8.48	76.5	20
Z2-103	Gazi ShW (west of rd)	25/03/2014	760	29.1	6.89	188	30.5	18.3	8.32	108	4.78	27	45.5
Z1-110	Fihoni Pri Sch	25/03/2014	115.5	30	6.47	37.9	8.25	4.09	4.24	12.6	0.77	7.9	1.03
Z2-111	Fihoni (nr. S11)	25/03/2014	266	30.2	6.74	208	11.1	8.5	1.06	34.2	1.74	13.6	11.6
Z2-112	Bumamani	25/03/2014	68.5	29.2	6.14	96	4.8	2.24	1.06	6.74	0.65	6.92	0.64
Z3-102	MDC Kitaruni (Teba)F	26/03/2014	675	27.2	7.05	119	44	1.25	0.36	75.5	17.8	38.6	11.3
Z3-29	Mchenzani Magaoni	25/03/2014	180	28.5	5.47	39.2	25.3	11.3	1.06	12.3	2.29	17.8	2.72
Z3-25	Zigira Mosque (F)	27/03/2014	277	27.8	7.09	67	22.6	8.34	3.18	31.5	2	21.6	3.33
Z3-30	Magaoni Mosque	25/03/2014	1014	30.1	6.31	53	256	11.4	< 0.01	65.5	13.6	106	4.01

Z3-87	Kinondo II	27/03/2014	1924	28.6	6.94	131	423	40.3	3.85	135	30.1	226	9.33
Z3-90	Makongeni Mosque	26/03/2014	2630	28.9	6.52	114	645	50	2.47	260	27.1	232	9.38
Z3-96	Kinondo IV	27/03/2014	3010	28.7	7.01	125	795	82.2	1.99	134	48.3	406	13.6
Z3-98	Kinondo III	27/03/2014	711	28.8	6.9	9	29.3	1.55	62.7	132	3.25	16	0.6
Z4-01	Kiuzini	27/03/2014	627	28.5	6.63	121	18.8	11.6	2.2	106	9.26	18.3	2.56
Z4-05	Mwabungo I	27/03/2014	564	28.2	6.89	120	21.3	15.4	1.01	87.9	11.3	18.8	3.29
Z4-06	Ukunda Set Scheme	27/03/2014	737	28.4	6.59	117	19	3.35	0.84	110	16.6	30.6	2.68
Z4-09	Mabakoni	27/03/2014	945	28.3	7.02	115	28.3	13.9	0.19	89.5	12.6	26	29.8
Z4-11	Mabakoni Mosque	27/03/2014	218	28.1	6.7	27.4	11.5	4.63	0.75	29.1	1.49	13.1	2.62
Z4-18	Mwabungo II	27/03/2014	827	29	6.7	136	68.7	25.3	2.83	115	13.6	46.3	4.16
Z4-24	Kilole Pri Sch (F)	27/03/2014	187.7	28.3	6.92	31	13.3	2.77	0.79	22.6	1.97	13.5	2.49
Z4-78	Neptune	27/03/2014	2450	29	7.04	0	697	69.2	113	131	37.1	328	9.66
Z4-85	Kinondo I	27/03/2014	850	29.2	6.79	59	81	15.9	2.77	115	11	55.1	2.64

Table 5, Appendix A: Physico-chemical parameters measured in the field and hydrochemical data for June 2014 field survey.

Code	*Localization*	*Data*	*Cond.*	*T*ª	*pH*	HCO_3	*Cl*	SO_4	NO_3	*Ca*	*Mg*	*Na*	*K*
			(µS/cm)	*°C*		*(mg/L)*	*(mg/L)*	*(mg/L)*	*(mg/L)*	*(mg/L)*	*(mg/L)*	*(mg/L)*	*(mg/L)*
Z1-140	Vumbu Shallow Well	07/06/2014	516	29.6	6.35	323	14.1	11.1	6.41	83.4	7.3	17.1	12.5
Z1-110	Fihoni Pri Sch	07/06/2014	206	28.9	6.98	98	13.6	9.55	23.8	29.8	0.87	11.3	1.33
Z1-116	Mwaembe, Msambweni	07/06/2014	658	28.2	6.79	373	36.2	17.1	27.3	111	9.96	26.8	2.47
Z1-122	Kidzumbani Mosque (Buda Rd)	07/06/2014	175.6	26.5	6.45	98.5	13	2.24	17.6	23.1	2.18	9.14	0.41
Z1-124	Gongonda South	07/06/2014	243	27.1	6.38	160	8.77	4.37	8.98	37.8	2.12	8.32	2.41
Z1-135	Madzi Kuko Mosque	07/06/2014	407	26.3	7.17	252	10	10.8	13.5	47.1	6.17	19.8	25.8
Z1-33	Munje Mosque	07/06/2014	597	28.6	7.1	377	19.6	7.29	7.16	114	4.37	23	2.81
Z1-70	Darigube Mosque, Ramisi	07/06/2014	882	28.2	6.4	210	143	61.3	16.3	61.6	12.8	95.5	25.3
Z2-103	Gazi ShW (west of rd)	07/06/2014	782	27.4	6.96	394	45	38	20.8	105	4.75	39.5	56.3
z2-104	Fihoni Salha Centre	07/06/2014	656	28	6.72	391	24.3	15.3	25	117	6.86	30.1	2
Z2-111	Fihoni (nr. S11)	07/06/2014	332	26.7	6.37	203	7.44	8.58	< 0.01	46.8	2.16	13	11.3
Z2-112	Bumamani	07/06/2014	106.1	27	6.09	57.1	4.54	3.2	2.92	14.5	0.95	6.32	0.53
Z3-24	Mchenzani Magaoni	07/06/2014	232	26.9	5.75	98.4	24	11.4	1.1	24.3	2.58	17.6	2.49
Z3-25	Zigira Mosque	08/06/2014	398	27.7	6.84	185	17.1	31.1	14.5	45.7	4.54	26.5	13
Z3-30	Magaoni Mosque	07/06/2014	1845	26.7	6.64	311	209	25.6	18.3	106	18.3	117	10.1
Z3-87	Kinondo II	08/06/2014	1590	27.8	6.79	336	337	36.2	5.08	124	18.1	191	4.04

Z3-90	Makongeni Mosque	08/06/2014	1950	28	6.48	435	430	23.5	35.7	248	13.4	160	2.16
Z3-96	Kinondo IV	06/06/2014	1968	27.2	7.49	290	473	54.7	1.14	110	32.7	261	9.24
Z3-98	Kinondo III	06/06/2014	726	28	6.92	347	36.1	2.24	48.2	138	3.27	19.1	0.4
Z4-01	Kiuzini	06/06/2014	633	28.5	6.85	431	19.6	11.5	3.27	112	9.9	17.8	2.37
Z4-05	Mwabungo I	06/06/2014	546	27.7	7.25	341	20.3	15.5	0.28	88.5	11.8	18.3	3.35
Z4-06	Ukunda Set Scheme	06/06/2014	728	28.7	6.85	508	18.5	3.64	0.66	115	17.6	30.6	2.56
Z4-08	Kibarani, Ukunda Set Scheme	06/06/2014	680	28.6	6.6	480	21.1	3.58	< 0.01	105	15	29.6	5.65
Z4-11	Mabakoni Mosque	06/06/2014	209	27.4	7.89	98.5	11.6	9.33	12.3	14	0.75	20.6	15.3
Z4-18	Mwabungo II	06/06/2014	835	28.5	6.83	442	64.7	25.5	2.33	121	14.5	46.8	3.54
Z4-24	Kilole Pri Sch (F)	08/06/2014	164.3	27.4	6.76	86.9	14.9	2.99	0.7	17.1	1.74	14	1.73
Z4-78	Neptune	06/06/2014	1641	28.4	6.94	271	375	47.8	11.8	104	28.1	193	6.86
Z4-85	Kinondo I	06/06/2014	839	28.3	6.98	396	74.5	15.9	3.98	119	10.8	53.6	2.2
Z3-130	Gonjora	07/06/2014	1315	25.7	7.14	188	194	3.98	228	120	31	96.5	2.1

Table6, Appendix A: Physico-chemical parameters measured in the field and hydrochemical data for March 2016 field survey.

Code	*Localization*	*Geology*	*Data*	*Cond.*	*T°*	*pH*	*Alkalinity*	*NH_4*	*Cl*	*SO_4*	*NO_3*	*Ca*	*Mg*	*Na*	*K*	*Fe*
				(µS/cm)	*°C*		*as mg/L HCO_3^-*	*(mg/L)*	*(mg/L)*	*(mg/L)*	*(mg/L)*	*(mg/L)*	*(mg/L)*	*(mg/L)*	*(mg/L)*	*(mg/L)*
Footprints School	Foot Print Childeren Home/School	Mazeras snd.	01/03/2016	343.6	27.9	5.6	67.1	0.0	43.1	31.9	1.1	2.5	6.9	44.3	4.0	2.88
Z4-11	Mabokoni Msikitini	Magarini s.	01/03/2016	218.6	28.9	6.0	97.6	0.0	14.5	4.5	1.4	23.6	0.8	13.3	0.5	0.06
A/04/12	Galu Multipurpose Group (GMG)	P.Corals	06/03/2016	949	30.5	6.8	323.4	0.0	61.1	27.4	2.8	114.8	14.5	44.3	4.1	0.07
Z4-18	Mwabungo _ Chiungoni	P.Corals	06/03/2016	950.0	29.4	6.9	305.1	0.0	60.8	21.7	20.0	114.1	13.0	42.8	3.6	0.04
Z4-78B	Neptune	P.Corals	06/03/2016	4423	30.6	7.2	238.0	0.0	1104.5	133.3	10.0	131.9	59.9	561.6	17.6	0.07
Z4-08	Ukunda Settlement Scheme	Kilindini s.	02/03/2016	828	29.1	6.6	378.3	0.0	18.8	3.4	1.5	108.8	13.0	30.0	2.4	0.05
Z4-06	Ukunda Settlement Scheme	Kilindini s.	02/03/2016	826	29.2	6.7	353.9	0.0	17.3	3.3	2.0	106.4	15.5	29.6	2.4	0.02
D/100/16	Ukunda Scheme Kwa Boga	Kilindini s.	02/03/2016	924	29.9	6.8	384.4	0.0	28.0	28.3	0.2	62.8	41.4	55.5	2.7	0.02
Z4-04	Mwabungo-Mwamua B	Kilindini s.	02/03/2016	631	29.3	7.0	256.3	0.0	20.0	16.7	1.3	81.5	10.8	18.0	3.0	0.03

Z4-MS	Mkambani Mosque	Magarini s.	01/03/2016	338.1	28.5	6.2	115.9	0.2	30.2	15.6	2.8	28.8	4.8	21.4	1.6	0.07
D/82/14	Mwanjamba Kwa Mwakassim A	Magarini s.	01/03/2016	89.6	28.9	5.2	12.2	0.0	10.3	5.0	1.1	0.5	0.4	13.0	1.5	0.01
Z4-85	Kinondo	P.Corals	06/03/2016	1010	30.3	6.9	353.9	0.0	60.6	11.2	7.5	115.9	11.7	56.5	3.0	0.03
Z4-24	Kilole Primary School	Kilindini s.	05/03/2016	221.5	29.0	6.4	61.0	0.0	15.8	2.5	1.8	21.3	1.4	13.7	2.0	0.11
Z3-25	Zigira Mosque	Kilindini s.	05/03/2016	537	28.6	7.8	61.0	0.0	93.0	5.6	13.1	37.0	4.1	45.9	4.6	0.00
D/63/13	Zigira Chiyaye B	Magarini s.	05/03/2016	182.7	28.8	5.4	48.8	0.0	14.9	4.7	1.0	1.7	0.7	32.1	1.4	0.03
D/68/13	Zigira Bodo C	Magarini s.	05/03/2016	175	28.7	5.8	79.3	0.0	10.3	9.2	2.0	3.0	0.8	29.7	1.7	0.13
Z3-30	Magaoni Mosque	Kilindini s.	03/03/2016	751	29.5	6.1	134.2	0.0	125.1	25.8	5.2	36.8	10.4	72.2	5.1	0.38
Z3-29	Mchenzani Magaoni	Kilindini s.	03/03/2016	376.9	27.9	6.6	128.1	0.0	23.3	12.8	0.8	45.4	2.7	16.8	2.8	0.03
DB/BM/HP	Bumamani	Kambe	03/03/2016	274.2	28.5	6.3	85.4	0.0	12.3	15.1	0.9	14.6	4.6	28.9	2.2	0.00
BH310	KISCOL Sugar Plantation	Mazeras snd.	04/03/2016	555	30.2	7.0	244.1	0.0	14.8	4.9	7.8	73.8	5.5	23.7	2.1	0.04
BH402	KISCOL Sugar Plantation	Mazeras snd.	04/03/2016	429.4	30.1	7.1	201.4	0.0	7.7	2.6	6.9	56.1	3.7	18.9	1.6	-0.02
NK-03	Nikaphu	Mazeras snd.	04/03/2016	760	31.2	6.9	140.3	1.2	161.6	2.2	0.2	28.1	17.3	133.2	9.3	-0.02

Z1-70	Darigube	Kilindini s.	11/03/2016	692	29.8	6.2	122.0	0.0	102.2	34.7	18.2	36.0	7.4	62.8	21.1	0.01
Z1-33	Munje Bujoni	P.Corals	11/03/2016	700	30.1	7.1	329.5	0.0	20.4	6.9	3.3	106.0	3.7	19.1	1.9	0.02
A/14/10	Munje Madukani	P.Corals	11/03/2016	723	29.6	6.7	341.7	0.0	21.6	5.5	5.2	117.3	3.8	17.8	1.7	0.02
Z3-87	Kinondo	P.Corals	06/03/2016	2171.0	29.5	6.8	360.0	0.0	296.5	31.3	5.7	134.9	25.7	233.9	7.4	0.00
Z3-90	Makongeni	P.Corals	08/03/2016	3153	30.6	6.6	408.8	0.0	541.1	43.7	20.1	269.0	31.9	238.9	9.3	0.14
A/05/11	Makongeni Kambini	P.Corals	01/03/2016	2197	29.3	6.5	402.7	0.0	469.7	46.2	9.8	194.4	17.8	211.3	8.1	0.01
HOTSPRING	Hotspring on the Tributary fo Ramisi River	Spring	10/03/2016	10240.0	59.3	7.3	744.4	>8	2640.1	0.2	0.7	32.9	8.1	1854.8	60.7	0.07
3KD01	Mwachande Bridge	SW	10/03/2016	5251	37.2	9.3	614.5	0.0	1948.2	2.0	0.2	21.2	16.3	1417.0	41.4	0.11
GD31	Shimba Hills Secondary School BH	Mazeras snd.	09/03/2016	567	28.3	6.4	238.0	0.0	33.4	52.4	1.5	32.2	17.8	57.9	5.9	1.19
MUK DAM	Mukurumudzi River- Base T Dam	SW	09/03/2016	195.7	33.0	7.1	61.0	0.0	20.3	3.6	0.3	10.0	3.6	17.0	3.6	0.09
Z1-125	Gongonda	Magarini s.	04/03/2016	100.1	28.4	5.3	18.3	0.0	11.8	5.6	2.9	2.8	1.2	11.9	1.5	0.04
Z1-124	Gongonda	Magarini s.	04/03/2016	288.6	28.8	6.2	128.1	3.0	8.9	5.6	0.2	41.7	1.5	8.3	1.8	0.66
D/16/10	Milalani-Nimbodze kwa Mwabiti	Kilindini s.	04/03/2016	683	29.5	6.8	360.0	0.0	11.4	4.4	4.1	105.3	3.7	15.6	5.0	0.03

Z1-121B	Milalani	Kilindini s.	05/03/2016	758	28.5	6.9	421.0	0.0	18.5	1.0	9.2	137.0	3.6	6.7	0.8	0.04
Z1-116	Mwaembe	P.Corals	11/03/2016	752	30.3	6.8	341.7	0.0	32.3	15.8	3.4	107.2	8.8	21.6	2.6	0.02
C/07/09	Kisimachande	P.Corals	11/03/2016	722	31.2	6.8	347.8	0.0	23.1	10.0	3.9	106.9	5.6	17.2	1.6	0.02
Z2-103	Gazi shallow well	P.Corals	05/03/2016	868	30.1	7.0	390.5	0.0	30.6	18.1	11.2	108.9	4.8	25.3	42.4	0.02
D/203/27	Marigiza - Baa Kanda (Voroni)	Kilindini s.	08/03/2016	638	31.2	6.8	262.4	0.0	32.8	2.1	13.8	104.0	3.5	9.7	1.8	0.05
DB/MS/LST	Vingujini opp Msambweni Police	P.Corals	05/03/2016	1156	29.9	6.8	299.0	0.0	61.1	10.5	0.2	113.3	16.3	74.5	6.5	2.59
Z1-135	Madzi Kuko Centre	Kilindini s.	02/03/2016	278	31.0	7.0	158.7	0.0	6.5	2.8	0.3	33.0	2.9	12.0	3.3	0.18
Z2-112	Bumamani	Magarini s.	03/03/2016	79.3	28.8	5.7	24.4	0.0	7.3	1.5	0.3	6.4	0.7	6.0	0.7	-0.01
Z1-140	Vumbu	Magarini s.	09/03/2016	681.0	28.9	6.6	353.9	0.0	13.8	16.0	0.7	77.9	17.8	18.8	9.3	0.05
Z2-104	Sala center	P.Corals	03/03/2016	710	29.1	6.7	353.9	0.0	18.0	12.1	1.2	101.1	6.2	23.5	2.1	0.05
Z1-110	Fihoni Primary School	Kilindini s.	03/03/2016	129.8	31.3	6.6	48.8	0.0	5.8	9.4	1.1	13.5	0.7	7.5	1.1	0.58
DB/FI/HP	Fihoni Chief's camp	Kambe	03/03/2016	846.0	29.8	7.1	262.4	0.0	55.8	48.2	0.0	63.4	23.2	59.3	4.0	0.18
Z3-96	Kinondo	P.Corals	08/03/2016	3594	28.5	7.0	299.0	0.0	612.0	79.6	5.4	126.4	45.7	413.9	11.8	0.08

E/29/01	Kinindo Amani Mosque	Pls-Plc	08/03/2016	967	29.3	6.7	335.6	0.0	91.5	7.7	1.7	131.5	7.2	40.5	1.6	0.18
A/09/11	Makongeni Bandani	P.Corals	08/03/2016	4409	29.7	6.9	299.0	0.0	1069.6	151.2	0.0	111.4	73.4	580.7	25.4	-0.02
MIVUMONI	Mivumoni Secondary School (BH)	Mazeras snd.	09/03/2016	252.5	29.9	5.0	61.0	0.0	10.1	11.8	4.3	2.9	3.7	37.5	2.9	0.11
C/15/10	Mivumoni	Mazeras snd.	09/03/2016	666	30.2	6.6	262.4	0.0	28.6	26.3	0.5	30.1	18.3	73.9	4.8	0.74
C/109/21	Amka village	Mazeras snd.	09/03/2016	499	27.8	6.4	213.6	0.0	16.3	24.0	1.2	37.4	12.1	45.4	4.6	0.36
C/12/12	Maphombe Primary	Mazeras snd.	10/03/2016	1072	30.4	6.3	128.1	0.0	188.0	50.3	3.4	26.9	22.8	141.1	4.7	0.07
C/06/12	Gazore	Mazeras snd.	10/03/2016	685	29.1	6.4	140.3	0.0	113.7	30.7	12.4	19.8	18.8	82.6	7.0	0.08
C/19/10	Mivumoni-Makutano	Magarini s.	10/03/2016	92.7	28.5	5.3	24.4	0.0	8.2	5.0	1.7	2.4	1.6	8.2	1.2	3.80
D/129/19	Mabokoni Msikitini	Magarini s.	01/03/2016	141	28.3	5.7	24.4	0.0	13.6	8.6	1.1	0.7	0.5	25.5	1.0	-0.01
DB/MH/CO	Muhaka I.C.P.E. Coastal Field St	Mazeras snd.	02/03/2016	462	29.8	7.1	140.3	0.0	18.5	5.3	5.3	48.2	5.2	25.4	2.1	0.00
Z1-141	Jabalini	P.Corals	13/03/2016	10979	30.0	6.7	305.1	0.5	3180.0	390.6	2.1	244.6	168.2	1620.0	46.5	0.01
UK-WL	Ukunda hand dug well	P.Corals	06/03/2016	1048	29.9	6.7	445.4	0.0	58.7	14.6	53.7	132.7	20.2	34.6	3.7	0.03
A/06/13	Kona Ya Chief/Mwagutu	P.Corals	06/03/2016	1086.0	30.0	6.8	384.4	0.0	43.3	15.4	48.2	122.22	20.71	44.68	3.59	0.04

D/103/16	Ukunda Scheme Kwa Madzugwe	Kilindini s.	08/03/2016	580.0	29.0	7.0	256.3	0.0	20.7	2.5	2.3	71.13	9.12	21.61	3.60	0.02
LUKORE-Sec. School	LUKORE-SH	Mazeras snd.	10/03/2016	2047.0	28.2	6.6	402.7	0.0	291.1	127.1	2.0	109.12	67.77	167.78	10.12	0.28
Z1-118	Mabatani	P.Corals	11/03/2016	720.0	29.2	6.7	360.0	0.2-0.5	11.0	1.2	3.3	123.50	2.65	10.21	1.11	0.03
VIN-WL	Vingujini well	Kilindini s.	11/03/2016	773.0	29.8	6.7	378.3	0.0	29.3	6.2	14.5	125.11	4.40	13.98	1.47	0.04
Base_BH_1	Base Titanium	Mazeras snd.	16/03/2016	527.0	28.9	6.9	183.1	0.0	59.3	29.8	6.3	42.62	7.73	46.14	3.05	-0.02
Base_BH_3	Base Titanium	Mazeras snd.	16/03/2016	690.0	28.0	6.9	274.6	0.0	44.2	16.4	0.3	86.98	4.61	34.21	3.86	0.07
Base_BH_7	Base Titanium	Mazeras snd.	16/03/2016	426.6	28.8	6.6	164.8	0.0	16.4	21.3	0.2	33.34	6.28	37.91	2.99	0.07
DB/KI/ST	Kibwaga Feeder School	Mazeras snd.	16/03/2016	553.0	28.2	6.5	225.8	0.0	34.8	26.4	0.5	21.43	15.59	59.44	3.10	0.73
A/06/12	Mvureni-Maweni	P.Corals	06/03/2016	2993	30.4	6.9	286.8	0.0	690.3	82.8	4.6	133.1	35.1	348.9	9.3	0.06

Appendix B. Supplementary information of Chapter 3: *E. coli* presence in each samples for March and June field campaigns.

Table 1, Appendix B: *E. coli* quantification results from CBT in MPN/100ml in March 2016. Green colour means safe, yellow means intermediate risk, orange means high risk and red means unsafe.

Code	*Aquagenx (bags)*	*Code*	*Aquagenx (bags)*	*Code*	*Aquagenx (bags)*
Footprints School	0,0	**A/14/10**	0,0	**Z2-112**	48,3
Z4-11	48,3	**Z3-87**	1,5	**Z1-140**	0,0
Z4-09	>100	**Z3-98**	>100	**Z2-104**	2,6
Z4-01	>100	**Z3-90**	>100	**Z1-110**	>100
A/04/12	0,0	**A/05/11**	>100	**DB/FI/HP**	0,0
Z4-18	>100	**HOTSPRING**	0,0	**Z3-96**	>100
A/06/12	1,2	**C108HWL**	>100	**E/29/01**	13,6
Z4-78B	>100	**3KD01**	48,3	**A/09/11**	0,0
Z4-08	48,3	**S1-3KD06**	>100	**MIVUMONI**	0,0
Z4-06	>100	**GD31**	0,0	**C/15/10**	0,0
D/100/16	13,6	**MUK DAM**	>100	**C/109/21**	0,0
Z4-04	>100	**MUK DWS**	>100	**C/12/12**	0,0
Z4-MS	>100	**Z1-122**	13,6	**C/06/12**	0,0
D/82/14	0,0	**Z1-125**	>100	**C/19/10**	0,0
Z4-85	>100	**Z1-124**	>100	**D/129/19**	0,0
Z4-24	>100	**D/16/10**	1,2	**DB/MH/CO**	0,0
Z3-25	>100	**Z1-121B**	>100	**Z1-141**	>100
D/63/13	0,0	**Z1-116**	13,6	**UK-WL**	0,0
D/68/13	0,0	**C/07/09**	0,0	**A/06/13**	0,0
Z3-30	48,3	**A/01/11**	0,0	**D/103/16**	0,0
Z3-29	13,6	**Z2-103**	>100	**LUKORE-SH**	48,3
DB/BM/HP	0,0	**D/203/27**	1,1	**Z1-118**	>100
BH310	13,6	**DB/MS/LST**	0,0	**VIN-WL**	0,0
BH402	0,0	**Z1-135**	>100	**Base_BH_1**	0,0
NK-03	0,0	**DB/KI/ST**	0,0	**Base_BH_3**	0,0
Z1-70	>100	**Z1-33**	>100	**Base_BH_7**	0,0

Table 2, Appendix B: *E. coli* quantification results from CBT in MPN/100ml in June 2016. Green colour means safe, yellow means intermediate risk, orange means high risk and red means unsafe.

Code	*Aquagenx (bags)*	*Code*	*Aquagenx (bags)*	*Code*	*Aquagenx (bags)*
Footprints School	0,0	**A/05/11**	>100	**Z1-110**	>100
Z4-11	48,3	**HOTSPRING**	0,0	**DB/FI/HP**	0,0
Z4-01	>100	**C108HWL**	>100	**Z3-96**	48,3
A/04/12	0,0	**3KD01**	48,3	**E/29/01**	9,6
Z4-18	48,3	**MUACHEMA**	>100	**A/09/11**	0,0
A/06/12	0,0	**S1-3KD06**	>100	**MIVUMONI**	0,0
Z4-78B	>100	**GD31**	0,0	**C/15/10**	0,0
Z4-08	>100	**MUK DAM**	>100	**C/109/21**	0,0
Z4-06	>100	**MUK DWS**	>100	**C/12/12**	0,0
D/100/16	48,3	**Z1-122**	13,6	**C/06/12**	0,0
Z4-04	>100	**Z1-125**	>100	**C/19/10**	0,0
Z4-MS	48,3	**Z1-124**	>100	**D/129/19**	0,0
D/82/14	0,0	**D/16/10**	0,0	**DB/MH/CO**	0,0
Z4-85	48,3	**Z1-121B**	>100	**Z1-141**	>100
Z4-24	>100	**Z1-116**	13,6	**UK-WL**	0,0
D/63/13	0,0	**C/07/09**	0,0	**D/103/16**	0,0
D/68/13	0,0	**A/01/11**	0,0	**LUKORE- SH**	0,0
Z3-30	>100	**Z2-103**	>100	**Z1-118**	>100
Z3-29	>100	**D/203/27**	13,6	**VIN-WL**	0,0
DB/BM/HP	0,0	**DB/MS/LST**	0,0	**Base_BH_3**	0,0
BH310	0,0	**Z1-135**	>100	**Base_BH_7**	0,0
Z1-70	>100	**Z2-112**	48,3	**DB/KI/ST**	0,0
Z1-33	48,3	**Z1-140**	1,5	**Z3-102B**	13.6
A/14/10	0,0	**Z2-104**	4,7	**BH302**	0,0
Z3-87	>100	**Z3-98**	>100	**C/05/09**	48.3
Z3-90	13,6	**C/03/09**	0,0		

Appendix C. Supplementary information of Chapter 4: Information used in the mixing model and equation applied to calculate the saline intrusion wedge.

Figure 1, Appendix C: Diagram process of the methodology applied to calculate net recharge.

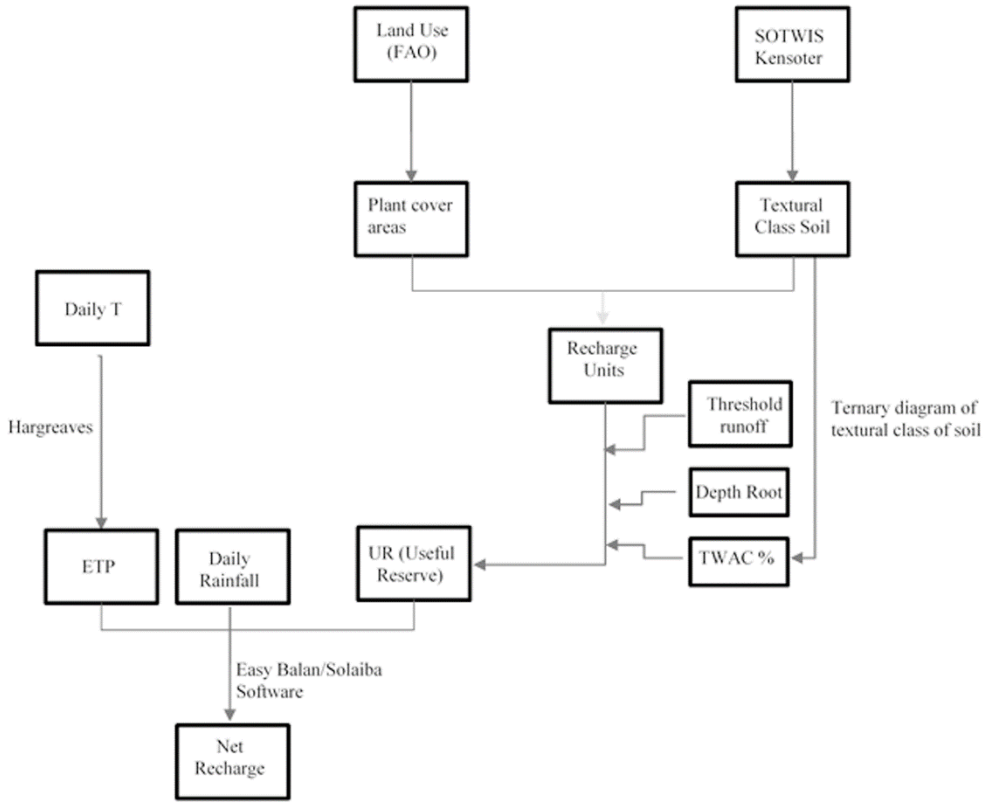

Table 1, Appendix C: Hydrochemical composition of the samples used as initial solutions for the geochemical model.

Sample	***T (ºC)***	***pH***	***HCO_3^-***	***Ca***	***K***	***Cl^-***	***SO_4^{2-}***	***Br^-***	***Si***	***Mg***	***Na***
Fresh sample	28.4	6.5	433.2	136	0.5	13	0.3	0.1	24.1	3.4	5.7
Saline sample	27.3	7	177	344.91	268.35	15844	2208.2	58.7	10.37	878.22	7138.30

Table 2, Appendix C: Groundwater level range and EC range of some monitored points of the shallow aquifer measured during and post- La Niña event (2016 and 2017).

Point	***Geology***	***Zone***	***Groundwater level depth (m b.g.l)***					***Electrical conductivity µS/cm***				
			The beginning of La Niña (January 2016)	The end of La Niña (March 2017)	After the first wet seasson (April 2017)	After the second wet seasson (December 2017)	Mean±SD	The beginning of La Niña (January 2016)	The end of La Niña (March 2017)	After the first wet seasson (April 2017)	After the second wet seasson (December 2017)	Mean±SD
Z4-85	P.Corals	4	9.89	9.8	9.81	9.78	9,77±0,08	829	959	941	899	891±51
Z4-78	P.Corals	4	8.24	8.4	8.24	8.15	8,2±0,08	2484	2652	2641	2598	2568±76
Z4-18	P.Corals	4	15.44	15.48	15.43	15.37	15,38±0,06	760	931	920	887	856±85
Z4-11	Magarini s.	4	12.65	16.07	16.1	14.11	14,59±1,06	120	366	358	210	256±100
Z4-05	Kilindini s.	4	22.62	23.4	23.42	22.74	23,05±0,23	628	586	594	582	585±30
Z4-01	Kilindini s.	4	23.19	23.3	23.33	23.27	23,19±0,1	687	681	666	678	667±21
Z3-98	P.Corals	3	11.73	11.7	11.71	11.36	11,51±0,35	786	905	901	805	816±49
Z3-90	P.Corals	3	7.97	8.4	8.49	6.19	7,26±0,88	1685	3622	3650	2594	2632±652
Z3-87	P.Corals	3	5.06	5.03	5	4.9	4,96±0,07	1722	2080	2100	1991	1922±115
Z3-30	Kilindini s.	2	5.1	5.66	5.62	3.24	4,57±0,93	1369	584	590	609	723±236
Z3-29	Kilindini s.	2	9.96	11.05	11.13	9.3	10,24±0,49	337	290	320	468	322±71
Z3-102B	P.Corals	2	No data	11.79	11.8	11.41	11,45±0,26	No data	589	591	580	586±6
Z2-112	Magarini s.	2	6.75	8.99	9.11	6.83	7,68±0,7	128	58	83	89	83±28
Z2-103	P.Corals	2	11.42	11.51	11.36	11.1	11,11±0,26	749	811	831	854	806±52

Z1-70	Kilindini s.	1	3	4.95	5.31	2.54	3,5±0,94	795	623	640	733	696±89
Z1-33	Kilindini s.	1	10.3	10.47	10.46	9.98	10,13±0,22	640	712	644	644	647±51
Z1-140	Magarini s.	2	12.4	12.6	12.9	12.17	12,28±0,34	582	662	661	595	581±37
Z1-135	Kilindini s.	2	4.37	No data	5.01	2.56	3,8±0,84	369	No data	260	443	328±84
Z1-125	Magarini s.	1	14.11	16.9	17.11	14.08	15,2±1,14	94	135	182	91	111±20
Z1-124	Magarini s.	1	14.66	15.01	No data	15.35	14,88±0,55	302	0	No data	648	439±185
Z1-122	Magarini s.	1	11.7	12.8	12.75	10.2	11,52±0,84	115	121	109	183	164±33
Z1-110	Kilindini s.	2	5.17	No data	No data	4.32	5,14±0,62	114	No data	No data	225	180±63
Z1-141	P.Corals	1	6.45	6.65	6.61	6.38	6,42±0,15	3999	3999	3999	3999	4138±924

Table 3, Appendix C: Electrical conductivity in µS/cm of diverse field survey from September 2013 to June 2016.

	September 2013			***March 2014***		***June 2014***			***March-May 2015***			***September 2015***		***March 2016***		***June 2016***	
Code	EC (µS/cm)	Code	EC (µS/cm)	Code	EC (µS/cm)	Code	EC (µS/cm)	Code	EC (µS/cm)	Code	EC (µS/cm)	Code	EC (µS/cm)	Code	EC (µS/cm)	Code	EC (µS/cm)
A/01/09	701	**C/32/11**	764	**Z1-110**	654	**Z1-110**	206	**A/01/09**	722	**D/10/09**	689	**Footprints School**	315	**Z4-11**	219	**Z4-11**	205
A/01/11	956	**C/33/11**	936	**Z1-116**	670	**Z1-116**	658	**A/01/11**	1004	**D/11/09**	574	**Z4-11**	136	**Z4-09**	619	**Z4-09**	
A/01/12	803	**D/01/09**	737	**Z1-118**	638	**Z1-122**	176	**A/02/09**	700	**D/113/17**	943	**Z4-09**	569	**Z4-01**	716	**Z4-01**	671
A/02/09	690	**D/04/09**	707	**Z1-121**	624	**Z1-124**	243	**A/02/11**	852	**D/117/17**	880	**Z4-01**	630	**A/04/12**	949	**A/04/12**	65
A/02/11	800	**D/05/09**	794	**Z1-122**	143	**Z1-125**	111	**A/02/12**	858	**D/118/17**	732	**A/05/12**	836	**Z4-18**	950	**Z4-18**	881
A/02/12	816	**D/06/09**	720	**Z1-124**	157	**Z1-135**	407	**A/02/13**	697	**D/13/10**	566	**Z4-18**	834	**A/06/12**	2993	**A/06/12**	2743
A/02/13	865	**D/07/09**	573	**Z1-125**	92	**Z1-33**	597	**A/03/09**	628	**D/137/15**	901	**LEISURE HOTEL**	1603	**Z4-78B**	4423	**Z4-78B**	3793
A/03/12	654	**D/09/09**	480	**Z1-135**	298	**Z1-70**	882	**A/04/09**	635	**D/144/20**	781	**A/06/12**	2557	**Z4-08**	828	**Z4-08**	406
A/03/13	872	**D/10/09**	795	**Z1-33**	596	**Z2-103**	782	**A/04/12**	810	**D/145/20**	859	**Z4-78B**	3614	**Z4-06**	826	**Z4-06**	769
A/04/09	614	**D/100/16**	860	**Z1-70**	705	**Z2-104**	656	**A/04/27**	1848	**D/150/20**	876	**Z4-08**	748	**D/100/16**	924	**D/100/16**	875
A/04/11	3999	**D/102/16**	738	**Z2-103**	760	**Z2-112**	106	**A/05/09**	672	**D/151/20**	753	**Z4-06**	735	**Z4-04**	631	**Z4-04**	592
A/04/12	752	**D/103/16**	510	**Z2-104**	116	**Z3-102**	846	**A/05/10**	670	**D/158/21**	894	**D/100/16**	708	**Z4-MS**	338	**Z4-MS**	364
A/04/27	1858	**D/104/16**	605	**Z2-112**	69	**Z3-25**	398	**A/05/13**	2138	**D/16/10**	680	**Z4-05**	547	**D/82/14**	90	**D/82/14**	92
A/05/09	640	**D/105/16**	715	**Z3-102**	675	**Z3-30**	1845	**A/06/10**	672	**D/17/10**	626	**Z4-MS**	311	**Z4-85**	1010	**Z4-85**	65
A/05/10	611	**D/11/09**	551	**Z3-29**	180	**Z3-87**	1590	**A/06/12**	2760	**D/20/10**	705	**D/82/14**	68	**Z4-24**	222	**Z4-24**	283
A/05/12	784	**D/110/16**	752	**Z3-25**	277	**Z3-90**	1950	**A/07/09**	651	**D/36/12**	670	**Z4-85**	879	**Z3-25**	537	**D/63/13**	170
A/05/13	2001	**D/113/17**	914	**Z3-30**	1014	**Z3-96**	1968	**A/07/12**	1175	**D/37/12**	3052	**Z4-24**	224	**D/63/13**	183	**D/68/13**	51

A/06/09	640	**D/114/16**	853	**Z3-87**	1924	**Z3-98**	726	**A/07/13**	963	**D/40/12**	248	**Z3-25**	355	**D/68/13**	175	**Z3-30**	735
A/06/10	638	**D/115/16**	1556	**Z3-90**	2630	**Z4-01**	633	**A/08/09**	687	**D/47/12**	127	**D/63/13**	153	**Z3-30**	751	**Z3-29**	342
A/06/12	2365	**D/118/17**	719	**Z3-96**	3010	**Z4-06**	728	**A/08/12**	1181	**D/48/13**	684	**D/68/13**	161	**Z3-29**	377	**DB/BM/HP**	256
A/06/13	924	**D/119/17**	487	**Z3-98**	711	**Z4-08**	680	**A/08/13**	1262	**D/51/13**	656	**Z3-30**	801	**DB/BM/HP**	274	**BH310**	510
A/07/09	613	**D/121/17**	283	**Z4-01**	627	**Z4-11**	209	**A/09/09**	679	**D/84/15**	752	**Z3-29**	343	**BH310**	555	**Z1-70**	820
A/07/11	1810	**D/123/17**	489	**Z4-05**	564	**Z4-18**	835	**A/09/11**	4270	**D/86/15**	662	**DB/BM/HP**	243	**BH402**	429	**Z1-33**	700
A/07/12	1016	**D/127/17**	354	**Z4-06**	737	**Z4-24**	164	**A/09/12**	1371	**D/90/15**	633	**BKH-310**	507	**NK-03**	760	**A/14/10**	667
A/07/13	921	**D/129/19**	134	**Z4-08**	710	**Z4-85**	839	**A/09/13**	1121	**D/98/16**	593	**BKH-402**	381	**Z1-70**	692	**Z3-87**	2011
A/08/09	619	**D/13/10**	562	**Z4-09**	945			**A/10/10**	1461	**D/99/16**	758	**NK-03**	922	**Z1-33**	700	**Z3-98**	830
A/08/12	1116	**D/130/19**	229	**Z4-11**	218			**A/11/12**	788			**Z1-70**	773	**A/14/10**	723	**Z3-90**	2360
A/08/13	1160	**D/137/15**	873	**Z4-18**	827			**A/12/10**	633			**Z1-33**	613	**Z3-87**	2171	**A/05/11**	1750
A/09/09	678	**D/144/20**	762	**Z4-24**	188			**A/12/12**	563			**A/14/10**	642	**Z3-98**	877	**HOTSPRING**	15792
A/09/11	3999	**D/145/20**	816	**Z4-78**	2450			**A/13/12**	895			**Z3-87**	1896	**Z3-90**	3153	**C108HWL**	5594
A/09/12	1294	**D/148/20**	917	**Z4-85**	850			**A/14/10**	676			**Z3-98**	720	**A/05/11**	2197	**3KD01**	3211
A/09/13	986	**D/150/20**	868					**A/14/12**	692			**Z3-90**	2310	**HOTSPRING**	10240	**TIWI 8.2**	450
A/10/12	1048	**D/158/21**	900					**A/15/10**	676			**A/05/11**	1851	**C108HWL**	7849	**TIWI 1**	1100
A/11/11	1911	**D/16/10**	628					**A/16/10**	1085			**LUKORE**	1313	**3KD01**	5251	**MUACHEMA TRIB**	505

A/11/12	745	**D/17/10**	613	**A/17/10**	1190	**HOTSPRING**	8600	**TIWI 8.2**	713	**S1-3KD06**	140
A/12/10	599	**D/18/10**	658	**A/18/10**	1897	**RAMISIUS**	5450	**TIWI 1**	1137	**GD31**	290
A/12/12	528	**D/20/10**	693	**B/02/09**	775	**RAMISIDWS**	2646	**S1-3KD06**	137	**MUK DAM**	230
A/13/11	773	**D/203/27**	640	**B/03/09**	701	**VUGA**	841	**GD31**	567	**MUK DWS**	210
A/13/12	831	**D/25/10**	92	**B/08/09**	106	**TIWI 8.2**	676	**MUK DAM**	196	**KINGOMBERO**	110
A/14/11	808	**D/36/12**	681	**B/10/09**	361	**TIWI 1**	944	**MUK DWS**	211	**Z1-122**	210
A/14/12	649	**D/37/12**	196	**B/14/10**	813	**MUACHEMA TRIB**	407	**KINGOMBERO**	112	**Z1-125**	112
A/17/10	1389	**D/38/12**	433	**B/15/10**	935	**3KD06-MUK**	136	**Z1-122**	224	**Z1-124**	325
A/18/10	1121	**D/40/12**	236	**B/16/10**	2070	**SHIMBA 2SCH**	634	**Z1-125**	100	**D/16/10**	592
B/03/09	676	**D/47/12**	122	**B/17/10**	3290	**MUK DAM**	191	**Z1-124**	289	**Z1-121B**	589
B/08/09	86	**D/48/13**	676	**B/21/10**	1391	**MUK DWS**	183	**D/16/10**	683	**Z1-116**	740
B/10/09	352	**D/49/13**	807	**B/24/10**	1727	**KINGOMBERO**	122	**Z1-121B**	758	**C/07/09**	666
B/12/10	466	**D/50/13**	687	**C/02/09**	614	**Z1-122**	203	**Z1-116**	752	**A/01/11**	1040
B/14/10	746	**D/51/13**	655	**C/03/09**	871	**Z1-125**	71	**C/07/09**	722	**Z2-103**	890
B/15/10	822	**D/52/13**	675	**C/03/12**	145	**Z1-124**	304	**A/01/11**	1052	**D/203/27**	610
B/16/10	1888	**D/54/13**	705	**C/04/09**	679	**Z1-130**	675	**Z2-103**	868	**DB/MS/LST**	1010

B/17/10	3110	**D/62/13**	306	**C/04/12**	442	**D/16/10**	649	**D/203/27**	638	**Z1-135**	254
B/18/10	668	**D/63/13**	171	**C/05/09**	1935	**Z1-121B**	695	**DB/MS/LST**	1156	**Z2-112**	41
B/21/10	1090	**D/67/13**	152	**C/06/09**	864	**Z1-116**	690	**Z1-135**	278	**Z1-140**	650
B/24/10	1566	**D/68/13**	169	**C/06/12**	341	**C/05/09**	686	**Z2-112**	79	**Z2-104**	610
C/02/09	544	**D/71/14**	219	**C/07/12**	239	**A/01/11**	938	**Z1-140**	681	**Z1-110**	180
C/03/09	768	**D/73/14**	537	**C/08/09**	656	**Z2-103**	780	**Z2-104**	710	**DB/FI/HP**	590
C/03/12	152	**D/75/14**	465	**C/08/12**	515	**Z3-102**	670	**Z1-110**	130	**Z3-96**	3300
C/04/09	1014	**D/84/15**	751	**C/10/12**	830	**B/MU/01**	546	**DB/FI/HP**	846	**E/29/01**	980
C/04/12	346	**D/85/15**	646	**C/109/21**	581	**DB/MS/LST**	864	**Z3-96**	3594	**A/09/11**	475
C/05/09	1758	**D/86/15**	638	**C/111/21**	340	**Z1-135**	367	**E/29/01**	967	**MIVUMONI**	260
C/06/09	790	**D/88/15**	1274	**C/119/22**	1182	**Z2-112**	186	**A/09/11**	4409	**C/15/10**	66
C/06/12	268	**D/90/15**	605	**C/12/12**	847	**Z1-140**	453	**MIVUMONI**	253	**C/109/21**	630
C/07/09	598	**D/91/15**	634	**C/120/22**	1165	**Z2-104**	633	**C/15/10**	666	**C/12/12**	66
C/07/12	436	**D/94/15**	616	**C/13/10**	101	**Z1-110**	175	**C/109/21**	499	**C/06/12**	313
C/08/09	590	**D/96/15**	137	**C/13/12**	1564	**DB/FI/HP**	708	**C/12/12**	1072	**C/19/10**	43
C/08/12	406	**D/97/15**	98	**C/14/10**	213	**Z3-96**	3353	**C/06/12**	685	**D/129/19**	49
C/109/21	548	**D/98/16**	558	**C/145/27**	172	**E/29/01**	755	**C/19/10**	93	**DB/MH/CO**	516
C/111/21	296	**D/99/16**	749	**C/15/10**	548	**A/09/11**	4087	**D/129/19**	141	**Z1-141**	9440

C/12/10	120	**C/16/12**	387	**MIVUMONI**	216	**DB/MH/CO**	462	**UK-WL**	1040
C/12/12	954	**C/17/10**	202	**C/15/10**	432	**Z1-141**	10979	**D/103/16**	539
C/120/22	1182	**C/17/13**	368	**C/109/21**	452	**UK-WL**	1048	**LUKORE-Sec. School**	70
C/13/10	94	**C/18/10**	115	**C/12/12**	872	**A/06/13**	1086	**Z1-118**	710
C/13/12	1024	**C/22/11**	289	**C/06/12**	315	**D/103/16**	580	**VIN-WL**	780
C/14/10	178	**C/23/11**	880	**C/19/10**	85	**LUKORE-Sec. School**	2047	**Base_BH_3**	590
C/145/27	130	**C/25/11**	134	**D/129/19**	131	**Z1-118**	720	**Base_BH_7**	370
C/15/10	408	**C/26/11**	898	**D/129/19**	123	**VIN-WL**	773	**DB/KI/ST**	500
C/16/12	134	**C/27/11**	1411	**DB/MH/CO**	493	**Base_BH_1**	527	**Z3-102B**	540
C/17/10	196	**C/28/11**	1544	**JABALINI**	9540	**Base_BH_3**	690	**BH302**	200
C/17/13	659	**C/32/11**	309	**HOME**	9540	**Base_BH_7**	427	**DIANI**	46750
C/18/10	98	**C/33/11**	1062			**DB/KI/ST**	553	**MSW BEACH**	12250
C/19/10	118	**D/01/09**	629					**KIS_21**	170
C/22/11	292	**D/04/09**	715					**KIS_65**	110
C/23/11	802	**D/06/09**	808					**GD14_5**	329
C/26/11	798	**D/07/09**	598					**GD14_ 35**	418

C/27/11	1252	**D/09/09**	494	**C/05/09**	894
C/28/11	1950			**C/03/09**	1435

Table 4, Appendix C: Data used to calculate the saline wedge progress.

Equation used to calculate the saline wedge progress: $L = \frac{K*\beta(1+\beta)*b^2}{2q_t}$ Where $q_t = \frac{W-abs_t}{coast\ lenght}$		
Equation used to calculate the saline wedge depth at different coastline distance: $Z^2 = \frac{2q_tX - WX^2}{K\beta}$		
L, *length of the saline wedge*	L_0= 7 meters	L_1= 9 meters
Z, *depth of the saline wedge at different coastline distance*	meters	
K, hydraulic conductivity of geological formation	*K*=100 m/d for coral formation *K*=10 m/d for Kilindini sands	
b, shallow aquifer thickness	*b*=30 meters	
W, recharge during La Niña event	*W*=158602 m^3/d	
Abs, groundwater abstraction	Abs_0=9535 m^3/d	Abs_1=34270 m^3/d
β, ratio of the difference between saltwater and fresh water densities to fresh water density, which means the saline interface is located 40 times the fresh water level over the sea water level in that point.	*β*=1/40	
X, *distance from the coast lin4*	meters	

Appendix D. Supplementary information of Chapter 5: Groundwater mass balance for each scenario.

Table 1, Appendix D: Water balance for each future scenario

Hm3/y	Dry_Normal_0ºC_Current						Dry_Normal_0ºC_Extreme					
	1st year	2nd year	3rd year	4th year	5th year	6th year	1st year	2nd year	3rd year	4th year	5th year	6th year
Recharge in	11.14	17.20	11.82	161.33	78.79	51.55	11.14	17.20	11.82	161.33	78.79	51.55
River Leakage in	33.46	34.51	35.15	34.00	34.35	34.55	53.80	55.08	56.05	54.47	54.85	55.10
TOTAL IN	44.59	51.70	46.97	195.32	113.14	86.10	64.94	72.28	67.87	215.80	133.65	106.65
Wells out	0.93	1.06	1.97	1.63	0.96	1.00	8.78	8.76	9.00	8.90	9.07	8.69
Constant Head out	75.56	64.74	60.70	78.84	76.78	62.61	76.45	64.79	60.61	78.69	76.52	62.31
River Leakage out	20.56	17.19	15.13	18.74	18.04	16.03	28.52	24.36	21.95	26.34	25.41	22.93
Drains out	69.83	58.09	51.67	65.50	61.20	58.86	75.95	64.13	57.58	71.66	67.08	64.72
TOTAL OUT	166.88	141.09	129.47	164.71	156.98	138.50	189.70	162.04	149.14	185.59	178.08	158.65
IN-OUT	-122.29	-89.38	-82.50	30.61	-43.84	-52.40	-124.76	-89.76	-81.27	30.21	-44.44	-52.00
Hm3/y	**VDry_Normal_0ºC_Current**						**VDry_Normal_0ºC_Extreme**					
	1st year	2nd year	3rd year	4th year	5th year	6th year	1st year	2nd year	3rd year	4th year	5th year	6th year
Recharge in	12.06	12.31	8.61	159.90	72.43	50.96	12.06	12.31	8.61	159.90	72.43	50.96
River Leakage in	33.32	34.57	35.32	34.09	34.38	34.53	33.38	34.70	35.47	34.26	34.59	34.74
TOTAL IN	45.38	46.88	43.93	193.99	106.82	85.49	45.44	47.01	44.09	194.16	107.02	85.70
Wells out	0.93	1.06	1.97	1.63	0.96	1.00	8.62	8.60	8.60	8.60	8.91	8.53
Constant Head out	75.74	64.85	60.60	77.61	73.21	61.37	72.83	61.03	56.58	73.52	69.02	57.12
River Leakage out	21.08	17.18	14.91	18.60	17.99	16.08	20.94	16.97	14.73	18.31	17.66	15.79
Drains out	70.54	57.70	51.01	64.59	60.80	58.63	70.12	56.77	49.90	63.34	59.37	57.06
TOTAL OUT	168.29	140.80	128.49	162.43	152.96	137.08	172.52	143.37	129.81	163.77	154.96	138.50
IN-OUT	-122.92	-93.91	-84.55	31.56	-46.14	-51.59	-127.07	-96.36	-85.73	30.39	-47.94	-52.80
Hm3/y	**VDry_Normal_2ºC_Current**						**VDry_Normal_2ºC_Extreme**					
	1st year	2nd year	3rd year	4th year	5th year	6th year	1st year	2nd year	3rd year	4th year	5th year	6th year
Recharge in	10.65	11.27	7.31	149.95	68.95	44.81	10.65	11.27	7.31	149.95	68.95	44.81

River Leakage in	33.33	34.59	35.34	34.20	34.49	34.73	33.40	34.72	35.49	34.37	34.70	34.94
TOTAL IN	43.99	45.86	42.65	184.15	103.44	79.55	44.05	45.98	42.81	184.32	103.64	79.75
Wells out	0.93	1.06	1.97	1.63	0.96	1.00	8.62	8.60	8.60	8.60	8.91	8.53
Constant Head out	75.69	64.76	60.53	76.49	72.27	60.96	72.78	60.94	56.50	72.39	68.07	56.71
River Leakage out	21.01	17.07	14.80	18.30	17.64	15.62	20.87	16.87	14.63	18.02	17.32	15.35
Drains out	70.40	57.49	50.79	62.50	59.64	56.11	69.98	56.56	49.68	61.26	58.22	54.54
TOTAL OUT	168.04	140.39	128.08	158.92	150.51	133.69	172.26	142.97	129.41	160.27	152.52	135.12
IN-OUT	-124.05	-94.53	-85.43	25.23	-47.07	-54.15	-128.21	-96.98	-86.60	24.05	-48.88	-55.37
Hm3/y	**VDry_Wet_0ºC_Current**						**VDry_Wet_0ºC_Extreme**					
	1st year	2nd year	3rd year	4th year	5th year	6th year	1st year	2nd year	3rd year	4th year	5th year	6th year
Recharge in	12.06	12.31	8.61	305.32	271.86	339.60	12.06	12.31	8.61	305.32	271.86	339.60
River Leakage in	33.32	34.57	35.32	32.08	30.66	29.55	33.38	34.70	35.47	32.25	30.90	29.77
TOTAL IN	45.38	46.88	43.93	337.40	302.52	369.15	45.44	47.01	44.09	337.57	302.76	369.37
Wells out	0.93	1.06	1.97	1.63	0.96	1.00	8.62	8.60	8.60	8.60	8.91	8.53
Constant Head out	75.18	64.32	60.20	89.47	101.11	112.61	72.27	60.50	56.17	85.38	96.93	108.39
River Leakage out	21.08	17.18	14.91	24.69	29.71	35.01	20.94	16.97	14.73	24.32	29.21	34.41
Drains out	70.49	57.67	50.97	108.82	116.47	146.98	70.07	56.73	49.86	107.52	114.96	145.22
TOTAL OUT	167.69	140.23	128.04	224.61	248.25	295.60	171.91	142.81	129.37	225.82	250.01	296.55
IN-OUT	-122.31	-93.35	-84.11	112.80	54.27	73.55	-126.47	-95.80	-85.28	111.75	52.75	72.82